

UNIVERSITY OF OKLAHOMA

GRADUATE COLLEGE

ASSOCIATION OF WINTER WEATHER VARIABILITY IN CENTRAL AND  
EASTERN NORTH AMERICA WITH TROPICAL PACIFIC SEA SURFACE  
TEMPERATURE

A DISSERTATION

SUBMITTED TO THE GRADUATE FACULTY

in partial fulfillment of the requirements for the

degree of

DOCTOR OF PHILOSOPHY

By

DAVID L. MONTROY

Norman, Oklahoma

2006

UMI Number: 3242289

UMI<sup>®</sup>

---

UMI Microform 3242289

Copyright 2007 by ProQuest Information and Learning Company.  
All rights reserved. This microform edition is protected against  
unauthorized copying under Title 17, United States Code.

---

ProQuest Information and Learning Company  
300 North Zeeb Road  
P.O. Box 1346  
Ann Arbor, MI 48106-1346

ASSOCIATION OF WINTER WEATHER VARIABILITY IN CENTRAL AND  
EASTERN NORTH AMERICA WITH TROPICAL PACIFIC SEA SURFACE  
TEMPERATURE

A DISSERTATION APPROVED FOR THE  
SCHOOL OF METEOROLOGY

BY

---

Peter J. Lamb

---

Michael B. Richman

---

Kelvin K. Droegemeier

---

David J. Stensrud

---

S. Lakshmiarahan

© Copyright by DAVID L. MONTROY 2006  
All Rights Reserved.

## ACKNOWLEDGEMENTS

Early portions of this research were funded by National Science Foundation Grant ATM 92-96119, USEPA Cooperative Agreement CR-819646010, National Oceanic and Atmospheric Administration (NOAA) Cooperative Agreement NA67RJ0150, and an American Meteorological Society graduate fellowship received by the author and cosponsored by the NOAA Office of Global Programs.

I would like to thank my advisor, Peter Lamb, for his guidance and help on the writing and editing of this manuscript. Over the last 15 years, Dr. Lamb has been an excellent instructor in how to most effectively and succinctly present research results, particularly those that are highly technical. Without his supervision and feedback, this manuscript would not approach its current quality. I am thankful for Dr. Lamb's support of this research since its beginning as an undergraduate honors thesis.

I am also indebted to my committee for their patient support in the completion of this research since its inception in Spring 1997. They provided key guidance on the proper adjustment on the scope of this research in its early stages, and this input was instrumental in focusing the analysis into a significant but manageable body of work for the purposes of completing this dissertation. Dr. Stensrud provided key guidance in this regard and encouraged me to focus on statistically based techniques to identify the novel relationships that are stated in this manuscript. Additionally, Dr. Varahan provided key personal support and encouragement to complete this research, and I thank him for his participation on my committee. Dr. Droegemeier has been a strong source of support – both professionally and personally – for me since my early days as an undergraduate. Finally, Dr. Richman has been a key advisor and constant supporter of this research and is responsible for helping excite me about multivariate analysis and the investigation of interannual climate patterns.

Further, a number of other scientists at the University of Oklahoma and representatives from other institutions provided key guidance and support. I would like to thank Dr. Xiaofeng Gong for providing key comments on early research results and for

his personal support and encouragement “in the trenches” in the OU Graduate Program. Additionally, I am indebted to Ms. Denise Russell during her time at the Williams Companies for her support (professionally and financially) of the continued advancement of this research while I was employed on her Market Analysis team. Mr. Chris Keyes and the team at Weathernews Americas also encouraged the completion of this work. Finally, Ms. Dawn Trammel and the team at Coral Energy in Houston took the lead on extra projects to provide me with the time required to complete the last stages of this research and complete a process begun nearly 10 years ago.

Finally, I am most thankful and deeply indebted to my family for their constant and patient support and encouragement through the whole process of completing this work. To Mom and Dad – I did it! Thank you for instilling in me the drive to complete what I started and for your encouragement. For my beautiful daughter Miranda, this research has been around longer than you, and you have been so patient in letting Daddy finish his “paych-d”. Too many times your Dad has been busy in his office on his work ... but now it’s time to catch up on those books and games and get started on that Lego house. I love you, Miranda. And to my loving wife Dana – You are the most understanding and patient woman there ever was. Ever since we were married, you have had a distracted husband with this ever-present task to complete. You have patiently endured nights and weekends with me in the office, “clacking away”, and have had to hear me talk about “the paper” for years. But through it all, you cheerfully encouraged me to complete this work that I began so many years ago and have provided unending love and support, as you always do. You were always there to help me along when the end seemed so far away. Your sacrifices gave me the time I needed to finish. And in the last week, you were instrumental in helping me present my results clearly and with confidence. Is there no end to your skills? You are and always will be my source of strength in all that I do, and I now have the rest of our life together to show you how dearly and deeply I love you.

## TABLE OF CONTENTS

TABLE OF CONTENTS .....	vi
LIST OF ILLUSTRATIONS .....	ix
LIST OF TABLES .....	xviii
ABSTRACT .....	xxiii
<b>CHAPTER 1 INTRODUCTION.....</b>	<b>1</b>
1.1 SYNOPSIS OF TROPICAL PACIFIC CLIMATE VARIATIONS.....	1
1.2 DETAILED REVIEW OF PREVIOUS RESEARCH.....	4
1.2.1 <i>Early tropical Pacific climate studies</i> .....	4
1.2.2 <i>Interannual climate variations in the tropics</i> .....	5
1.2.3 <i>Global climate teleconnections from the tropical Pacific</i> .....	6
1.2.4 <i>Other modes of interannual climate variations</i> .....	9
1.3 PROBLEM IDENTIFICATION.....	12
<b>CHAPTER 2 STRATIFICATION OF TROPICAL PACIFIC SEA-SURFACE TEMPERATURE ANOMALY EVENTS .....</b>	<b>15</b>
2.1 PREAMBLE .....	15
2.2 DEFINITION OF TROPICAL PACIFIC SSTA EVENTS.....	16
2.2.1 <i>Data</i> .....	16
2.2.2 <i>Methodology</i> .....	17
2.2.3 <i>SSTA Events for 1950-2000</i> .....	20
2.3 OTHER ATMOSPHERIC/OCEANIC PHENOMENA.....	21
2.3.1 <i>Arctic Oscillation/North Atlantic Oscillation</i> .....	21
2.3.2 <i>Pacific Decadal Oscillation</i> .....	24
2.4 SELECTION OF PRIMARY SST EVENTS .....	27
<b>CHAPTER 3 MONTHLY TELECONNECTIONS BETWEEN TROPICAL PACIFIC SSTA EVENTS AND NORTH AMERICAN WINTER CLIMATE .....</b>	<b>30</b>
3.1 PREAMBLE .....	30
3.2 NORTH AMERICAN CLIMATE DATA .....	30
3.3 METHODOLOGY .....	31
3.4 RESULTS .....	31
3.4.1 <i>North American Precipitation – Post-1993 Events</i> .....	32
3.4.2 <i>North American Temperature</i> .....	39
3.4.3 <i>Comparison of 1950-92 North American Temperature Composites to Post 1993 Events</i> .....	51
3.4.4 <i>Event Consistency</i> .....	56
3.5 SUMMARY.....	60

<b>CHAPTER 4 ASSOCIATIONS BETWEEN TROPICAL PACIFIC SSTA EVENTS AND DISTRIBUTIONS OF DAILY WEATHER EVENTS OVER NORTH AMERICA.....</b>	<b>63</b>
4.1 PREAMBLE .....	63
4.2 DATA AND METHODOLOGY .....	64
4.3 PRECIPITATION RESULTS .....	65
4.3.1 <i>Associations with Eastern Tropical Pacific SSTA Events.....</i>	<i>65</i>
4.3.2 <i>Associations with Central Tropical Pacific SSTA Events Only.....</i>	<i>106</i>
4.4 TEMPERATURE RESULTS.....	109
4.4.1 <i>Associations with Eastern Tropical Pacific SSTA Events.....</i>	<i>109</i>
4.5 SUMMARY OF DAILY DISTRIBUTION FINDINGS AND FOCUS FOR CHAPTER 5 .....	129
<b>CHAPTER 5 LARGER-SCALE ATMOSPHERIC PHENOMENA ASSOCIATED WITH SHIFTS IN NORTH AMERICAN DAILY WEATHER EVENT DISTRIBUTIONS DURING WARM TROPICAL PACIFIC SSTA EVENTS.....</b>	<b>137</b>
5.1 PREAMBLE .....	137
5.2 DATA	138
5.2.1 <i>NCEP/NCAR Reanalysis Data.....</i>	<i>138</i>
5.2.2 <i>Cyclone Tracks.....</i>	<i>139</i>
5.3 METHODOLOGY .....	140
5.3.1 <i>Large-Scale Atmospheric Patterns Associated with warm TP SSTAs.....</i>	<i>140</i>
5.3.2 <i>Intra-Month Characteristics of Anomalous North American Precipitation and Temperature.....</i>	<i>140</i>
5.3.3 <i>Antecedent Atmospheric Conditions for Target Daily Periods .....</i>	<i>141</i>
5.4 LARGE-SCALE ATMOSPHERIC FEATURES LINKED TO WARM TP SSTA EVENTS .	141
5.4.1 <i>Seasonal and Monthly Composites .....</i>	<i>141</i>
5.4.2 <i>Intra-month characteristics .....</i>	<i>146</i>
5.4.3 <i>Individual event differences .....</i>	<i>149</i>
5.5 CHARACTERISTICS OF ANOMALOUS NORTH AMERICA WEATHER ASSOCIATED WITH WARM TROPICAL PACIFIC SSTA EVENTS .....	156
5.5.1 <i>Northern U.S. Great Plains and Southern Canadian Prairies – Warm and Dry (November-February).....</i>	<i>157</i>
5.5.2 <i>Dry Eastern Midwest and Wet-Cool South (January-March).....</i>	<i>165</i>
5.5.3 <i>Warm Eastern U.S. (December).....</i>	<i>169</i>
5.5.4 <i>Warm Daily Minimum Temperatures in Central U.S. Plains (February) and Northern/Central Plains to Ohio Valley (March).....</i>	<i>172</i>
5.6 SUMMARY.....	174
<b>CHAPTER 6 SUMMARY AND CONCLUSIONS .....</b>	<b>178</b>
6.1 PREAMBLE .....	178
6.2 ASSOCIATIONS BETWEEN TROPICAL PACIFIC SSTAs AND MONTHLY AVERAGES OF DAILY MAXIMUM AND MINIMUM TEMPERATURES .....	178

6.3	DAILY DISTRIBUTION PROPERTIES OF MONTHLY PRECIPITATION AND TEMPERATURE TELECONNECTION RELATIONSHIPS.....	180
6.4	DURATION OF DAILY PRECIPITATION AND TEMPERATURE ANOMALY PERIODS AND ANTECEDENT ATMOSPHERIC CONDITIONS .....	182
6.5	INFLUENCE OF OTHER ATMOSPHERIC MODES ON TELECONNECTIONS FROM TROPICAL PACIFIC TO NORTH AMERICA .....	184
6.6	SYNOPSIS OF ASSOCIATION BETWEEN TROPICAL PACIFIC SSTAS AND NORTH AMERICAN PRECIPITATION AND TEMPERATURE .....	186
6.7	COMMENTS ON CONTEXT PROVIDED BY KEY ATMOSPHERIC FLOW STUDIES .....	187
6.8	FRAMEWORK FOR FUTURE MODELING INVESTIGATIONS .....	189
	<b>REFERENCES .....</b>	<b>193</b>

## LIST OF ILLUSTRATIONS

Fig. 2.1: Region of the tropical Pacific for which sea surface temperature anomaly (SSTA) data were analyzed in order to define SSTA events.....	16
Fig. 2.2: Spatial loading patterns for SSTA Principal Components described in Section 2.2.2.....	18
Fig. 2.3: Principal Component score time series for SSTA modes associated with the spatial loading patterns in Fig. 2.2. ....	19
Fig. 2.4: Correlation between December-January-February Arctic Oscillation index of Thompson and Wallace (2000) and seasonal mean surface temperature. (Calculations were performed using the NCEP/NCAR Reanalysis data and analysis tools available from the NOAA/ESRL Physical Science Division, Boulder Colorado from their web site <a href="http://www.cdc.noaa.gov/">http://www.cdc.noaa.gov/</a> ).....	22
Fig. 2.5: Composite December-February 500mb geopotential height anomalies (gpm, from 1968-1996 climatology) for (a) 1959-60, 1962-63, 1965-66, and 1968-69 and (b) 1969-70, 1976-77, 1978-79, 1984-85, 1985-86, and 2000-01. (Calculations were performed using the NCEP/NCAR Reanalysis data and analysis tools available from the NOAA/ESRL Physical Science Division, Boulder Colorado from their web site <a href="http://www.cdc.noaa.gov/">http://www.cdc.noaa.gov/</a> ).....	24
Fig. 2.6: Time series of monthly PDO index from 1900 through July 2002. Data have been standardized by month over the entire data range. Further details are given in Section 2.3.2. Index data were obtained from Mantua (2005).....	25
Fig. 2.7: Correlation between December-January-February seasonal average of index in Fig. 2.6 and seasonal mean (a) sea-level pressure over the Northern Hemisphere, (b) surface precipitation rate, and (c) surface temperature. (d) As in (c) but for January only. (Calculations were performed using the NCEP/NCAR Reanalysis data and analysis tools available from the NOAA/ESRL Physical Science Division, Boulder Colorado from their web site <a href="http://www.cdc.noaa.gov/">http://www.cdc.noaa.gov/</a> ).....	26
Fig. 3.1: Composite monthly precipitation anomalies (mm) for warm (left column) and cold (right column) SSTA VPC1 events during November-March for 1950-92. Constituent years of each composite are listed on right side of each panel. Maps on side of each panel delineate areas for which regional statistical significance was computed and presented, as in Table 3.1 below. (Taken from Montroy et al. 1998; their Fig. 4).....	33
Fig. 3.2: Observed precipitation anomalies (mm) for individual months for November 1992-March 1993.....	34
Fig. 3.3: As in Fig. 3.2 but for November 1994-March 1995.....	36

Fig. 3.4: As in Fig. 3.2 but for November 1997-March 1998.....	37
Fig. 3.5: As in Fig. 3.2 but for November 1999-March 2000.....	38
Fig. 3.6: Composite monthly averaged daily temperature anomalies (°C) for warm SSTA VPC1 events during 1950-92 for December-April. Color shading follows scale at right. Left (right) column gives anomalies in daily maximum (minimum) temperature. An “X” is plotted at stations where the composite value is significantly different from zero at the 90% level. Field significances (FS) and explained variances (EV) appear at the bottom of each panel in %, and constituent years of composites are listed at right of each panel. Small maps at sides locate numbered regions in Table 3.3. ....	42
Fig. 3.7: As in Fig. 3.6, but for cold SSTA VPC1 events. Small maps at sides locate numbered regions in Table 3.4.....	45
Fig. 3.8: As in Fig. 3.6 but for October-November for warm SSTA VPC1 events. Numbers in side maps locate regions numbered in Table 3.3. ....	49
Fig. 3.9: As in Fig. 3.8 but for cold SSTA VPC1 events. Numbers in side maps locate regions numbered in Table 3.4. ....	50
Fig. 3.10: Observed mean daily maximum (left column) and minimum (right column) temperature anomalies (°C) for individual months for November 1992 through March 1993.....	52
Fig. 3.11: As in Fig. 3.10 but for November 1994 through March 1995.....	53
Fig. 3.12: As in Fig. 3.10 but for November 1997 through March 1998.....	54
Fig. 3.13: As in Fig. 3.10 but for November 1999 through March 2000.....	55
Fig. 3.14: Average of Arctic Oscillation index (standardized units, as defined in Section 2.3.1) for December through March, for 1958-2001. Indicated year corresponds to the January-March of the constituent months.....	57
Fig. 4.1: (a) Actual Event Frequency from Table 4.1 for January-March in south Florida region demarcated in inset map for the indicated range (mm d <sup>-1</sup> ) during warm, neutral, and cold SSTA VPC1 events as defined in Section 2.2. (b) Amount of precipitation accumulated during January-March (mm d <sup>-1</sup> ) from daily precipitation amounts in the indicated size range. Sum over all precipitation size ranges for each SSTA event type equals corresponding January-March total in top section of Table 4.1. ....	70
Fig. 4.2: (a) As in Fig. 4.1a, but for far southeast U.S./central Florida region demarcated in thumbnail map. (b) As in Fig. 4.1b, but for far southeast U.S./central Florida region. (c) As in (a) but for North-South Carolina region. (d) As in (b) but for North-South Carolina region. ....	73

Fig. 4.3: (a) Regionally averaged station precipitation anomalies ( $\text{mm d}^{-1}$ ) from 1950-92 mean for January, February, and March and seasonal total (January-March) during warm SSTA VPC1 events for far southeast U.S./central Florida region as delineated in Table 4.2. (b) As in (a) but for cold TP SSTA events. ....	76
Fig. 4.4: As in Fig. 4.1 but for November precipitation in (a)-(b) Florida, (c)-(d) North-South Carolina, and (e)-(f) the Gulf Coast regions. ....	79
Fig. 4.5: Difference in total November precipitation received in Table 4.8 during warm and cold TP SSTA events compared to neutral TP SSTA events by precipitation category for (a) North-South Carolina region in Fig. 4.4c and (b) Gulf Coast region Fig. 4.4e.....	82
Fig. 4.6: As in Fig. 4.4, but for Oklahoma-Illinois track (a)-(b) and Texas (c)-(d) for November.....	82
Fig. 4.7: Regionally averaged station precipitation anomalies ( $\text{mm d}^{-1}$ ) from 1950-92 mean for November during warm SSTA VPC1 events for regions delineated in Table 4.7. ....	83
Fig. 4.8: As in Fig. 4.7, but for cold TP SSTA events.....	84
Fig. 4.9: As in Fig. 4.1 but for January-February precipitation in (a)-(b) southwestern Appalachian Mountains and (c)-(d) eastern Midwest region.....	87
Fig. 4.10: (a) As in Fig. 2.1a but for January-February precipitation for southwestern Appalachian Mountains as delineated in Table 4.9. (b) As in (a) but for eastern Midwest region in Table 4.10. ....	89
Fig. 4.11: As in Fig. 4.10 but for cold SSTA VPC1 events.....	90
Fig. 4.12: As in Fig. 4.1 but for November-January precipitation in eastern Montana (a)-(b) and southern Alberta-Manitoba (c)-(d).....	94
Fig. 4.13: As in Fig. 4.5, but for total November-January precipitation for (a) eastern Montana region in Fig. 4.12a and (b) southern Alberta-Manitoba region in Fig. 4.12c.....	95
Fig. 4.14: (a) As in Fig. 2.1a but for November-January precipitation for eastern Montana region as delineated in Table 4.13. Indicated year corresponds to January of November-January season. (b) As in (a), but for November-January precipitation for southern Alberta-Manitoba region delineated in Table 4.14. (c) As in (b) but for cold SSTA events.....	97
Fig. 4.15: (a) As in Fig. 4.1a but for January precipitation in north Texas region (upper right) delineated in Table 4.17. (b) As in Fig. 4.2b, but for January precipitation in north Texas region in (a). (c)-(d) As in (a)-(b) but for March	

precipitation in Oklahoma-Kansas region (upper right) in Table 4.17. (e)-(f) As in (c)-(d) but for northern Great Plains region (upper right).....	100
Fig. 4.16: Average January precipitation anomaly from 1950-92 mean in $\text{mm d}^{-1}$ for north Texas region delineated in Table 4.17.....	102
Fig. 4.17: Average March precipitation anomaly from 1950-92 mean in $\text{mm d}^{-1}$ for Oklahoma-Kansas and Northern Great Plains regions delineated in Table 4.17....	103
Fig. 4.18: (a) As in Fig. 4.1a but for December precipitation in the east Texas-Louisiana region (upper right). (b) As in Fig. 4.1b, but for December precipitation in east Texas-Louisiana region. ....	104
Fig. 4.19: Average December precipitation anomaly from 1950-92 mean in $\text{mm d}^{-1}$ for east Texas-Louisiana region delineated in Table 4.17. ....	105
Fig. 4.20: (a) As in Fig. 4.1a but for April precipitation in mid-Atlantic region delineated in Table 4.17 during SSTA UPC1 events. (b) As in Fig. 4.1b, but for April precipitation in mid-Atlantic region during SSTA UPC1 events.....	107
Fig. 4.21: Average April precipitation anomaly from 1950-92 mean in $\text{mm d}^{-1}$ for mid-Atlantic region delineated in Table 4.19. ....	108
Fig. 4.22: (a) Frequency (indicated by solid line) of daily maximum temperatures ( $^{\circ}\text{C}$ ) during neutral SSTA VPC1 events in December-February for North Dakota region delineated in inset map, and associated anomaly (indicated by bars) during warm and cold SSTA VPC1 events. (b) As in (a) but for daily minimum temperatures. Category containing seasonal 1950-2000 mean daily temperature extreme ( $^{\circ}\text{C}$ ) is indicated by solid gray line. Dashed gray lines provide approximate indication of seasonal mean $\pm$ one standard deviation.....	110
Fig. 4.23: As in Fig. 4.22 but for western Pennsylvania during December.....	112
Fig. 4.24: As in Fig. 4.22 but for southern Quebec during February-April.....	113
Fig. 4.25: As in Fig. 4.22 but for southern Manitoba during March-April.....	113
Fig. 4.26: Observed seasonal or monthly average daily maximum (solid bar) and minimum (open bar) temperature anomalies (in $^{\circ}\text{C}$ ) in years classified as warm SSTA VPC1 events for (a) North Dakota region (Fig. 4.22) in December-February, and (b) western Pennsylvania region (Fig. 4.23) in December. ....	114
Fig. 4.27: As in Fig. 4.26 but for cold SSTA VPC1 events for (a) southern Quebec region (Fig. 4.24) during February-April, and (b) southern Manitoba region (Fig. 4.25) during March-April.....	115
Fig. 4.28: As in Fig. 4.22 but for southeast Texas region during December-February.	117

Fig. 4.29: As in Fig. 4.22 but for western Kansas-Oklahoma region during December. ....	117
Fig. 4.30: As in Fig. 4.22 but for northern Georgia during January. ....	119
Fig. 4.31: As in Fig. 4.22 but for southeast Texas during January. ....	119
Fig. 4.32: As in Fig. 4.22 but for eastern Colorado-western Kansas during February. .	120
Fig. 4.33: As in Fig. 4.22 but for western Kansas-Oklahoma during February-March. ....	121
Fig. 4.34: As in Fig. 4.26 but for (a) northern Georgia region (Fig. 4.30) in January, (b) southeast Texas region (Fig. 4.31) in January, and (c) eastern Colorado/western Kansas region in February (Fig. 4.32).....	123
Fig. 4.35: As in Fig. 4.27 but for (a) southeast Texas region (Fig. 4.28) during December-February, (b) western Kansas/Oklahoma region (Fig. 4.29) during December, and (c) western Kansas/Oklahoma region (Fig. 4.33) during February-March. ....	124
Fig. 4.36: As in Fig. 4.22 but for southern Minnesota region during October-November.....	126
Fig. 4.37: As in Fig. 4.22 but for eastern Nebraska region during October-November. ....	126
Fig. 4.38: As in Fig. 4.22 but for north Texas region during October-November.....	128
Fig. 4.39: As in Fig. 4.26 but during warm October-November SSTA VPC1 events for (a) southern Minnesota region (Fig. 4.36), (b) eastern Nebraska region (Fig. 4.37), and (c) north Texas region (Fig. 4.38). (d) As in (c) but for cold SSTA events.....	130
Fig. 5.1: (a) Composite SST anomalies (contoured, °C) and sea-surface temperatures (shaded, °C, bottom scale) during December-February for the warm SSTA VPC1 events listed in Table 2.3. (b) Climatological average sea-surface temperatures (shaded, °C, bottom scale) for December-February based on 1950-1999.....	142
Fig. 5.2: Composite December-February wind anomalies ( $m s^{-1}$ ) for warm SSTA events (in Table 2.3) for (a) 200mb zonal wind and (b) 200mb meridional wind ( $m s^{-1}$ ). Composite December-February wind anomalies of (c) vertical motion ( $mb s^{-1}$ ) and (d) meridional wind ( $m s^{-1}$ ) for cross section from 1000mb to 100mb averaged over 175°W to 155°W.....	143
Fig. 5.3: Composite December-February (a) 500mb geopotential heights (contours, gpm) and anomalies (shaded, gpm, bottom scale) and (b) sea level pressure (contours, mb) and anomalies (shaded, mb, bottom scale) during warm SSTA VPC1 events.....	144

Fig. 5.4: As in Fig. 5.2a but for individual monthly composite 200mb zonal wind anomalies ( $\text{m s}^{-1}$ ) for November through March. ....	145
Fig. 5.5: Observed 500mb heights (light green lines, gpm), anomalies (black lines, gpm), average vorticity (shaded, in $10^{-5} \text{ s}^{-1}$ ), and position of local maximum negative daily 500mb geopotential height anomalies (denoted by “L”) of at least 60m magnitude during (a) December-February 1957-58 and (b) December-February 1982-83. Size of letter “L” for plotted centers is proportional to size of 500mb height anomaly. Dashed barbell lines locate time-longitude cross-sections in Fig. 5.6. ....	148
Fig. 5.6: Time-longitude pattern of daily mean 500mb height anomalies (gpm, averaged from $45^{\circ}\text{N}$ to $55^{\circ}\text{N}$ ) from $140^{\circ}\text{E}$ to $40^{\circ}\text{W}$ during December-February (a) 1957-1958 and (b) 1982-83. ....	149
Fig. 5.7: (a) Observed December-February 500mb heights (gpm) averaged from $45^{\circ}\text{N}$ to $55^{\circ}\text{N}$ for warm TP SSTA events in Table 2.3 compared to average for 1968-96 (thick solid line). (b) Average SSTs ( $^{\circ}\text{C}$ ) compared to average for 1979-95 (thick solid line) along the equator from $165^{\circ}\text{W}$ to $140^{\circ}\text{W}$ for warm SSTA events in Table 2.3. ....	151
Fig. 5.8: As in Fig. 5.5 but for warm TP SSTA event in 1965-66. ....	152
Fig. 5.9: As in Fig. 5.8 but for positive 500mb height anomaly centers plotted with an “H”. ....	152
Fig. 5.10: Observed 500mb geopotential height (solid lines) and anomalies (shading) in geopotential meters for (a) 1 December 1972 and (b) 11 December 1972. Shading is given by indicated legend. ....	154
Fig. 5.11: As in Fig. 5.10 but for average from 17 December 1972 to 31 January 1973. ....	155
Fig. 5.12: As in Fig. 5.10 but for average from 1-28 February 1973. ....	155
Fig. 5.13: As in Fig. 5.10 but for average from 1 December 1992 to 28 February 1993. ....	156
Fig. 5.14: Daily temperature anomalies ( $^{\circ}\text{C}$ , based on 1950-2000 average) for indicated stations in the northern U.S. Great Plains. Each row in the table corresponds to one day from November through March. Order of stations in column is Station 1 Tmax, Station 1 Tmin, Station 2 Tmax, Station 2 Tmin, etc., with station numbers according to number in inset map. Data are presented for November-March periods for warm SSTA events in Table 5.1 plus two other events (1976-77 and 1987-88) for comparison. Year indicated in column headings corresponds to January-March. Temperature ( $^{\circ}\text{C}$ ) shading is according to given legend. ....	157

- Fig. 5.15: Analysis of length of positive TAPs for average daily maximum temperatures in the North Dakota region (as delineated in Table 4.21) during December-February. A positive TAP is a period with consecutive daily maximum temperature anomalies (based on 1950-2000 average) of at least 3°C. Histogram bars: Average frequency (left axis) of positive TAPs with the duration indicated on abscissa during the warm SSTA events in Table 5.1 (dark bars) and all other years (lighter bars). Plotted diamonds: Percentage of time (right axis) that a TAP of that duration occurred during warm SSTA events. (For example, 100% = All TAPs with that length occurred during a warm TP SSTA event.) Solid thin line: Percentage (right axis) of years that are warm TP SSTA events (8 events divided by 52 periods = 18%). ..... 159
- Fig. 5.16: Time evolution composites (TECs) (as defined in Section 5.3.3) of 500mb geopotential height anomalies (gpm) for days preceding onset of warm temperatures in North Dakota (as delineated in Table 4.21) during December-February of warm TP SSTA composite. TECs correspond to (a) Day (0), the day that the target anomaly period (TAP) began, (b) Day (-2), two days before TAP beginning, (c) Day (-4), (d) Day (-6), (e) Day (-8), and (f) Day (-10). ..... 161
- Fig. 5.17: As in Fig. 5.16 but where Day (0) corresponds to the end of the Target Anomaly Period (TAP). ..... 162
- Fig. 5.18: Tracks of extratropical cyclones (in SLP) during December-February for selected warm eastern TP SSTA events as recorded in the NASA Atlas of Extratropical Storm Tracks (NASA 2005). Tracks given for December-February of (a) 1982-83, (b) 1986-87, (c) 1991-92, and (d) 1997-98. Small numbers represent the day of the season that particular cyclone was observed. .... 164
- Fig. 5.19: As in Fig. 5.18 but for (a) 1965-66 and (b) 1992-93. .... 164
- Fig. 5.20: As in Fig. 5.15, but for length of wet events over all stations in Georgia (delineated in inset map, upper right) during January-March. A wet event was defined as at least one day with at least 1 mm of precipitation. .... 165
- Fig. 5.21: As in Fig. 5.20, but for periods of zero precipitation for stations in the eastern Midwest (as delineated in Table 4.10) during January-February. .... 166
- Fig. 5.22: As in Fig. 5.15, but for maximum temperature averaged over all stations in Alabama-Georgia (delineated in inset map, upper right) during January. .... 166
- Fig. 5.23: As in Fig. 5.14, but for daily precipitation totals (mm) from November through March observed at stations from the northern U.S. Plains to Florida. Inset map gives order of stations within each SSTA event column. Small letters at foot of column further indexes stations as Northern Plains (“NPL”, Columns 1-4), Midwest (“M”, Columns 5-7), and Florida (“FL”, Columns 8-10). Year indicated in column headings corresponds to January-March. Precipitation shading (mm) is according to given legend. .... 167

Fig. 5.24: As in Fig. 5.16 but for precipitation in Georgia (inset map in Fig. 5.20) for January-February-March.....	168
Fig. 5.25: As in Fig. 5.16 but for precipitation in southeast Texas (see inset map #6 in Fig. 3.6) for November- February.....	169
Fig. 5.26: As in Fig. 5.14 but for December daily maximum and minimum temperatures (°C) for stations in Pennsylvania indicated in inset map. Order of stations in column is Station 1 Tmax, Station 1 Tmin, Station 2 Tmax, Station 2 Tmin, etc. Column heading corresponds to year of following January (in order to facilitate comparison to Fig. 5.14). .....	170
Fig. 5.27: As in Fig. 5.15 but for positive TAPs in western Pennsylvania region as delineated in Table 4.22. ....	170
Fig. 5.28: As in Fig. 5.16 but for positive TAPs in western Pennsylvania.....	171
Fig. 5.29: As in Fig. 5.14 but for February daily minimum temperatures (°C) for stations in eastern Colorado/western Kansas indicated in inset map. Order of stations in column is Station 1 Tmin, Station 2 Tmin, Station 3 Tmin, etc.....	172
Fig. 5.30: As in Fig. 5.15 but for negative TAPs in eastern Colorado/western Kansas region as delineated in Table 4.29. ....	173
Fig. 5.31: As in Fig. 5.16 but for negative TAPs in eastern Colorado/western Kansas region during all years except warm SSTA events. ....	174
Fig. 5.32: Illustration of the role of the positive phase of the Arctic Oscillation on the 500mb geopotential height patterns during warm TP SSTA events. Black lines provide position of negative and positive anomaly centers during warm TP SSTA events and gray lines provide displaced positions during positive Arctic Oscillation phases. ....	175
Fig. 5.33: Illustration of the role of the negative phase of the Arctic Oscillation on the 500mb geopotential height patterns during warm TP SSTA events. Black lines provide position of negative and positive anomaly centers during warm TP SSTA events and gray lines provide displaced positions during negative Arctic Oscillation phases. ....	176
Fig. 6.1: Illustration of key atmospheric processes and North American precipitation and temperature associations during a typical warm TP SSTA event. ....	183
Fig. 6.2: Composite December-February SSTAs (°C) during 1982-83, 1986-87, 1991-92, 1992-93, and 1997-98 using optimal interpolation SST data of Reynolds et al. (2002). ....	188
Fig. 6.3: Yearly North Pacific Index provided by the Climate Analysis Section, NCAR, Boulder, USA. Index represents the area-weighted sea level pressure	

from 30-65°N latitude and 160°E-140°W. Method of calculation is as in  
Trenberth and Hurrell (1994). Figure reproduced from Hurrell (2006). Smooth  
trend line is obtained using 11-year running mean. .... 190

## LIST OF TABLES

<p>Table 2.1: Tropical Pacific SSTA events during 1993-2000 examined in this study. Dates in parentheses are listed when the event based on the SSTA PC in the second column ended in a different month. ....</p>	21
<p>Table 2.2: Individual monthly classification of November-March 1950-2000 with respect to all atmospheric and oceanic phenomena discussed in previous sections of this Chapter, abbreviated as defined there. The year in the left-hand column refers to the year of the January-March. “H” indicates a high-index (<math>&gt; +0.97\sigma</math>) phase of that index, and “L” indicates a low-index (<math>&lt; -0.97\sigma</math>) phase. If neither the high nor the low index criteria are met, the sign of the index is plotted with a plus or minus symbol or with a “0”. ....</p>	28
<p>Table 2.3: Primary warm SSTA events for which physical/dynamical aspects of the teleconnection linkage chain from the tropical Pacific to North America will be documented in Chapter 5. ....</p>	29
<p>Table 3.1: Statistics for monthly average precipitation anomalies over selected regions in composites based on SSTA VPC1, as presented in MRL98 and present Fig. 3.1. Region numbers pertain to shaded areas in small maps along sides of present Fig. 3.1. For warm and cold events, “CA” denotes the composite regional precipitation anomaly (mm), “FR” the fraction of composite members for which the regional mean anomaly has the same sign as the overall composite anomaly (CA), and “SIG” is the regional significance level. Boldface entries have regional significance above 95%. (Taken from Montroy et al. 1998; their Table 1).....</p>	34
<p>Table 3.2: Summary of regions with monthly anomalies of daily maximum (Tmax) and minimum (Tmin) temperatures significantly associated with TP SSTA events. ....</p>	40
<p>Table 3.3: Statistics for monthly averaged daily maximum (Tmax) and minimum (Tmin) temperature anomalies over selected regions in composites based on warm SSTA VPC1 events presented in Fig. 3.6. Numbered regions are delineated in small side maps in Figs. 3.6 (1-13) and 3.8 (14-17). For maximum and minimum temperature, “CA” denotes the composite regional temperature anomaly (<math>^{\circ}\text{C}</math>), “FR” the fraction of composite members for which the regional mean anomaly has the same sign as the overall composite anomaly (CA), and “SIG” is the regional significance level. Boldface entries have regional significance above 90%. ....</p>	43
<p>Table 3.4: As in Table 3.3, but for cold SSTA VPC1 events. Numbered regions are delineated in the small side maps in Figs. 3.7 (1-8) and 3.9 (9-12).....</p>	46
<p>Table 3.5: Regional averages of station precipitation anomalies (mm) from indicated 1950-92 average for individual months from January through March and</p>	

seasonal total (JFM) during warm and cold SSTA VPC1 events. Region definitions are provided by small map. Bold (italic) font indicates totals for which the anomaly is greater than +25 mm (less than -25 mm). Second and third columns from left also give JFM average Arctic Oscillation and Pacific Decadal Oscillation index values as defined in Section 2.3. Center highlighted row provides average JFM precipitation totals for 1950-92. ....	57
Table 3.6: As in Table 3.5 but for individual regions during November. Region definitions are provided by small maps at right. ....	58
Table 3.7: As in Table 3.5 but for eastern Montana and Southern Alberta-Manitoba region during November-December-January. Note that year refers to the last month (January). For example, the line for 1958 includes data from November 1957, December 1957, and January 1958. ....	59
Table 3.8: Observed monthly composite anomaly for indicated regions in Fig. 3.6 (indexed by Table 3.3) during the individual constituent years when warm TP SSTAs were present, as defined in Section 2.2. Anomalies for years that did not meet the threshold temperature criteria for warm events are grayed out. Shading and bold font are according to given legend. ....	61
Table 4.1: Daily January-March precipitation event statistics for south Florida region (shown in map in upper left corner) during TP SSTA event categories defined in Section 2.2.3 and used to create the 1950-1992 warm and cold composites in Fig. 3.1 and to select warm and cold event years during 1993-2000 (Section 3.4.1). Neutral SSTA events are all years not defined as warm or cold events. Top section (“Aggregate Statistics”): Monthly or seasonal composite precipitation total, and anomaly from 1950-92 mean (“Anom,” comparable to composite anomaly on Fig. 3.1, but including post-1992 events), in mm d <sup>-1</sup> . Second section (“Relative Event Frequency”): Total number of daily (non-zero) precipitation events, percentage of events that fall into the indicated categories, and average daily precipitation event size (mm d <sup>-1</sup> ). Third section (“Quartile”): Quartile statistics on the daily non-zero precipitation events. Fourth section (“Actual Event Frequency”): Average number of days with non-zero precipitation totals that occurred in the indicated month/season during composites of indicated type of SSTA event. Non-zero Actual Event Frequency less than 0.1 indicated by “< 0.1”. ....	67
Table 4.2: As in Table 4.1, but for far southeast U.S./central Florida region shown in map in upper left corner. ....	68
Table 4.3: As in Table 4.1 but for North-South Carolina region shown in upper left corner. ....	69
Table 4.4: Top: Total seasonal or monthly accumulated precipitation (mm d <sup>-1</sup> ) by precipitation category for south Florida region delineated in top left hand corner of Table 4.1 (as in Fig. 4.1b). Rows of precipitation categories represent daily	

totals. Columns are presented in  $\text{mm d}^{-1}$  averaged over indicated season or month. Last row (“TOTAL”) matches corresponding value in top section of Table 4.1. Bottom: Percent contribution to monthly or seasonal composite precipitation total. Non-zero percent contributions less than 1% are indicated by “< 1%”. Column headings correspond to TP SSTA event type, as in Table 4.1..... 72

Table 4.5: As in Table 4.4 but for far southeast U.S./central Florida region delineated in top left hand corner of Table 4.2.....	74
Table 4.6: As in Table 4.4 but for North-South Carolina delineated in top left hand corner of Table 4.3.....	75
Table 4.7: As in Table 4.1 but for individual regions (delineated in map in top row) during November. ....	78
Table 4.8: As in Table 4.4 but for individual regions during November as delineated in Table 4.7. ....	81
Table 4.9: As in Table 4.1 but for southwestern Appalachian mountains (upper left) during January-February. ....	85
Table 4.10: As in Table 4.1 but for eastern Midwest (upper left) during January-February. ....	86
Table 4.11: As in Table 4.4 but for southwestern Appalachian mountains (as delineated in upper left corner of Table 4.9) during January-February. ....	87
Table 4.12: As in Table 4.4 but for eastern Midwest (as delineated in upper left corner of Table 4.10) during January-February. ....	88
Table 4.13: As in Table 4.1 but for eastern Montana region (upper left) during November-December-January. ....	92
Table 4.14: As in Table 4.1 but for southern Alberta-Manitoba region (upper left) during November-December-January.....	93
Table 4.15: As in Table 4.4 but for eastern Montana region (as delineated in upper left corner of Table 4.13) during November-December-January. ....	95
Table 4.16: As in Table 4.4 but for southern Alberta-Manitoba region (as delineated in upper left corner of Table 4.14) during November-December-January. ....	96
Table 4.17: As in Table 4.1 but for individual regions in the Central and Southern U.S. Great Plains during January and March and eastern Texas-Louisiana in December. ....	99

Table 4.18: As in Table 4.4 but for individual regions (delineated in Table 4.17) in the Central and Southern Plains during January and March and in eastern Texas-Louisiana in December. ....	101
Table 4.19: As in Table 4.1 but for mid-Atlantic region (upper left) during April SSTA UPC1 events.....	106
Table 4.20: As in Table 4.4 but for mid-Atlantic region delineated in Table 4.19 during April SSTA UPC1 events.....	108
Table 4.21: For North Dakota region (delineated in upper right inset map in Fig. 4.22a), cumulative sum of frequency anomaly (compared to neutral SSTA events; displayed in Fig. 4.22) of daily maximum (Tmax, °C) and daily minimum (Tmin, °C) temperatures (in days) during December-February warm and cold SSTA VPC1 events. Sums are computed for daily extremes below seasonal 1950-2000 mean minus one standard deviation (“< Mean-1σ”), below seasonal mean (“< Mean”), above seasonal mean (“> Mean”), and above the seasonal mean + one standard deviation (“> Mean+1σ”). Seasonal mean and ±1σ range are indicated in Fig. 4.22. ....	111
Table 4.22: As in Table 4.21, but for western Pennsylvania region during December (Fig. 4.23).....	112
Table 4.23: As in Table 4.21, but for southern Quebec region during February-April (Fig. 4.24).....	114
Table 4.24: As in Table 4.21, but for southern Manitoba region during March-April (Fig. 4.25).....	114
Table 4.25: As in Table 4.21, but for southeast Texas region during December-February (Fig. 4.28). ....	118
Table 4.26: As in Table 4.21, but for western Kansas-Oklahoma region during December (Fig. 4.29). ....	118
Table 4.27: As in Table 4.21, but for southeast Texas region during January (Fig. 4.31).....	119
Table 4.28: As in Table 4.21, but for northern Georgia region during January (Fig. 4.30).....	119
Table 4.29: As in Table 4.21, but for eastern Colorado-western Kansas region during February (Fig. 4.32). ....	120
Table 4.30: As in Table 4.21, but for western Kansas-Oklahoma region during February-March (Fig. 4.33). ....	121

Table 4.31: As in Table 4.21, but for southern Minnesota region during October-November (Fig. 4.36).....	127
Table 4.32: As in Table 4.21, but for eastern Nebraska region during October-November (Fig. 4.37).....	127
Table 4.33: As in Table 4.21, but for north Texas region during October-November (Fig. 4.38).....	128
Table 4.34: Summary of daily precipitation event characteristics associated with TP SSTA events.....	132
Table 4.35: Summary of daily maximum and minimum event coherencies with TP SSTA events.....	134
Table 4.36: Key regions and associated precipitation/temperature characteristics used to define target anomaly periods and focus examination of antecedent atmospheric conditions. ....	136
Table 5.1: As in Table 2.3, primary SSTA events for which physical/dynamical aspects of the teleconnection linkage chain from the tropical Pacific to North America will be documented. ....	138

## ABSTRACT

Many authors have statistically documented the seasonal precipitation and temperature patterns linked to tropical Pacific (TP) SST anomaly (SSTA) events. Only recently have changes in the daily distributions of observed surface precipitation and temperature begun to be analyzed in this context. But no extensive linkage of TP SSTs with daily North American weather observations has been established.

The present research contributes to the need for such a linkage using a comprehensive set of analyses relating monthly composite patterns to daily atmospheric flow. First, the approach used in an earlier analysis of precipitation data is applied to monthly averages of daily maximum/minimum temperatures during warm and cold TP SSTA events, providing a set of regions with notable precipitation or temperature anomalies during warm and cold TP SSTA events. The associated series of daily precipitation and temperature anomalies during warm TP SSTA events are examined to document the change in the frequency of daily observations, the duration of consecutive days of daily anomalies, and the antecedent North Pacific-North American atmospheric conditions. Additionally, for all results, the modulation of the TP SSTA-North American teleconnections by other atmospheric modes is examined.

The monthly composite temperature analyses demonstrated that, similar to the earlier precipitation analysis, the patterns of monthly average daily temperature extremes yielded previously unknown regions associated with TP SSTAs. In particular, new regions found to be characterized by strong temperature anomalies included the eastern U.S. (warm, December), the central U.S. Great Plains (warm, February), and the U.S. Great Plains (cool, October-November) during warm TP SSTA events, and south central Canada (March-April) and the southern U.S. Great Plains (warm, December-April) during cold TP SSTA events. Additionally, the observed monthly precipitation/temperature anomalies during SSTA events after 1992 exhibited strong similarities to the features common to the 1950-92 events.

The analysis of North American daily precipitation and temperature distributions during warm and cold TP SSTA events identified unique changes. In the southeastern

U.S., increased precipitation during January-March warm TP SSTA events was generally linked to more frequent daily precipitation totals above 10 mm, while the increased November precipitation in similar regions resulted from increased daily precipitation totals of all amounts. Further, below average January precipitation in the southwestern Appalachian Mountain region during warm TP SSTA events was associated with the lack of occurrence of very large (>25 mm) daily precipitation totals. During cold TP SSTA events, below average November precipitation principally was associated with reduced frequency of larger (>10 mm) precipitation events. Similarly unique relationships were identified in monthly average daily temperature extremes. Cooler than average February daily minimum temperatures in the central U.S. Great Plains mainly arose from the lack of occurrence of observations well below the monthly mean. Also, cooler than average daily maximum temperatures in the southern U.S. were associated principally with relatively few observations well above the monthly mean. For many other locations, the shifts in the daily maximum and minimum temperature distributions were quantified.

The surface climate anomalies with the longest duration are the temperature anomalies in the northern U.S. Great Plains and south-central Canada during warm TP SSTA events. During warm TP SSTA events, these regions observed noticeably warmer than average temperatures that last for as many as 14 consecutive days during December-March. Other regions exhibited anomalies with shorter durations. For all regions, the key feature was the location of positive geopotential height anomalies located over North America and the placement of negative geopotential height anomalies in the north Pacific Ocean. This anomalous upper tropospheric longwave pattern develops as a cyclonic system moves off northeast Asia into the north Pacific Ocean to the region of favorable development north of the TP SSTAs and remains there until dissipating before another system moves off northeast Asia.

The Arctic Oscillation (AO) was shown to materially modify the teleconnection between the TP and North American climate in both its positive and negative phases. Particularly, the AO modulates the placement of the negative geopotential height anomalies in the north Pacific Ocean and the positive geopotential height anomalies over

North America. These changes in atmospheric flow then bring about differences in the associated precipitation and temperature anomalies.

# Chapter 1

## Introduction

### 1.1 Synopsis of tropical Pacific climate variations

Tropical Pacific sea-surface temperatures (SSTs) have been recognized for about a century as a potential principal driver of global climate. The earliest research includes that of Lockyer and Lockyer (1902, 1904), who first identified an oscillation in sea-level pressure (SLP) between Sydney (Australia) and Buenos Aires (Argentina) with an interannual period (3.8 years), and later demonstrated this oscillation to have correlations with SLP fields across the globe. Nearly 25 years later, this global-scale association was named the Southern Oscillation by Sir Gilbert Walker (e.g., 1924), who continued to demonstrate the global nature of its variations and correlations. Moreover, Murphy (1923) discussed the “Countercurrent” that created periodic warm waters off the coast of Peru, a phenomenon that had already been recognized in the 16th century by fishermen in coastal areas of Peru and linked to the demise of their fishing season. He identified this “Countercurrent” as the El Niño phenomenon (now known to be closely related to Walker’s Southern Oscillation).

These initial investigations into the Southern Oscillation were the pioneering research in an area that has blossomed into a major international effort. Following a more than 30-year gap in significant research, in the mid-1960s Norwegian meteorologist Jacob Bjerknes (1966, 1969) added an atmosphere-ocean interaction perspective to the understanding of tropical Pacific (TP) climate variations by proposing that abnormal warming of equatorial ocean temperatures arises from a weakening of the surface trade winds. He further connected the atmospheric and oceanic variations and was the first to propose a positive feedback mechanism linking the weakening of the trade winds to an increase in eastern TP SSTs, thereby decreasing the east-west SST and SLP gradient, further weakening the trade winds, etc. Also in 1966, Dutch meteorologist and geophysicist Hendrik Berlage (1966) further investigated the association among Djakarta,

Easter Island, and Greenland SLP, as well as TP SSTs, and further noted that high pressure over Indonesia often followed a cold winter in northwest Europe. Later, at the University of Hawaii, German mathematician and oceanographer Klaus Wyrtki (1975) identified more of the oceanographic features of El Niño/Southern Oscillation events. All of these pioneering research papers were then followed by the seminal work by American researchers Eugene Rasmusson and Thomas Carpenter (1982) that described the “canonical” El Niño event. Following several pioneering investigations into the teleconnections between TP climate indices and global climate patterns (e.g., Ropelewski and Halpert 1986, 1996) and early numerical modeling of El Niño events (e.g., Cane and Zebiak 1985, Zebiak and Cane 1987, Latif et al. 1994), analysis and prediction of TP SSTs (and often SSTs for the whole Pacific basin) became the subject of major research initiatives in countries spanning the globe, including the United States, Canada, Brazil, Australia, Japan, India, Germany, and the United Kingdom, to name only a few.

The above studies illustrate that the logical chain of deductive reasoning has been followed in the study of interannual TP climate variations and its influence on global climate. The earliest works presented limited statistical associations and were largely descriptive investigations outlining the characteristics of TP climate events. Then, beginning in the mid-1960s, many studies (particularly those of Bjerknes) presented robust physical theories explaining the interannual TP variations and describing the joint atmospheric and oceanic evolution during El Niño/Southern Oscillation events, culminating in the above landmark study by Rasmusson and Carpenter (1982). With this initial physical framework in place and as more events occurred (and more high quality data sets were developed), observational studies in the last 25 years have focused on applying a battery of univariate and multivariate statistical methods to elucidate the signature of interannual TP climate variations in global climate fields. Further, the advancement of computing technology and development of robust global climate models (GCMs) promoted the rapid growth of GCM simulations and coupled ocean-atmosphere models of the atmospheric response to TP sea-surface temperature anomaly (SSTA) events. Consequently, knowledge of interannual TP climate variations has grown (arguably necessarily) from the most general and theoretical hypotheses to much more intricate and detail-oriented postulations rooted in analyses of 150 years of marine

meteorological data and the numerical model simulations prompted by analyses of those data.

The present research seeks to build upon the extensive existing research on the influence of TP SSTs on North American climate, by bringing the physical understanding developed from the late 1960s through the late 1980s to bear in the statistical analysis of daily weather events. While recent investigations have demonstrated statistically significant TP associations with North American climate in monthly mean fields (e.g., Montroy 1997, Livezey et al. 1997, Montroy et al. 1998), and other preliminary investigations have shown some promising associations with the frequency of daily weather events (e.g., Mo and Higgins 1998), no studies have provided a comprehensive documentation and synthesis of the patterns of daily weather events that create the aggregate seasonal and monthly mean TP-related teleconnections. Further, no study has presented a comprehensive physical understanding of the link between TP SSTAs and North American weather on the daily time scale. This understanding must not only explain the associations for the majority of cases but also provide insight into why certain SSTA events do not show the associations that are present for most such events.

The present study addresses the above points in a 3-step process. First, the central and eastern North American regions exhibiting a notable statistical association with warm and cold TP SSTAs in monthly precipitation and temperature are identified using an earlier precipitation study (Montroy et al. 1998) supplemented by new counterpart analyses of daily maximum and minimum temperature. Second, for the target regions for warm and cold TP SSTA events, the statistical properties of the daily temperature/precipitation data are described, providing some insight into the nature of how the monthly associations arise. Third, those findings are combined with a focused intraseasonal analysis of the observed weather patterns during warm TP SSTA events to form an understanding of the physical relationships connecting the TP variations to the evolution of daily weather systems over North America. In this process, additional insight is provided whenever possible on why these relationships are not present during certain TP SSTA events by examining the state of other major climate system components impacting North American climate.

## **1.2 Detailed review of previous research**

### *1.2.1 Early tropical Pacific climate studies*

For over a century now, atmospheric scientists have been investigating observed regional manifestations of global climate variations for application in all facets of society. Some of the earliest such studies focused on the Indian monsoon and its relationship to a range of larger-scale surface meteorological variables. As noted in Kumar et al. (1998), H. F. Blanford issued “tentative” forecasts of Indian monsoon seasonal rainfall from 1882 to 1885 and later related the failure of Indian monsoons to variations in preceding snowfall in the Himalayas (Blanford 1884). He subsequently used these snowfall variations as one of three monsoon rainfall predictors in operational forecasts (Blanford 1886).

To improve upon Blanford’s Indian monsoon operational forecasting, Sir Gilbert Walker embarked on an extensive global study of the interrelationships among several large-scale meteorological variables (e.g., surface pressure, surface wind, rainfall). In so doing, Walker (e.g., 1923) described the global extent of the SLP oscillation earlier identified by Hildebrandsson (1897) and Lockyer and Lockyer (e.g., 1902) that is captured by the out-of-phase relation between Sydney (Australia) and Buenos Aires (Argentina). Walker (1924) named this phenomenon the “Southern Oscillation” and later documented its association with global wind and rainfall patterns while proposing some underlying associated physical mechanisms (e.g., Walker and Bliss 1930). His definition of the Southern Oscillation as “the barometrically recorded exchange of mass along the complete circumference of the globe in tropical latitudes” exemplifies the general acceptance of the Southern Oscillation as a global phenomenon. Interestingly, Walker did not use SSTs in the development of the physical mechanisms for the Southern Oscillation-global climate relationships, but instead focused on previously proposed and researched climate drivers such as sunspot number, incoming solar radiation, and polar ice. The end result of these early pioneering investigations into the regularity, robustness, and scope of major global climate variations was a well-documented statistical structure outlining the regions of influence of the major modes of global climate variations, with the leading mode showing major centers of action in the tropical Pacific.

### 1.2.2 *Interannual climate variations in the tropics*

After a 30-year (post-Walker) absence of research into interannual TP climate variations, resurgent interest beginning in the early 1960s added some physical understanding to the statistical structure developed in the early 20<sup>th</sup> century. Bjerknes (1966) capitalized on data collection during the International Geophysical Year (1957-58) – which fortuitously coincided with a strong El Niño event – and physically linked a weakening in the eastern and central TP surface southeast trade winds to the anomalous warming of eastern TP SSTs. This was one of the first recognitions of the ocean-atmosphere coupling and positive feedback (as explained below) that occurs during El Niño/Southern Oscillation events. Similarly, Berlage (1966) also associated atmospheric with oceanic variations in relating Djakarta SLP to SSTs at Puerto Chicama (Peru) as well as SLP variations as far afield as Greenland. Bjerknes (1969) added a more formal connection between Walker’s Southern Oscillation and SST variations. Bjerknes showed that a warming of the equatorial Pacific SSTs decreases the intensity of the Walker Circulation through a reduction in the west-to-east SST gradient across the equatorial Pacific, thereby reducing the east-to-west SLP gradient, and the southeasterly surface winds in the lower branch of the Walker Circulation. He went on to further describe the connections to TP precipitation patterns as well. This work completed the physical understanding of the evolution of atmospheric variations in the TP and marked a tremendous shift in the focus of interannual climate studies. The landmark nature of Bjerknes’ work was recognized by Rasmusson and Carpenter (1982), who state this “remarkable synthesis of Bjerknes ... marked a shift in emphasis from statistical analysis to more physically-oriented diagnostic studies” (p. 355).

In the 1970s, the physical investigation of TP climate variations illuminated the associated variations in oceanic processes and variables during SSTA events. Wyrtki (1975) connected the Southern Oscillation and El Niño-related TP SSTs from an oceanographic standpoint. During “normal” conditions, surface trade winds “pile up” relatively warm water in the western TP and cause the thermocline to be deeper there than further east in the equatorial Pacific. When the trade winds weaken in the presence of relatively warm SSTs (per Bjerknes’ arguments), the warm water in the western TP “sloshes” back eastward and raises the thermocline in the west as a consequence of the

eastward propagation of an internal equatorial Kelvin wave. When this Kelvin wave reaches the South American coast, the thermocline in that region is depressed, further contributing to warmer SSTs there.

This pioneering work by Bjerknes and Wyrtki outlining the physical characteristics and mechanisms of the ocean-atmosphere coupling during El Niño events permitted a comprehensive description of the typical El Niño event to be produced in the early 1980s. In a landmark paper, Rasmusson and Carpenter (1982) documented the two-year evolution of TP surface wind, SST, and rainfall patterns characteristic of six El Niño events (1951-52, 1953-54, 1957-58, 1965-66, 1969-70, and 1972-73). Using in-situ measurements of SSTs and surface winds, they analyzed the evolution of these atmospheric and oceanic fields over a 33-month period extending from April of the year preceding El Niño initiation through to the December of the year following El Niño maturity. They demonstrated the westward propagation of SSTAs from the South American coast to the western equatorial Pacific and the associated westerly surface wind anomalies (i.e., weakened easterlies), representing a decrease in the intensity of the Walker Circulation, consistent with the findings of Bjerknes. Further, they found evidence supporting Wyrtki's (1975) proposal that an intensification of the tropical easterlies precedes El Niño formation and serves as the trigger mechanism that allows the above equatorial Kelvin wave to develop and move eastward, eventually depressing the thermocline in the eastern Pacific and at the South American coast, causing the initial abnormal warming of SSTs there, beginning the cycle of events that promotes the positive feedback mechanism first proposed by Bjerknes (1966).

### *1.2.3 Global climate teleconnections from the tropical Pacific*

Following the physical atmosphere-ocean interaction investigations in the 1960s and 1970s, much subsequent research has examined the seasonal-mean (global and regional) climate patterns associated with El Niño/Southern Oscillation (ENSO) events. Some of the more comprehensive ENSO-related studies include Ropelewski and Halpert (1986, 1987, 1989, 1996; hereafter RH86, RH87, RH89, RH96) and Halpert and Ropelewski (1992, hereafter HR92), which used harmonic dial analysis of the Southern Oscillation Index (SOI) to document (conservatively) accompanying global seasonal

precipitation and temperature patterns. For North America, Ropelewski and Halpert (1986) identified the most robust seasonal climate associations linked to negative (low index) SOI events (i.e., warm TP SSTA events) to include the generally wet and cool winter conditions observed over the southeastern U.S. and the simultaneously generally warm conditions over western Canada. However, their conservative approach was on “defining those areas of the continent over which the ENSO response is both **consistent** and **strong**” (p. 2352). They also required that seasonal relationships span at least five months.

Following the significant investigations of Ropelewski and Halpert, other research added more detail to their seasonal analysis. Kiladis and Diaz (1989) added a little more temporal resolution by compositing 3-month average warm TP SST event global climate anomalies (temperature and precipitation) and subtracted from them cold TP SST event anomaly counterparts, which assumed a linear relationship between TP SSTs and regional climate. Other representative regional investigations into seasonal SST-climate associations involved Australian precipitation (e.g., Nicholls 1989), Brazilian rainfall (Ward and Folland 1991), western U.S. streamflow (Kahya and Dracup 1994), and U. S. snowfall (Kunkel and Angel 1999; Smith et al. 2001). Wolter et al. (1999) took a slightly different approach by concentrating on the risk of extreme seasonal precipitation and temperature occurrence during ENSO events defined by SOI extremes (upper or lower 20% of historical record). Thus, instead of focusing on only whether the observed anomaly during ENSO events is different from normal, their analysis examined the probability of seasonal-mean extreme climate (i.e., the tails of the seasonal mean distribution).

In the last 10 years, earlier global and regional seasonal research has been extended by more detailed studies documenting monthly associations between TP SSTAs and extratropical climate, particularly for North America. For sets of warm and cold SSTA events based on a central TP region closely associated with TP precipitation and indicative of ENSO occurrence, Livezey et al. (1997, hereafter L97) composited monthly U.S. precipitation, surface temperature, and 700mb geopotential height patterns. A more comprehensive examination of the central and eastern North American precipitation

patterns linked to TP SSTs was undertaken by Montroy (1997, hereafter M97), who identified Principal Components (PCs) of TP SSTA variability and documented the statistically significant monthly linear precipitation anomaly patterns for the SSTA PC score extremes. Later, Montroy et al. (1998, hereafter MRL98) used composite analysis to document the nonlinear relationships between four similarly derived SSTA PCs and observed monthly precipitation in the same region. In relating monthly precipitation totals from a high spatial resolution data set (described in, e.g., Gong and Richman 1995) to several different SSTA modes, M97 and MRL98 substantially extended the aforementioned seasonal studies by comprehensively documenting the intraseasonal and interannual variability of North American precipitation and relating it to SSTAs across the entire TP basin instead of just in one small region (e.g., as in L97). A broadly similar approach was taken by Mo and Higgins (1998), who identified the western U.S. precipitation patterns (on a much coarser latitude-longitude grid than that used in M97 and MRL98) linked to enhanced convection in several different regions spanning the TP. Further, using month-to-month SOI signs and tendencies, Stone and Auliciems (1992) documented contemporaneous and lag relationships with monthly Australian precipitation, upon which Stone et al. (1996a) built by documenting the potential predictability of global rainfall based on the same two-month patterns of SOI sign and tendency.

With monthly climate teleconnections thus having been documented comprehensively for some key affected regions, recent work has been motivated to identify interannual TP climate variations that occur on sub-monthly scales. For example, using the operational MRF model run by the National Centers for Environmental Prediction (NCEP), Compo et al. (2001) showed substantial differences in the ensemble variance of the simulated response to the 1986-87 El Niño and 1988-89 La Niña in January-March 500mb heights at the synoptic (2-7 day), intraseasonal (8-45 day), monthly average (30-day), and seasonal average (90-day) time scales over the Pacific Ocean, North America, and other regions of the globe. Also, Barsugli et al. (1999) used an innovative approach involving the operational MRF to demonstrate that SST forcing influences could appear in medium-range forecasts as early as forecast day 5 over North America. With these modeling studies finding some associations between TP SST

forcing and modes of model variability on a daily scale, properly designed investigations using daily observational data now are necessary to provide additional support and identify other related daily observed temperature and precipitation patterns.

In recent years, some preliminary studies have examined observational daily data for associations with TP SSTs, but no comprehensive statistical analysis has been performed on a continental scale. One specifically focused statistical investigation into daily data distributions is Higgins et al. (1996), which examined the associations between SOI extremes and the frequency of U.S. daily precipitation anomalies (on a coarse grid) exceeding 10 percent of the seasonal mean value. Later, Higgins et al. (2000) similarly analyzed 3-day precipitation accumulations along the western U.S. coast. Cayan et al. (1999) also analyzed ENSO-related shifts in the distributions of daily streamflow and precipitation during the western U.S. cold season, while Janowiak and Bell (1998) conducted a similar study for U.S. temperature, precipitation, and snowfall. In an earlier study for eastern Australia, Nicholls and Kariko (1993) associated the length and frequency of rainfall events with Southern Oscillation phases. However, no investigation has fully examined on a continental scale the patterns of daily weather events that typically occur during warm TP SSTA events and how variations in those patterns impact regional temperature and precipitation patterns. As explained below, the present inquiry addresses these issues.

#### *1.2.4 Other modes of interannual climate variations*

Aside from interannual modes of TP-related climate variability, during the last 25 years other major modes have also been identified and analyzed separately for signatures in global climate, though the interplay between them and the TP mode is not always well documented. These other modes of interannual variability are represented by the North Atlantic Oscillation (NAO), the Arctic Oscillation (AO), and the Pacific Decadal Oscillation (PDO). Rogers (1984) analyzed *extremes* of the Southern Oscillation and NAO and identified similarities in their teleconnection patterns. The NAO and many of the major modes of atmospheric variability were documented in the landmark investigation of Wallace and Gutzler (1981), which used correlation analysis of the 700mb geopotential height field to highlight four major modes, including the NAO, the

North Pacific Oscillation (later termed the PDO), the Pacific/North American pattern, and a “zonally symmetric seesaw” later named by Thompson and Wallace (1998) as the AO and which includes the NAO. Wallace and Gutzler’s study was followed by Barnston and Livezey (1987), who used Rotated PC analysis of the 700mb monthly mean Northern Hemisphere height field to identify the major atmospheric modes by season. The end result of these investigations is a thorough analysis of atmospheric variability on seasonal timescales and an identification of the principal modes in the Northern Hemisphere.

The NAO is one of the most significant modes of variation particularly for the Atlantic Ocean and Europe. The first recognition of the atmospheric fluctuations in Greenland associated with the NAO dates back over 200 years to the diary entries by the missionary Hans Egede Saabye from 1770-78 (van Loon and Rogers 1978). Walker and Bliss (1932) was one of the first studies to document global climate variations linked to what is now known as the NAO. Generally, the NAO represents a north-south mass oscillation over the North Atlantic Ocean, with one node located over Greenland and the other centered near the Azores (Lamb and Pepler 1987). The positive phase of the NAO usually brings about warmer than normal winters in the Northeast U.S. and in Europe, and below normal temperatures in Greenland (Walker and Bliss 1932; van Loon and Rogers 1978; Wallace and Gutzler 1981; Lamb and Pepler 1987). The work of van Loon and Rogers (1978) examined north Atlantic and European geopotential height field variations linked to the NAO, while Wallace and Gutzler (1981) expanded the analysis of associated geopotential height fields to the northern Hemisphere. Hurrell (1995) further documented the significant interannual and interdecadal characteristics of the NAO.

Another larger mode of atmospheric variability for the northern hemisphere as a whole is the Arctic Oscillation (AO). The AO, also known as the Northern Hemisphere Annular Mode was first defined by Thompson and Wallace (1998). It involves a “see-saw” of the winter (November-April) sea-level pressure anomalies from 20°N to the North Pole and is evident on both interannual and intraseasonal time scales. The manifestation of the AO on intraseasonal time scales has led the Climate Prediction Center to include the AO as a predictor in their seasonal outlooks, monthly outlooks, and 8-14 day outlooks (e.g., CPC 2006). This variation at the surface has associations that

extend into the stratosphere (Thompson and Wallace 1998), whereby a positive phase of the AO is characterized by an enhanced winter polar vortex. Thompson and Lorenz (2004) have also shown where the AO seems to be manifest in the tropical troposphere, in addition to the tropical stratosphere, as noted in Thompson and Wallace (1998), and that the linkage is strongest during cold TP SSTA events. In the present context, a particularly important implication of these AO investigations is that the polar vortex variations and other atmospheric variations to which it is dynamically linked can influence TP climate, including by modulating the linkage between TP SSTAs and extratropical (including North American) climate. The extent to which the AO (and NAO) help modulate the TP-based North American climate associations is an additional key focus of the present research.

A further source of climate system forcing that has been used to explain intraseasonal and interannual variations in North American extratropical climate is North Pacific (NP) SSTAs, as documented particularly in the extensive research of Jerome Namias. Namias (1959) was the first to discuss the possible physical linkage between NP SSTAs and the overlying winter atmosphere, including a possible feedback mechanism that would allow the SSTAs to persist for long durations (e.g., summer 1957 through winter 1957-58 in the case studied by Namias 1959). Namias (e.g., 1969) then followed this hypothesis by proposing that the observed duration of NP SSTAs during the 1960s could help explain some of the observed climate variations over North America during that decade, thereby allowing the SSTAs to be used in seasonal forecasting, an approach further supported by later studies (e.g., Namias and Cayan 1981, Barnett and Somerville 1983). The GCM simulations of Kushnir et al. (2002) later confirmed that an ocean-atmosphere feedback mechanism was present in the North Pacific, consistent with the mechanism hypothesized by Namias (1959, 1969); however, their limited GCM investigation was not able to sustain the overlying atmospheric circulation as shown by Namias. Kushnir et al. (2002) did propose two other physical mechanisms that can link the NP atmosphere and ocean, but stated that the best way to examine the linkage is not necessarily through a direct linear response of the atmosphere to NP SSTAs, but instead through examining “potentially subtle changes in the probability distributions of internal modes of variability” (p. 2253). Kushnir et al.’s (2002) inability to replicate the

observationally based investigations of Namias further demonstrates the need for coupling observational studies with modeling studies.

### **1.3 Problem Identification**

Consequently, although a tremendous amount of research has been completed linking interannual TP SSTAs to global and regional temperature and precipitation patterns, the specific associations between the TP and daily weather event frequencies remains substantially under-investigated. This is manifest in the absence of a comprehensive physical description of how “information” from the anomalous TP SSTA events induces different continental weather patterns on a day-to-day timescale. Following the extensive physical diagnostic studies of the 1960s and 1970s, the statistical teleconnections between TP SSTAs and North American climate have been fully documented using seasonal and monthly mean data. But the association to daily distributions of weather events has only begun to be investigated. And while some studies have proposed physical explanations for portions of the teleconnection linkage chain between the TP and North American climate – such as for frequencies of heavy daily precipitation events (Mo and Higgins 1998) – there still remains no unified physical explanation on the daily level of how many seasonal and monthly mean relationships arise.

The present research addresses this need through a unique analysis of daily surface climate data for central and eastern North America and underlying regional climate system behavior across the TP and NP as well as North America. First, the classification of TP SSTA events is reviewed, with information added on the phase of other key modes of climate variability (Chapter 2), followed by a replication of the same monthly analyses performed for central and eastern North America by MRL98 (on precipitation) for maximum and minimum temperatures (Chapter 3). Then, comprehensive observational analyses utilizing high-quality, fine-resolution daily data sets are used to identify the sub-seasonal precipitation and temperature characteristics of previously identified North American regional climate patterns accompanying extreme TP SST events (Chapter 4). This provides insight into the nature of the daily weather events that aggregate to monthly and seasonal time-mean patterns. Lastly, a physical

understanding of how TP SSTAs impact evolution of daily weather events is presented (Chapter 5). This final treatment includes examining the larger-scale atmospheric conditions using a “two-path” approach. First, the atmospheric conditions over the NP and North America are documented for the warm TP SSTA events examined here by compositing atmospheric fields. Then, the antecedent atmospheric conditions for the daily events that significantly deviate from normal and substantially contribute to the observed composite anomalies in Chapter 3 are described by analyzing composite daily atmospheric patterns and extratropical cyclone tracks over the Pacific Ocean and North America. Comparing the results from each branch of this two-path analysis permits the establishment of a physical understanding of how TP SSTAs cause changes in daily weather patterns.

To further support the understanding obtained, Chapter 5 also investigates the years during which the sign and/or magnitude of the observed North American seasonal climate anomaly substantially deviates from the composite mean. The goal is to determine why the event did not produce a regional surface climate anomaly consistent with the composite, citing whenever possible the additional atmospheric modes introduced above and described in Chapter 2. This analysis of atmospheric modes outside the TP helps address the relative impact of other views on the control on extratropical climate, particularly the North Polar-centered views based on the Arctic Oscillation and the North-Pacific-SST-centered views advocated by Namias. The physical understanding of the teleconnection linkage chain from the abnormally warm TP SSTs to the observed surface climate in central and eastern North America is summarized at the end of Chapter 5 and in Chapter 6.

The goal of this research is not to specifically attribute any individual North American weather system as arising “because of” TP SSTA events. The atmosphere is inherently chaotic, and the occurrence of TP SSTA events on seasonal-to-interannual climate time scales cannot be stated as the sole cause for the formation of any trough, front, or other synoptic-scale feature over North America. Instead, the focus is to document how atmospheric conditions combine during TP SSTA events to create an atmospheric environment that favors certain characteristics of weather systems. To

create a comprehensive and robust understanding of how atmospheric information travels from the TP to the extratropics, statistically derived daily distribution characteristics are combined with composites of atmospheric conditions and a physically based justification for how they are related to the daily surface climate distributions.

In order to provide the most useful extension of existing literature, the present study will focus specifically on warm and cold TP SSTA events in the traditional El Niño region for the statistical analysis in Chapters 3 and 4, and then will focus on warm TP SSTA events in Chapter 5. The focus in Chapter 5 follows the extensive investigation of the atmospheric flow during El Niño events (i.e., warm TP SSTA events), which provides a solid foundation for the present study to develop a physical teleconnection linkage chain from the TP to North America. For all Chapters, the principal months examined will be October through March, the period exhibiting the most robust seasonal and monthly associations with the classical El Niño regions (i.e., the central and eastern TP).

## Chapter 2

### Stratification of Tropical Pacific Sea-Surface Temperature Anomaly Events

#### 2.1 Preamble

The first step in identifying the physical and dynamical processes that transmit climate teleconnections to North America during tropical Pacific (TP) SSTA events is defining appropriately the SSTA events. Previous authors have used a wide range of definitions of warm and cold TP SSTA events, ranging from SOI-based classifications (e.g., Ropelewski and Halpert 1986) to standard seasonal mean SSTA classifications based on observations in a single region (e.g., northern Peru SSTs measured by Ship Track 1 for Rasmusson and Carpenter 1982) to monthly SSTAs in a small region of the TP (Livezey et al. 1997). Some techniques have also used multiple data sources to define ENSO events (e.g., the Multivariate ENSO Index of Wolter and Timlin 1998).

Previous research has demonstrated that using multivariate statistical techniques to define TP SSTA events can help identify statistically significant associations with North American precipitation. Montroy (1997, hereafter M97) identified three Principal Components (PCs) of TP SSTA for 1950-1992 variability and the statistically significant monthly linear central and eastern North American precipitation anomaly patterns associated with the SSTA PC score extremes. Montroy et al. (1998, hereafter MRL98) extended this research in two ways. First, the TP SSTA domain was expanded to include SSTAs west of 140°E. This permitted the identification of four (compared to M97's three) SSTA PCs that had statistically significant associations with monthly North American precipitation totals using the same precipitation data set. Second, MRL98 additionally identified regions of North America with monthly precipitation totals exhibiting nonlinear associations with TP SSTAs. The present research uses the same multivariate method to identify TP SSTA events but will extend the time period for which SSTA events are identified from 1950-1992 to 1950-2000.

To interpret fully the impact of TP SSTA events on North American climate on time scales of months to decades, the possible modulating influences of other important atmospheric/oceanic phenomena must be considered. These include the Arctic Oscillation (e.g., Thompson and Wallace 1998), the North Atlantic Oscillation (e.g., van Loon and Rogers 1978; Lamb and Pepler 1987), and the Pacific Decadal Oscillation (e.g., Mantua et al. 1997). In some cases, these other oscillations have been shown to work together with SOI or TP SSTA events (e.g., Thompson and Lorenz 2004). In the present work, these other influences will be used to help explain climate anomalies that did not match the composite anomaly obtained for all TP SSTA events. These events will be defined using indices of these phenomena and will be investigated as necessary.

The following sections provide the methodology for defining TP SSTA events (Section 2.2) as well as synopses of the other atmospheric/oceanic phenomena considered as potential modulating influences on teleconnections between TP SSTA events and North American climate (Section 2.3).

## 2.2 Definition of Tropical Pacific SSTA Events

### 2.2.1 Data

The SSTA data used in this study come from the same source as in M97 and MRL98 but have been extended to include more recent years. Monthly mean SST data were extracted from the Climate Prediction Center's global reconstructed SST data set (Smith et al. 1996) on a  $2^\circ$  latitude-longitude grid for the TP region spanning  $19^\circ\text{S}$ - $19^\circ\text{N}$

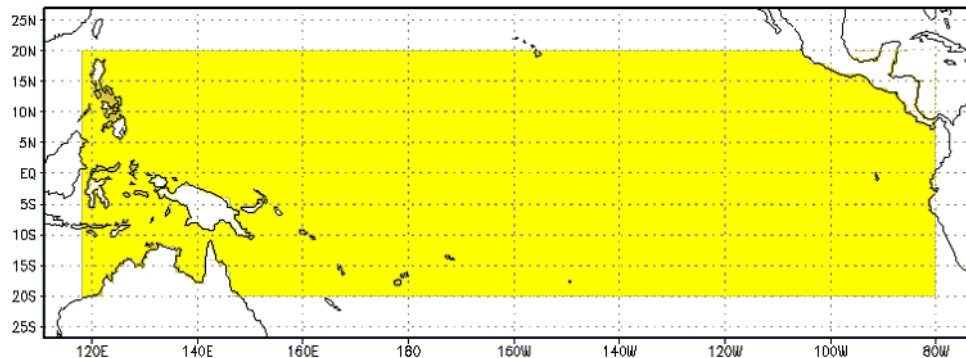


Fig. 2.1: Region of the tropical Pacific for which sea surface temperature anomaly (SSTA) data were analyzed in order to define SSTA events.

and from 119°E to the west coast of the Americas (Fig. 2.1). Full details on this data set's construction are given in Smith et al. (1996). While M97 and MRL98 focused on the 1950-92 time period, the present research has extended the study period to 1950-2000 to include recent pronounced TP SSTA events (1997-98 El Niño and 1999-2000 La Niña).

### 2.2.2 Methodology

The methodology for defining TP SSTA events in this study closely follows that of M97 and MRL98. Here, as in those studies, Principal Component (PC) analysis was applied to the TP SSTAs for the domain in Fig. 2.1, but the present study recomputes the PCs for the extended time period of 1950-2000. Unrotated PCs (UPCs) were first derived from the inter-grid cell correlation matrix in an S-mode sense (Richman 1986, p. 305). Utilizing similar truncation tests as in M97 and MRL98 – scree test (Cattell 1966), eigenvalue separation criterion (North et al. 1982), and “point teleconnection patterns” (Richman 1986, pp. 303-304) – the resulting unrotated spatial loading patterns then were examined in conjunction with the associated eigenvalues to determine that three modes explaining 61.9% of the SSTA variance contained nonrandom signal. These three modes were retained and then rotated to the Varimax criterion (Kaiser 1958) in order to obtain SSTA modes that are more representative than unrotated modes of the physical variability present in the data set (Horel 1981; Richman 1986). Both sets of SSTA modes – the UPCs and Varimax-rotated PCs (VPCs) – then were examined, and four PCs were retained for further use in the subsequent climate analyses (see Fig. 2.2 for loading patterns and Fig. 2.3 for score time series). These four PCs, the first UPC and all three VPCs, represent very similar SSTA modes to those described in MRL98, with the set emphasizing the same four regions of TP SSTA variability as in MRL98: central tropical Pacific (UPC1), eastern tropical Pacific (VPC1), western Pacific horseshoe (VPC2), and far western tropical Pacific (VPC3).

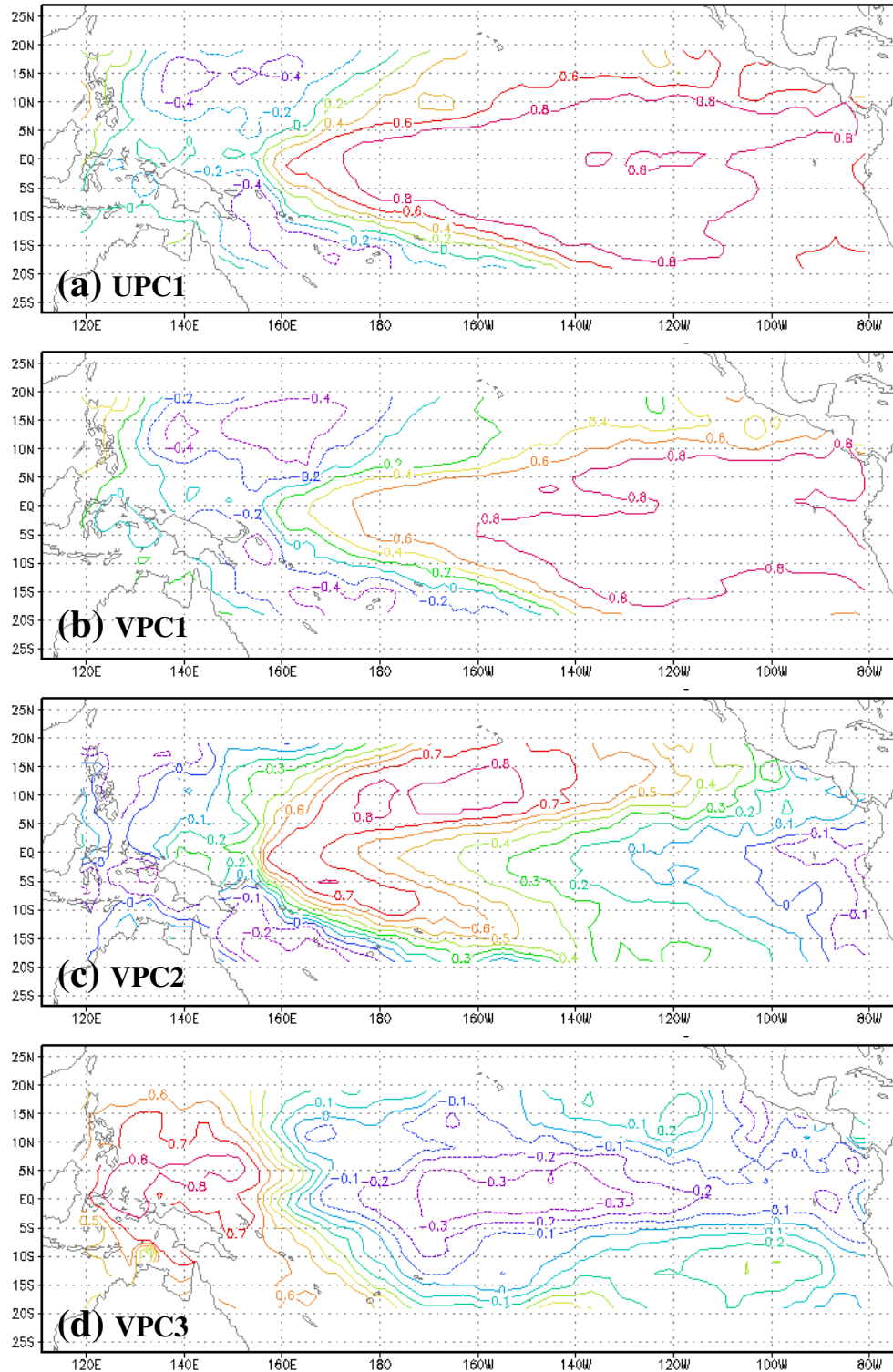


Fig. 2.2: Spatial loading patterns for SSTA Principal Components described in Section 2.2.2.

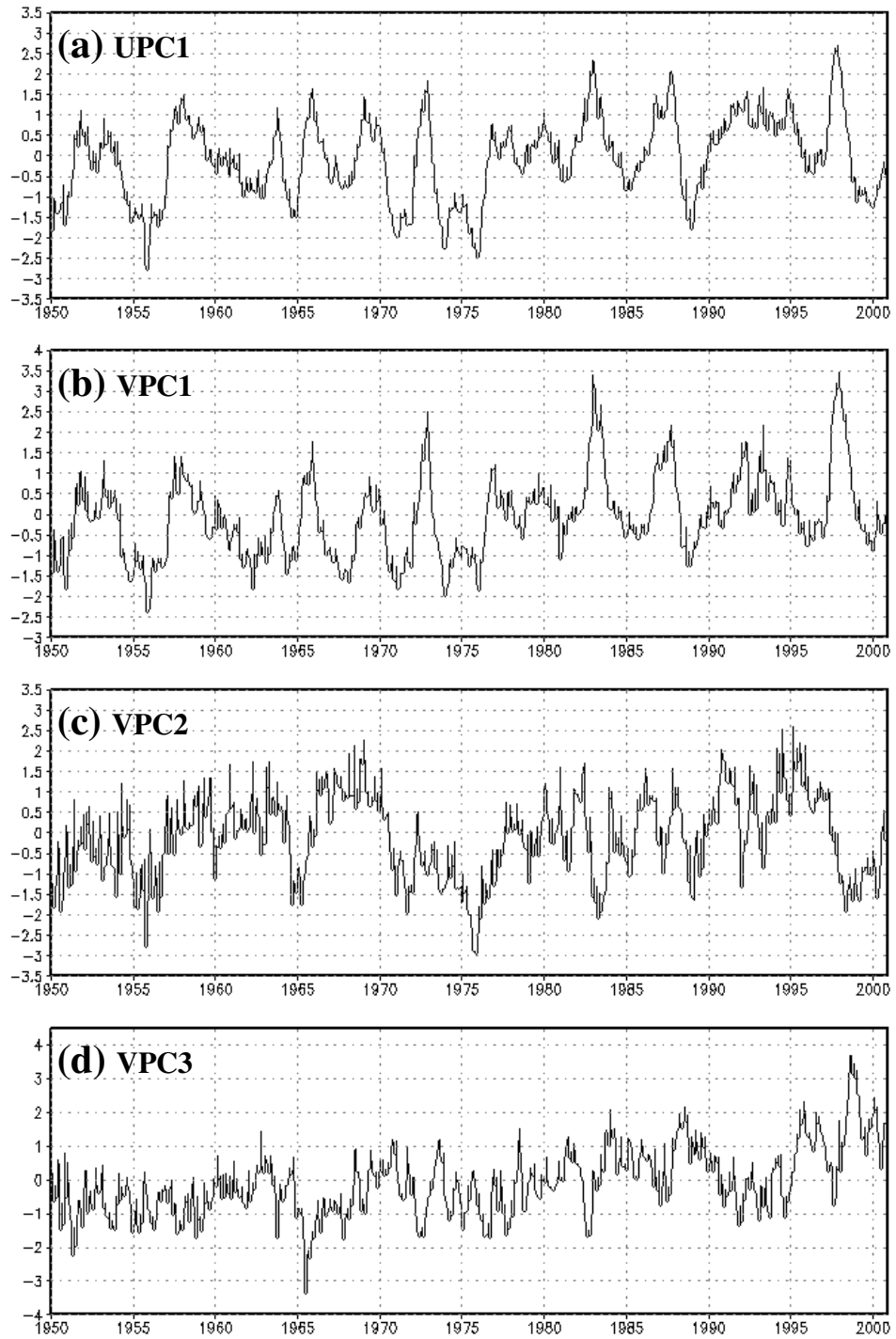


Fig. 2.3: Principal Component score time series for SSTA modes associated with the spatial loading patterns in Fig. 2.2.

Warm and cold SSTA event months were identified for different regions of the tropical Pacific using the associated score time series from the four SSTA PC modes identified above. MRL98 used a score threshold of  $\pm 0.97$  to define such events, which represents the critical  $t$  value for a student's  $t$  distribution with 43 degrees of freedom (one for each year from 1950-92, the original time period examined in that study) with a two-tailed hypothesis test using  $\alpha = 0.3333$ . This approach effectively classified one-sixth of the distribution as warm events and one-sixth as cold events, with two thirds being in the "neutral" category. For the present study, the same threshold is used, as increasing the degrees of freedom to 51 to correspond to the 1950-2000 analysis period does not alter the critical  $t$  value for the target  $\alpha$  value.

### 2.2.3 SSTA Events for 1950-2000

The SSTA events to be examined in the present research include the central and eastern TP SSTA events that were previously used in MRL98, plus additional events for 1993-2000. There were no instances where the PC scores calculated for this study caused a month to be re-classified compared to MRL98's scores based on 1950-1992. Table 2.1 lists the four primary SSTA events during 1993-2000 for VPC1 (and UPC1) during the November-March season. These events included (1) the warm central and eastern TP SSTA event extending into summer 1993, (2) a warm central and eastern TP SSTA event from November through January in 1994-1995, (3) a warm central and eastern TP SSTA event corresponding to the major El Niño from May 1997 through September 1998, and (4) a cold central TP SSTA event from September 1999 through March 2000. All of these events will be examined to highlight monthly regional temperature associations (Chapter 3) and identify the daily precipitation and temperature distribution characteristics for particular regions (Chapter 4). The investigation into physical/dynamical reasons for the observed features in the teleconnection linkage chain from the TP to North America (Chapter 5) will focus on select November-March periods. Further details are given in Section 2.4.

Table 2.1: Tropical Pacific SSTA events during 1993-2000 examined in this study. Dates in parentheses are listed when the event based on the SSTA PC in the second column ended in a different month.

<b>Period</b>	<b>SSTA PC</b>	<b>Anomaly Sign</b>	<b>Event Type</b>
Jan 1993 - Jul 1993	VPC1 / UPC1	Positive	El Niño
Nov 1994 - Jan 1995 (Mar 1995)	VPC1 (UPC1)	Positive	El Niño
May 1997 - Sep 1998 (May 1998)	VPC1 (UPC1)	Positive	El Niño
Sep 1999 - Mar 2000	UPC1	Negative	La Niña

### 2.3 Other Atmospheric/Oceanic Phenomena

This section discusses additional climate system components that have been identified as having associations with North American climate or that have been shown to have modulating influences on teleconnections between the TP and North American climate. This information is provided here as background for further consideration, as the monthly associations summarized in Chapter 3 are further refined in Chapter 4 and connected to atmospheric variations in Chapter 5.

#### 2.3.1 Arctic Oscillation/North Atlantic Oscillation

As defined by Thompson and Wallace (1998, 2000), the term Arctic Oscillation (AO) refers to the leading mode of variability of Northern Hemisphere wintertime sea-level pressure. The AO first was evaluated for November-April (Thompson and Wallace 1998) and later was expanded to all months of the year (Thompson and Wallace 2000), using an AO index based on the first UPC of Northern Hemisphere sea-level pressure anomalies (SLPA) for 1958-1997 poleward of 20°N. The positive phase of the AO is characterized by an increased Arctic polar vortex, which brings strong westerlies over North America and helps to keep the coldest winter air in northern Canada. Increased westerlies over the North Atlantic Ocean also bring relatively warm conditions and increased precipitation into northern Europe (Hodges 2000). Conversely, the negative AO index phase has a diminished north polar vortex, providing more opportunity to have cold Arctic air spill into the U.S. and reducing the advection of warm/moist water from the Gulf Stream into Europe.

Some recent studies have explicitly linked the AO to North American winter temperature anomalies, particularly in the eastern U.S. and Canada. Thompson and Wallace (1998) showed that the November-April average surface air temperature over the U.S. east of the Rocky Mountains and in Canada from Alberta through Manitoba is positively correlated with the AO index – meaning warm winters during positive AO phase and cold during the negative AO phase – while much of the Canadian province of Nunavut (located east of the Northwest

Territories and north of Manitoba) is negatively correlated with the AO index. These associations are documented in Fig. 2.4. Thompson and Wallace (2000) further attributed the above positive correlation to warm temperature advection in the lower troposphere. Higgins et al. (2002), citing the AO as the dominant mode of extratropical Northern Hemisphere atmospheric variability, extended this seasonal analysis to examine daily U.S. temperature extremes, which were defined in their study by daily temperatures in the upper/lower 10% of the winter distribution. They found that the positive (negative) AO index phase was characterized by more (fewer) warm temperature extremes and fewer (more) cold temperature extremes. This is broadly consistent with the linear correlation between the AO index and surface temperatures shown in Fig. 2.4.

In the present study, AO events will be defined using the index described above from Thompson and Wallace (2000). They computed the first UPC of NCEP/NCAR Reanalysis SLP data using data from 1958 to 1997. Thompson (2005) expanded the time

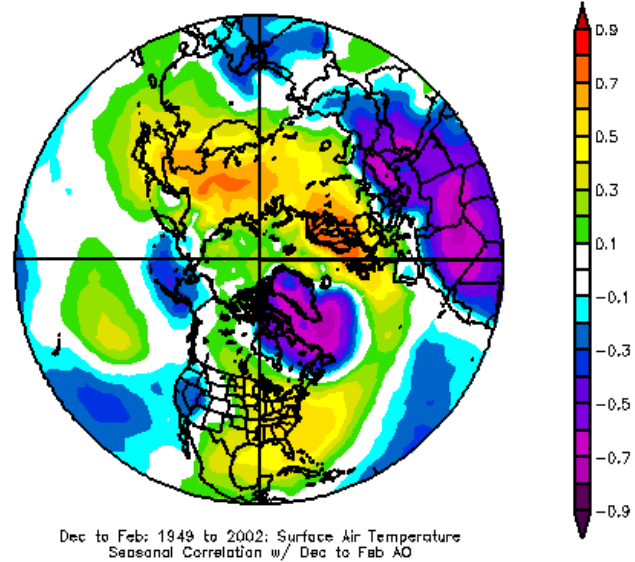


Fig. 2.4: Correlation between December-January-February Arctic Oscillation index of Thompson and Wallace (2000) and seasonal mean surface temperature. (Calculations were performed using the NCEP/NCAR Reanalysis data and analysis tools available from the NOAA/ESRL Physical Science Division, Boulder Colorado from their web site <http://www.cdc.noaa.gov/>.)

period to 1899 through 2000 by projecting the associated Reanalysis SLP data (after 1997) and the SLP data of Trenberth and Paolino (1980) (before 1958) onto the UPC coefficients. AO extreme events here are defined using thresholds of  $\pm 0.97$ , paralleling MRL98's criteria on the standardized UPC score data and that for the SSTA PCs in the present study (see Section 2.2). This criterion is more stringent than Higgins et al. (2002), who used a threshold of  $\pm 0.5$  (on standardized indices) to define high/low (i.e., positive/negative) index phases of the AO. Since the AO index is primarily used in the present study to explain outliers with respect to the TP SSTA-North American climate connection, this higher threshold will permit the use of only the strongest AO events to try to explain outliers.

Due to multidecadal trends in the Pacific Ocean, the observed atmospheric flow patterns during the negative phase of the AO have changed. Many studies have documented the presence of decadal-scale shifts in the climatology of atmospheric variables (e.g., Trenberth and Hurrell 1994, Graham 1994) and ecological data (e.g., Ebbesmeyer et al. 1991), and these trends are evident in the atmospheric flow patterns related to the AO. For four December-February seasons characterized by a negative AO before 1970, the composite 500mb geopotential height anomalies were positive in the northern Pacific Ocean (Fig. 2.5a), but for six seasons after 1970 the height anomalies in the same region were negative (Fig. 2.5b). Consequently, in the present study, when examining the role of the AO in the teleconnections between the TP and North America, the relative differences in the AO flow pattern before and after 1970 will be used to interpret the AO modulation of the TP teleconnections.

While it is recognized as a major mode of variability in the Northern Hemisphere, the North Atlantic Oscillation will not be used here, as it is a regional manifestation of the AO. Hurrell (1995) demonstrated that the NAO had associations with wintertime U.S. surface temperature, similar to those described in Thompson and Wallace (2000) for the AO. However, because the NAO does not explain as much surface air temperature variance in North America as the AO (Wallace 2000; Higgins et al. 2002), it will not be used to explain modulations of the connection between TP SSTAs and North American climate in the present study.

(a)

(b)



Fig. 2.5: Composite December-February 500mb geopotential height anomalies (gpm, from 1968-1996 climatology) for (a) 1959-60, 1962-63, 1965-66, and 1968-69 and (b) 1969-70, 1976-77, 1978-79, 1984-85, 1985-86, and 2000-01. (Calculations were performed using the NCEP/NCAR Reanalysis data and analysis tools available from the NOAA/ESRL Physical Science Division, Boulder Colorado from their web site <http://www.cdc.noaa.gov/>.)

### 2.3.2 Pacific Decadal Oscillation

The Pacific Decadal Oscillation (PDO) refers to the inter-decadal atmospheric/oceanic variations centered in the northern Pacific Ocean. This mechanism has been observed by different authors with different indices computed using EOF-based analyses on north Pacific SLP anomalies and SSTAs. The term “Pacific Decadal Oscillation” was first used by Mantua et al. (1997) and Zhang et al. (1997), who used PCA of SSTAs in the Pacific Ocean north of 20°N to identify the oscillation. Power et al. (1999a) called this same phenomenon the “Interdecadal Pacific Oscillation” and compared four different indices measuring the variability, all of which were well correlated, with correlation magnitudes between 0.8 and 0.95. The high (low) index phase of the PDO is characterized by abnormally cold (warm) ocean temperatures in the north Pacific Ocean. Mantua et al.’s (1997) PDO index has exhibited substantial variability on decadal time scales (Fig. 2.6), switching from the low index phase in 1950-76 to the high index phase in 1977-99, consistent with the observation of many authors (e.g., Trenberth and Hurrell 1994) of a pronounced global climate shift around 1976-77.

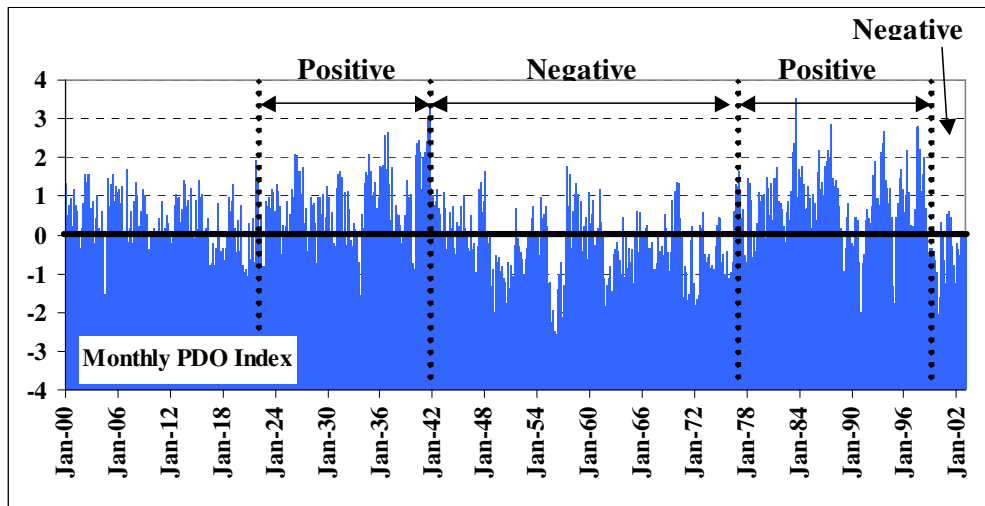


Fig. 2.6: Time series of monthly PDO index from 1900 through July 2002. Data have been standardized by month over the entire data range. Further details are given in Section 2.3.2. Index data were obtained from Mantua (2005).

Some recent studies have suggested the PDO plays an important role in the teleconnections between the tropical Pacific and North American climate. Gershunov and Barnett (1998) separated El Niño and La Niña events according to phase of the PDO (which they term the "North Pacific Oscillation") by separating the period of record according to regime shifts that "have been confirmed by independent analyses to have occurred in 1925, 1947, and 1977" in SST, SLP, and other indices. They demonstrated that during El Niño (La Niña), January-February-March precipitation and sea-level pressure relationships were strongest during high (low) index phase of the PDO. They hypothesized that the modulation of the teleconnections comes in part via the Aleutian Low, which is deepened (filled) when El Niño (La Niña) coincides with high (low) PDO years. Indeed, these associations are evident in the correlation between December-January-February sea-level pressure with the PDO index (Fig. 2.7a), with correlation values in the Aleutian Low region exceeding -0.8. The PDO is also negatively correlated with precipitation from east Texas to Ohio-western Pennsylvania (Fig. 2.7b), a region MRL98 has shown to be linked to below normal precipitation (especially for January-February) during warm TP SSTA events.

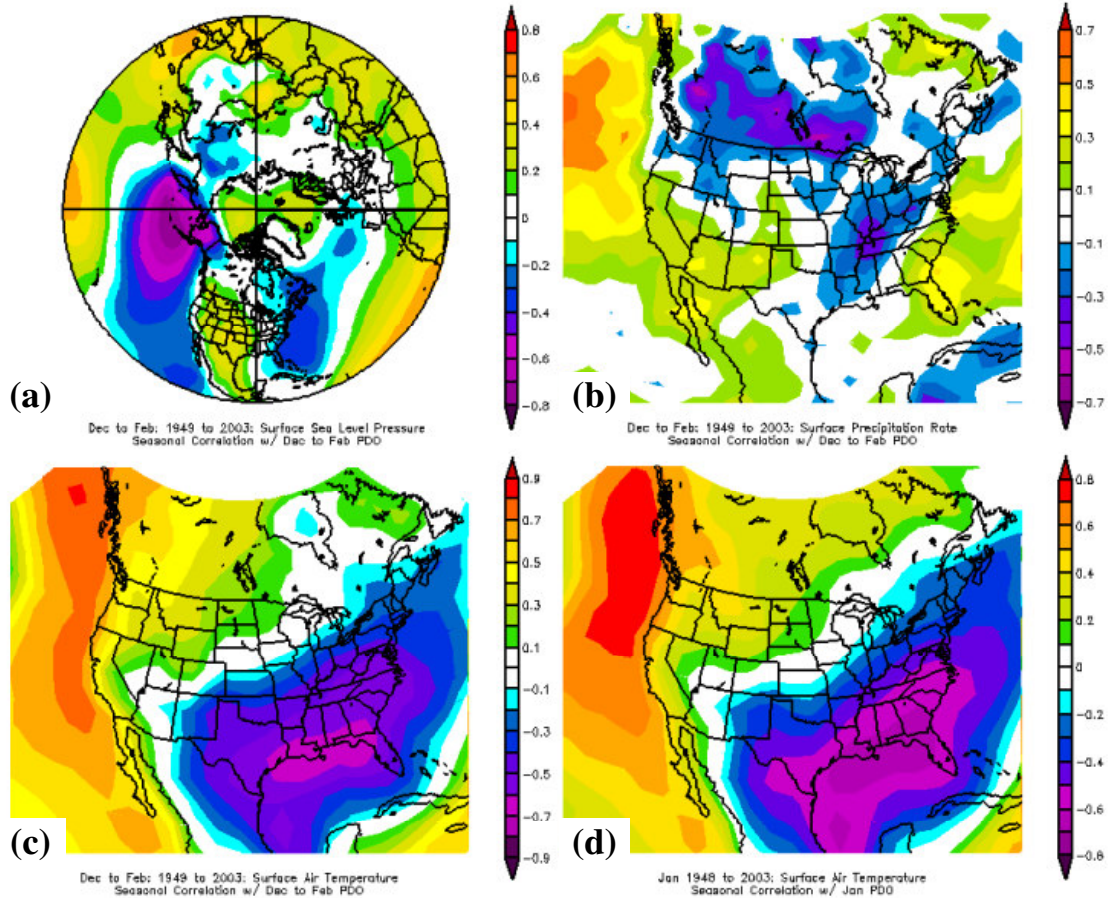


Fig. 2.7: Correlation between December-January-February seasonal average of index in Fig. 2.6 and seasonal mean (a) sea-level pressure over the Northern Hemisphere, (b) surface precipitation rate, and (c) surface temperature. (d) As in (c) but for January only. (Calculations were performed using the NCEP/NCAR Reanalysis data and analysis tools available from the NOAA/ESRL Physical Science Division, Boulder Colorado from their web site <http://www.cdc.noaa.gov/>.)

Here, the phase of the PDO will be defined using the index in Fig. 2.6 calculated by Mantua et al. (1997). This index is the time series of the first EOF mode of Pacific SSTs north of 20°N spanning 1900-1993. Mantua (2005) calculated index data through 2000 by projecting the more recent SST data onto the EOF mode. PDO events will be defined using a standardized PDO index (with a base period of 1971-2000) with an event threshold of  $\pm 0.97$ , following the classification of months based on the sign of SSTAs in different regions of the Pacific as outlined in Section 2.2.2, which will approximately designate one sixth of the months as high index and one sixth as low index.

## **2.4 Selection of Primary SST Events**

A summary of the individual warm and cold TP SSTA events found in the present research is given in Table 2.2 on a monthly basis. The individual monthly SSTA event classification follows MRL98 by using UPC1 and VPC1-3; however this table extends these classifications to show the state of the other major climate system phenomena discussed above. All indices have been standardized by calendar month for the observed period of record. When the sign and/or magnitude of monthly anomalies during individual constituent events notably depart from the sign and magnitude of the composite anomalies between SSTA events and North American climate (Chapter 3), the phases of these other phenomena were examined (Chapters 4 and 5). The extremes in these other phenomena were analyzed to determine if they occurred during any of the individual constituent years that do not match the sign and/or magnitude of the composite field.

In order to focus the development of a teleconnection linkage chain during warm TP SSTA events in Chapter 5, the individual monthly classifications given in Table 2.2 have been used to identify the November-March periods characterized by generally positive SSTAs. For a November-March period to be classified as a key warm SSTA event for the purposes of Chapter 5, at least 3 of the 5 months should be a warm SSTA VPC1 event using the method outlined in Section 2.2. These key events (listed in Table 2.3) will be used in the event by event analysis of the evolution of atmospheric patterns in the presence of TP SSTAs in order to identify the physical/dynamical features of the teleconnection linkage chain (Chapter 5).

Table 2.2: Individual monthly classification of November-March 1950-2000 with respect to all atmospheric and oceanic phenomena discussed in previous sections of this Chapter, abbreviated as defined there. The year in the left-hand column refers to the year of the January-March. “H” indicates a high-index ( $> +0.97\sigma$ ) phase of that index, and “L” indicates a low-index ( $< -0.97\sigma$ ) phase. If neither the high nor the low index criteria are met, the sign of the index is plotted with a plus or minus symbol or with a “0”.

(JFM) Year	UPC1					VPC1					VPC2					VPC3					SOI					AO					PDO															
	N	D	J	F	M	N	D	J	F	M	N	D	J	F	M	N	D	J	F	M	N	D	J	F	M	N	D	J	F	M	N	D	J	F	M											
1950			L	L	L			L	L	L	-			-		-		-	L	L			-	+	+	H	H			-	-	L	L	L	L											
1951	L	L	L	-	L	L	L	L	-	-						+	-	+	-	-			-			H	H	+	-		-	L	L	L	L											
1952	H	+	+	+	+	H	+	+	+	+			L		+		+	+	+			+			L	L	L	L	0	-	H	+	L	L	L	-										
1953	-	-	+	+	+	-	-	+	+	+																L	-	L	+	L			+	-	+	-	L									
1954	-	-	+	-	-	+	+	+	+	+			L		-		-		-						+	+	-	-	-	-	+	+	L	L	-	-										
1955	L	L	L	L	L	L	L	L	-	L			-	L	L	L	L	-					+	H	-	H	+			-	-	L	+	+	+	L	L									
1956	L	L	L	L	L	L	L	L	L			-	-	-	L	L									H	+	H	H	+	L	-	L	+	L	L	L	L	L								
1957	L	L	-	+	+	L	L	L	-	+															+	+	+	-	-	H	-	L	L	L	L	-	+									
1958	H	H	H	H	H	H	H	H					L	L	L	-	-						+	+	+	H	+	L	-	L	L	-	L	-	L	L	-	+								
1959	+	+	+	+	+	+	+	+	+	+			L	-	L	L	L									H	H	-	-		L	L	+		L	L	+	+								
1960	-	-	-	-	+	-	-	-	-	+			-	+	+	+	+								+	+	0	-	+	L	-	L	L	L	H	+	+	+	-							
1961	-	+	-	+	-	-	-	-	-			+	-	+	+	+									H	+	+	+	L	-	-	+	+	H	+	+	+	+								
1962	-	-	-	-	-	-	L	L	L																+	+	+	+	+	H	H	-	-	L	H	-	L	L	L	L	L					
1963	-	L	-	-	-	-	L	-	L	-			+	+	+	+	+									H	H	+	0	H	+	+	L	-	L	L	+	-	-	-	-					
1964	+	+	+	-	-	+	+	+	-	-			-	-	-	-	-									+	+	+	+	+	L	+	-	-	L	L	+	-	-	-						
1965	L	L	-	-	-	-	-	-	-	-			-	L	-	-	-									0	-	-	+	+	-	-	-	L	-	L	L	+	+	+						
1966	H	H	H	+	+	H	H	H	+	+			L	L	L	L	L								L	0	L	-	L	L	+	L	+	L	-	-	+	+	-	L						
1967	-	-	-	-	-	-	-	-	L	L																H	H	+	+	+	+	+	L	-	+	H	L	-	-	-	L					
1968	-	-	-	-	-	L	L	L	L	L			L	L	-	L										-	+	H	-	-	-	L	L	H	-	-	-	-	-	-						
1969	+	+	H	H	+	+	+	+	+	+			-	-	-	L										0	L	L	-	L	-	L	L	-	L	L	-	L	L	-	-					
1970	+	+	+	+	+	+	+	+	-	+			+	+	+	+	+									+	+	+	H	+	+	+	+	L	L	0	+	L	L	+	+	+	H			
1971	L	L	L	L	L	L	L	L	L	L			H	+	H	+										H	H	+	H	H	+	+	+	+	+	+	+	+	+	+	+	+				
1972	L	L	-	-	-	-	L	L	-	+			+	+	+	+										+	0	+	+	+	+	+	+	+	+	+	+	+	+	+	+	+				
1973	H	H	H	+	+	H	H	H	+	+			-	-	-	-										-	L	-	L	+	+	+	+	+	+	+	+	+	+	+	+	+	+			
1974	L	L	L	L	L	L	L	L	L	L			+	+	+	+											H	H	H	H	H	-	-	+	+	+	+	+	+	+	+	+	+			
1975	L	L	L	-	L	-	L	-	-	-			-	-	L	L	L	L									0	-	+	H	+	+	+	+	+	+	+	+	+	+	+	+	+			
1976	L	L	L	L	L	L	L	L	L	L			-	-	-	L	L									H	H	H	H	H	+	+	+	+	+	+	+	+	+	+	+	+	+			
1977	+	+	+	+	+	+	H	H	H	+	+			+	+	+	+									+	-	-	H	L	-	L	L	L	+	H	H	H	H	+	+	+	+			
1978	+	+	+	+	+	+	+	+	+	+			L	L	-	L										L	L	-	L	-	+	-	-	L	+	-	-	+	H	H	+	+	+			
1979	+	+	+	+	+	+	+	+	+	+			-	-	-	-	+													H	-	-	+	+	+	+	+	+	+	+	+	+	+	+		
1980	+	+	H	+	+	+	+	+	+	+			+	+	+	+	+										-	L	+	0	L	+	+	+	+	+	+	+	+	+	+	+	+	+		
1981	+	+	-	-	-	+	+	L	-	-			+	+	+	+	+										-	+	-	L	L	-	-	L	+	+	+	+	+	+	+	+	+			
1982	+	+	+	+	+	+	+	+	+	+			H	+	+	+	+										H	H	+	+	+	+	+	+	+	+	+	+	+	+	+	+	+	+		
1983	H	H	H	H	H	H	H	H	H	H			L	+	+	+	+										L	L	L	L	L	L	L	L	L	L	L	L	L	L	L	L	L	L		
1984	+	+	+	+	+	+	+	+	+	+			H	+	H	H	H										-	+	+	+	+	+	+	+	+	+	+	+	+	+	+	+	+	+	+	
1985	-	-	-	-	-	-	-	-	+	+			+	+	+	+	+										+	+	+	+	+	+	+	+	+	+	+	+	+	+	+	+	+	+	+	
1986	-	-	+	+	+	-	-	-	-	+			+	H	+	+	+										+	+	+	H	H	+	+	+	+	+	+	+	+	+	+	+	+	+	+	
1987	H	H	+	H	H	H	H	H	H	H			+	+	+	+	+										L	L	-	L	L	-	L	+	+	+	+	+	+	+	+	+	+	+	+	
1988	H	H	H	+	+	H	H	H	+	+			H	+	H	H	H	H									+	+	+	+	+	+	+	+	+	+	+	+	+	+	+	+	+	+	+	
1989	L	L	L	L	L	-	L	L	-	-			H	+	H	+	+											H	H	H	H	+	+	+	+	+	+	+	+	+	+	+	+	+	+	
1990	-	+	+	+	+	+	+	+	+	+			+	+	+	+	+										-	+	-	L	L	+	+	+	+	+	+	+	+	+	+	+	+	+	+	
1991	+	+	+	+	+	-	+	+	-	-																		-	+	-	L	+	+	+	+	+	+	+	+	+	+	+	+	+	+	
1992	H	H	H	H	H	+	H	H	H	H			L	-	L	-											L	L	L	L	+	+	+	+	+	+	+	+	+	+	+	+	+	+	+	
1993	+	+	H	H	H	+	+	H	H	H			+	+	+	+	+										-	L	L	L	L	+	+	+	+	+	+	+	+	+	+	+	+	+	+	+
1994	H	H	+	+	+	+	+	+	+	+			+	+	+	+	+										0	-	-	L	+	+	+	+	+	+	+	+	+	+	+	+	+	+	+	+
1995	H	H	H	H	H	H	H	H	+	+			+	+	+	+	+										L	-	-	+	+	+	+	+	+	+	+	+	+	+	+	+	+	+	+	+
1996	+	+	-	-	+	-	-	-	-	+			H	H	H	H	H	H									0	-	+	-	+	+	+	+	+	+	+	+	+	+	+	+	+	+	+	
1997	+	-	-	+	+	-	-	-	+	+			H	H	H	+	+										+	+	+	H	L	+	+	+	+	+	+	+	+	+	+	+	+	+	+	
1998	H	H	H	H	H	H	H	H	H	+	+			+	+	+	+										L	L	L	L	L	-	-	L	+	+	+	+	+	+	+	+	+	+	+	+
1999	-	-	L	-	-	+	+	+	+	+			H	H	H	H	H											H	H	H	+	+	+	+	+	+	+	+	+	+	+	+	+	+	+	
2000	L	L	L	L	L	-	-	-	-	+			H	H	H	H	H											H	H	+	+	+	+	+	+	+	+	+	+	+	+	+	+	+	+	

Table 2.3: Primary warm SSTA events for which physical/dynamical aspects of the teleconnection linkage chain from the tropical Pacific to North America will be documented in Chapter 5.

<b>Period</b>	<b>Event Type</b>
1957-58	El Niño
1965-66	El Niño
1972-73	El Niño
1982-83	El Niño
1986-87	El Niño
1991-92	El Niño
1992-93	El Niño
1997-98	El Niño

## Chapter 3

### Monthly Teleconnections between Tropical Pacific SSTA Events and North American Winter Climate

#### 3.1 Preamble

Using the TP SSTA event definitions as noted in Table 2.2 and Section 2.2, the monthly North American precipitation and temperature patterns associated with the SSTA PCs during November-March are presented in the following sections. The present research builds upon previous monthly SSTA-surface climate associations in three particular ways. First, the analysis period is extended beyond that of Montroy (1997, hereafter M97) and Montroy et al. (1998, hereafter MRL98) to include warm and cold SSTA events through 2000. Second, MRL98's techniques that were applied to monthly precipitation totals are here used to document associations for daily maximum and minimum temperature. Lastly, the present research indicates whether extremes in other climate phenomena (Section 2.3) may be linked to individual months where the sign and/or magnitude of the observed North American precipitation/temperature anomaly is not consistent with that of the overall composite anomaly.

#### 3.2 North American Climate Data

The principal data set used in this study to identify the North American climate patterns associated with TP SSTA events is the same high-resolution set of daily precipitation totals and daily maximum/minimum temperature observations for an approximately 1° latitude-longitude grid east of the Rocky Mountains, as was used in earlier studies (e.g., Gong and Richman 1995, MRL98, Skinner et al. 1999). The data set includes 766 stations, and there are no missing data, as missing values were substituted using data from a nearby station. For the present research, the daily precipitation values were summed for individual calendar months (as in MRL98), and the daily maximum and minimum temperature values were averaged for individual months. The fine spatial

resolution of this data set permits clear delineation of specific regions in the eastern two-thirds of North America exhibiting particular associations with TP SSTAs.

### **3.3 Methodology**

The compositing methodology used here for the monthly averages of daily maximum and minimum temperature data exactly follows that for the precipitation data in MRL98. For the SSTA events defined in Section 2.2, composite individual calendar monthly temperature anomalies are produced, as well as composite patterns for periods of two and three consecutive months when the monthly composite fields varied little from month to month. In the multiple-month cases, at least two months in the season must have the same SSTA PC classification as defined in Section 2.2. Significance testing for monthly averages of daily maximum and minimum temperature is performed here in three ways, as in MRL98 for precipitation. First, a local  $t$  test is applied to each station composite anomaly to assess whether it is significantly different from zero at the 90% level. Second, the field significance is assessed by randomly reshuffling the precipitation or temperature fields 1000 times, recomputing the composites, and repeating the local significance test. The field significance is the percentage of reshuffled anomalies with fewer significant stations than in the original composite. Finally, a regional significance test is computed by applying a  $t$  test to the average anomaly for clusters of stations whose composite anomalies are locally significant.

### **3.4 Results**

The major associations between TP SSTA events and central and eastern North American precipitation and temperature anomalies are now summarized. First, the precipitation patterns during TP SSTA events after 1992 are examined for consistency with the MRL98 composites derived from 1950-92 (reproduced here in Fig. 3.1, with associated regional statistics in Table 3.1). Next, composite maximum and minimum temperatures are presented for the same 1950-1992 analysis period for the months of November-March, followed by a similar comparison of the monthly temperature patterns during TP SSTA events after 1992 to the pre-1992 composite patterns. (However, if an association begins in March and extends into April or begins in October and extends in to November, then the October or April associations also are discussed.) Use of the same

1950-92 study period facilitated the comparison of the temperature composites to the precipitation composites of MRL98. Lastly, the consistency of the anomaly through each composite's constituent members is investigated, with coincident occurrences between outliers in constituent years and extremes in the other climate phenomena in Section 2.3 being noted for further investigation in Chapter 5.

#### *3.4.1 North American Precipitation – Post-1993 Events*

Composite patterns of central and eastern North American precipitation during 1950-92 were fully documented in MRL98 for TP SSTA events very similar to those represented here by Fig. 2.2 and Fig. 2.3. The full details of these associations are not recited here, but the key composite patterns are reproduced in the present Fig. 3.1.

The following sub-sections document the key consistencies and inconsistencies between the composites based on 1950-92 (and documented in MRL98) and the observed precipitation during the SSTA events that occurred from 1993 through 2000 (listed in Table 2.1 and plotted in Figs. 3.2-3.5), and further note where the impact of other climate phenomena can help explain any outliers in the events from 1993 through 2000. This comparison occurs through visual inspection of the maps of individual monthly precipitation anomalies during November-March 1993-2000 (calendar months during which precipitation anomalies were significantly related to SSTA VPC1 in MRL98) for the structures evident in the MRL98 1950-92 composites. The comparison here of the precipitation anomalies during the 1997-98 El Niño to the 1950-92 composites in MRL98 is an extension of the “Note Added in Proof” in that paper, which was based on lower-resolution Climate Division data (NCDC 2005) that were immediately available at the time.

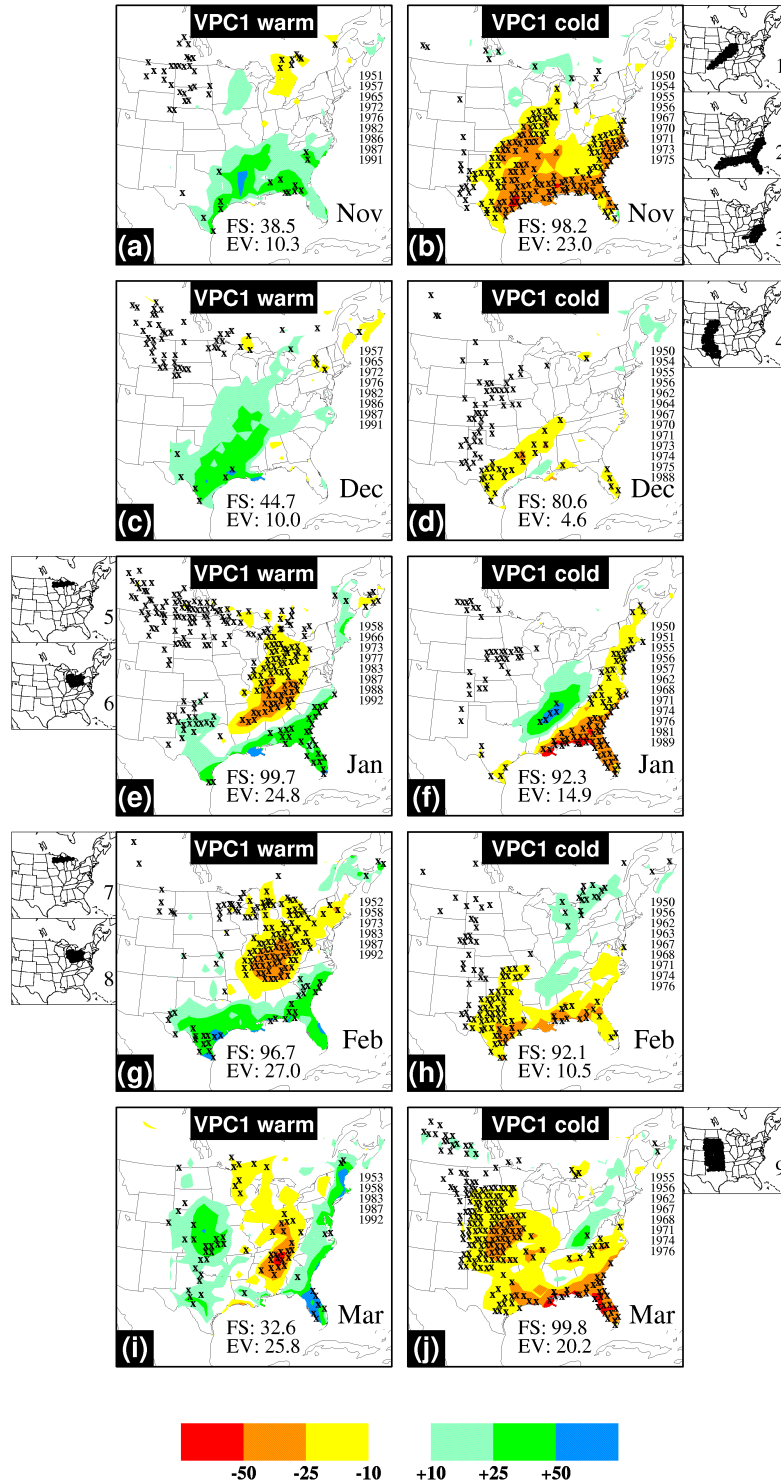


Fig. 3.1: Composite monthly precipitation anomalies (mm) for warm (left column) and cold (right column) SSTA VPC1 events during November-March for 1950-92. Constituent years of each composite are listed on right side of each panel. Maps on side of each panel delineate areas for which regional statistical significance was computed and presented, as in Table 3.1 below. (Taken from Montroy et al. 1998; their Fig. 4)

Region	Location	Time period	Warm events			Cold events		
			CA	FR	SIG	CA	FR	SIG
1	Oklahoma–Illinois	Nov	1.8	5/9	13.7	<b>-21.6</b>	<b>7/9</b>	<b>99.0</b>
2	Atlantic and Gulf of Mexico coast	Nov	23.2	7/9	93.2	<b>-31.8</b>	<b>9/9</b>	<b>100.0</b>
3	Southern Atlantic coast	Nov	16.2	7/9	78.1	<b>-24.8</b>	<b>9/9</b>	<b>99.9</b>
4	Texas to Nebraska	Dec	14.1	5/8	82.5	<b>-6.3</b>	<b>12/13</b>	<b>99.3</b>
5	Northern Wisconsin–Michigan	Jan	<b>-7.0</b>	<b>7/8</b>	<b>97.7</b>	-1.8	8/12	24.7
6	Lake Erie region	Jan	<b>-16.1</b>	<b>8/8</b>	<b>99.9</b>	3.3	6/12	28.1
7	Northern Wisconsin–Michigan	Feb	<b>-11.6</b>	<b>6/6</b>	<b>99.5</b>	5.2	6/9	61.6
8	Lake Erie region	Feb	<b>-18.7</b>	<b>6/6</b>	<b>98.2</b>	7.4	6/9	62.3
9	Central plains	Mar	19.0	5/5	93.2	<b>-18.2</b>	<b>8/8</b>	<b>99.9</b>

Table 3.1: Statistics for monthly average precipitation anomalies over selected regions in composites based on SSTA VPC1, as presented in MRL98 and present Fig. 3.1. Region numbers pertain to shaded areas in small maps along sides of present Fig. 3.1. For warm and cold events, “CA” denotes the composite regional precipitation anomaly (mm), “FR” the fraction of composite members for which the regional mean anomaly has the same sign as the overall composite anomaly (CA), and “SIG” is the regional significance level. Boldface entries have regional significance above 95%. (Taken from Montroy et al. 1998; their Table 1)

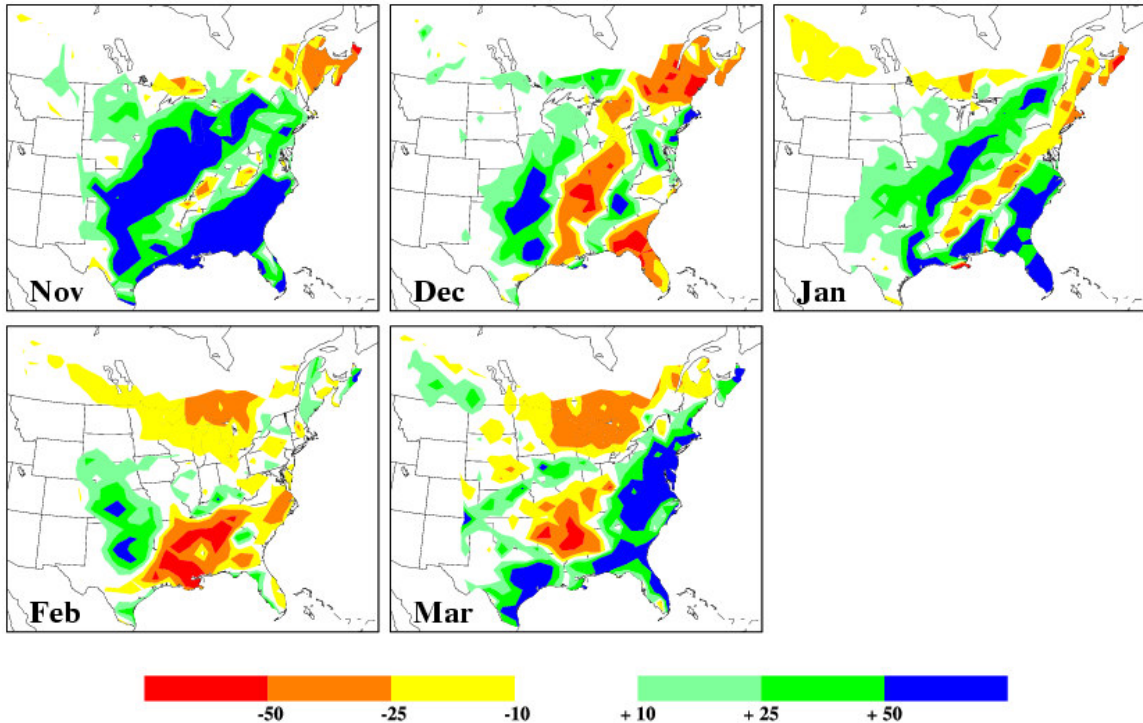


Fig. 3.2: Observed precipitation anomalies (mm) for individual months for November 1992–March 1993.

#### 3.4.1.1 EL NIÑO 1992-93

Most of the key features of the November-March MRL98 warm SSTA VPC1 event precipitation composites are reflected in the observed November 1992-March 1993 precipitation anomalies. Fig. 3.2 shows that during each month except for February, spatially extensive above normal precipitation occurred over parts of the southern and southeastern U.S. in similar locations as positive composite precipitation anomalies in MRL98's warm SSTA VPC1 event composites (Fig. 3.1). Additionally, a narrow band of below normal precipitation was observed along the western edge of the Appalachian Mountains from northern Mississippi to the mid-Atlantic coast to Maine, matching a similar feature in MRL98's composite. Further, below normal precipitation was observed in south-central Canada during January 1993 in a similar location as a coherency of negative precipitation anomalies in MRL98's composite. The intraseasonal evolution of the 1992-1993 precipitation anomalies in southern Canada also supports the association with TP SSTAs. MRL98's composite (Fig. 3.1a,c,e) indicates below normal precipitation in south central Canada during November-January is associated with warm eastern TP SSTAs. During November 1992-January 1993, only January was classified as a warm SSTA VPC1 event (Table 2.2) and only in January 1993 was below normal precipitation observed in south-central Canada.

There were two notable differences between the MRL98 composite features and observed precipitation from November 1992-March 1993. The negative composite anomalies in MRL98's composite around the Great Lakes region in January (Fig. 3.1e) did not have a corresponding negative observed anomaly during January 1993, as a wide band of above normal precipitation was observed from Arkansas to Indiana to New York state (Fig. 3.2), although the feature is present in February and March. Also, the February 1993 precipitation anomalies were generally characterized by positive precipitation anomalies only in Texas-Oklahoma and not along the Atlantic and Gulf of Mexico coasts (Fig. 3.2) as indicated in MRL98's composite. Further, the negative observed precipitation anomalies centered over Louisiana and Mississippi were located farther south than indicated by the MRL98 composites (Fig. 3.1g).

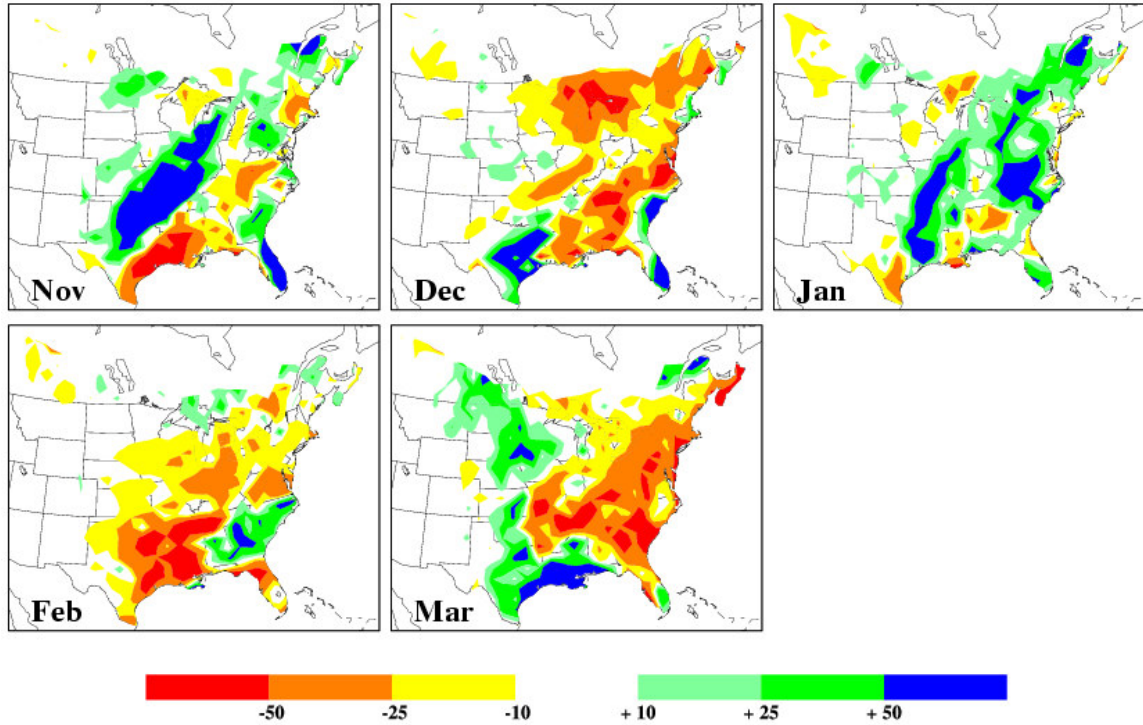


Fig. 3.3: As in Fig. 3.2 but for November 1994-March 1995.

#### 3.4.1.2 EL NIÑO 1994-95

The observed precipitation anomalies during November 1994-January 1995 are very inconsistent with MRL98's composite anomalies. Fig. 3.3 indicates below normal November 1994 precipitation was observed over the southeastern U.S. region where MRL98's composite had positive anomalies (Fig. 3.1a), with similar differences holding for December precipitation (Fig. 3.1c). Precipitation anomalies in January 1995 were positive in parts of Florida and the Carolinas/mid-Atlantic coast as in MRL98's composites (Fig. 3.1e); however, negative anomalies were not observed around Kentucky and Tennessee, but instead occurred farther south in Louisiana-Mississippi-Alabama (Fig. 3.3).

The inconsistency of the winter of 1994-95 with the warm SSTA VPC1 event composites of MRL98 could be associated with a low index phase of the PDO. For example, none of the eight Januarys used to create the 1950-92 composite in MRL98 (Fig. 3.1e) were characterized by a strong low index phase of the PDO. However, this

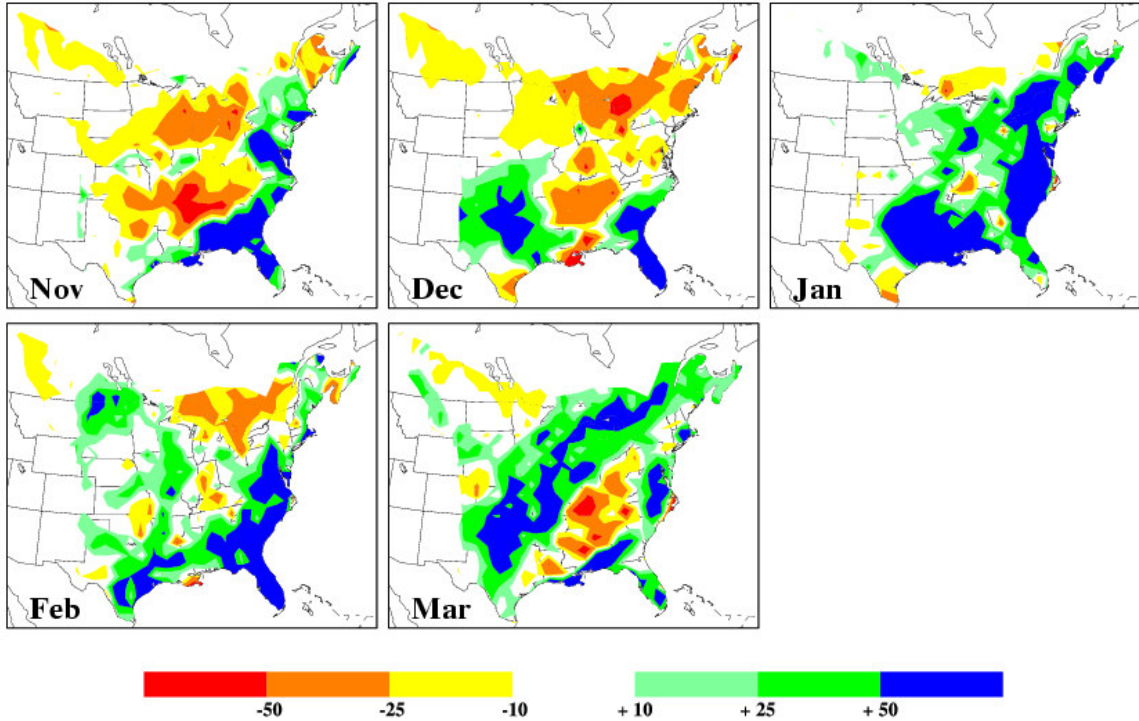


Fig. 3.4: As in Fig. 3.2 but for November 1997-March 1998.

characterized January 1995 (Table 2.2), and low index phases of the PDO typically produce above normal rainfall in exactly the region indicated by the MRL98 composites to have below normal rainfall (Fig. 2.7b). The roles of these competing climate system processes will be further explored in Chapter 5.

#### 3.4.1.3 EL NIÑO 1997-98

The observed precipitation anomalies during the very strong November 1997-March 1998 El Niño period correspond well with the composite anomalies based on 1950-92 warm SSTA VPC1 events. Fig. 3.4 demonstrates that positive November (December) precipitation anomalies spanned much of the southeast U.S. (southeast and south-central U.S.), consistent with that indicated by the 1950-92 composite anomalies (Fig. 3.1a,c). Further positive anomalies occurred in January-March along the Gulf of Mexico and Atlantic coast, as well as the extension of positive anomalies northward into the southern and central U.S. Great Plains to Kansas, all as in MRL98's warm VPC1 composites. The dry anomalies in south-central Canada (November-January) and (to a

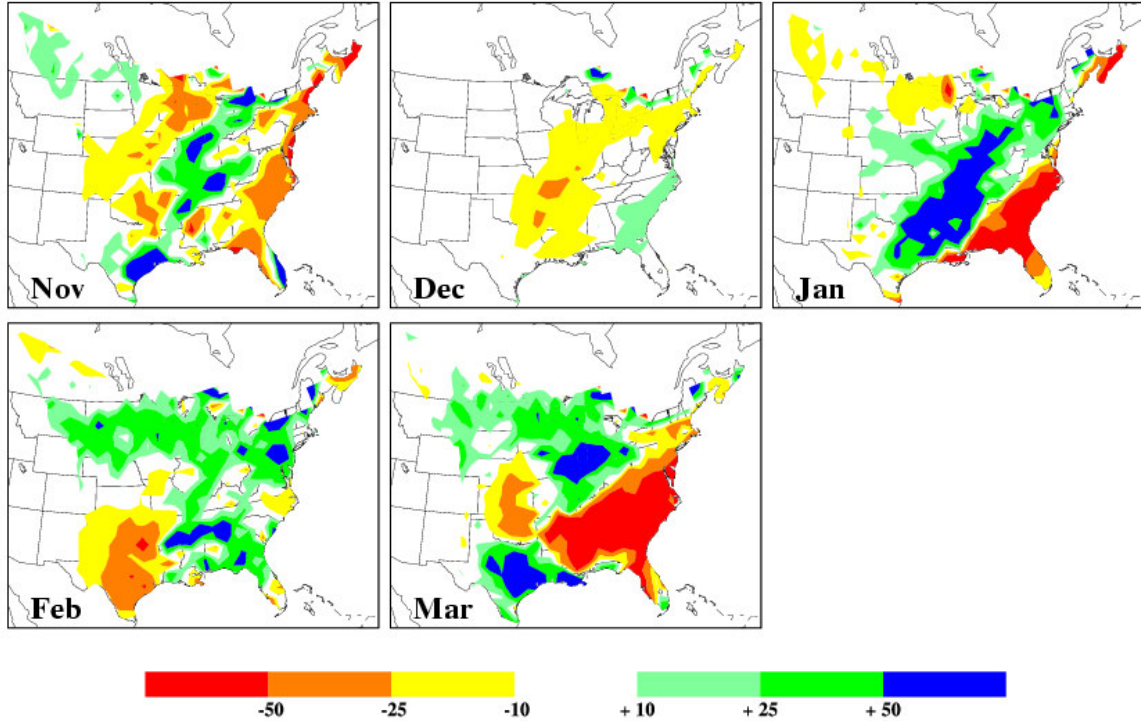


Fig. 3.5: As in Fig. 3.2 but for November 1999-March 2000.

lesser extent) the Ohio River area (January-March, strongest in March) also are present, although the features did seem to develop earlier (November-December) in 1997-98 than in the 1950-92 composite (Fig. 3.1a,c). These results are consistent with those outlined in the preliminary “Note Added in Proof” in MRL98, although the present results provide further confirmation of the south-central Canada association. Additionally, the present results indicate that the wet Gulf-southeast coast/dry inland association evident in observed November-December 1997 precipitation anomalies (which matched the MRL98 composite) also was observed for October 1997 precipitation anomalies.

#### 3.4.1.4 LA NIÑA 1999-2000

The observed anomalies during the November 1999-March 2000 La Niña period correspond very well with the MRL98 composites based on 1950-92 cold TP SSTA events. Fig. 3.5 indicates that negative precipitation anomalies were observed in large areas of the southern U.S. Great Plains and the southeastern U.S for November through March. These drier than normal conditions geographically coincide with the negative

precipitation coherencies in the MRL98 VPC1 cold SSTA composite (Fig. 3.1). Additionally, during January-March, most of the Ohio River valley and far inland areas of the Southeast U.S. observed positive precipitation anomalies, also consistent with the indication in MRL98's composites (Fig. 3.1f,h,i). Further, the lack of below normal precipitation anomalies in December in the immediate eastern Gulf/east coastal areas of the Southeast U.S. matches the features in the MRL98 composites, as does the observation of below normal precipitation in the central U.S. Great Plains in March.

### 3.4.2 *North American Temperature*

The regions of monthly average daily maximum/minimum temperature anomalies exhibiting significant associations with November-March TP SSTA events are summarized in Table 3.2 and documented in the following sections. To check the consistency of the maximum and minimum temperature composites based on warm SSTA VPC1 events, the composites here are (as in MRL98) based on 1950-92, and maximum/minimum temperature patterns characteristic of individual post-1993 SSTA events listed in Table 2.1 are compared with these composite anomalies. The same methodology is used here as for the precipitation data from 1993-2000 in Section 3.4.1. The SSTA composites from 1950-92 are given in Figs. 3.6-3.9 and described first below in this section, with their regional statistics appearing in Tables 3.3-3.4. The anomalies observed during the post-1992 SSTA events are presented in Figs. 3.10-3.13 and are discussed further below in Section 3.4.3.

#### 3.4.2.1 U.S.-CANADIAN BORDER AND SOUTHERN TIER OF U.S. (DECEMBER-APRIL; SSTA VPC1)

Fig. 3.6 shows that during warm SSTA VPC1 (eastern TP) events, many regions of the northern U.S. and southern Canada exhibit warm air temperature anomalies during December-April, when the southern U.S. simultaneously experiences cold anomalies. These opposite associations are concentrated in the northern Great Plains/southern Canadian prairies, versus the U.S. Atlantic coast and Gulf of Mexico coast. While these relationships are broadly similar for both the maximum temperature and minimum temperature fields, there are some notable month-to-month differences in the structure of the composite anomaly fields. The individual regions with coherent composite anomalies

Table 3.2: Summary of regions with monthly anomalies of daily maximum (Tmax) and minimum (Tmin) temperatures significantly associated with TP SSTA events.

Region	Period	SSTA Event Type	Section	Tmax	Tmin
Northern Plains / Southern Canadian Prairies	Dec-Mar	Warm VPC1	3.4.2.1	Strong Warm	Warm with approximately the same magnitude Dec-Jan but warm and stronger in Feb-Mar, extending into Texas, too
Atlantic coast	Dec	Warm VPC1	3.4.2.1	Warm	Warm
Southeast U.S. / Texas	Jan (~Feb)	Warm VPC1	3.4.2.1	Strong Cool	Strong Cool
Southeast U.S.	Apr	Warm VPC1	3.4.2.1	Cool	Stronger Cool and extend into TX/OK/IL
Mid-Atlantic	Apr	Warm VPC1	3.4.2.1	Cool	None
Central U.S.	Oct-Nov	Warm VPC1	3.4.2.2	Cool	Only weak in Nov, somewhat in the Northeast
Southern Plains	Dec-Apr	Cold VPC1	3.4.2.1	Warm	Barely present
U.S.-Canada border	Feb-May	Cold VPC1	3.4.2.1	Cool	Cool

also have high regional significance, as shown in Table 3.3. Further, these associations have a high degree of nonlinearity compared to the composite anomalies associated with cold SSTA VPC1 events (Fig. 3.7). The details of these associations are now summarized here.

Fig. 3.6 suggests that the generally warm conditions that occur in southern Canada and the northern U.S. during warm SSTA VPC1 events are reflected in both the maximum and minimum temperature fields in almost every calendar month from December through March. Coherent positive anomalies with high local significance are present in all months from December through February in the northern U.S. Great Plains and southern Canadian prairies. The field significance of these composites is relatively high in all months, especially for maximum temperature in December-January and minimum temperature in February-April. Furthermore, the months that do not have high field significances have composite anomalies with a broadly similar structure to that of months with high field significance. In the northern Great Plains, the association has high local and regional significance for both maximum and minimum temperatures. For example, the North Dakota region has regional significance above 99% for the December-February period as a whole and above 90% in all individual months, except

for January maximum temperatures (Table 3.3). This North Dakota association is especially strong in minimum temperatures in February-March and also extends farther southeast into eastern Colorado and northwest Texas in February (Fig. 3.6f) and southeast to northern Missouri/Illinois for March (Fig. 3.6h). The considerable strength of the minimum temperature associations in February-March is further supported by the high regional significances for those areas (e.g., 96.6% in east Colorado-western Kansas, 99.7% in Minnesota-Wisconsin for minimum temperatures; Table 3.3).

The geographical location and seasonal timing of the generally warm conditions in southern Canada and the northern U.S. Great Plains during warm SSTA VPC1 events suggest a possible physical land-atmosphere interaction with the negative precipitation association identified for the same area by MRL98. MRL98 found that November-January precipitation in south-central Canada and the northern U.S. Great Plains typically is below normal during warm SSTA VPC1 events. Reduced precipitation in this area leads to reduced snow depth and ground cover during those months. With such reduced snow cover, as temperatures warm in February-March, the snow cover will disappear more rapidly than otherwise would be the case. Normally, more prolonged snow cover would help keep minimum temperatures low due to the additional cooling from increased outgoing longwave radiation (compared to vegetative cover or other non-frozen ground cover) and reflection of incoming short-wave radiation. But if the snow cover disappears, this would reduce nighttime cooling in February-March as suggested by Fig. 3.6e,g. This association will be further utilized in Chapter 5 when the physical associations between North American climate patterns and TP SSTAs are explained in more depth.

December daily maximum temperatures in the mid-Atlantic region and northeast U.S. also are significantly related to warm SSTA VPC1 events. Positive maximum temperature anomalies with high local significance span much of the Northeast and Atlantic coast for December (Fig. 3.6a). Furthermore, positive daily minimum temperature anomalies also are widespread there, albeit while only locally significant at scattered stations. However, the maximum temperature anomalies also have high regional significance, as shown in the examples of the Three Rivers (96.7%), Chesapeake Bay (98.4%), and western Pennsylvania (98.4%) regions (Table 3.3).

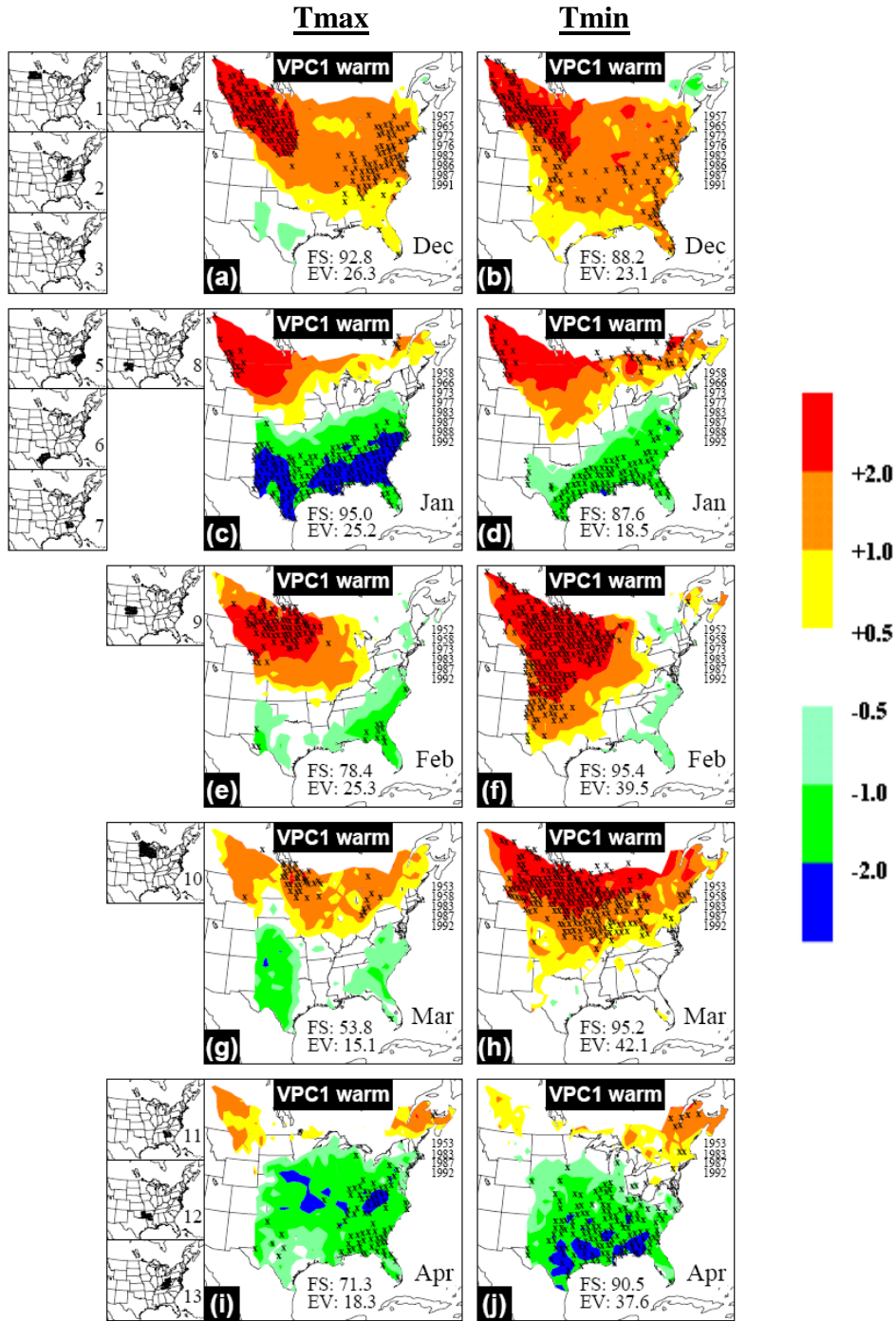


Fig. 3.6: Composite monthly averaged daily temperature anomalies ( $^{\circ}\text{C}$ ) for warm SSTA VPC1 events during 1950-92 for December-April. Color shading follows scale at right. Left (right) column gives anomalies in daily maximum (minimum) temperature. An “X” is plotted at stations where the composite value is significantly different from zero at the 90% level. Field significances (FS) and explained variances (EV) appear at the bottom of each panel in %, and constituent years of composites are listed at right of each panel. Small maps at sides locate numbered regions in Table 3.3.

Table 3.3: Statistics for monthly averaged daily maximum (Tmax) and minimum (Tmin) temperature anomalies over selected regions in composites based on warm SSTA VPC1 events presented in Fig. 3.6. Numbered regions are delineated in small side maps in Figs. 3.6 (1-13) and 3.8 (14-17). For maximum and minimum temperature, “CA” denotes the composite regional temperature anomaly (°C), “FR” the fraction of composite members for which the regional mean anomaly has the same sign as the overall composite anomaly (CA), and “SIG” is the regional significance level. Boldface entries have regional significance above 90%.

Region #	Location	Time Period	Figure	Tmax			Tmin		
				CA	FR	SIG	CA	FR	SIG
1	North Dakota	Dec-Feb	Fig. 3.6	<b>2.08</b>	<b>8/11</b>	<b>99.0</b>	<b>2.50</b>	<b>8/11</b>	<b>99.2</b>
		Dec		<b>2.23</b>	<b>8/11</b>	<b>97.9</b>	<b>2.37</b>	<b>8/11</b>	<b>97.7</b>
		Jan		1.99	8/11	87.4	<b>2.35</b>	<b>7/11</b>	<b>92.1</b>
		Feb		<b>1.92</b>	<b>7/11</b>	<b>95.7</b>	<b>2.67</b>	<b>7/11</b>	<b>96.3</b>
2	Three Rivers	Dec	Fig. 3.6	<b>1.35</b>	<b>7/10</b>	<b>96.7</b>	<b>1.61</b>	<b>9/10</b>	<b>97.2</b>
3	Chesapeake Bay	Dec	Fig. 3.6	<b>1.20</b>	<b>9/10</b>	<b>98.4</b>	<b>1.26</b>	<b>9/10</b>	<b>97.4</b>
4	Western Pennsylvania	Dec	Fig. 3.6	<b>1.50</b>	<b>9/10</b>	<b>98.4</b>	<b>1.51</b>	<b>9/10</b>	<b>96.5</b>
5	Carolinas	Jan	Fig. 3.6	<b>-1.47</b>	<b>7/11</b>	<b>95.6</b>	-0.56	7/11	58.6
6	Southeast Texas	Jan	Fig. 3.6	<b>-1.31</b>	<b>9/11</b>	<b>95.2</b>	-0.93	8/11	89.9
7	Northern Georgia	Jan	Fig. 3.6	<b>-1.46</b>	<b>7/11</b>	<b>96.0</b>	-0.65	7/11	65.2
8	Western Texas	Jan	Fig. 3.6	<b>-1.86</b>	<b>9/11</b>	<b>99.7</b>	-0.12	6/11	19.2
9	East Colorado-Western Kansas	Feb	Fig. 3.6	-0.39	4/8	29.9	<b>1.78</b>	<b>7/8</b>	<b>96.6</b>
10	Minnesota-Wisconsin	Mar	Fig. 3.6	0.90	5/7	86.1	<b>2.06</b>	<b>6/7</b>	<b>99.7</b>
11	Northern Georgia	Apr	Fig. 3.6	<b>-1.48</b>	<b>6/6</b>	<b>99.6</b>	<b>-1.22</b>	<b>5/6</b>	<b>97.1</b>
12	Eastern Oklahoma-Arkansas	Apr	Fig. 3.6	-1.14	5/6	79.9	<b>-1.58</b>	<b>6/6</b>	<b>99.9</b>
13	Three Rivers	Apr	Fig. 3.6	<b>-1.44</b>	<b>6/6</b>	<b>99.1</b>	-0.40	4/6	84.8
14	Southern Minnesota	Oct-Nov	Fig. 3.8	<b>-1.15</b>	<b>9/12</b>	<b>99.3</b>	-0.49	8/12	72.6
		Oct		<b>-1.05</b>	<b>10/12</b>	<b>99.1</b>	-0.41	4/12	63.3
		Nov		<b>-1.25</b>	<b>9/12</b>	<b>93.2</b>	-0.58	6/12	61.6
15	Eastern Nebraska	Oct-Nov	Fig. 3.8	<b>-1.32</b>	<b>10/12</b>	<b>99.6</b>	-0.19	7/12	35.5
		Oct		<b>-1.37</b>	<b>10/12</b>	<b>99.7</b>	-0.17	4/12	31.4
		Nov		<b>-1.27</b>	<b>9/12</b>	<b>95.7</b>	-0.20	6/12	27.3
16	Northern Texas	Oct-Nov	Fig. 3.8	<b>-1.04</b>	<b>9/12</b>	<b>97.3</b>	-0.43	9/12	74.7
		Oct		<b>-0.82</b>	<b>8/12</b>	<b>90.8</b>	-0.49	8/12	79.7
		Nov		<b>-1.27</b>	<b>9/12</b>	<b>95.7</b>	-0.36	8/12	49.8
17	Western Texas	Oct-Nov	Fig. 3.8	<b>-1.12</b>	<b>8/12</b>	<b>97.9</b>	-0.17	8/12	38.2
		Oct		-0.69	8/12	88.0	-0.06	5/12	13.9
		Nov		<b>-1.57</b>	<b>8/12</b>	<b>97.9</b>	-0.28	8/12	46.7

In the southern U.S., anomalously cold conditions generally are associated with warm TP SSTA VPC1 events primarily in January and (to a lesser extent) February-March. Fig. 3.6 shows that the composite temperature fields for both maximum and minimum temperatures exhibit locally significant anomalies over a wide area from Texas to the southern Atlantic coast in January, with both fields having high field significances (95.0% for maximum temperature and 87.6% for minimum temperature). The associations are strong for both daily maximum and minimum temperatures; however, the anomalies are more extensive in Texas and the southern Great Plains in daily maximum temperatures than in minimum temperatures. This is further reflected in the regional significance of the western Texas region (99.7% for maximum temperatures vs. 19.2% for minimum). Also, Table 3.3 shows that the regional significances for other areas are much higher in maximum temperatures than minimum temperatures – e.g., Carolinas (95.6% in maximum temperatures vs. 58.6% in minimum temperatures), and northern Georgia (96.0% vs. 65.2%). But in southeast Texas, the association has reasonably high regional significance in both maximum temperature (95.2%) and minimum temperature (89.9%).

The above cold association in the southern U.S. during warm SSTA VPC1 events also is physically consistent with the precipitation results in MRL98. They demonstrated that during January-March, warm SSTA VPC1 events are associated with positive precipitation anomalies from Texas to the southern Atlantic coast. Higher monthly precipitation amounts likely are associated with more frequent cloudy days, limiting incoming solar radiation and therefore the daily maximum temperature. The generally cooler daytime temperatures also are associated with cooler minimum temperatures. However, while the daytime clouds help cool the atmosphere, nocturnal cloudiness may reduce radiative cooling, possibly helping explain the relatively weaker composite minimum temperature anomalies. This issue will be explored further in Chapter 5.

Contrasting the above results from Fig. 3.6 with the cold VPC1 SSTA patterns in Fig. 3.7 illustrates strong nonlinear associations between North American daily temperatures and TP SSTAs. Negative (positive) maximum temperature anomalies in the central and southern Great Plains during December-March are locally significant for

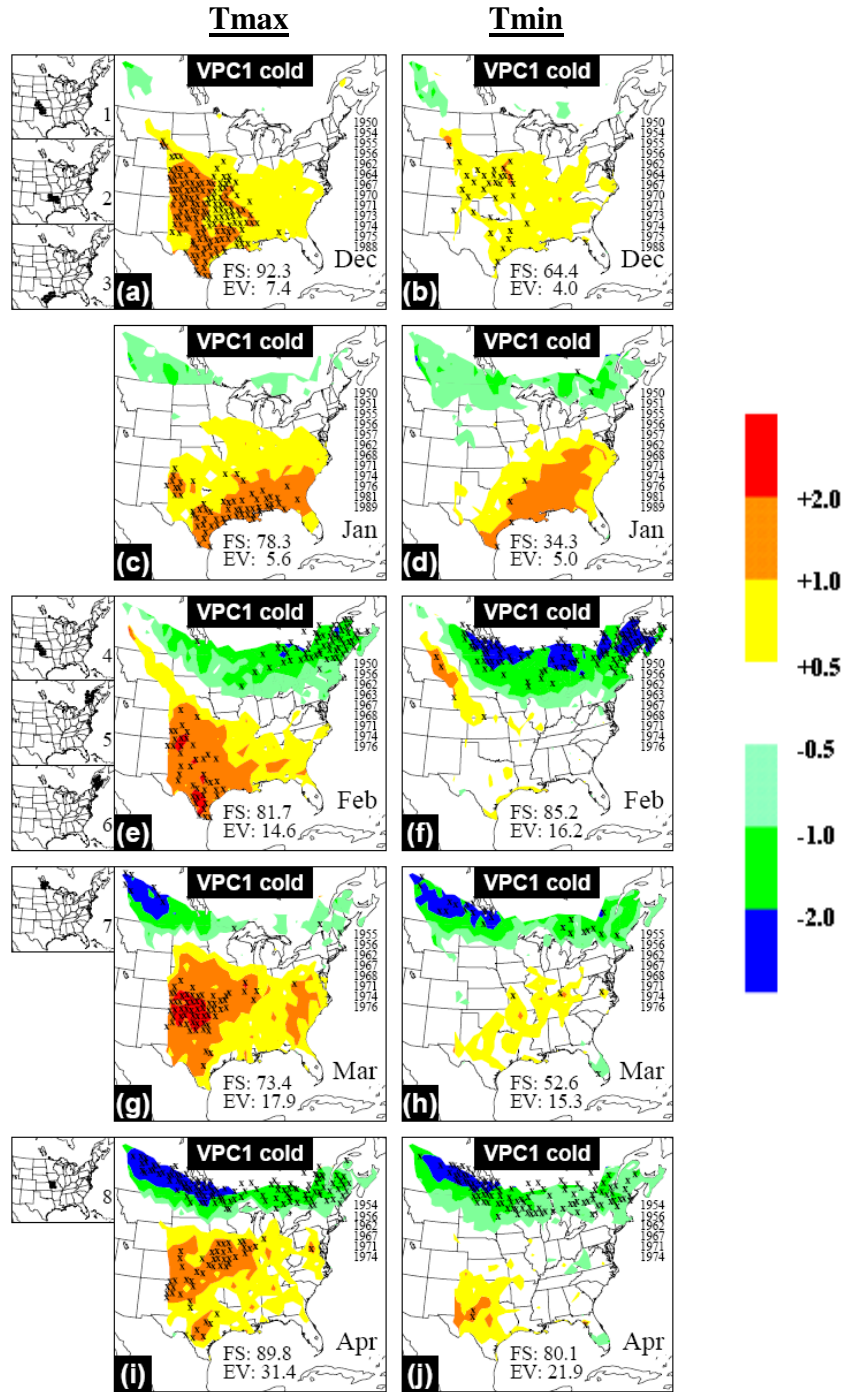


Fig. 3.7: As in Fig. 3.6, but for cold SSTA VPC1 events. Small maps at sides locate numbered regions in Table 3.4.

Table 3.4: As in Table 3.3, but for cold SSTA VPC1 events. Numbered regions are delineated in the small side maps in Figs. 3.7 (1-8) and 3.9 (9-12).

Region #	Location	Time Period	Figure	Max			Min		
				CA	FR	SIG	CA	FR	SIG
1	Western Kansas-Oklahoma	Dec	Fig. 3.7	<b>1.71</b>	<b>10/12</b>	<b>99.9</b>	<b>0.59</b>	<b>9/12</b>	<b>90.9</b>
2	Eastern Oklahoma-Arkansas	Dec	Fig. 3.7	<b>0.93</b>	<b>9/12</b>	<b>97.1</b>	0.50	8/12	71.6
3	Southeast Texas	Dec-Feb	Fig. 3.7	<b>1.03</b>	<b>9/12</b>	<b>98.6</b>	0.63	7/12	86.2
		Dec		<b>1.22</b>	<b>9/12</b>	<b>99.3</b>	0.62	8/12	83.4
		Jan		0.82	8/12	82.7	0.60	8/12	63.2
		Feb		1.04	8/12	88.1	0.69	6/12	72.3
4	Western Kansas-Oklahoma	Feb-Mar	Fig. 3.7	<b>1.95</b>	<b>9/10</b>	<b>99.9</b>	-0.04	6/10	8.5
		Feb		<b>1.49</b>	<b>6/10</b>	<b>90.2</b>	-0.15	6/10	25.8
		Mar		<b>2.38</b>	<b>10/10</b>	<b>100.0</b>	0.08	5/10	13.2
5	Southern Quebec	Feb-Apr	Fig. 3.7	<b>-0.75</b>	<b>5/7</b>	<b>92.0</b>	-0.94	6/7	88.8
		Feb		-1.14	4/7	83.1	-1.46	4/7	85.3
		Mar		-0.52	5/7	55.3	-1.14	4/7	70.4
		Apr		-0.59	6/7	68.7	-0.20	3/7	34.7
6	Maine-New Brunswick	Feb-Apr	Fig. 3.7	<b>-0.67</b>	<b>6/7</b>	<b>91.5</b>	-0.90	6/7	88.8
		Feb		-1.06	5/7	88.0	<b>-1.52</b>	<b>4/7</b>	<b>91.2</b>
		Mar		-0.47	5/7	53.7	-1.00	4/7	69.5
		Apr		-0.47	5/7	70.8	-0.17	4/7	34.0
7	Southern Manitoba	Mar-Apr	Fig. 3.7	<b>-1.22</b>	<b>7/10</b>	<b>93.8</b>	<b>-1.51</b>	<b>9/10</b>	<b>99.4</b>
		Mar		<b>-1.62</b>	<b>9/10</b>	<b>96.0</b>	<b>-2.51</b>	<b>9/10</b>	<b>99.0</b>
		Apr		-0.80	6/10	57.7	-0.48	6/10	47.5
8	Western Missouri	Apr	Fig. 3.7	<b>1.76</b>	<b>6/6</b>	<b>98.7</b>	0.64	4/6	58.9
9	Southern Minnesota	Oct-Nov	Fig. 3.9	0.56	7/11	79.0	0.35	7/11	60.4
		Oct		0.97	7/11	88.0	0.70	9/11	81.3
		Nov		0.13	7/11	16.4	-0.01	3/11	2.0
10	Eastern Nebraska	Oct-Nov	Fig. 3.9	0.47	6/11	72.5	0.19	4/11	42.5
		Oct		0.75	7/11	73.2	0.42	6/11	67.1
		Nov		0.19	6/11	25.4	-0.04	5/11	7.1
11	Northern Texas	Oct-Nov	Fig. 3.9	0.59	8/11	89.8	-0.03	7/11	8.7
		Oct		0.57	7/11	77.6	0.32	6/11	57.1
		Nov		0.62	7/11	82.6	-0.39	7/11	63.2
12	Western Texas	Oct-Nov	Fig. 3.9	<b>0.92</b>	<b>8/11</b>	<b>96.9</b>	-0.11	6/11	33.0
		Oct		<b>0.97</b>	<b>9/11</b>	<b>94.5</b>	0.03	6/11	5.5
		Nov		0.87	9/11	86.7	-0.26	6/11	53.9

warm (cold) eastern TP SSTA events, but the magnitude of the anomalies in southeast Texas is larger for warm TP SSTA events (-1.31°C, Table 3.3) compared to cold TP SSTA events (+0.82°C, Table 3.4). Further, the positive maximum temperature anomalies for December, February, and March in the cold TP SSTA event composites (Fig. 3.7a,e,g) are locally significant, while the corresponding negative anomalies in the warm TP SSTA event composites (Fig. 3.6a,e,g) are not. Similarly, some locally significant positive maximum temperature anomalies covered western Kansas-Oklahoma in the February composite (Fig. 3.7e,g). Table 3.4 shows the regional significance of all

of these anomalies exceeds 90%. However, anomalies at the corresponding stations in the warm TP SSTA event composite, while negative (Fig. 3.6e,g), are not locally significant. Thus, the structure of the temperature anomalies in the composites based on cold TP SSTA events generally differs from that of the anomalies in the corresponding composites based on warm TP SSTA events (Fig. 3.6).

Fig. 3.6 and Table 3.3 additionally suggest that widespread negative temperature anomalies span much of the southeast U.S. in April during warm SSTA VPC1 events after appearing in smaller geographical areas in March. Negative April daily maximum and minimum temperature anomalies span much of the area from South Dakota to New York and southward to the Gulf coast (Fig. 3.6i-j), with the most stations with high locally significant anomalies being in the minimum temperature composite, which has a high field significance (90.5%) and explains over 37% of the variance in April minimum temperatures. In parts of Georgia-Alabama, the relationship is present for both daily maximum and minimum temperatures, as shown by the high regional significance of the northern Georgia area in both fields (99.6% and 97.1%; Table 3.3). But, in other areas, the minimum temperature composite is the only field with high regional significance (e.g., eastern Oklahoma-Arkansas 79.9% for maximum temperatures vs. 99.9% for minimum; Table 3.3). Only scattered areas have higher regional significance in the maximum temperatures compared to minimum temperatures (e.g., Three Rivers, 99.1% vs. 84.8%; Table 3.3). The negative daily maximum temperature anomalies span a larger geographical area in the April composite than in the March composite (Fig. 3.6g-h), where smaller coherencies of negative temperature anomalies cover the middle and southern Atlantic states and parts of the southern Plains but are not locally significant.

Comparing Fig. 3.7 with Fig. 3.6 shows that in the central and southern Great Plains from February-April, both maximum and minimum temperatures are nonlinearly related to eastern TP SSTAs. During warm SSTA VPC1 events, locally significant minimum temperature anomalies in February are limited to Kansas and western Texas only (Fig. 3.6f), while during cold SSTA VPC1 events, locally significant warm anomalies also reach from Texas to Kansas in February and cover much of western Kansas and Oklahoma in March (Fig. 3.7f,h). In April, while cool maximum temperature

anomalies span nearly all of the central plains in the cold VPC1 composites (Fig. 3.7i), they are not locally significant, while in the corresponding warm event composite, warm anomalies are locally significant from northwest Texas to western Missouri (Fig. 3.7i). The February-March maximum temperature anomalies over western Kansas-Oklahoma have high regional significance for that entire season and for the individual months (99.9% for February-March, 90.2% for February, 100% for March; Table 3.4), as do the April maximum temperature anomalies in western Missouri (98.7%; Table 3.4).

In contrast, during the same February-April period, temperature anomalies along the U.S.-Canadian border have a generally linear relationship with eastern TP SSTAs with fewer nonlinear characteristics. Fig. 3.7 shows that cold maximum and minimum temperature anomalies span large stretches of the U.S.-Canadian border in the individual monthly composites for February-April, while warm maximum and minimum temperature anomalies are present there in the warm SSTA VPC1 composites (Fig. 3.6e-j). Also, the coherency in southern Manitoba in March-April does have high regional significance in March for both maximum and minimum temperatures (Table 3.4). However, the locally significant anomalies are more spatially extensive for the cold SSTA VPC1 composites, covering southeastern Canada in February and much of the U.S.-Canadian border in April. Table 3.4 also shows that the regional significance of the temperature anomalies in southern Quebec and Maine-New Brunswick is not high in any individual month. Consistent with the above results, the monthly average daily temperature anomalies along the U.S.-Canadian border generally have linear associations with TP SSTAs, but the areas with the highest statistical significance vary.

#### 3.4.2.2 GREAT PLAINS (OCTOBER-NOVEMBER, SSTA VPC1)

October and November daily maximum temperatures in portions of the Great Plains exhibit a broadly linear association with eastern TP SSTAs, with highest statistical significance during warm SSTA events. In both the October and November warm SSTA composite (Fig. 3.8a,c), positive anomalies cover much of the U.S. Great Plains from Texas to Minnesota-Wisconsin, with field significance above 95% for both months. Further, the composite anomalies during warm SSTA events for southern Minnesota and eastern Nebraska have high regional significance (above 99% in the October-November

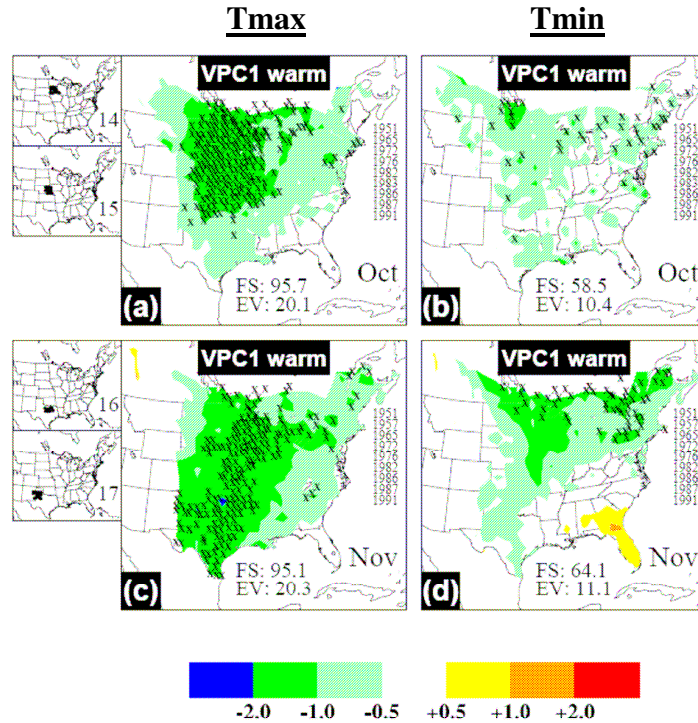


Fig. 3.8: As in Fig. 3.6 but for October-November for warm SSTA VPC1 events. Numbers in side maps locate regions numbered in Table 3.3.

combined statistics) and only 2 or 3 years (out of 12) where the sign of the anomaly in the individual year does not match that of the composite anomaly (Table 3.3). In the daily maximum temperature composites based on cold SSTA VPC1 events, negative daily October maximum temperature anomalies are present in the same region that exhibited positive daily maximum temperature anomalies in the warm SSTA VPC1 composite, but are not locally significant (Fig. 3.9a). During November, negative anomalies of monthly average daily maximum temperature are present in Texas only (Fig. 3.9c), with regional significance of 86.7% (Table 3.4). This indicates that the monthly average of daily maximum temperature in Texas is somewhat linearly related to TP SSTAs, but November average daily maximum temperature in the central and northern U.S. Plains is nonlinearly related to TP SSTAs.

October and November average daily minimum temperatures are nonlinearly related to TP SSTAs principally in the northeastern U.S. in October and the southeastern U.S. in November. During warm TP SSTA events, negative composite anomalies of

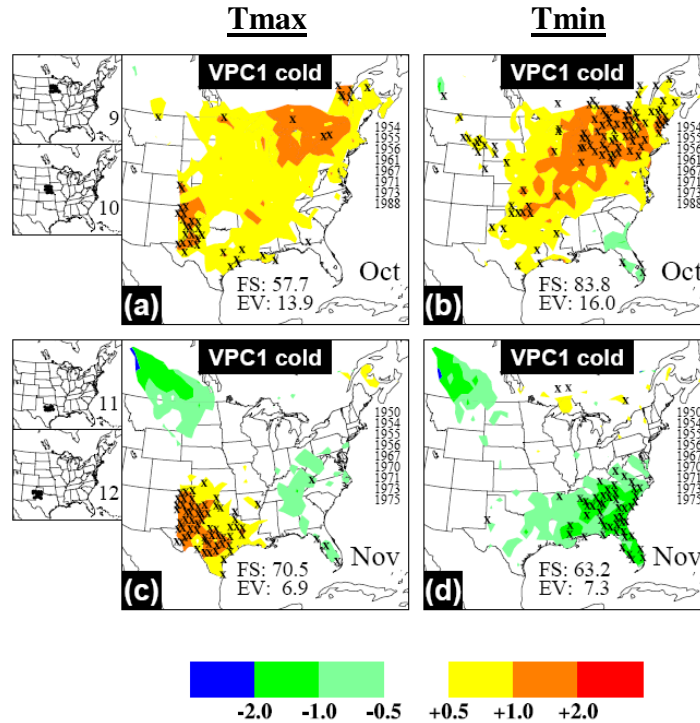


Fig. 3.9: As in Fig. 3.8 but for cold SSTA VPC1 events. Numbers in side maps locate regions numbered in Table 3.4.

monthly average daily minimum temperatures span portions of the northeast U.S. in November only (Fig. 3.8d), while the October composite does not exhibit extensive areas of statistically significant anomalies (Fig. 3.8b). In the counterpart cold TP SSTA event composites (Fig. 3.9b,d), statistically significant positive composite anomalies cover the Great Lakes and northeastern U.S. in October, while the November composite exhibits negative anomalies in the southeastern U.S. Additionally, the structure of these composite anomalies of monthly average daily minimum temperature (Fig. 3.8b,d; Fig. 3.9b,d) differs considerably from the corresponding composites for daily maximum temperatures (Fig. 3.8a,c; Fig. 3.9a,c). Consequently, October (November) average daily minimum temperatures in the northeast (southeast) U.S. are nonlinearly related to TP SSTAs.

### *3.4.3 Comparison of 1950-92 North American Temperature Composites to Post 1993 Events*

Three (one) winter seasons after 1992 were characterized as warm (cold) SSTA VPC1 events and exhibited some interesting similarities with and differences to the above associations derived for 1950-92. Comparisons of each of these events to the warm/cold SSTA VPC1 composites for daily maximum and minimum temperature for December-March (Fig. 3.6) are summarized in the following sections. In all events, at least two months exhibited strong similarities to the warm and cold SSTA VPC1 daily maximum and minimum temperatures composites for 1950-92 events, with the temperature anomalies during the strong 1997-98 El Niño exhibiting the closest similarities to the temperature anomalies for the composite of 1950-92 events.

#### *3.4.3.1 EL NIÑO 1992-93*

The North American temperature anomalies during the 1992-93 El Niño broadly parallel the anomalies in the northern Great Plains in the January and March warm SSTA VPC1 composites, but not in that for February. Fig. 3.10 shows that in January, negative maximum temperature anomalies occurred across much of the U.S. Great Plains, an area also shown to have below normal maximum temperatures during 1950-92 events (Fig. 3.6). Additionally, some positive temperature anomalies were observed across the northern tier of the study domain for January daily maximum (but much less so for daily minimum) and March daily maximum and minimum temperatures, matching that observed during 1950-92 El Niño events (Fig. 3.6c-d,g-h). But key differences with the pre-1992 events are evident in the southern half of the U.S. for January 1993, where no negative daily maximum or minimum temperature anomalies were observed, as the 1950-92 SSTA event composite indicated. Further, the areal extent of the January and March positive temperature anomalies in the northern part of the domain was not as large as indicated in the corresponding warm SSTA VPC1 composite (Fig. 3.6g-h), and the February 1993 daily maximum and minimum temperature anomalies are negative across most of the whole domain, the opposite sign to the February composite anomalies (Fig. 3.6e-f).

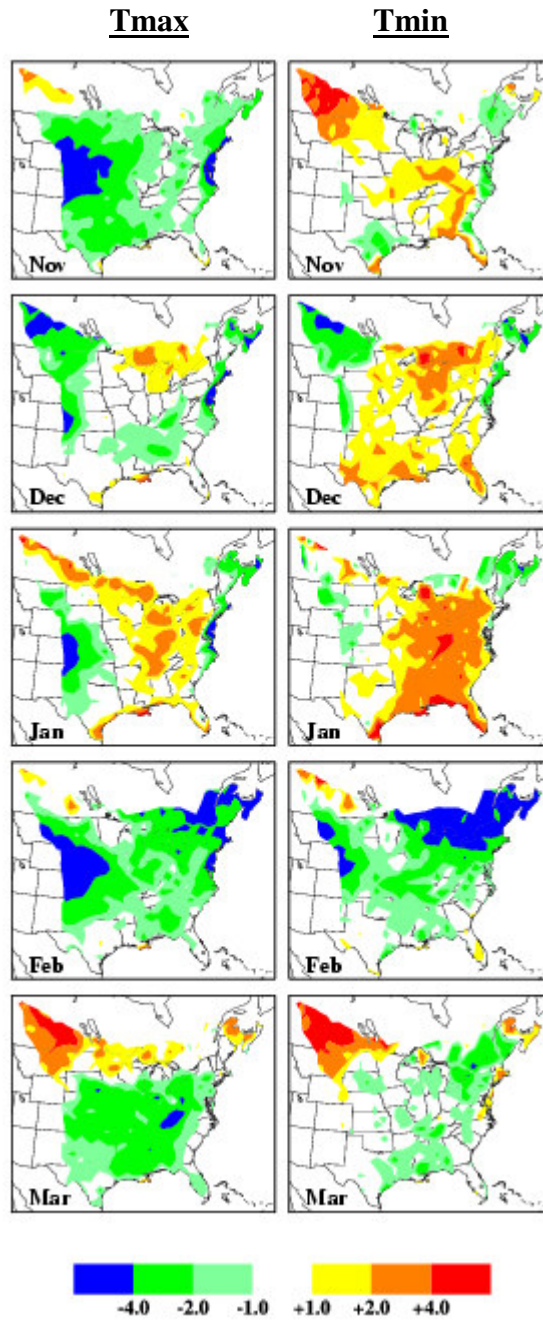


Fig. 3.10: Observed mean daily maximum (left column) and minimum (right column) temperature anomalies ( $^{\circ}\text{C}$ ) for individual months for November 1992 through March 1993.

### 3.4.3.2 EL NIÑO 1994-95

During the warm SSTA VPC1 event from November 1994 through January 1995, the December and January average daily maximum and minimum temperature anomalies had similar spatial coherencies to those in the corresponding 1950-92 composites. Fig. 3.11 shows that large areas of strong positive daily maximum and minimum temperature anomalies spanned much of the domain in December and the northern third of the domain in January, similar to the corresponding composites for those months (Fig. 3.6a-d). The same anomaly pattern characterized November 1994, whereas the counterpart November VPC1 composite shows primarily negative anomalies (Fig. 3.8c-d). However, the large stretch of negative temperature anomalies across the southern part of the domain in the January composite is not present for January 1995, although the positive anomalies are weakest there. In February and March 1995, the positive anomalies are weakest and the negative anomalies are strongest across the southern part of the domain.

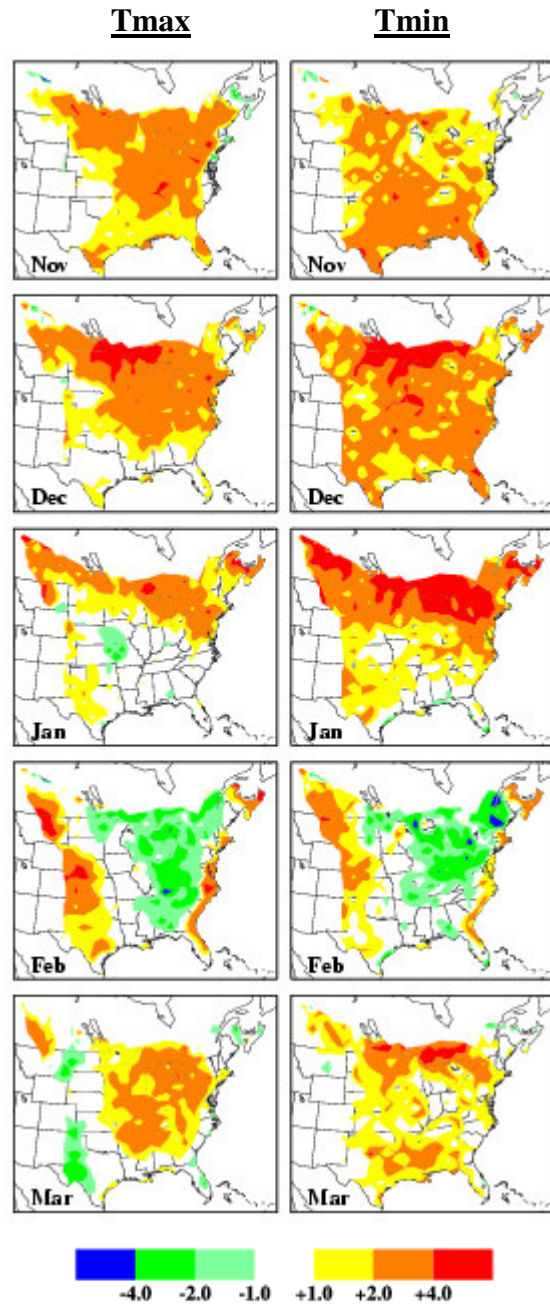


Fig. 3.11: As in Fig. 3.10 but for November 1994 through March 1995.

### 3.4.3.3 EL NIÑO 1997-98

The strong 1997-98 El Niño event featured nearly all of the North American daily temperature anomaly characteristics of the warm 1950-92 SSTA VPC1 event composite.

Fig. 3.12 indicates that warm anomalies in both daily maximum and minimum temperature exceeding 2°C were observed in south central Canada and the northern Great Plains during December, across nearly the entire domain in January, and the northern two-thirds of the domain in February. The daily maximum and (especially) minimum temperature anomalies in March 1998 also exceeded +1°C in a large region centered on the Great Lakes and extending into New England. The maximum temperature anomalies for this month were positive in interior New England but negative in the southern and central U.S. Great Plains. All of these coherencies strongly parallel those in the warm SSTA VPC1 composites (Fig. 3.6), with the sole exception of the negative composite January temperature association from Texas to the Carolinas.

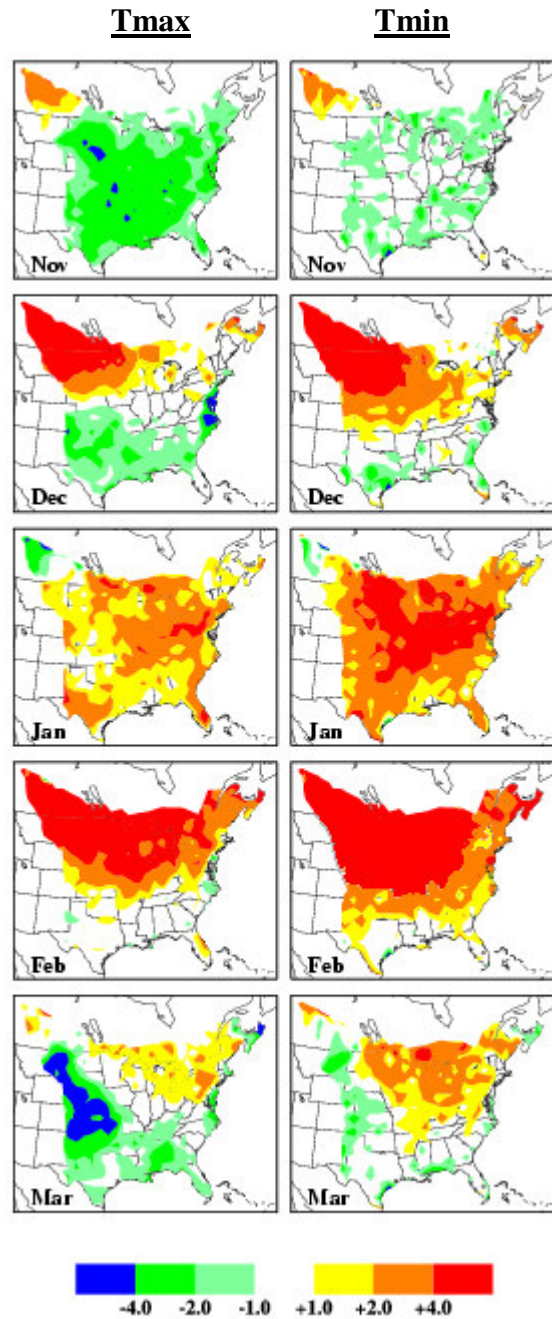


Fig. 3.12: As in Fig. 3.10 but for November 1997 through March 1998.

### 3.4.3.4 LA NIÑA 1999-2000

The observed North American temperature anomalies during the 1999-2000 La Niña event only exhibited temperature anomalies corresponding to the cold SSTA VPC1 composite where the composite indicated warm surface temperature anomalies. Fig. 3.13 indicates that throughout November-March 1999-2000, the monthly average daily maximum and minimum temperature anomalies were above average in much of the eastern two-thirds of North America. The anomalies in monthly average daily maximum temperature are geographically coincident with corresponding positive composite values in the southern Plains in November-March and in the southeastern U.S. in February-March (Fig. 3.7a,c,e,g; Fig. 3.9c). Positive anomalies in monthly average daily minimum temperature correspond to the cold SSTA VPC1 composite only in the central Plains in December and in Texas in January (Fig. 3.7b,d). The observed November-March 1999-2000 temperature anomalies exhibit no negative anomalies corresponding to the negative coherency in the cold SSTA VPC1 composite,

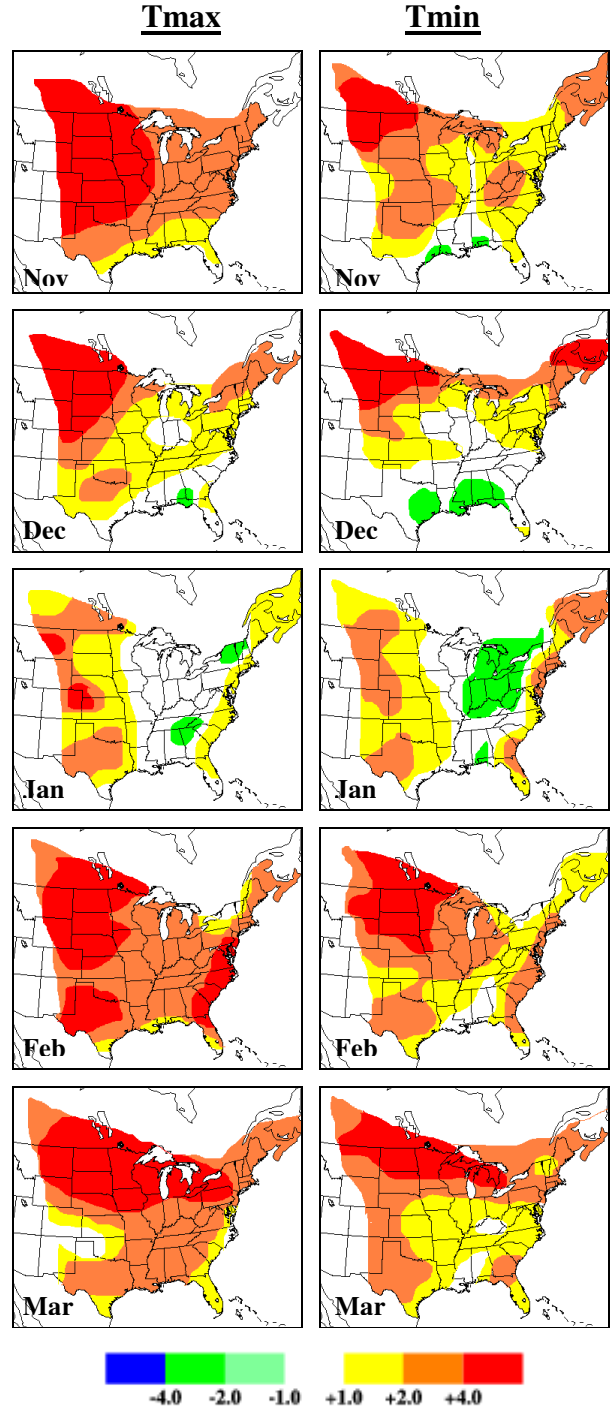


Fig. 3.13: As in Fig. 3.10 but for November 1999 through March 2000.

except in southern Ontario for average daily minimum temperatures in January 2000 (Fig. 3.13).

#### 3.4.4 *Event Consistency*

Now the consistency of the observed precipitation and temperature anomalies between individual TP SSTA events is examined. Specifically, years during which the sign of the observed precipitation or temperature anomaly does not match the sign of the composite anomaly are identified and reconciled with extremes in the other atmospheric phenomena described in Section 2.3. Years that are “exceptions” for multiple regions will be further examined in Chapter 5.

##### 3.4.4.1 NORTH AMERICAN PRECIPITATION

Table 3.5 indicates that the generally wet (dry) conditions along the Atlantic and Gulf of Mexico coasts during warm (cold) SSTA VPC1 events in January-March shown by MRL98 and confirmed further above are characteristic of individual event years except during certain years when the Arctic Oscillation is positive (1967, 1973, 1992). In all seven warm SSTA VPC1 events except 1973 and 1992, the total JFM precipitation anomaly in south Florida exceeded +25 mm. These two years also produced the lowest JFM precipitation total of any SSTA VPC1 event for the Southeast U.S./Central Florida region, and two of the three lowest totals for the North-South Carolina region (Table 3.5). Moreover, every warm SSTA VPC1 event season had at least one heavy precipitation month (anomaly > 75 mm) in south Florida except in 1973 and 1992. During cold SSTA VPC1 events, all JFM precipitation totals in south Florida were below normal with at least one monthly anomaly below -25 mm, except for 1967, a year that also produced the only JFM season among cold SSTA VPC1 events with two above normal precipitation months in the far southeast U.S. and central Florida region. All three of these years during which the sign of the observed anomaly did not match that of the composite anomaly exhibited a positive phase of the Arctic Oscillation (Table 2.2, Fig. 3.14). Consequently, these three years with positive AO were characterized by a suppression of the above average precipitation typically characteristic of warm TP SSTA events.

Table 3.5: Regional averages of station precipitation anomalies (mm) from indicated 1950-92 average for individual months from January through March and seasonal total (JFM) during warm and cold SSTA VPC1 events. Region definitions are provided by small map. Bold (italic) font indicates totals for which the anomaly is greater than +25 mm (less than -25 mm). Second and third columns from left also give JFM average Arctic Oscillation and Pacific Decadal Oscillation index values as defined in Section 2.3. Center highlighted row provides average JFM precipitation totals for 1950-92.



Year	JFM AO	JFM PDO	VPC1 Event	South Florida				Southeast U.S. / Central FL				North and South Carolina			
				Jan	Feb	Mar	JFM	Jan	Feb	Mar	JFM	Jan	Feb	Mar	JFM
1958	-1.04	0.15	Warm	<b>143.8</b>	<i>-28.6</i>	<i>77.2</i>	<b>192.5</b>	-5.0	-7.8	<b>32.2</b>	19.4	7.1	3.9	4.3	15.4
1973	0.39	-0.52	Warm	<b>26.4</b>	5.9	-2.8	<b>29.4</b>	14.3	0.6	<b>70.1</b>	<b>84.9</b>	1.2	<b>37.8</b>	<b>36.0</b>	<b>75.0</b>
1983	-0.19	0.84	Warm	<b>80.3</b>	<b>192.9</b>	<b>57.7</b>	<b>330.9</b>	6.5	<b>66.4</b>	<b>75.3</b>	<b>148.2</b>	0.9	<b>68.0</b>	<b>103.2</b>	<b>172.2</b>
1987	-0.73	1.33	Warm	9.9	-3.4	<b>105.7</b>	<b>112.3</b>	<b>62.0</b>	<b>49.8</b>	<b>44.3</b>	<b>156.2</b>	<b>65.7</b>	24.1	15.2	<b>105.0</b>
1992	0.44	0.13	Warm	-22.6	14.3	0.3	-8.0	<b>70.1</b>	<b>29.1</b>	-14.3	<b>84.9</b>	-9.0	-12.6	-11.8	<i>-33.4</i>
1993	0.66	0.13	Warm	<b>118.1</b>	0.8	22.0	<b>141.0</b>	<b>65.1</b>	-13.7	<b>45.0</b>	<b>96.3</b>	<b>61.1</b>	-13.7	<b>56.7</b>	<b>104.1</b>
1998	-0.36	0.98	Warm	0.6	<b>108.9</b>	<b>50.8</b>	<b>160.4</b>	<b>71.0</b>	<b>89.0</b>	<b>42.5</b>	<b>202.5</b>	<b>74.7</b>	<b>89.0</b>	5.6	<b>169.3</b>
1950-92			Average	<b>53.9</b>	<b>57.1</b>	<b>67.6</b>	<b>178.6</b>	<b>111.0</b>	<b>109.8</b>	<b>128.7</b>	<b>349.4</b>	<b>108.5</b>	<b>98.0</b>	<b>115.3</b>	<b>321.8</b>
1950	0.10	-1.67	Cold	<i>-48.1</i>	<i>-33.0</i>	<i>-22.9</i>	<i>-104.0</i>	<i>-77.8</i>	<i>-63.6</i>	13.6	<i>-127.7</i>	<i>-52.4</i>	<i>-64.4</i>	-18.0	<i>-134.8</i>
1955	-0.71	-0.76	Cold	<i>-13.3</i>	<i>-37.8</i>	<i>-37.8</i>	<i>-89.0</i>	<i>-4.7</i>	<i>-26.9</i>	<i>-97.0</i>	<i>-128.6</i>	-15.8	-23.0	<i>-58.9</i>	<i>-97.7</i>
1956	-0.34	-2.09	Cold	<i>-19.8</i>	<i>-33.9</i>	<i>-55.8</i>	<i>-109.5</i>	<i>-39.1</i>	12.6	-15.8	<i>-42.3</i>	<i>-60.8</i>	<b>46.5</b>	<i>-27.6</i>	<i>-41.9</i>
1962	-0.44	-1.11	Cold	<i>-23.6</i>	<i>-39.8</i>	1.9	<i>-61.5</i>	-6.2	<i>-35.8</i>	7.1	<i>-34.9</i>	<b>31.6</b>	-10.6	<b>30.1</b>	<b>51.1</b>
1967	0.51	-0.53	Cold	<i>-5.9</i>	<i>-1.1</i>	<i>-23.6</i>	<i>-30.6</i>	11.5	3.6	<i>-91.8</i>	<i>-76.7</i>	-11.8	5.3	<i>-67.9</i>	<i>-74.4</i>
1968	0.02	-0.55	Cold	<i>-37.2</i>	3.1	<i>-42.8</i>	<i>-76.9</i>	<i>-56.4</i>	<i>-58.2</i>	<i>-74.1</i>	<i>-188.8</i>	2.8	<i>-66.4</i>	<i>-37.8</i>	<i>-101.4</i>
1971	-0.38	-1.47	Cold	<i>-36.6</i>	<i>-26.6</i>	<i>-54.6</i>	<i>-117.7</i>	<i>-37.2</i>	<b>30.0</b>	12.1	4.9	7.1	23.8	<b>36.9</b>	<b>67.8</b>
1974	-0.20	-1.07	Cold	<i>-23.3</i>	<i>-45.4</i>	<i>-54.6</i>	<i>-123.2</i>	<i>-5.6</i>	-11.2	<i>-25.7</i>	<i>-42.5</i>	1.2	19.3	<i>-28.8</i>	<i>-8.3</i>
1976	0.36	-1.11	Cold	<i>-36.9</i>	3.9	<i>-54.3</i>	<i>-87.2</i>	<i>-25.1</i>	<i>-65.8</i>	-2.2	<i>-93.1</i>	-23.3	<i>-64.1</i>	-15.8	<i>-103.2</i>

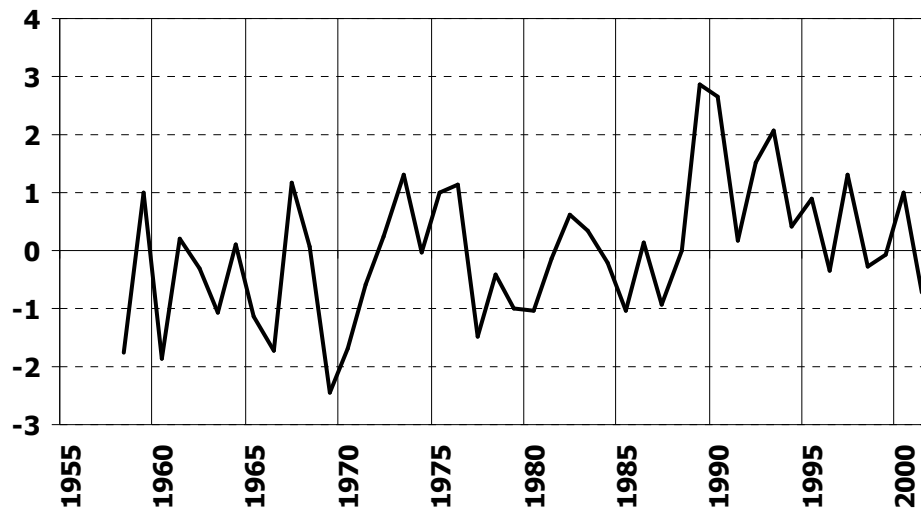


Fig. 3.14: Average of Arctic Oscillation index (standardized units, as defined in Section 2.3.1) for December through March, for 1958-2001. Indicated year corresponds to the January-March of the constituent months.

Table 3.6: As in Table 3.5 but for individual regions during November. Region definitions are rovided by small maps at right.

Year	Nov PDO	VPC1 Event	November					
			Carolinas	Florida	Gulf Coast	Texas	OK-IL Track	
1951	-1.48	Warm	18.3	<b>27.9</b>	21.3	<u>-35.1</u>	-2.4	 North-South Carolina
1957	-0.37	Warm	<b>79.8</b>	<u>-28.2</u>	<b>79.5</b>	<b>69.3</b>	1.2	 Florida
1965	-0.63	Warm	<u>-35.1</u>	<u>-27.6</u>	<u>-37.5</u>	-0.3	<u>-42.9</u>	 Gulf Coast
1972	-0.04	Warm	<b>53.7</b>	<b>85.5</b>	<b>33.3</b>	15.0	<b>38.1</b>	 Texas
1976	0.36	Warm	3.9	13.5	<b>53.7</b>	-11.1	<u>-48.0</u>	 OK-IL Track
1982	0.25	Warm	3.6	8.1	14.4	<b>57.0</b>	18.6	
1986	-0.07	Warm	<b>34.5</b>	1.8	<b>94.5</b>	<b>45.9</b>	-7.5	
1987	-0.73	Warm	12.0	<b>76.8</b>	21.3	<b>51.0</b>	24.9	
1991	-0.14	Warm	<u>-26.4</u>	<u>-32.1</u>	-22.2	-14.4	<b>26.7</b>	
1994	0.24	Warm	9.0	<b>82.2</b>	-23.7	<u>-45.0</u>	<b>62.7</b>	
1997	0.44	Warm	<b>42.6</b>	<b>49.5</b>	<b>104.1</b>	9.0	-9.9	
1950-92		Average	76.5	60.0	99.6	83.1	58.8	
1950	0.10	Cold	<u>-42.3</u>	<u>-27.0</u>	<u>-71.4</u>	<u>-61.8</u>	<u>-33.9</u>	
1954	0.06	Cold	-9.3	<b>31.2</b>	<u>-35.1</u>	-24.3	<u>-42.6</u>	
1955	-0.71	Cold	-21.3	<u>-27.6</u>	<u>-48.6</u>	<u>-58.5</u>	<u>-45.6</u>	
1956	-0.34	Cold	<u>-42.6</u>	<u>-47.4</u>	<u>-69.6</u>	-23.4	-18.6	
1967	0.51	Cold	-9.3	<u>-35.4</u>	<u>-59.7</u>	<u>-38.7</u>	<u>-27.6</u>	
1970	-0.95	Cold	<u>-25.2</u>	<u>-47.4</u>	<u>-55.2</u>	<u>-58.2</u>	<u>-33.0</u>	
1971	-0.38	Cold	-11.1	-8.1	<u>-29.7</u>	-22.2	-13.5	
1973	0.39	Cold	<u>-43.2</u>	-20.1	9.9	<u>-32.1</u>	1.8	
1975	0.27	Cold	-16.5	<u>-25.2</u>	-8.7	<u>-36.9</u>	11.1	

Table 3.6 indicates that the generally dry conditions across much of the southern U.S. shown by MRL98 during cold November SSTA VPC1 events is consistent through all of the individual event years except during some years with negative PDO phase. During 1954, 1971, 1973, and 1975 (especially the latter 3 events), anomalies of the opposite sign of the monthly composite or the smallest in magnitude occur in all regions except Texas. During 1971, 1973, and 1975, November was characterized by the low index phase of the PDO (Table 2.2, Fig. 2.6).

Table 3.7: As in Table 3.5 but for eastern Montana and Southern Alberta-Manitoba region during November-December-January. Note that year refers to the last month (January). For example, the line for 1958 includes data from November 1957, December 1957, and January 1958.

Year	NDJ AO	NDJ PDO	VPC1 Event	Eastern Montana				Southern Alberta-Manitoba			
				Nov	Dec	Jan	NDJ	Nov	Dec	Jan	NDJ
1958	-0.55	-0.14	Warm	0.3	-10.4	-9.9	-20.0	1.6	-7.8	-8.4	-14.7
1966	-0.92	-0.31	Warm	-4.3	-5.6	-1.9	-11.8	14.0	-0.6	5.6	19.0
1973	0.29	-0.02	Warm	-9.6	2.2	-9.6	-17.0	-2.2	0.8	-17.1	-18.4
1977	-0.99	1.20	Warm	0.3	-5.3	7.4	2.4	-10.2	4.5	-5.0	-10.7
1983	0.65	0.21	Warm	-7.1	9.5	-5.3	-2.9	-7.1	-2.0	-7.8	-16.8
1992	0.53	0.20	Warm	2.5	-9.0	-9.3	-15.8	-5.6	0.8	-5.3	-10.0
1998	-0.55	0.78	Warm	-2.8	-7.0	-2.5	-12.3	-11.5	-12.3	5.9	-17.9
1950-92			Average	13.0	11.2	14.0	38.2	17.1	16.5	19.8	53.4
1951	-0.99	-1.26	Cold	-0.6	-1.4	-4.0	-6.1	0.3	-1.4	4.3	3.3
1955	-0.16	0.14	Cold	-10.9	-9.8	-6.8	-27.5	-6.5	-11.8	2.2	-16.1
1956	-0.78	-2.29	Cold	6.5	1.4	-7.1	0.8	11.8	7.0	3.7	22.5
1957	0.25	-1.40	Cold	-1.9	-3.9	0.0	-5.8	-1.6	9.8	-7.4	0.8
1968	0.00	-0.34	Cold	-3.4	3.6	-0.9	-0.7	4.7	8.1	1.6	14.3
1971	0.04	-0.97	Cold	3.1	-2.0	<b>28.5</b>	<b>29.7</b>	6.2	1.7	14.6	22.5
1974	-0.01	-1.00	Cold	5.0	5.9	-4.7	6.2	12.1	9.5	17.7	<b>39.3</b>
1976	0.52	-1.31	Cold	8.7	4.2	-5.3	7.6	-2.5	11.8	-3.4	5.9
1989	0.77	-0.34	Cold	-4.7	2.5	9.3	7.2	-3.4	1.1	7.1	4.8

Table 3.7 suggests that for the November-January season, in the southern Canadian prairies, the only years during which MRL98's observed seasonal anomaly is positive (while the overall composite anomaly is negative) correspond to negative phases of the Arctic Oscillation. Of the 7 warm VPC1 SSTA events, the eastern Montana average precipitation anomaly exceeds climatology only in 1977, while the southern Alberta-Manitoba region only exceeds climatology in 1966 (Table 3.7). Both of these years correspond to low index phases of the Arctic Oscillation (Table 2.2, Fig. 3.14).

#### 3.4.4.2 NORTH AMERICAN TEMPERATURE

Consistent with the situation demonstrated above for North American precipitation, the sign of observed regional anomalies of monthly average daily maximum/minimum temperature during warm TP SSTA events does not match that of the corresponding composite during some negative phases of the Arctic Oscillation and positive phases of the PDO. During warm TP SSTA events in December-January-

February (Fig. 3.6a-f), monthly average daily maximum and minimum temperature anomalies across the northern U.S. and southern Canada are not consistent with the composite anomaly during negative AO years. Table 3.8 shows that for 1966 and 1977, the North Dakota region observed notable negative temperature anomalies, and both of these were characterized by a negative Arctic Oscillation index during January (Table 2.2; Fig. 3.14). In addition, the southeast U.S. exhibited somewhat warmer than normal temperature anomalies in 1992, 1993, 1995, and 1998 (Table 3.8). These years fall within the period when the PDO index shifted to a positive phase (Fig. 2.6).

On an individual monthly scale, December temperatures during warm SSTA VPC1 events were not consistent with the sign of the SSTA VPC1 composites during negative AO or positive PDO years. Table 3.8 shows that for several regions stretching in the eastern U.S., only a few SSTA events were characterized by negative temperature anomalies. The years with cooler than normal temperatures (and associated AO and PDO phase as noted in Table 2.2) were 1976 (negative AO, positive PDO), 1986 (positive AO, positive PDO), and 1997 (negative AO, positive PDO).

### **3.5 Summary**

This Chapter has presented the monthly average daily maximum/minimum temperature patterns for central and eastern North America associated with TP SSTA events, complementing the precipitation-based work of MRL98. Statistically significant associations have been identified for each month from October through March for daily maximum and minimum temperatures. The separate analysis of monthly average daily maximum and minimum temperatures during warm and cold SSTA events yielded the identification of previously undocumented regions with temperatures associated with TP SSTAs. Further, the nonlinear aspects of the relationship between temperatures in each of these regions and TP SSTAs have been documented. Nonlinearities in the association between monthly average daily maximum/minimum temperatures and TP SSTAs were identified for most of the target anomaly regions.

Table 3.8: Observed monthly composite anomaly for indicated regions in Fig. 3.6 (indexed by Table 3.3) during the individual constituent years when warm TP SSTAs were present, as defined in Section 2.2. Anomalies for years that did not meet the threshold temperature criteria for warm events are grayed out. Shading and bold font are according to given legend.

Maximum Temperature												
Year	Northern_Plains			Atlantic_Coast			Southeast_US					
	North Dakota	East Colo-West KS	MN-WI	Three Rivers	Chespk Bay	Western PA	Southeast TX		North GA	West TX		
	DJF	Feb	Mar	Dec	Dec	Dec	Jan	Jan	Jan	Jan		
1958	<b>5.7</b>	<b>3.8</b>	<b>3.3</b>	<b>2.8</b>	<b>1.3</b>	<b>2.4</b>	-3.1	-0.8	-2.8	-1.4		
1966	-1.3	-0.6	-0.4	2.2	1.1	2.2	-3.1	-3.5	-3.2	<b>-4.1</b>		
1973	0.9	-3.0	0.1	1.5	1.9	1.4	-0.2	-3.0	-1.1	-3.9		
1977	-2.3	-0.1	<b>-4.7</b>	-1.6	-2.0	-2.3	<b>-6.6</b>	<b>-5.5</b>	<b>-7.1</b>	-3.6		
1983	<b>3.8</b>	-0.3	<b>2.7</b>	<b>4.6</b>	<b>2.6</b>	<b>4.5</b>	-2.7	-1.4	-2.2	-2.6		
1987	<b>5.2</b>	0.5	4.0	-0.5	0.2	0.2	-1.5	-0.8	-1.5	-1.9		
1988	2.5	-2.7	0.6	1.7	0.9	1.2	-4.0	-2.6	-3.1	-3.3		
1992	<b>5.2</b>	<b>1.3</b>	<b>2.5</b>	<b>2.0</b>	<b>2.0</b>	<b>2.4</b>	0.5	-1.9	0.2	-2.2		
1993	-1.9	<b>-6.3</b>	-0.7	*****	*****	*****	1.0	-0.7	0.8	-2.3		
1995	1.0	1.3	2.2	3.0	2.6	3.1	0.1	0.8	0.2	0.2		
1998	3.9	-0.7	3.5	-0.4	0.2	0.7	1.5	2.8	1.4	2.0		
<b>COMPOSITE</b>	<b>2.07</b>	<b>-0.61</b>	<b>1.20</b>	<b>1.53</b>	<b>1.08</b>	<b>1.58</b>	<b>-1.65</b>	<b>-1.51</b>	<b>-1.67</b>	<b>-2.10</b>		

Minimum Temperature												
Year	Northern_Plains			Atlantic_Coast			Southeast_US					
	North Dakota	East Colo-West KS	MN-WI	Three Rivers	Chespk Bay	Western PA	Southeast TX		North GA	West TX		
	DJF	Feb	Mar	Dec	Dec	Dec	Jan	Jan	Jan	Jan		
1958	<b>5.2</b>	1.7	2.7	1.6	1.1	1.9	-2.4	-1.2	-2.1	0.5		
1966	-1.6	-0.6	<b>5.2</b>	1.3	0.1	2.5	-1.8	-2.1	-2.0	-2.9		
1973	0.8	-0.8	0.4	3.2	2.9	3.1	-0.2	-2.9	-0.6	-0.9		
1977	-3.4	-1.9	<b>-6.5</b>	<b>-4.4</b>	-2.8	<b>-4.6</b>	<b>-5.6</b>	<b>-4.3</b>	<b>-5.7</b>	-3.4		
1983	<b>4.9</b>	2.0	<b>4.7</b>	<b>4.1</b>	3.0	3.1	-0.6	-1.3	-1.3	-0.7		
1987	<b>6.2</b>	2.0	<b>4.6</b>	0.6	0.3	0.9	-0.7	-0.9	-0.4	-0.2		
1988	2.2	-1.3	<b>4.9</b>	1.6	0.8	1.4	-2.7	-2.7	-2.4	-1.5		
1992	<b>5.4</b>	3.0	4.0	1.7	0.9	0.9	0.8	0.2	0.6	1.0		
1993	-1.6	-2.1	-0.6	*****	*****	*****	2.7	-0.2	3.0	0.7		
1995	2.5	1.7	3.6	2.4	2.7	1.7	0.9	0.8	0.7	1.9		
1998	<b>6.1</b>	2.6	<b>6.7</b>	1.1	0.4	1.9	2.6	2.6	2.2	2.0		
<b>COMPOSITE</b>	<b>2.43</b>	<b>0.58</b>	<b>2.70</b>	<b>1.32</b>	<b>0.94</b>	<b>1.28</b>	<b>-0.64</b>	<b>-1.09</b>	<b>-0.73</b>	<b>-0.32</b>		

KEY: 4.0 greater than 4 °C    -1.0 less than -1 °C    \*\*\*\*\* Not a monthly SST event  
1.0 greater than 1 °C    -4.0 less than -4 °C

Additionally, the composite temperature associations derived from SSTA events during 1950-92 and described in this Chapter, as well as the precipitation associations documented in MRL98 have been compared with the observed anomalies during three warm and one cold SSTA event during 1993-2000. In general, the three warm TP SSTA events exhibited all of the precipitation and temperature anomalies exhibited in the composites based on SSTA events during 1950-92, except for the precipitation anomalies during the 1994-95 El Niño and the cooler than normal temperature anomalies only in the

southern U.S. during the during the 1997-98 El Niño. During the 1999-2000 La Niña event, the observed precipitation anomalies corresponded well with the cold SSTA event composite based on 1950-92 events, although the observed temperature anomalies only matched the positive anomalies in the U.S. Great Plains in the corresponding temperature composites.

Further, this Chapter has identified the years during which the observed anomalies were not consistent with the sign of the corresponding precipitation/temperature composite based on warm SSTA events. These “exception” years were frequently found to follow extremes of the AO. In Chapter 5, when physical linkages between the North American climate patterns and TP SSTAs are sought, the global atmospheric processes involved in the Arctic Oscillation will be considered as a possible means of explaining events when the observed climate departs from the composite anomaly. Note that while some exceptions years based on the extremes of the PDO were identified, the focus of the analysis of exception years in Chapter 5 will be on the AO due to the multiple regions observing precipitation/temperature anomalies with a relationship to TP SSTAs influenced by extremes of the AO.

## Chapter 4

### **Associations between Tropical Pacific SSTA Events and Distributions of Daily Weather Events over North America**

#### **4.1 Preamble**

Previous researchers already have documented the monthly associations between TP SSTA events and North American precipitation and temperature. Montroy (1997, hereafter M97) documented the linear relationships between central and eastern North American precipitation and TP SSTAs, while Montroy et al. (1998, hereafter MRL98) identified the nonlinear associations. The latter study extended the previous work of Livezey et al. (1997, hereafter L97), which also documented the temperature, precipitation, and 700mb height patterns linked to one key area of SSTAs in the central TP. And in Chapter 3 above, for the first time, the nonlinearities of the relationships between monthly mean maximum and minimum temperatures and TP SSTAs were established, following MRL98's analysis of monthly precipitation. These studies significantly extended previous research identifying seasonal relationships between El Niño/Southern Oscillation events and global climate (e.g., Ropelewski and Halpert 1986, 1996; Kiladis and Diaz 1989), in part because M97, MRL98, and Chapter 3 above all benefited from use of the fine resolution data set analyzed in the present study (see Section 3.2). This data set permitted the identification of TP SSTA associations with monthly mean precipitation and monthly mean temperatures (daily maximum and minimum, separately) not previously recognized.

However, even though several studies (including the present research described in Chapter 3) have outlined the monthly associations between TP SSTAs and North American climate, relatively few have focused on the frequencies of daily weather events that aggregate to monthly and seasonal relationships. As outlined in Section 1.2.3, only a few studies have examined distributions of daily weather events, including Janowiak and Bell (1998), who examined some of the changes in event distributions for daily

temperature, precipitation, and snowfall in the U.S. during El Niño-Southern Oscillation events. Also, Higgins et al. (1996, 2000) investigated the interannual variability of frequencies of daily (and 3-day accumulated) precipitation extremes for the U.S. on a relatively coarse grid ( $2.5^\circ$  longitude by  $2.0^\circ$  latitude) based on TP outgoing longwave radiation. But none of these investigations focused on identifying the changes in daily distributions within a monthly time scale, and none used a high-resolution data set like the one employed here (see Section 3.2).

To provide additional physical insight into the nature of the monthly teleconnection patterns identified in Chapter 3, this Chapter analyzes statistics on the changes in frequency and intensity of daily weather events associated with the monthly teleconnection relationships described in Chapter 3. The regions outlined in Chapter 3 to exhibit locally significant composite anomalies (i.e., Table 3.3 and Table 3.4) are used to focus the analysis here. These analyses help elucidate the nature of the monthly teleconnection relationships and therefore contribute additional insight into the physical nature of those teleconnections, consistent with the overarching objective of the current research.

## **4.2 Data and Methodology**

The first step in documenting the relation of daily weather event distributions to TP SSTA events was to identify the individual stations for which monthly precipitation or temperature has a significant monthly or seasonal relationship with TP SSTA events. This was done by examining the maps of composite monthly precipitation anomalies (in MRL98) and temperature anomalies (in Chapter 3) based on TP SSTA events from 1950-1992 and identifying the stations (in the fine resolution data set described in Section 3.2) in the key regions where the composite monthly anomaly was especially strong and spatially coherent. This provided, for each monthly or seasonal relationship, a set of associated stations exhibiting similar pronounced monthly/seasonal anomalies. Next, for each such station, the monthly average statistics provided in MRL98 and Chapter 3 were extended by using daily event statistics to document the weather system characteristics associated with the monthly linkages.

The statistical properties of the daily event distributions are presented below using a variety of formats. First, histograms are used to examine the relative frequency of events during warm, cold, and neutral TP SSTA events. Second, sets of tables and figures present statistical properties of the distributions. For precipitation, these properties include: (a) the average monthly and seasonal anomaly in  $\text{mm d}^{-1}$ ; (b) the “Relative Event Frequency,” which is the percentage of nonzero precipitation events in a series of amount ranges; (c) the average nonzero event size; (d) the maximum/minimum and quartile statistics for the nonzero daily precipitation events; and (e) the “Actual Event Frequency,” which is the average number of days per month or season that a precipitation event of the indicated size occurs. For the target regions, the monthly or seasonal precipitation anomaly is further analyzed to determine the contribution to that anomaly from precipitation events in certain categories, as well as the percentage contribution of each event category to the overall precipitation total. Lastly, documentation is provided for the sign consistency among individual constituent years used in the MRL98 composites plus, if any, additional years after 1992. For the results based on monthly average daily maximum and minimum temperature, similar statistical properties are documented.

### **4.3 Precipitation Results**

The details of the daily precipitation results now are presented. In this section, the associations are separated according to the SSTA TP PC used to define the events. Results are provided for both warm and cold TP SSTA events for November-March, the target analysis months for the present study. However, if an association begins in March and extends into April or begins in October and extends into November, then the October or April associations also are discussed.

#### *4.3.1 Associations with Eastern Tropical Pacific SSTA Events*

The following sections deal with all North American regions exhibiting an association with either warm or cold eastern TP SSTA events during October-March, as indicated by SSTA VPC1 (Fig. 2.2b, Fig. 2.3b). Many of these regions correspond to

areas with monthly precipitation totals that MRL98 found to have statistically significant linkages to the occurrence of warm or cold eastern TP SSTA events, as shown in Fig. 3.1. However, as noted in MRL98, not all of these relationships are linear, which is defined as having a statistically significant association during cold eastern TP SSTA events that is equal in magnitude and opposite in sign to a similar statistically significant association during warm eastern TP SSTA events. These nonlinear associations also are highlighted below.

#### 4.3.1.1 ATLANTIC AND GULF OF MEXICO COASTS (JANUARY-MARCH)

Using a monthly time scale, MRL98 demonstrated that coastal areas in the southeastern U.S. during each month from January through March are characterized by a linear relation involving generally above (below) normal precipitation during warm (cold) SSTA VPC1 events (Fig. 3.1). They noted that average monthly composite anomalies during this period exceeded 25 mm in each month (equivalent to approximately  $0.9 \text{ mm d}^{-1}$ ). Both the warm and cold SSTA monthly composite precipitation anomalies were found to be statistically significant using field and local significance tests. This linear relationship is consistent with the findings of previous authors who conducted seasonal (e.g., Ropelewski and Halpert 1996) and monthly (e.g., L97) investigations into precipitation related to warm TP SSTA events.

However, the more specific, daily-based analysis in the present study highlights nonlinearities in the composite monthly precipitation anomalies in Fig. 3.1. Table 4.1 shows that the composite precipitation anomaly over south Florida during warm SSTA VPC1 events exceeds  $+1.0 \text{ mm d}^{-1}$  in each individual month from January to March (Fig. 3.1e,g,i), but is greatest during January ( $+1.65 \text{ mm d}^{-1}$ ) and smallest in March ( $+1.43 \text{ mm d}^{-1}$ ). Conversely, the composite anomaly during cold SSTA VPC1 events for January and February (about  $-0.85 \text{ mm d}^{-1}$ ) is around half the magnitude of the corresponding warm anomaly – but is larger in March when the cold SSTA VPC1 monthly precipitation anomaly ( $-1.23 \text{ mm d}^{-1}$ ) is close to the same size as the corresponding warm SSTA VPC1 anomaly ( $+1.43 \text{ mm d}^{-1}$ ). Table 4.2 and Table 4.3 show similar relationships in the far southeast U.S./central Florida and North-South Carolina regions although, unlike the south Florida region, the March precipitation

		January-March Season			January			February			March		
		Warm	Neutral	Cold	Warm	Neutral	Cold	Warm	Neutral	Cold	Warm	Neutral	Cold
<b>Aggregate Statistics</b>	Total (mm d <sup>-1</sup> )	3.50	1.94	1.00	3.38	1.63	0.86	3.52	1.97	1.21	3.61	2.21	0.95
	Anom (mm d <sup>-1</sup> )	1.52	-0.05	-0.99	1.65	-0.10	-0.87	1.48	-0.08	-0.83	1.43	0.03	-1.23
<b>Relative Event Frequency</b>	Num Events	1260	4807	905	429	1670	346	408	1594	304	423	1543	255
	< 5 mm	49%	56%	63%	49%	60%	73%	51%	56%	57%	47%	52%	58%
	5-10 mm	14%	16%	17%	15%	16%	17%	14%	16%	18%	13%	16%	18%
	10-25 mm	20%	18%	14%	18%	17%	7%	19%	19%	19%	22%	19%	16%
	25-50 mm	13%	7%	5%	12%	6%	3%	13%	7%	6%	14%	9%	7%
	50-100 mm	4%	2%	1%	5%	1%	1%	3%	2%	0%	4%	3%	1%
	100-200 mm	< 1%	< 1%	0%	0%	< 1%	0%	< 1%	< 1%	0%	< 1%	1%	0%
	>200 mm	0%	0%	0%	0%	0%	0%	0%	0%	0%	0%	< 1%	0%
	Avg Size (mm)	12.37	9.26	6.32	11.54	7.83	5.25	11.25	9.00	7.07	14.29	11.08	6.87
<b>Quartile</b>	Max (mm)	112.27	231.14	74.17	97.79	154.94	61.47	112.27	118.36	56.64	105.41	231.14	74.17
	3rd Quartile (mm)	17.53	11.43	7.62	16.76	9.59	5.33	16.76	10.92	10.67	20.32	13.97	9.53
	Median (mm)	5.08	3.56	2.79	5.08	3.05	2.03	4.57	3.56	3.43	5.33	4.32	3.30
	1st Quartile (mm)	1.27	1.02	0.76	1.27	1.02	0.76	1.02	1.02	1.02	1.52	1.27	1.02
	Min (mm)	0.25	0.25	0.25	0.25	0.25	0.25	0.25	0.25	0.25	0.25	0.25	0.25
<b>Actual Event Frequency</b>	ALL EVENTS	22.5	16.7	12.6	7.7	5.8	4.8	7.3	5.5	4.2	7.6	5.4	3.5
	< 5 mm	11.1	9.4	7.9	3.8	3.5	3.5	3.7	3.1	2.4	3.6	2.8	2.1
	5-10 mm	3.2	2.7	2.2	1.2	0.9	0.8	1.0	0.9	0.8	1.0	0.9	0.6
	10-25 mm	4.4	3.0	1.8	1.4	1.0	0.3	1.4	1.0	0.8	1.6	1.0	0.6
	25-50 mm	2.9	1.2	0.6	0.9	0.4	0.1	0.9	0.4	0.3	1.1	0.5	0.2
	50-100 mm	0.9	0.3	0.1	0.4	< 0.1	< 0.1	0.3	0.1	< 0.1	0.3	0.2	< 0.1
	100-200 mm	0.1	0.1	0.0	0.0	< 0.1	0.0	< 0.1	< 0.1	0.0	< 0.1	< 0.1	0.0
	>200 mm	0.0	< 0.1	0.0	0.0	0.0	0.0	0.0	0.0	0.0	0.0	< 0.1	0.0

Table 4.1: Daily January-March precipitation event statistics for south Florida region (shown in map in upper left corner) during TP SSTA event categories defined in Section 2.2.3 and used to create the 1950-1992 warm and cold composites in Fig. 3.1 and to select warm and cold event years during 1993-2000 (Section 3.4.1). Neutral SSTA events are all years not defined as warm or cold events. Top section (“Aggregate Statistics”): Monthly or seasonal composite precipitation total, and anomaly from 1950-92 mean (“Anom,” comparable to composite anomaly on Fig. 3.1, but including post-1992 events), in mm d<sup>-1</sup>. Second section (“Relative Event Frequency”): Total number of daily (non-zero) precipitation events, percentage of events that fall into the indicated categories, and average daily precipitation event size (mm d<sup>-1</sup>). Third section (“Quartile”): Quartile statistics on the daily non-zero precipitation events. Fourth section (“Actual Event Frequency”): Average number of days with non-zero precipitation totals that occurred in the indicated month/season during composites of indicated type of SSTA event. Non-zero Actual Event Frequency less than 0.1 indicated by “< 0.1”.

		January-March Season			January			February			March		
		<i>Warm</i>	<i>Neutral</i>	<i>Cold</i>	<i>Warm</i>	<i>Neutral</i>	<i>Cold</i>	<i>Warm</i>	<i>Neutral</i>	<i>Cold</i>	<i>Warm</i>	<i>Neutral</i>	<i>Cold</i>
<b>Aggregate Statistics</b>	Total (mm d <sup>-1</sup> )	5.14	3.86	2.98	4.89	3.54	2.72	5.01	3.92	3.06	5.51	4.14	3.17
	Anom (mm d <sup>-1</sup> )	1.26	-0.02	-0.90	1.31	-0.04	-0.86	1.09	0.00	-0.86	1.36	-0.02	-0.99
<b>Relative Event Frequency</b>	Num Events	8326	37023	8231	2966	13000	2847	2531	11899	2579	2829	12124	2805
	< 5 mm	37%	41%	45%	49%	51%	64%	47%	49%	46%	41%	44%	54%
	5-10 mm	16%	17%	19%	14%	19%	15%	14%	17%	21%	15%	15%	17%
	10-25 mm	26%	24%	23%	23%	20%	14%	24%	22%	22%	23%	22%	20%
	25-50 mm	16%	13%	10%	12%	8%	5%	11%	10%	8%	14%	13%	8%
	50-100 mm	5%	4%	3%	1%	2%	1%	4%	2%	2%	7%	4%	1%
	100-200 mm	1%	< 1%	< 1%	< 1%	< 1%	0%	1%	< 1%	1%	< 1%	1%	< 1%
	>200 mm	< 1%	< 1%	< 1%	0%	0%	0%	0%	0%	0%	0%	0%	0%
Avg Size (mm)	16.14	13.61	11.66	14.58	11.93	10.61	16.08	13.40	12.43	17.83	15.62	12.01	
<b>Quartile</b>	Max (mm)	264.16	286.26	231.14	195.58	231.39	193.04	160.53	211.33	157.73	264.16	286.26	231.14
	3rd Quartile (mm)	21.59	18.29	15.24	19.81	16.51	13.84	22.10	18.29	15.24	23.37	20.57	16.26
	Median (mm)	8.89	7.11	6.10	7.62	6.35	5.33	9.14	7.37	6.35	10.16	7.87	6.35
	1st Quartile (mm)	2.54	2.03	1.78	2.03	1.78	1.52	2.54	2.03	2.03	2.79	2.29	2.29
	Min (mm)	0.25	0.25	0.25	0.25	0.25	0.25	0.25	0.25	0.25	0.25	0.25	0.25
<b>Actual Event Frequency</b>	ALL EVENTS	29.7	25.7	22.9	10.6	9.0	7.9	9.0	8.3	7.2	10.1	8.4	7.8
	< 5 mm	11.0	10.6	10.2	5.2	4.6	5.1	4.2	4.1	3.3	4.1	3.7	4.2
	5-10 mm	4.6	4.4	4.3	1.5	1.7	1.2	1.2	1.4	1.5	1.5	1.3	1.3
	10-25 mm	7.9	6.3	5.4	2.4	1.8	1.1	2.2	1.8	1.6	2.3	1.9	1.6
	25-50 mm	4.7	3.3	2.3	1.3	0.7	0.4	0.9	0.8	0.6	1.4	1.1	0.6
	50-100 mm	1.4	1.0	0.7	0.2	0.2	0.1	0.4	0.2	0.2	0.7	0.3	0.1
	100-200 mm	0.2	0.1	0.1	< 0.1	< 0.1	0.0	0.1	< 0.1	0.1	< 0.1	0.1	< 0.1
>200 mm	< 0.1	< 0.1	< 0.1	0.0	0.0	0.0	0.0	0.0	0.0	0.0	0.0	0.0	

Table 4.2: As in Table 4.1, but for far southeast U.S./central Florida region shown in map in upper left corner.

		January-March Season			January			February			March		
		<i>Warm</i>	<i>Neutral</i>	<i>Cold</i>	<i>Warm</i>	<i>Neutral</i>	<i>Cold</i>	<i>Warm</i>	<i>Neutral</i>	<i>Cold</i>	<i>Warm</i>	<i>Neutral</i>	<i>Cold</i>
<b>Aggregate Statistics</b>	Total (mm d <sup>-1</sup> )	4.54	3.52	3.03	4.43	3.43	3.07	4.49	3.44	2.97	4.68	3.70	3.05
	Anom (mm d <sup>-1</sup> )	0.97	-0.05	-0.54	0.93	-0.07	-0.43	1.00	-0.06	-0.53	0.97	-0.02	-0.67
<b>Relative Event Frequency</b>	Num Events	4255	19865	4834	1504	6913	1829	1262	6285	1384	1489	6667	1621
	< 5 mm	41%	44%	45%	37%	50%	46%	36%	46%	46%	40%	45%	45%
	5-10 mm	17%	19%	22%	18%	19%	23%	21%	20%	22%	20%	17%	24%
	10-25 mm	26%	25%	24%	25%	23%	23%	22%	23%	24%	21%	24%	22%
	25-50 mm	13%	10%	8%	15%	8%	7%	16%	9%	8%	16%	12%	9%
	50-100 mm	3%	2%	1%	4%	1%	1%	3%	2%	1%	3%	2%	< 1%
	100-200 mm	< 1%	< 1%	0%	0%	0%	0%	1%	0%	0%	< 1%	< 1%	0%
	>200 mm	0%	0%	0%	0%	0%	0%	0%	0%	0%	0%	0%	0%
	Avg Size (mm)	13.09	11.12	9.80	12.29	10.64	9.22	13.80	10.65	10.26	13.30	12.07	10.06
<b>Quartile</b>	Max (mm)	127.00	137.16	93.22	102.11	132.08	86.87	127.00	121.92	93.22	114.81	137.16	88.65
	3rd Quartile (mm)	17.78	15.24	13.21	17.78	14.48	12.19	18.03	15.24	14.48	17.78	16.00	13.72
	Median (mm)	7.37	6.35	5.84	7.11	5.84	5.08	7.62	6.10	6.35	7.37	6.86	5.84
	1st Quartile (mm)	2.03	2.03	2.03	1.78	1.78	1.52	2.54	1.78	2.54	2.29	2.29	2.03
	Min (mm)	0.25	0.25	0.25	0.25	0.25	0.25	0.25	0.25	0.25	0.25	0.25	0.25
<b>Actual Event Frequency</b>	ALL EVENTS	32.0	29.0	28.3	11.3	10.1	10.7	9.5	9.2	8.1	11.2	9.7	9.5
	< 5 mm	13.0	12.7	12.7	4.2	5.0	4.9	3.5	4.3	3.7	4.5	4.3	4.2
	5-10 mm	5.5	5.6	6.1	2.1	1.9	2.4	2.0	1.8	1.8	2.2	1.7	2.3
	10-25 mm	8.4	7.2	6.8	2.9	2.3	2.5	2.1	2.1	1.9	2.4	2.4	2.1
	25-50 mm	4.0	2.9	2.3	1.7	0.8	0.8	1.5	0.8	0.6	1.8	1.2	0.8
	50-100 mm	1.0	0.6	0.3	0.4	0.1	0.1	0.3	0.2	0.1	0.3	0.2	< 0.1
	100-200 mm	< 0.1	< 0.1	0.0	0.0	0.0	0.0	0.1	0.0	0.0	< 0.1	< 0.1	0.0
>200 mm	0.0	0.0	0.0	0.0	0.0	0.0	0.0	0.0	0.0	0.0	0.0	0.0	

Table 4.3: As in Table 4.1 but for North-South Carolina region shown in upper left corner.

anomalies during cold SSTA VPC1 events follow the pattern of January and February, where the cold SSTA event anomalies are smaller in magnitude than the corresponding warm SSTA VPC1 event anomalies. The far southeast U.S./central Florida region (Table 4.2) observed warm SSTA VPC1 event precipitation anomalies ranging from  $+1.09 \text{ mm d}^{-1}$  (February) to  $+1.36 \text{ mm d}^{-1}$  (March), with the largest composite anomaly during cold TP SSTA events of  $-0.99 \text{ mm d}^{-1}$  (March). During neutral TP SSTA events, the composite monthly precipitation anomalies for all three regions considered above remained notably near zero, much different from the associated anomalies for warm and cold TP SSTA events. Very similar results were obtained for North-South Carolina (Table 4.3).

The above increase (decrease) in January and February precipitation in south Florida during warm (cold) TP SSTA events is associated with more (less) frequent daily precipitation totals of all sizes, but especially between 25-100  $\text{mm d}^{-1}$ . Fig. 4.1 shows that during warm (cold) TP SSTA events in the January-March (JFM) season, the Actual Event Frequency in Table 4.1 is higher (lower) than in neutral TP SSTA events across all precipitation categories. During warm SSTA events in JFM, 11.1 days have

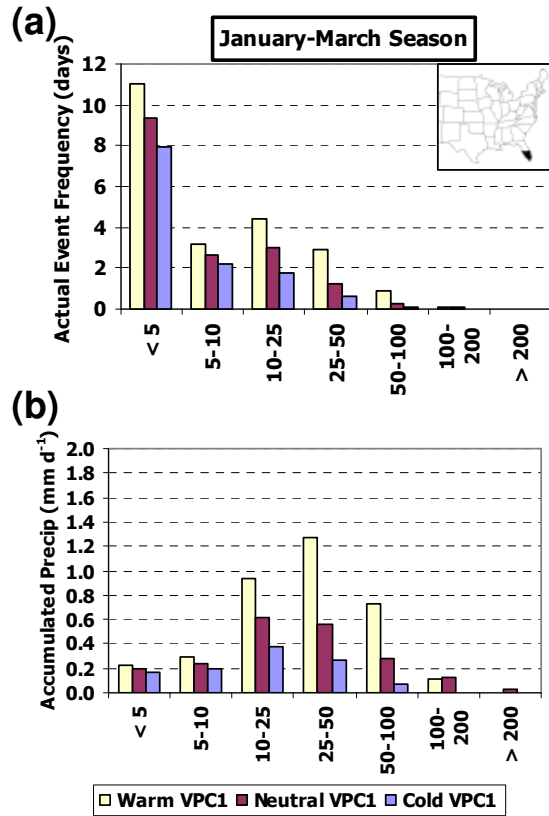


Fig. 4.1: (a) Actual Event Frequency from Table 4.1 for January-March in south Florida region demarcated in inset map for the indicated range ( $\text{mm d}^{-1}$ ) during warm, neutral, and cold SSTA VPC1 events as defined in Section 2.2. (b) Amount of precipitation accumulated during January-March ( $\text{mm d}^{-1}$ ) from daily precipitation amounts in the indicated size range. Sum over all precipitation size ranges for each SSTA event type equals corresponding January-March total in top section of Table 4.1.

precipitation less than 5 mm, compared to 7.9 days during cold SSTA VPC1 events. In total, over all precipitation categories in JFM, the south Florida region experienced precipitation on 22.5 (12.6) days during warm (cold) SSTA VPC1 events, compared to 16.7 days during neutral SSTA events (Fig. 4.1a). Table 4.1 further shows that this same relationship was present in the individual months as well, with an Actual Event Frequency of all daily precipitation events of 7.7, 7.3, and 7.6 days during warm TP SSTA events in January, February, and March, (respectively), more than the approximately 5.5 during neutral SSTA events. Further, cold TP SSTA events experienced fewer days with precipitation compared to neutral SSTA events, ranging from 4.8 in January to 3.5 in March. Lastly, Table 4.1 shows that during each individual month, the Relative Event Frequency for events between 25 and 100 mm d<sup>-1</sup> was higher (lower) during warm (cold) TP SSTA events compared to neutral SSTA events. Of all daily precipitation event size categories, the greatest increase during warm TP SSTA events (relative to cold and neutral SSTA events) was between 25-50 mm d<sup>-1</sup>. On average, 13% of the total precipitation events in JFM during warm SSTA VPC1 events were in that range, compared to 7% (5%) during neutral (cold) SSTA VPC1 events. Similar increases were present for the individual months from January to March, although the Relative Event Frequency for January daily totals between 50-100 mm d<sup>-1</sup> increased more during warm events (5%) compared to neutral events (1%) than in other months.

The daily precipitation totals with size between 25-50 mm d<sup>-1</sup> contributed most to the overall monthly and seasonal composite totals in south Florida during warm SSTA VPC1 events (Table 4.4). Precipitation events with this size contributed 36% to the overall January-March seasonal composite total, compared to 27% (25%) during neutral (cold) SSTA events, and also contributed similarly large fractions to the individual monthly composite anomalies. Comparatively large relative contributions from events of 50-100 mm d<sup>-1</sup> occurred as well during January, where 25% of the precipitation anomaly comes from events of this size, compared to 7% (10%) during neutral (cold) SSTA events (Table 4.4, Fig. 4.1b). During warm SSTA VPC1 events, of the total JFM composite precipitation of 3.51 mm d<sup>-1</sup>, nearly 2.0 mm d<sup>-1</sup> (1.272 + 0.715 = 1.987) originates from precipitation events with size between 25-100 mm d<sup>-1</sup> (Table 4.4).

Precip Category	January-March Season			January			February			March		
	Warm	Neutral	Cold	Warm	Neutral	Cold	Warm	Neutral	Cold	Warm	Neutral	Cold
<5	0.229	0.193	0.161	0.228	0.199	0.210	0.234	0.208	0.145	0.225	0.173	0.127
5-10	0.288	0.240	0.188	0.306	0.239	0.200	0.295	0.262	0.209	0.264	0.220	0.158
10-25	0.929	0.612	0.336	0.848	0.574	0.209	0.908	0.664	0.505	1.028	0.604	0.311
25-50	1.272	0.552	0.248	1.147	0.457	0.154	1.318	0.557	0.319	1.356	0.641	0.279
50-100	0.715	0.232	0.065	0.855	0.113	0.089	0.683	0.213	0.032	0.603	0.369	0.072
100-200	0.072	0.096	0.000	0.000	0.052	0.000	0.081	0.063	0.000	0.136	0.171	0.000
>200	0.000	0.010	0.000	0.000	0.000	0.000	0.000	0.000	0.000	0.000	0.030	0.000
<b>TOTAL</b>	<b>3.505</b>	<b>1.935</b>	<b>0.999</b>	<b>3.385</b>	<b>1.634</b>	<b>0.862</b>	<b>3.519</b>	<b>1.966</b>	<b>1.210</b>	<b>3.612</b>	<b>2.208</b>	<b>0.947</b>

Precip Category	January-March Season			January			February			March		
	Warm	Neutral	Cold	Warm	Neutral	Cold	Warm	Neutral	Cold	Warm	Neutral	Cold
<5	7%	10%	16%	7%	12%	24%	7%	11%	12%	6%	8%	13%
5-10	8%	12%	19%	9%	15%	23%	8%	13%	17%	7%	10%	17%
10-25	26%	32%	34%	25%	35%	24%	26%	34%	42%	28%	27%	33%
25-50	36%	29%	25%	34%	28%	18%	37%	28%	26%	38%	29%	29%
50-100	20%	12%	7%	25%	7%	10%	19%	11%	3%	17%	17%	8%
100-200	2%	5%	0%	0%	3%	0%	2%	3%	0%	4%	8%	0%
>200	0%	1%	0%	0%	0%	0%	0%	0%	0%	0%	1%	0%

Table 4.4: Top: Total seasonal or monthly accumulated precipitation ( $\text{mm d}^{-1}$ ) by precipitation category for south Florida region delineated in top left hand corner of Table 4.1 (as in Fig. 4.1b). Rows of precipitation categories represent daily totals. Columns are presented in  $\text{mm d}^{-1}$  averaged over indicated season or month. Last row (“TOTAL”) matches corresponding value in top section of Table 4.1. Bottom: Percent contribution to monthly or seasonal composite precipitation total. Non-zero percent contributions less than 1% are indicated by “< 1%”. Column headings correspond to TP SSTA event type, as in Table 4.1.

The increase (decrease) of precipitation in other parts of the southeastern U.S. during warm (cold) eastern TP SSTA events, relative to neutral events, was associated with more (less) frequent daily precipitation totals of almost all sizes, but especially between 10 and 100  $\text{mm d}^{-1}$ . The Actual Event Frequency of daily precipitation amounts in the far southeast U.S./central Florida region (Table 4.2; Fig. 4.2a) and North-South Carolina region (Table 4.3; Fig. 4.2c) was higher (lower) for each category between 10-100  $\text{mm d}^{-1}$  during warm (cold) TP SSTA events compared to neutral TP SSTA events. For the January-March season, the far southeast U.S./central Florida (North-South Carolina) region averaged 29.7 (32.0) total days of precipitation, compared to 25.7 (29.0) during neutral TP SSTA events and 22.9 (28.3) during cold TP SSTA events. The individual monthly Actual Event Frequencies exhibited similar differences in warm-neutral-cold SSTA events for daily precipitation amounts exceeding 10  $\text{mm d}^{-1}$  (Table 4.2, Table 4.3). The Relative Event Frequencies for both the January-March season and the individual months also increased (decreased) during warm (cold) SSTA

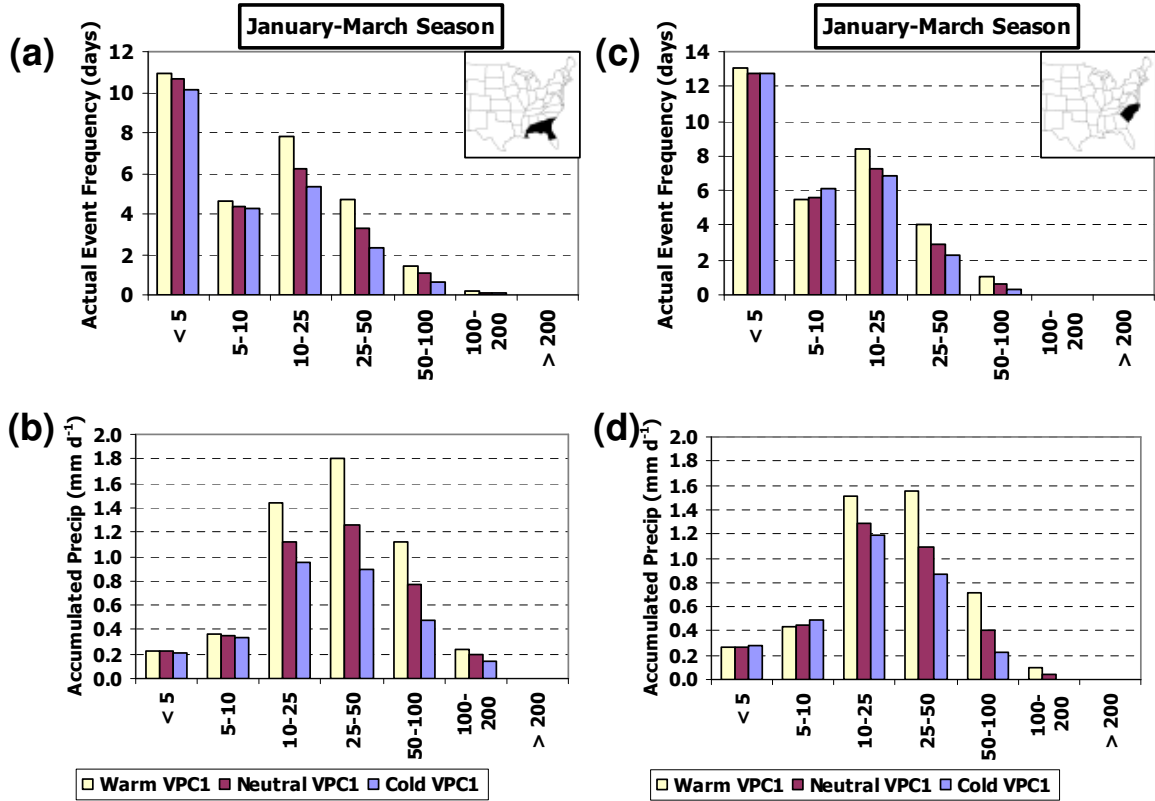


Fig. 4.2: (a) As in Fig. 4.1a, but for far southeast U.S./central Florida region demarcated in thumbnail map. (b) As in Fig. 4.1b, but for far southeast U.S./central Florida region. (c) As in (a) but for North-South Carolina region. (d) As in (b) but for North-South Carolina region.

events (compared to neutral SSTA events) for daily precipitation amounts from 10-100 mm d<sup>-1</sup> in both regions, except for amounts between 50-100 mm d<sup>-1</sup> in the far southeast U.S./central Florida region in January and between 10-25 mm d<sup>-1</sup> in the North-South Carolina region for the individual months of February and March (Table 4.2, Table 4.3).

For the aforementioned changes in daily precipitation event frequency for the far southeast U.S./central Florida and North-South Carolina regions, moderate sized daily precipitation amounts contributed the most to the seasonal precipitation total. For the JFM season, the daily precipitation amounts received during warm (cold) TP SSTA events increased (decreased) the most for categories between 25-100 mm d<sup>-1</sup> for both the far southeast U.S./central Florida and North-South Carolina regions relative to neutral TP

SSTA events (Fig. 4.2b,d). For warm events, the total relative contribution from these precipitation categories was about 2.9 (1.797 + 1.042 = 2.839) mm d<sup>-1</sup> (55%) of the 5.14 mm d<sup>-1</sup> seasonal average for the far southeast U.S./central Florida region (Table 4.5) and 2.3 (1.549 + 0.717 = 2.266) mm d<sup>-1</sup> (50%) of the 4.54 mm d<sup>-1</sup> seasonal total for the North-South Carolina region (Table 4.6), compared to 51% (45%) and 43% (35%) (respectively) for each region during neutral (cold) SSTA VPC1 events. While events with size 10-25 mm d<sup>-1</sup> also made important relative contributions to the seasonal precipitation total in each region, the relative contribution was noticeably lower during warm TP SSTA events compared to neutral and cold TP SSTA events – 28% (warm) vs. 29% (neutral) and 32% (cold) for the far southeast U.S./central Florida region (Table 4.5) and 33% (warm) vs. 37% (neutral) and 39% (cold) for North-South Carolina (Table 4.6). The relative contributions to the JFM seasonal total from the individual months for the 25-50 mm category similarly exhibited increases (decreases) during warm (cold) SSTA events of approximately 2-4% for both the far southeast U.S./central Florida region (Table 4.5) and the North-South Carolina region (Table 4.6) compared to neutral TP SSTA events. While the Relative Event Frequencies for the 50-100 mm category also increased (decreased) for the North-South Carolina region, those for the far southeast U.S./central Florida region only increased (decreased) during warm (cold) TP SSTA events in January-February (February-March).

Precip Category	January-March Season			January			February			March		
	Warm	Neutral	Cold	Warm	Neutral	Cold	Warm	Neutral	Cold	Warm	Neutral	Cold
<5	0.224	0.218	0.214	0.249	0.230	0.212	0.215	0.219	0.216	0.207	0.200	0.215
5-10	0.370	0.330	0.337	0.383	0.367	0.332	0.362	0.363	0.330	0.364	0.320	0.329
10-25	1.443	1.121	0.943	1.418	1.138	0.923	1.435	1.167	0.939	1.476	1.065	0.968
25-50	1.797	1.248	0.878	1.670	1.137	0.734	1.811	1.289	0.945	1.912	1.322	0.961
50-100	1.042	0.733	0.474	0.927	0.554	0.455	0.951	0.707	0.483	1.238	0.937	0.484
100-200	0.246	0.170	0.119	0.242	0.095	0.061	0.234	0.158	0.127	0.260	0.256	0.171
>200	0.019	0.022	0.014	0.000	0.014	0.000	0.000	0.015	0.000	0.055	0.037	0.040
<b>TOTAL</b>	<b>5.141</b>	<b>3.862</b>	<b>2.979</b>	<b>4.889</b>	<b>3.536</b>	<b>2.716</b>	<b>5.008</b>	<b>3.918</b>	<b>3.061</b>	<b>5.512</b>	<b>4.136</b>	<b>3.168</b>

Precip Category	January-March Season			January			February			March		
	Warm	Neutral	Cold	Warm	Neutral	Cold	Warm	Neutral	Cold	Warm	Neutral	Cold
<5	4%	6%	7%	5%	7%	8%	4%	6%	7%	4%	5%	7%
5-10	7%	9%	11%	8%	10%	12%	7%	9%	11%	7%	8%	10%
10-25	28%	29%	32%	29%	32%	34%	29%	30%	31%	27%	26%	31%
25-50	35%	32%	29%	34%	32%	27%	36%	33%	31%	35%	32%	30%
50-100	20%	19%	16%	19%	16%	17%	19%	18%	16%	22%	23%	15%
100-200	5%	4%	4%	5%	3%	2%	5%	4%	4%	5%	6%	5%
>200	< 1%	1%	< 1%	0%	< 1%	0%	0%	< 1%	0%	1%	1%	1%

Table 4.5: As in Table 4.4 but for far southeast U.S./central Florida region delineated in top left hand corner of Table 4.2.

Precip Category	January-March Season			January			February			March		
	Warm	Neutral	Cold	Warm	Neutral	Cold	Warm	Neutral	Cold	Warm	Neutral	Cold
<5	0.289	0.267	0.278	0.289	0.278	0.306	0.256	0.271	0.254	0.282	0.252	0.271
5-10	0.440	0.445	0.483	0.419	0.449	0.522	0.467	0.438	0.453	0.436	0.446	0.470
10-25	1.506	1.291	1.190	1.608	1.284	1.282	1.414	1.311	1.145	1.488	1.281	1.140
25-50	1.549	1.086	0.856	1.470	0.999	0.757	1.539	1.072	0.848	1.638	1.186	0.963
50-100	0.717	0.411	0.221	0.640	0.394	0.199	0.695	0.340	0.265	0.813	0.491	0.202
100-200	0.056	0.024	0.000	0.025	0.022	0.000	0.123	0.006	0.000	0.028	0.043	0.000
>200	0.000	0.000	0.000	0.000	0.000	0.000	0.000	0.000	0.000	0.000	0.000	0.000
<b>TOTAL</b>	<b>4.538</b>	<b>3.524</b>	<b>3.028</b>	<b>4.431</b>	<b>3.426</b>	<b>3.065</b>	<b>4.494</b>	<b>3.438</b>	<b>2.965</b>	<b>4.684</b>	<b>3.699</b>	<b>3.046</b>

Precip Category	January-March Season			January			February			March		
	Warm	Neutral	Cold	Warm	Neutral	Cold	Warm	Neutral	Cold	Warm	Neutral	Cold
<5	6%	8%	9%	6%	8%	10%	6%	8%	9%	6%	7%	9%
5-10	10%	13%	16%	9%	13%	17%	10%	13%	15%	9%	12%	15%
10-25	33%	37%	39%	36%	37%	42%	31%	38%	39%	32%	35%	37%
25-50	34%	31%	28%	33%	29%	25%	34%	31%	29%	35%	32%	32%
50-100	16%	12%	7%	14%	11%	6%	15%	10%	9%	17%	13%	7%
100-200	1%	1%	0%	1%	1%	0%	3%	< 1%	0%	1%	1%	0%
>200	0%	0%	0%	0%	0%	0%	0%	0%	0%	0%	0%	0%

Table 4.6: As in Table 4.4 but for North-South Carolina delineated in top left hand corner of Table 4.3.

For this Atlantic and Gulf of Mexico coast region during January-March, only one (two) of the warm (cold) TP SSTA event composite constituent years were characterized by observed precipitation anomalies that did not match the sign of the composite precipitation anomaly. For example, Fig. 4.3a shows that for the far southeast U.S./central Florida region (Table 4.2), of all the warm SSTA event years, only 1958 exhibited a very small January-March seasonal precipitation anomaly with opposite sign to the composite, mainly due to small negative anomalies in January and February and a relatively small positive anomaly in March. During this winter, the AO index was in a strong negative phase in February and March (Table 2.2). (The interrelation of the negative AO phase and warm SSTA VPC1 events will be explored in Chapter 5.) For cold SSTA events in 1967 and 1971, the observed seasonal precipitation anomaly for this region was positive (instead of negative as in the composite anomaly) for two of the three individual months during the January-March season in 1967, and for the January-March 1971 season (Fig. 4.3b). However, there are no distinguishing global climate system characteristics (e.g., AO, PDO) of these years with respect to the other cold TP SSTA event years (Table 2.2).

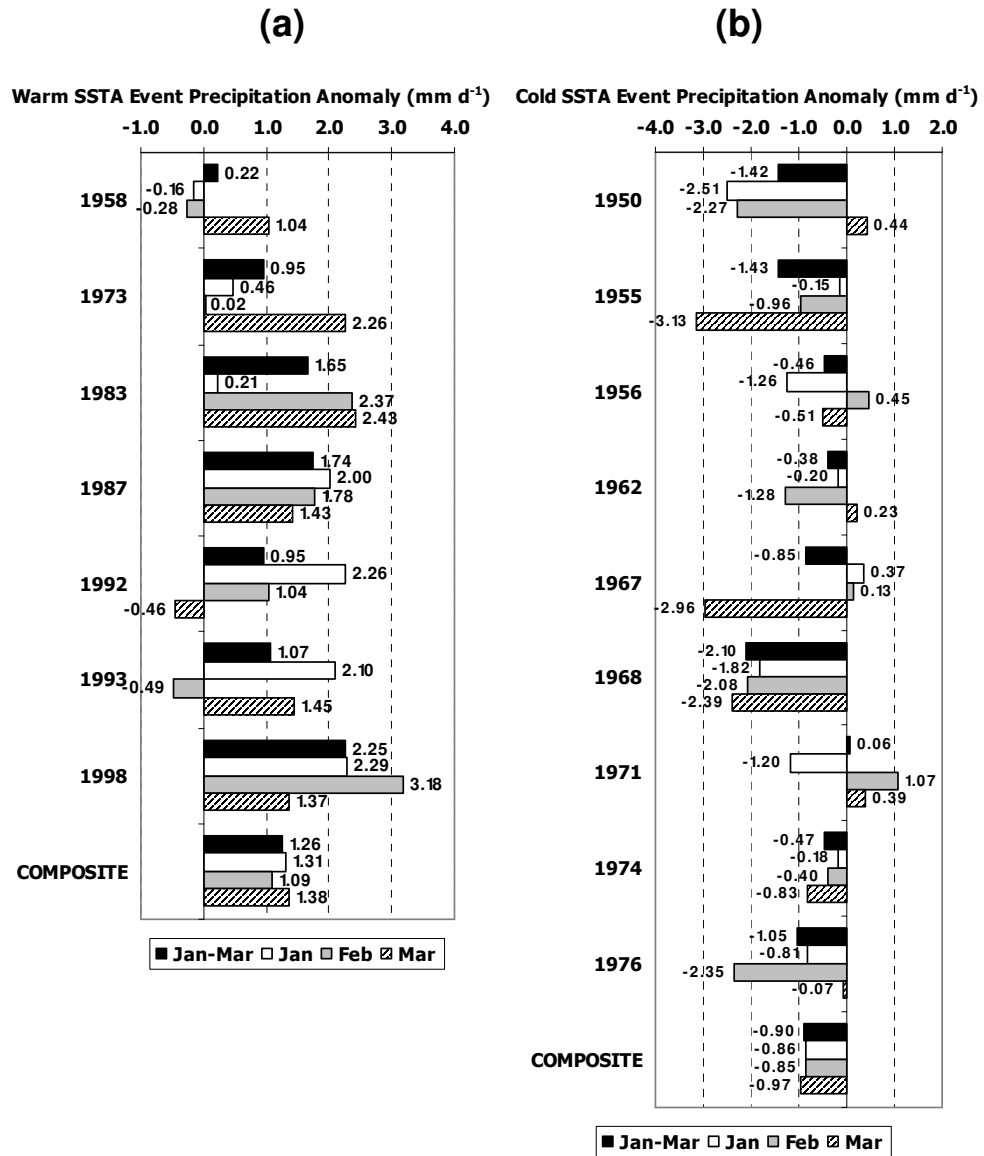


Fig. 4.3: (a) Regionally averaged station precipitation anomalies ( $\text{mm d}^{-1}$ ) from 1950-92 mean for January, February, and March and seasonal total (January-March) during warm SSTA VPC1 events for far southeast U.S./central Florida region as delineated in Table 4.2. (b) As in (a) but for cold TP SSTA events.

#### 4.3.1.2 SOUTHERN AND MIDWEST U.S. (NOVEMBER)

MRL98 demonstrated that during November, some regions of the southeastern U.S. near the Atlantic and Gulf of Mexico coasts exhibited a broadly linear precipitation relationship with TP SSTAs, while inland areas from Texas to the Midwest had a

nonlinear such relationship. The warm November TP SSTA VPC1 event composite (Fig. 3.1a) exhibited continuous positive precipitation anomalies from southeast Texas to Arkansas to Florida and the Carolinas, but the anomalies were not locally significant. In the corresponding cold SSTA event composite, statistically significant negative composite precipitation anomalies spanned the Gulf and Atlantic coastal areas from the Carolinas to Florida to southeast Texas and exceeded -25 mm for the month (about  $-0.85 \text{ mm d}^{-1}$ ) in many areas (Fig. 3.1b). Also in the cold November TP SSTA VPC1 event composite, statistically significant negative composite precipitation anomalies stretched from Oklahoma to Illinois, with no corresponding association in the warm SSTA event composite. The linear portion of this relationship is consistent with the findings of previous authors who conducted monthly (e.g., L97, M97) investigations into precipitation related to TP SSTA events. The finer resolution characteristics of the broad linear association along the southern Atlantic and Gulf Coast and the nonlinearities will now be discussed using the present daily-based approach.

The composite November precipitation anomalies in Florida are associated with an increase (decrease) in the frequency of precipitation events of all sizes during warm (cold) TP SSTA events, while the rest of the Gulf Coast and the North-South Carolina exhibit this characteristic only for heavier precipitation events. In the Florida, Gulf Coast, and North-South Carolina regions, the Actual Event Frequency (Table 4.7) was higher during warm TP SSTA events than during neutral SSTA events in each precipitation event category (Fig. 4.4a,c,e). Conversely, during cold TP SSTA events, the Actual Event Frequency was lower than the corresponding neutral SSTA values in most precipitation categories, except for daily amounts exceeding  $50 \text{ mm d}^{-1}$  in Florida and between  $5\text{-}10 \text{ mm d}^{-1}$  in North-South Carolina. Additionally, Table 4.7 indicates that the average daily precipitation event size is slightly higher (lower) for warm (cold) SSTA events in Florida (11.0 mm/9.2 mm/8.5 mm for warm/neutral/cold SSTAs) and the Gulf Coast (16.7 mm/14.4 mm/10.6 mm), but the relationship is less pronounced for North-South Carolina (10.9 mm/10.7 mm/8.4 mm).

																
		North-South Carolina			Florida			Gulf Coast			Texas			OK-IL Track		
		<i>Warm</i>	<i>Neutral</i>	<i>Cold</i>	<i>Warm</i>	<i>Neutral</i>	<i>Cold</i>	<i>Warm</i>	<i>Neutral</i>	<i>Cold</i>	<i>Warm</i>	<i>Neutral</i>	<i>Cold</i>	<i>Warm</i>	<i>Neutral</i>	<i>Cold</i>
<b>Aggregate Statistics</b>	Total (mm d <sup>-1</sup> )	3.14	2.58	1.73	2.78	1.95	1.23	4.34	3.35	1.96	3.20	3.00	1.45	2.15	2.11	1.21
	Anom (mm d <sup>-1</sup> )	0.59	0.03	-0.82	0.78	-0.05	-0.77	1.03	0.03	-1.36	0.43	0.22	-1.32	0.19	0.15	-0.75
<b>Relative Event Frequency</b>	Num Events	3402	8228	2034	1357	3399	624	2046	5038	1190	1804	4465	787	3749	9714	2232
	< 5 mm	48%	56%	53%	58%	64%	62%	43%	46%	54%	51%	51%	58%	52%	48%	55%
	5-10 mm	16%	16%	25%	15%	15%	16%	16%	16%	18%	17%	16%	21%	22%	18%	20%
	10-25 mm	22%	18%	16%	17%	12%	15%	20%	22%	16%	20%	19%	13%	18%	23%	19%
	25-50 mm	11%	7%	5%	7%	6%	3%	15%	11%	9%	10%	10%	6%	7%	8%	5%
	50-100 mm	3%	2%	1%	2%	2%	3%	6%	5%	2%	2%	4%	2%	2%	2%	1%
	100-200 mm	0%	1%	0%	1%	1%	1%	1%	1%	0%	1%	< 1%	0%	< 1%	0%	< 1%
≥200 mm	0%	0%	0%	0%	0%	< 1%	0%	0%	0%	0%	0%	0%	0%	0%	0%	
	Avg Size (mm)	10.9	10.7	8.4	11.0	9.2	8.5	16.7	14.4	10.6	13.5	14.0	12.6	9.1	10.0	7.2
<b>Quartile</b>	Max (mm)	144.78	198.12	109.73	228.35	165.10	265.43	169.42	307.34	124.97	215.90	230.38	96.52	104.65	170.18	130.81
	3rd Quartile (mm)	15.75	13.97	10.92	12.70	9.65	8.64	22.61	20.32	12.70	17.27	19.05	14.10	12.45	13.72	9.65
	Median (mm)	5.59	5.08	4.32	3.56	3.05	2.79	7.87	7.62	5.08	6.10	7.11	5.08	5.08	5.33	3.81
	1st Quartile (mm)	1.52	1.27	1.27	1.02	1.02	1.02	2.03	2.03	1.78	1.78	2.03	1.52	1.78	1.52	1.27
	Min (mm)	0.25	0.25	0.25	0.25	0.25	0.25	0.25	0.25	0.25	0.25	0.25	0.25	0.25	0.25	0.25
<b>Actual Event Frequency</b>	ALL EVENTS	8.8	7.3	6.5	7.7	6.6	4.3	8.1	6.8	5.7	7.5	6.3	4.0	7.0	6.2	5.1
	< 5 mm	4.2	4.1	3.4	4.5	4.3	2.7	3.5	3.1	3.1	3.8	3.2	2.3	3.6	3.0	2.8
	5-10 mm	1.4	1.2	1.6	1.2	1.0	0.7	1.3	1.1	1.0	1.2	1.0	0.8	1.5	1.1	1.0
	10-25 mm	2.0	1.4	1.0	1.3	0.8	0.6	1.6	1.5	0.9	1.5	1.2	0.5	1.2	1.4	0.9
	25-50 mm	1.0	0.5	0.4	0.6	0.4	0.1	1.2	0.7	0.5	0.8	0.6	0.2	0.5	0.5	0.3
	50-100 mm	0.2	0.2	0.1	0.2	0.1	0.1	0.5	0.3	0.1	0.1	0.2	0.1	0.1	0.1	< 0.1
	100-200 mm	0.0	< 0.1	0.0	0.1	< 0.1	0.1	0.1	< 0.1	0.0	< 0.1	< 0.1	0.0	< 0.1	0.0	< 0.1
≥200 mm	0.0	0.0	0.0	0.0	0.0	< 0.1	0.0	0.0	0.0	0.0	0.0	0.0	0.0	0.0	0.0	

Table 4.7: As in Table 4.1 but for individual regions (delineated in map in top row) during November.

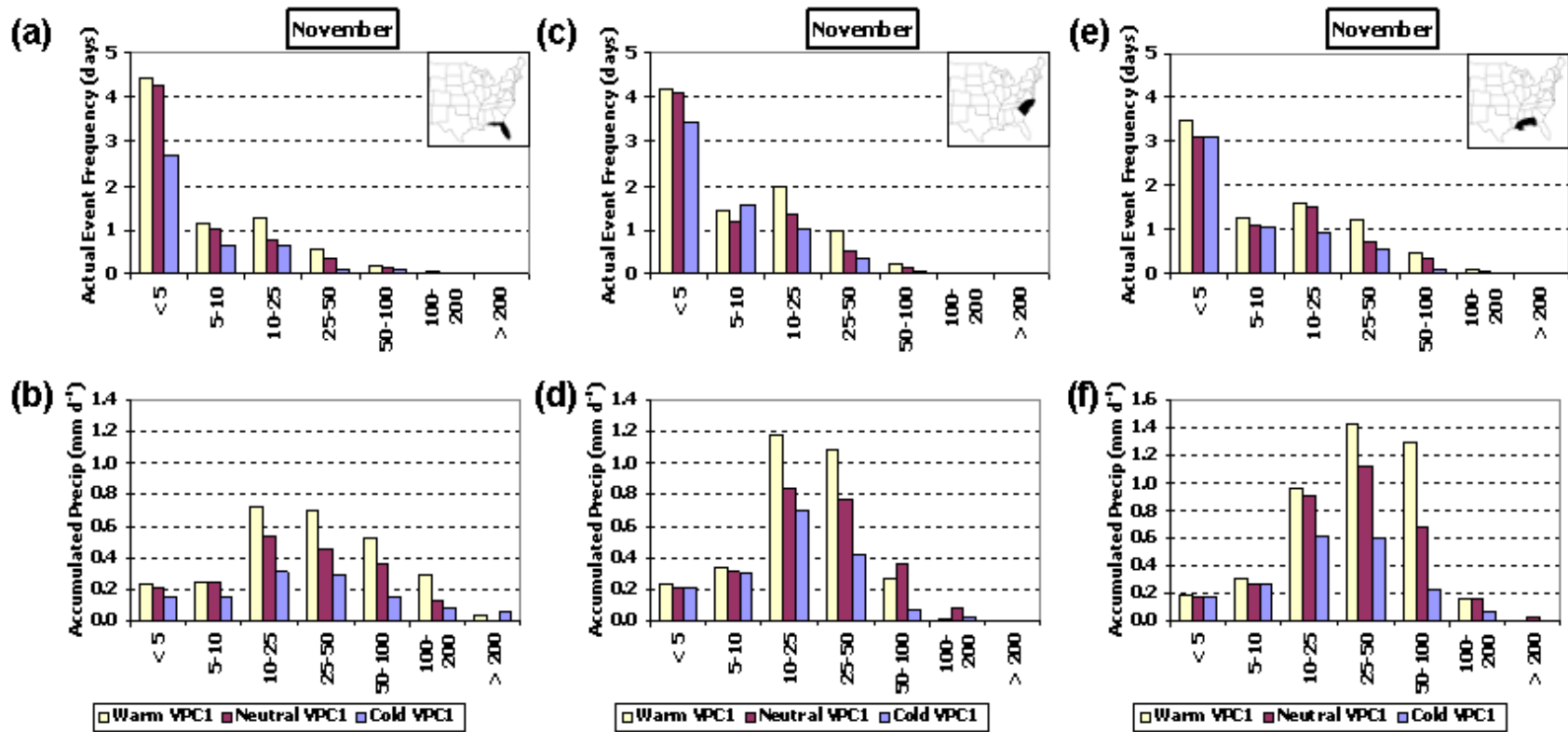


Fig. 4.4: As in Fig. 4.1 but for November precipitation in (a)-(b) Florida, (c)-(d) North-South Carolina, and (e)-(f) the Gulf Coast regions.

While the changes in November daily precipitation event frequency during warm (cold) TP SSTA events described in the previous paragraph bring about generally higher (lower) precipitation received from all daily precipitation amount categories compared to neutral SSTA events, the categories for moderate sized precipitation amounts exhibited the most linear characteristics. For Florida, the November precipitation received during warm (cold) TP SSTA events was higher (lower) than that observed during neutral TP SSTAs for all daily precipitation categories (Fig. 4.4b; Table 4.8). But the North-South Carolina (Fig. 4.4d) and Gulf Coast (Fig. 4.4f) regions only observed an increase (decrease) during warm (cold) TP SSTA events in total precipitation for daily amounts of 10-50 mm d<sup>-1</sup> and 10-100 mm d<sup>-1</sup>, respectively. For North-South Carolina, daily precipitation amounts between 10-25 mm d<sup>-1</sup> and 25-50 mm d<sup>-1</sup> during warm November TP SSTA events exceeded that during neutral SSTA events by 0.34 mm and 0.31 mm, respectively (Fig. 4.5). Similarly, for the Gulf Coast region, daily precipitation amounts between 25-50 mm d<sup>-1</sup> (50-100 mm d<sup>-1</sup>) during warm November TP SSTA events exceeded that during neutral SSTA events by 0.31 mm (0.61 mm) (Fig. 4.5). In addition, for both of these regions, the amount of precipitation received from daily totals between 10-100 mm d<sup>-1</sup> during cold TP SSTA events was lower than that during neutral TP SSTA events by similar margins (from -0.14 to -0.51 mm d<sup>-1</sup>) (Fig. 4.5).

For the aforementioned nonlinear associations in Texas and along a track from Oklahoma to Illinois, the negative composite November anomalies arose primarily from a decrease in frequency of larger precipitation events. In both regions, the average Actual Event Frequency (Fig. 4.6a,c; Table 4.7) and amount of November precipitation received (Fig. 4.6b,d; Table 4.8) in each category during cold SSTA events decreased compared to neutral SSTA events. However, most of the precipitation arose from daily totals less than 25 mm (Fig. 4.6b,d; Table 4.8). For the Oklahoma-Illinois track (Texas) region, 75% (50%) of the precipitation came from events smaller than 25mm during cold SSTA events, compared to 58% (41%) during neutral SSTA events (Table 4.8). This suggests that during cold November SSTA events, storm systems that normally would produce high precipitation in these regions do not occur.

Precip Category	North-South Carolina			Florida			Gulf Coast			Texas			OK-IL Track		
	Warm	Neutral	Cold	Warm	Neutral	Cold	Warm	Neutral	Cold	Warm	Neutral	Cold	Warm	Neutral	Cold
<5	0.238	0.208	0.209	0.238	0.213	0.153	0.193	0.189	0.176	0.199	0.164	0.114	0.218	0.183	0.179
5-10	0.344	0.309	0.307	0.247	0.246	0.161	0.309	0.267	0.268	0.305	0.280	0.165	0.354	0.275	0.244
10-25	1.189	0.845	0.709	0.721	0.537	0.318	0.961	0.912	0.616	0.883	0.801	0.446	0.834	0.756	0.483
25-50	1.089	0.777	0.419	0.707	0.480	0.294	1.427	1.116	0.604	1.067	0.975	0.454	0.511	0.607	0.224
50-100	0.271	0.364	0.065	0.527	0.363	0.158	1.297	0.687	0.221	0.592	0.611	0.271	0.212	0.256	0.073
100-200	0.013	0.078	0.023	0.297	0.130	0.087	0.158	0.158	0.072	0.121	0.172	0.000	0.019	0.030	0.010
>200	0.000	0.000	0.000	0.043	0.000	0.061	0.000	0.036	0.000	0.030	0.011	0.000	0.000	0.000	0.000
<b>TOTAL</b>	<b>3.145</b>	<b>2.583</b>	<b>1.731</b>	<b>2.780</b>	<b>1.949</b>	<b>1.233</b>	<b>4.345</b>	<b>3.345</b>	<b>1.958</b>	<b>3.197</b>	<b>2.995</b>	<b>1.450</b>	<b>2.147</b>	<b>2.106</b>	<b>1.213</b>

Precip Category	Carlinas			Florida			Gulf Coast			Texas			OK-IL Track		
	Warm	Neutral	Cold	Warm	Neutral	Cold	Warm	Neutral	Cold	Warm	Neutral	Cold	Warm	Neutral	Cold
<5	8%	8%	12%	9%	11%	12%	4%	5%	9%	6%	5%	8%	10%	9%	15%
5-10	11%	12%	18%	9%	13%	13%	7%	8%	14%	10%	9%	11%	17%	13%	20%
10-25	38%	33%	41%	26%	28%	26%	22%	27%	31%	28%	27%	31%	39%	36%	40%
25-50	35%	30%	24%	25%	24%	24%	33%	33%	31%	33%	33%	31%	24%	29%	18%
50-100	9%	14%	4%	19%	19%	13%	30%	21%	11%	19%	20%	19%	10%	12%	6%
100-200	< 1%	3%	1%	11%	7%	7%	4%	5%	4%	4%	6%	0%	1%	1%	1%
>200	0%	0%	0%	2%	0%	5%	0%	1%	0%	1%	< 1%	0%	0%	0%	0%

Table 4.8: As in Table 4.4 but for individual regions during November as delineated in Table 4.7.

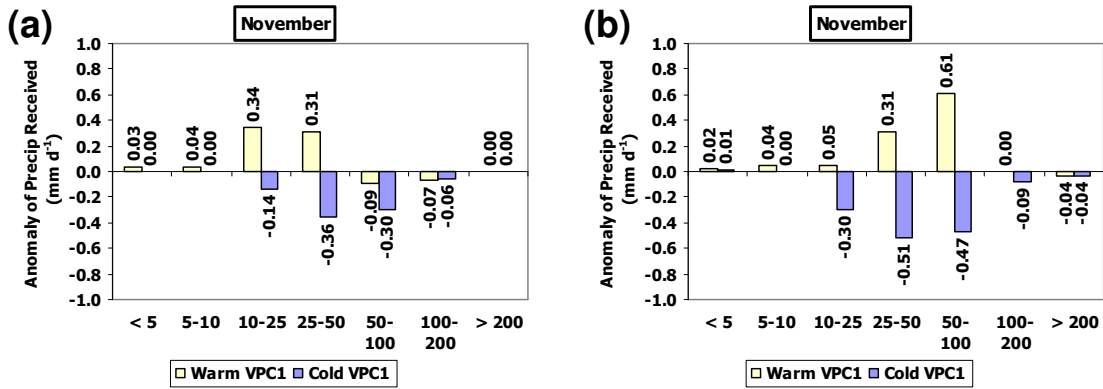


Fig. 4.5: Difference in total November precipitation received in Table 4.8 during warm and cold TP SSTA events compared to neutral TP SSTA events by precipitation category for (a) North-South Carolina region in Fig. 4.4c and (b) Gulf Coast region Fig. 4.4e.

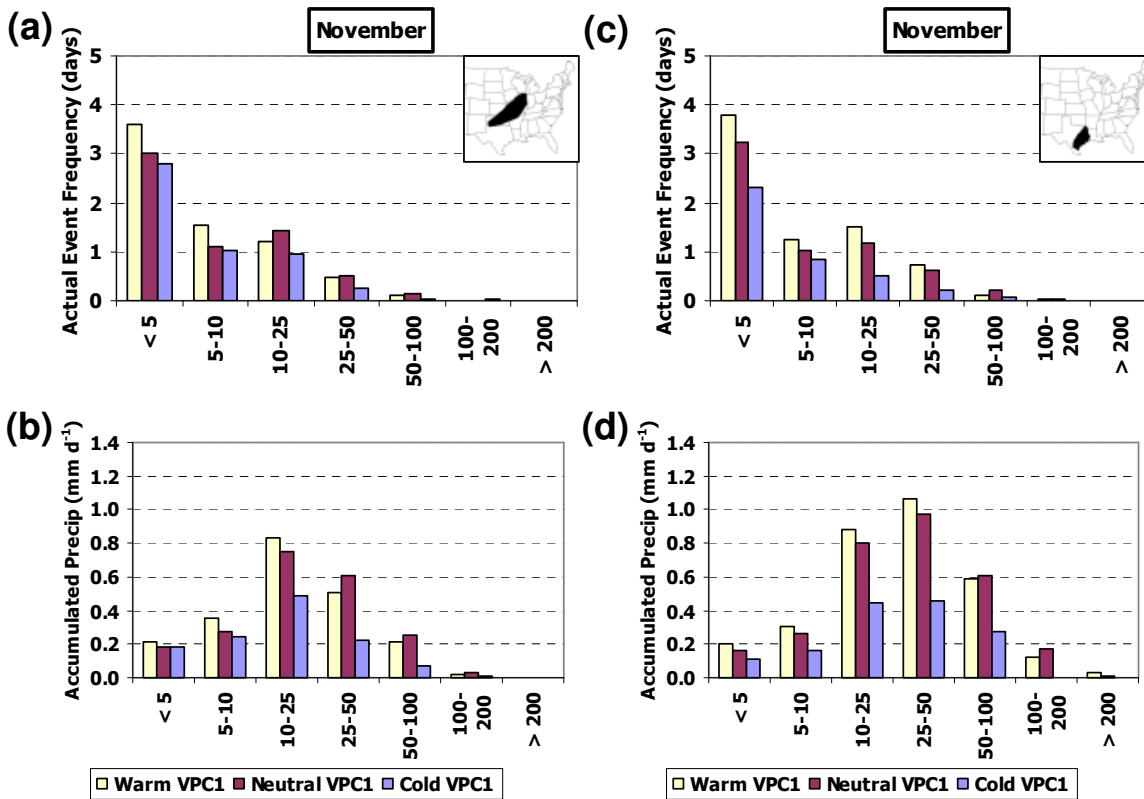


Fig. 4.6: As in Fig. 4.4, but for Oklahoma-Illinois track (a)-(b) and Texas (c)-(d) for November.

The observed November precipitation anomaly for two of the warm TP SSTA composite constituent years was notably different from the corresponding composite average values for North-South Carolina, Florida, and the Gulf Coast. Fig. 4.7 shows that in 1965, 1991, and 1994, more than one of the regions exhibited strong negative observed precipitation anomalies, while the composite average was positive. During these years, the PDO was entering a negative phase in 1965 and was in a negative phase in 1991, but was in a positive phase in 1994 (Table 2.2). The influence of the PDO in the physical teleconnection linkage chain from the TP to North American climate will be investigated in Chapter 5.

For cold November TP SSTA events, three of the composite constituent years exhibited observed regional anomalies that did not match the sign of the composite anomaly. Fig. 4.8 shows that positive precipitation anomalies were observed in 1954 (Florida), 1973 (Gulf Coast, OK-IL Track), and 1975 (OK-IL Track) while the composite anomaly for all of these regions was negative. Of these three “exception years”, two (1973 and 1975) were characterized by a strong negative PDO index in November (Table 4.2).

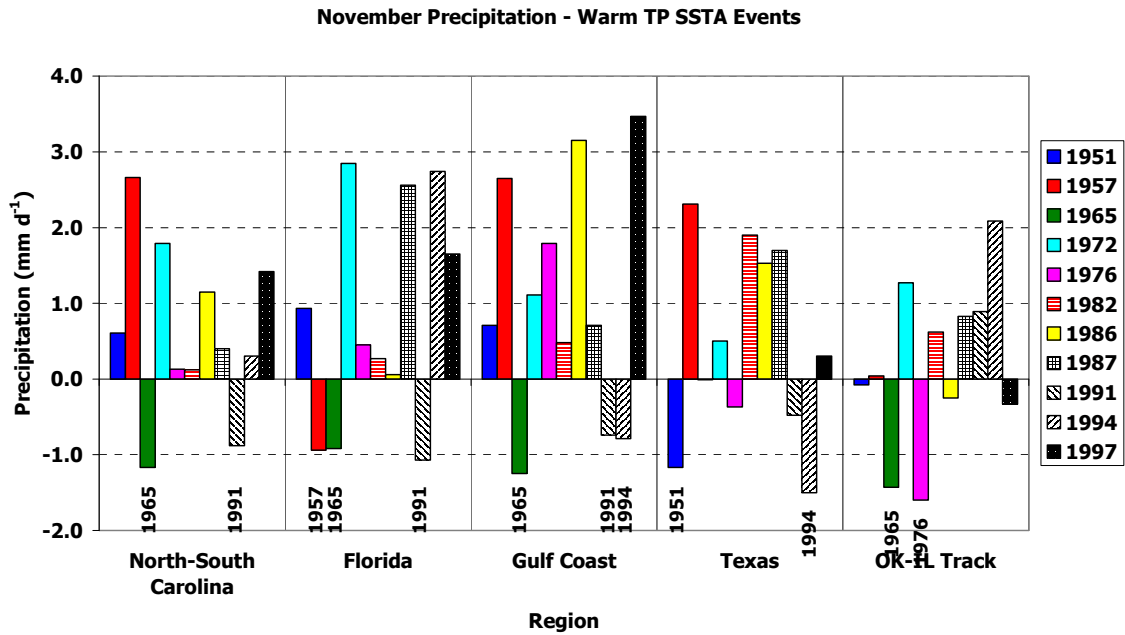


Fig. 4.7: Regionally averaged station precipitation anomalies ( $\text{mm d}^{-1}$ ) from 1950-92 mean for November during warm SSTA VPC1 events for regions delineated in Table 4.7.

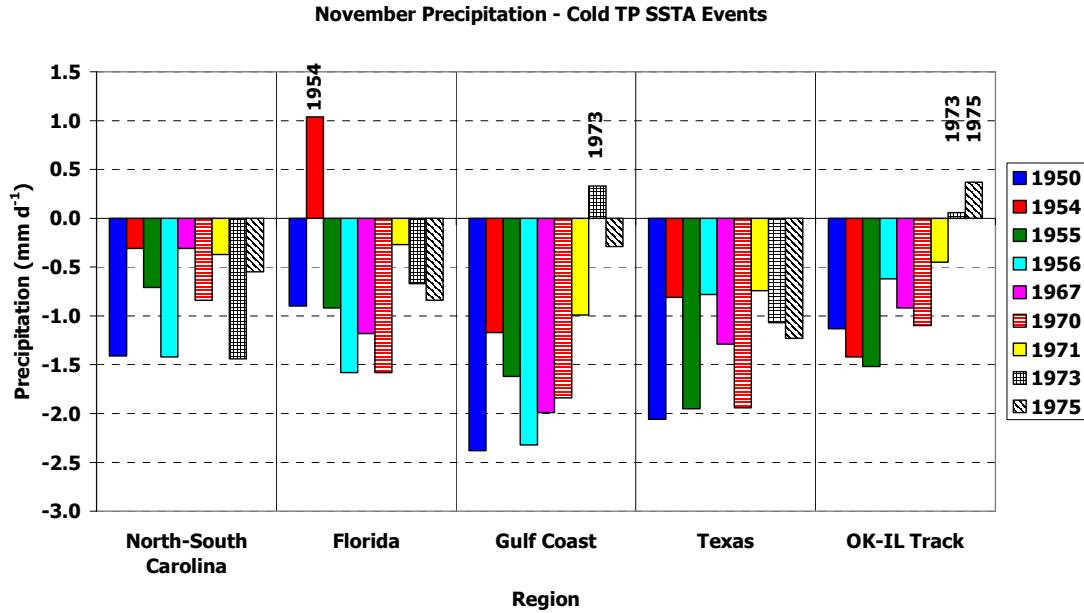


Fig. 4.8: As in Fig. 4.7, but for cold TP SSTA events.

#### 4.3.1.3 SOUTHWESTERN APPALACHIAN MOUNTAINS AND EASTERN MIDWEST (JANUARY-MARCH)

An association first identified by M97 and MRL98 involved generally dry (wet) conditions in the southwestern Appalachian Mountains and eastern Midwest during warm (cold) eastern TP SSTA events in January and February. MRL98 highlighted the nonlinearity of this feature using local and regional significance testing during the warm and cold eastern TP SSTA events. Specifically, the coherency was (was not) locally significant during warm (cold) eastern TP SSTA events (Fig. 3.1e-j). The association with warm SSTAs had large spatial extent during January and February with much smaller extent in March (but farther south than in January-February). Composite anomalies during the warm event years selected by MRL98 exceeded +25 mm (about  $0.90 \text{ mm d}^{-1}$ ) during each month. Note that while the above association does extend into March, it is not geographically coincident with the anomalies in February. Consequently, further analysis of daily distributions in this section will focus on January-February.

More specific analysis of the average anomalies in the present study indicates the warm SSTA event association in the southwestern Appalachian Mountains and eastern



		January-February Season			January			February		
		Warm	Neutral	Cold	Warm	Neutral	Cold	Warm	Neutral	Cold
<b>Aggregate Stats</b>	Total (mm d <sup>-1</sup> )	3.37	4.00	5.67	2.99	3.96	5.85	3.80	4.04	5.48
	Anom (mm d <sup>-1</sup> )	-0.78	-0.16	1.52	-1.11	-0.14	1.75	-0.41	-0.17	1.28
<b>Relative Event Freq</b>	Num Events	1610	11185	2358	842	5854	1306	768	5331	1052
	< 5 mm	41%	40%	36%	40%	39%	34%	33%	38%	30%
	5-10 mm	20%	19%	17%	21%	18%	14%	15%	17%	17%
	10-25 mm	28%	26%	27%	28%	28%	28%	34%	28%	30%
	25-50 mm	10%	11%	14%	9%	12%	17%	15%	13%	15%
	50-100 mm	2%	3%	6%	3%	4%	7%	3%	3%	8%
	100-200 mm	< 1%	< 1%	< 1%	0%	< 1%	0%	0%	< 1%	< 1%
>200 mm	0%	0%	0%	0%	0%	0%	0%	0%	0%	
	Avg Size (mm)	11.61	12.74	15.44	10.24	12.41	14.88	13.12	13.10	16.14
<b>Quartile</b>	Max (mm)	100.58	164.34	113.79	72.90	164.34	108.97	100.58	154.43	113.79
	3rd Quartile (mm)	15.49	16.76	21.08	12.95	16.51	20.32	17.78	17.27	21.65
	Median (mm)	6.99	7.11	8.64	5.84	7.11	7.87	8.51	7.11	9.65
	1st Quartile (mm)	2.54	2.29	2.54	2.03	2.03	2.54	2.54	2.54	3.05
	Min (mm)	0.25	0.25	0.25	0.25	0.25	0.25	0.25	0.25	0.25
<b>Actual Event Freq</b>	ALL EVENTS	17.9	19.1	22.5	9.4	10.0	12.4	8.5	9.1	10.0
	< 5 mm	7.3	7.7	8.2	3.7	3.9	4.3	2.8	3.5	3.0
	5-10 mm	3.5	3.6	3.8	1.9	1.8	1.8	1.3	1.6	1.7
	10-25 mm	5.0	5.1	6.0	2.6	2.8	3.5	2.9	2.5	3.0
	25-50 mm	1.8	2.2	3.2	0.8	1.2	2.1	1.3	1.2	1.5
	50-100 mm	0.3	0.5	1.3	0.2	0.4	0.8	0.2	0.3	0.8
	100-200 mm	< 0.1	< 0.1	< 0.1	0.0	< 0.1	0.0	0.0	< 0.1	< 0.1
>200 mm	0.0	0.0	0.0	0.0	0.0	0.0	0.0	0.0	0.0	

Table 4.9: As in Table 4.1 but for southwestern Appalachian mountains (upper left) during January-February.

Midwest was strongest in January and February, respectively, and further that for the Appalachians, the cold SSTA event association was stronger than its warm counterpart. Table 4.9 shows that the average composite anomaly over the southwestern Appalachian Mountains region during warm eastern TP SSTA events decreased from  $-1.11 \text{ mm d}^{-1}$  in January to  $-0.41 \text{ mm d}^{-1}$  in February, but during both months the average anomaly magnitude during cold SSTA events was much larger than for the corresponding cold event anomaly –  $+1.75 \text{ mm d}^{-1}$  (cold) vs.  $-1.11 \text{ mm d}^{-1}$  (warm) for January, and  $+1.21 \text{ mm d}^{-1}$  (cold) vs.  $-0.41 \text{ mm d}^{-1}$  (warm) in February. For the eastern Midwest region (Table 4.10), the anomaly during warm SSTA events in February ( $-0.71 \text{ mm d}^{-1}$ ) is nearly double that in January ( $-0.36 \text{ mm d}^{-1}$ ). In contrast to the southwestern Appalachian Mountain region, the magnitude of the average precipitation anomaly during cold SSTA events in the eastern Midwest was much closer to that during warm SSTA events. These relationships further refine MRL98’s finding of a nonlinear relationship between precipitation in these regions and TP SSTAs.



		January-February Season			January			February		
		Warm	Neutral	Cold	Warm	Neutral	Cold	Warm	Neutral	Cold
<b>Aggregate Stat</b>	Total (mm d <sup>-1</sup> )	1.19	1.72	2.20	1.38	1.73	2.15	0.98	1.70	2.25
	Anom (mm d <sup>-1</sup> )	-0.53	0.00	0.48	-0.36	-0.02	0.40	-0.71	0.01	0.55
<b>Relative Event Freq</b>	Num Events	2148	16680	3169	1238	9020	1639	910	7660	1530
	< 5 mm	70%	67%	60%	62%	59%	50%	66%	59%	53%
	5-10 mm	16%	17%	19%	18%	19%	20%	18%	18%	19%
	10-25 mm	12%	13%	17%	17%	17%	23%	14%	17%	21%
	25-50 mm	1%	3%	4%	3%	4%	6%	2%	4%	7%
	50-100 mm	0%	< 1%	< 1%	0%	1%	2%	0%	1%	< 1%
	100-200 mm	0%	0%	< 1%	0%	0%	< 1%	0%	0%	0%
	>200 mm	0%	0%	0%	0%	0%	0%	0%	0%	0%
	Avg Size (mm)	4.93	5.62	6.73	5.14	5.48	6.39	4.64	5.79	7.10
<b>Quartile</b>	Max (mm)	48.26	79.50	106.43	48.26	79.50	106.43	48.01	77.47	55.37
	3rd Quartile (mm)	6.10	6.60	8.64	6.35	6.35	8.89	5.59	6.86	8.64
	Median (mm)	2.29	2.54	3.56	2.54	2.54	3.30	2.03	2.79	3.56
	1st Quartile (mm)	0.76	1.02	1.27	0.76	1.02	1.02	0.76	1.02	1.27
	Min (mm)	0.25	0.25	0.25	0.25	0.25	0.25	0.25	0.25	0.25
<b>Actual Event Freq</b>	ALL EVENTS	15.6	18.6	19.7	9.0	10.1	10.2	6.6	8.5	9.5
	< 5 mm	10.9	12.5	11.8	5.5	6.0	5.1	4.3	5.0	5.0
	5-10 mm	2.5	3.2	3.7	1.6	1.9	2.0	1.2	1.6	1.8
	10-25 mm	1.9	2.4	3.3	1.6	1.7	2.3	0.9	1.5	2.0
	25-50 mm	0.2	0.5	0.8	0.3	0.4	0.6	0.1	0.4	0.7
	50-100 mm	0.0	0.1	0.1	0.0	0.1	0.2	0.0	0.1	< 0.1
	100-200 mm	0.0	0.0	< 0.1	0.0	0.0	< 0.1	0.0	0.0	0.0
>200 mm	0.0	0.0	0.0	0.0	0.0	0.0	0.0	0.0	0.0	

Table 4.10: As in Table 4.1 but for eastern Midwest (upper left) during January-February.

During warm (cold) eastern TP SSTA events, the negative (positive) precipitation anomaly in the southwestern Appalachian Mountains arises from a decrease (increase) in the frequency of relatively heavy precipitation events. During January-February, the Actual Event Frequency for the southwestern Appalachian Mountains region in Table 4.9 decreased slightly during warm TP SSTA events (relative to neutral SSTA events) for daily precipitation totals exceeding 25 mm d<sup>-1</sup>, but increased notably during cold SSTA events for precipitation amounts between 10-100 mm d<sup>-1</sup> (Fig. 4.9a). The January-February precipitation received from events with size in these ranges during warm TP SSTA events was less than that received during neutral TP SSTA events, but for cold TP SSTAs the precipitation received was higher in all categories, especially for events exceeding 10 mm d<sup>-1</sup> (Fig. 4.9b; Table 4.11). Consequently, it appears that during warm SSTA events, the southwestern Appalachian mountain region did not receive as many precipitation events exceeding 50 mm d<sup>-1</sup> in January-February, but especially in January.

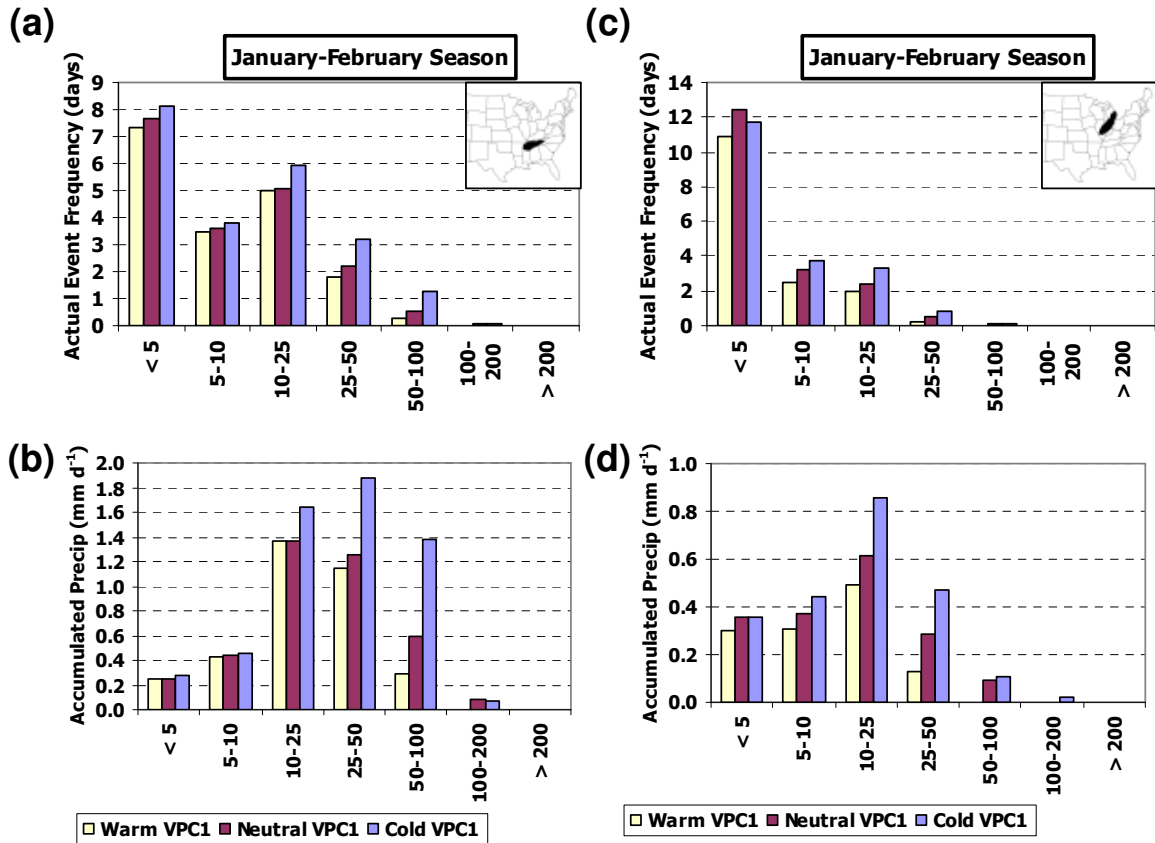


Fig. 4.9: As in Fig. 4.1 but for January-February precipitation in (a)-(b) southwestern Appalachian Mountains and (c)-(d) eastern Midwest region.

Precip Category	January-February Season			January			February		
	Warm	Neutral	Cold	Warm	Neutral	Cold	Warm	Neutral	Cold
<5	0.249	0.254	0.269	0.286	0.248	0.294	0.210	0.261	0.241
5-10	0.420	0.437	0.459	0.447	0.436	0.486	0.391	0.437	0.428
10-25	1.349	1.372	1.638	1.218	1.367	1.648	1.494	1.379	1.627
25-50	1.042	1.255	1.849	0.708	1.208	2.031	1.413	1.308	1.647
50-100	0.292	0.588	1.373	0.330	0.604	1.292	0.250	0.570	1.462
100-200	0.019	0.089	0.086	0.000	0.097	0.096	0.040	0.080	0.075
>200	0.000	0.000	0.000	0.000	0.000	0.000	0.000	0.000	0.000
<b>TOTAL</b>	<b>3.372</b>	<b>3.995</b>	<b>5.674</b>	<b>2.988</b>	<b>3.959</b>	<b>5.848</b>	<b>3.798</b>	<b>4.036</b>	<b>5.480</b>

Precip Category	January-February Season			January			February		
	Warm	Neutral	Cold	Warm	Neutral	Cold	Warm	Neutral	Cold
<5	7%	6%	5%	10%	6%	5%	6%	6%	4%
5-10	12%	11%	8%	15%	11%	8%	10%	11%	8%
10-25	40%	34%	29%	41%	35%	28%	39%	34%	30%
25-50	31%	31%	33%	24%	31%	35%	37%	32%	30%
50-100	9%	15%	24%	11%	15%	22%	7%	14%	27%
100-200	1%	2%	2%	0%	2%	2%	1%	2%	1%
>200	0%	0%	0%	0%	0%	0%	0%	0%	0%

Table 4.11: As in Table 4.4 but for southwestern Appalachian mountains (as delineated in upper left corner of Table 4.9) during January-February.

Precip Category	January-February Season			January			February		
	Warm	Neutral	Cold	Warm	Neutral	Cold	Warm	Neutral	Cold
<5	0.298	0.360	0.355	0.323	0.368	0.342	0.270	0.351	0.369
5-10	0.302	0.373	0.441	0.344	0.383	0.434	0.254	0.362	0.448
10-25	0.478	0.611	0.856	0.565	0.618	0.894	0.383	0.605	0.813
25-50	0.115	0.283	0.450	0.151	0.287	0.331	0.075	0.278	0.582
50-100	0.000	0.089	0.083	0.000	0.072	0.127	0.000	0.107	0.035
100-200	0.000	0.000	0.011	0.000	0.000	0.021	0.000	0.000	0.000
>200	0.000	0.000	0.000	0.000	0.000	0.000	0.000	0.000	0.000
<b>TOTAL</b>	<b>1.193</b>	<b>1.716</b>	<b>2.196</b>	<b>1.383</b>	<b>1.728</b>	<b>2.149</b>	<b>0.983</b>	<b>1.703</b>	<b>2.247</b>

Precip Category	January-February Season			January			February		
	Warm	Neutral	Cold	Warm	Neutral	Cold	Warm	Neutral	Cold
<5	25%	21%	16%	23%	21%	16%	27%	21%	16%
5-10	25%	22%	20%	25%	22%	20%	26%	21%	20%
10-25	40%	36%	39%	41%	36%	42%	39%	36%	36%
25-50	10%	16%	20%	11%	17%	15%	8%	16%	26%
50-100	0%	5%	4%	0%	4%	6%	0%	6%	2%
100-200	0%	0%	1%	0%	0%	1%	0%	0%	0%
>200	0%	0%	0%	0%	0%	0%	0%	0%	0%

Table 4.12: As in Table 4.4 but for eastern Midwest (as delineated in upper left corner of Table 4.10) during January-February.

The decrease in January-February precipitation in the eastern Midwest region primarily resulted from a decrease in the frequency of all daily precipitation amounts during warm eastern TP SSTA events, but during cold SSTA events, the precipitation increase arose primarily from more frequent precipitation with daily amounts between 10-50 mm d<sup>-1</sup>. During January-February, the Actual Event Frequency for this region in Table 4.10 decreased for precipitation events of all sizes during warm SSTA events (relative to neutral SSTA conditions) and increased during cold SSTA events for precipitation amounts greater than 5 mm d<sup>-1</sup> (Fig. 4.9c). The amount of precipitation received during warm TP SSTA events (Table 4.12) is substantially below the corresponding totals received during neutral SSTA events for precipitation events of all sizes (Fig. 4.9d). For cold SSTA events, the daily precipitation size ranges from which the amount of precipitation received was substantially above that received during neutral SSTA events was limited to sizes between 10-50 mm d<sup>-1</sup> (Fig. 4.9d). Consequently, relative to neutral SSTA events, the eastern Midwest region observed a decrease in precipitation during warm SSTA events due to reduced frequency of daily precipitation amounts of all sizes, while during cold TP SSTA events, total precipitation increased due to more frequent heavier (i.e., greater than 10 mm d<sup>-1</sup>) precipitation events, similar to the southwestern Appalachian mountain region.

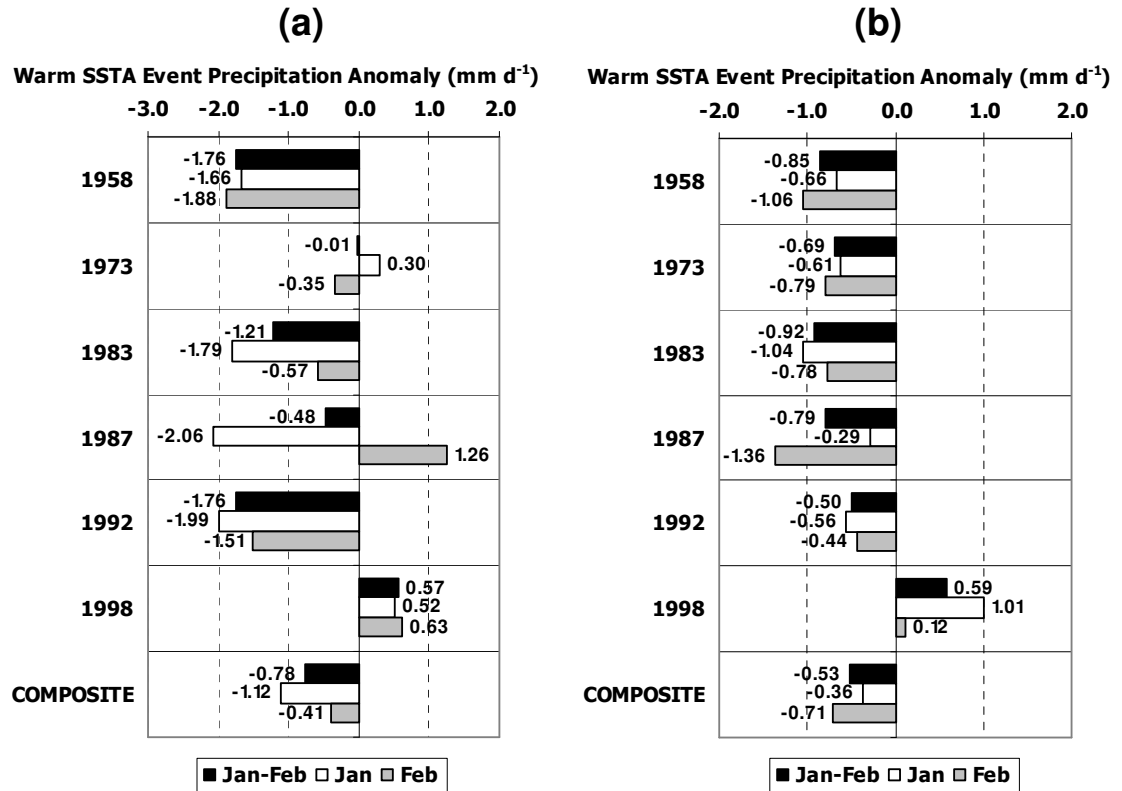


Fig. 4.10: (a) As in Fig. 2.1a but for January-February precipitation for southwestern Appalachian Mountains as delineated in Table 4.9. (b) As in (a) but for eastern Midwest region in Table 4.10.

Fig. 4.10 and Fig. 4.11 indicate that the composite constituent years during which the sign of the observed anomaly for the two aforementioned regions did not match that of the composite anomaly were 1973 and 1998 (warm SSTAs) and 1968 and 1976 (cold SSTAs), but there were no key distinguishing climate system characteristics of these years. The warm SSTA “exception years” of 1973 and 1998, aside from being traditional El Niño events, with a clear propagation of SSTAs from the eastern TP to the central TP, exhibited no distinguishing patterns in the other climate system phenomena described in Section 2.3. Although the January-March Arctic Oscillation (AO) was positive in 1973 – the same year when the January-February southwestern Appalachian mountain region observed near normal (instead of below normal) precipitation – the AO also was positive in 1992 (Table 2.2) when precipitation in the southwestern Appalachian mountain region was below normal. In 1998, both the eastern Midwest and southwestern Appalachian

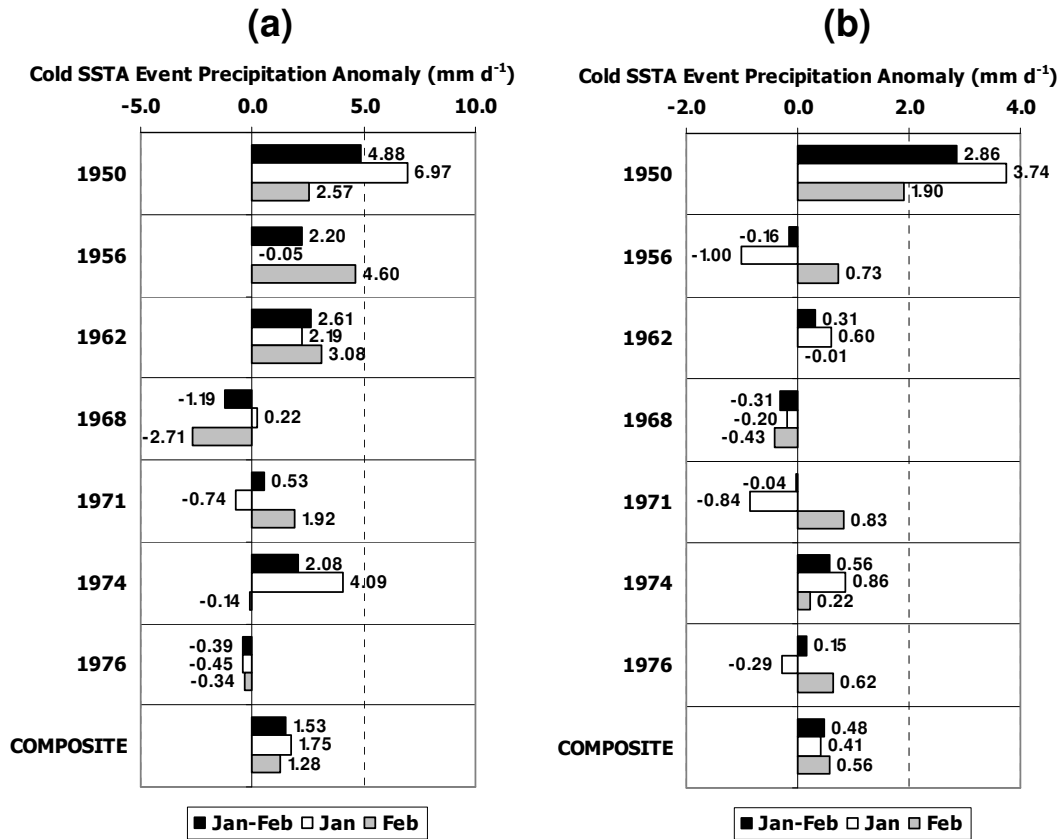


Fig. 4.11: As in Fig. 4.10 but for cold SSTA VPC1 events.

mountain regions experienced above normal precipitation, contrary to the composite anomaly, but the January-March AO and PDO were negative and positive, respectively, similar to many of the other composite anomalies.

During both of the cold SSTA VPC1 event “exception years”, the Arctic Oscillation was in the positive phase. In both 1968 and 1976, when the southwestern Appalachian mountain region experienced below normal precipitation (instead of above normal as in the overall composite), the January-March PDO was negative, just like all other cold SSTA VPC1 events, but the AO was positive (Table 2.2).

#### 4.3.1.4 CANADIAN PRAIRIES-NORTHERN U.S. GREAT PLAINS (NOVEMBER-JANUARY)

Another previously undiscovered relationship identified in MRL98 involved precipitation in the Northern U.S. Great Plains and southern Canadian prairies. MRL98

demonstrated that during November-December-January, southern Alberta-Manitoba, eastern Montana, and the Dakotas exhibited negative precipitation anomalies during warm eastern TP SSTA events (Fig. 3.1a,c,e). During cold TP SSTA events, smaller positive composite precipitation anomalies were present in Canada only (Fig. 3.1b,d,f). The association was mostly linear in southern Alberta-Manitoba, and more nonlinear in Montana and the Dakotas. During this season, statistically significant composite anomalies around -10 mm (about  $-0.11 \text{ mm d}^{-1}$ ) spanned these areas.

The present research supports MRL98's finding that the eastern Montana region exhibited the most nonlinear characteristics, but the southern Alberta-Manitoba region also demonstrated some linear features. In eastern Montana (Table 4.13), the individual monthly composite anomalies during warm TP SSTA events in December-January were similar and approximately twice the size of the November anomaly; however, the anomalies in all months during cold TP SSTA events were near zero. In southern Alberta-Manitoba (Table 4.14), the magnitude of the individual monthly composite anomalies in November-January during warm TP SSTA events was as much as  $0.05 \text{ mm d}^{-1}$  larger than the corresponding composite anomalies during cold TP SSTA events.

In both areas, the negative composite November-January precipitation anomalies during warm TP SSTA events arose from decreases (relative to neutral SSTA events) in the frequency of all daily precipitation totals, with the southern Alberta-Manitoba region exhibiting increased precipitation event frequency during cold TP SSTA events. The Actual Event Frequency for the November-January season during warm TP SSTA events in eastern Montana (Table 4.13) and southern Alberta-Manitoba (Table 4.14) was lower compared to neutral SSTA events for all daily precipitation amounts, although the greatest decrease occurred for totals of less than 5 mm (Fig. 4.12a,c). The Actual Event Frequency for eastern Montana (southern Alberta-Manitoba) for daily precipitation amounts less than 5 mm decreased from nearly 13 (17) days per November-January season during neutral TP SSTA events to 9 (14) days during warm TP SSTA events. Similarly, during cold TP SSTA events, the Actual Event Frequency in southern Alberta-Manitoba increased for all daily precipitation amounts (Fig. 4.12c) while that for eastern Montana was higher than during warm SSTA events in all categories (Fig. 4.12d).

		November-January Season			November			December			January		
		<i>Warm</i>	<i>Neutral</i>	<i>Cold</i>	<i>Warm</i>	<i>Neutral</i>	<i>Cold</i>	<i>Warm</i>	<i>Neutral</i>	<i>Cold</i>	<i>Warm</i>	<i>Neutral</i>	<i>Cold</i>
<b>Aggregate Stats</b>	Total (mm d <sup>-1</sup> )	0.29	0.46	0.44	0.34	0.46	0.43	0.24	0.45	0.40	0.29	0.49	0.48
	Anom (mm d <sup>-1</sup> )	-0.14	0.04	0.01	-0.09	0.03	0.00	-0.17	0.05	0.00	-0.16	0.04	0.03
<b>Relative Event Frequency</b>	Num Events	1882	10450	2658	594	2964	805	541	3548	883	747	3938	970
	< 5 mm	86%	84%	83%	80%	80%	83%	86%	87%	83%	92%	88%	83%
	5-10 mm	11%	12%	13%	14%	15%	14%	12%	10%	13%	7%	9%	13%
	10-25 mm	3%	3%	4%	5%	4%	3%	2%	2%	4%	2%	2%	4%
	25-50 mm	< 1%	< 1%	0%	1%	< 1%	0%	0%	< 1%	0%	0%	< 1%	0%
	50-100 mm	0%	0%	0%	0%	0%	0%	0%	0%	0%	0%	0%	0%
	100-200 mm	0%	0%	0%	0%	0%	0%	0%	0%	0%	0%	0%	0%
>200 mm	0%	0%	0%	0%	0%	0%	0%	0%	0%	0%	0%	0%	
	Avg Size (mm)	2.66	2.87	2.84	3.30	3.20	2.99	2.39	2.73	2.73	2.34	2.74	2.80
<b>Quartile</b>	Max (mm)	38.10	33.02	21.59	38.10	33.02	19.81	28.96	31.24	21.59	27.94	33.02	20.32
	3rd Quartile (mm)	3.05	3.56	3.56	3.81	4.06	3.81	3.05	3.30	3.30	2.54	3.30	3.81
	Median (mm)	1.52	1.78	1.78	1.78	1.78	2.03	1.52	1.78	1.52	1.27	1.78	1.78
	1st Quartile (mm)	0.76	0.76	0.76	0.76	0.76	0.76	0.76	0.76	0.76	0.76	0.76	0.76
	Min (mm)	0.25	0.25	0.25	0.25	0.25	0.25	0.25	0.25	0.25	0.25	0.25	0.25
<b>Actual Event Frequency</b>	ALL EVENTS	10.5	15.4	14.8	3.3	4.4	4.5	3.0	5.2	4.9	4.2	5.8	5.4
	< 5 mm	9.0	12.9	12.3	2.6	3.5	3.7	2.6	4.5	4.1	3.8	5.1	4.5
	5-10 mm	1.2	1.9	2.0	0.5	0.7	0.6	0.4	0.5	0.7	0.3	0.5	0.7
	10-25 mm	0.3	0.5	0.5	0.2	0.2	0.1	0.1	0.1	0.2	0.1	0.1	0.2
	25-50 mm	< 0.1	< 0.1	0.0	0.0	< 0.1	0.0	< 0.1	< 0.1	0.0	0.0	< 0.1	0.0
	50-100 mm	0.0	0.0	0.0	0.0	0.0	0.0	0.0	0.0	0.0	0.0	0.0	0.0
	100-200 mm	0.0	0.0	0.0	0.0	0.0	0.0	0.0	0.0	0.0	0.0	0.0	0.0
>200 mm	0.0	0.0	0.0	0.0	0.0	0.0	0.0	0.0	0.0	0.0	0.0	0.0	

Table 4.13: As in Table 4.1 but for eastern Montana region (upper left) during November-December-January.

		November-January Season			November			December			January		
		<i>Warm</i>	<i>Neutral</i>	<i>Cold</i>	<i>Warm</i>	<i>Neutral</i>	<i>Cold</i>	<i>Warm</i>	<i>Neutral</i>	<i>Cold</i>	<i>Warm</i>	<i>Neutral</i>	<i>Cold</i>
<b>Aggregate Stats</b>	Total (mm d <sup>-1</sup> )	0.45	0.61	0.71	0.44	0.57	0.62	0.46	0.60	0.73	0.45	0.65	0.78
	Anom (mm d <sup>-1</sup> )	-0.15	0.01	0.12	-0.11	0.01	0.07	-0.13	0.00	0.13	-0.19	0.01	0.14
<b>Relative Event Frequency</b>	Num Events	6888	31989	9196	2070	8891	2674	2241	10928	3078	2577	12170	3444
	< 5 mm	86%	84%	80%	87%	80%	78%	86%	86%	80%	89%	87%	80%
	5-10 mm	11%	13%	16%	9%	15%	14%	8%	12%	15%	10%	10%	15%
	10-25 mm	3%	3%	4%	4%	5%	7%	5%	2%	4%	< 1%	3%	5%
	25-50 mm	< 1%	< 1%	< 1%	0%	< 1%	1%	1%	0%	< 1%	0%	< 1%	0%
	50-100 mm	0%	0%	0%	0%	0%	0%	0%	0%	0%	0%	0%	0%
	100-200 mm	0%	0%	0%	0%	0%	0%	0%	0%	0%	0%	0%	0%
>200 mm	0%	0%	0%	0%	0%	0%	0%	0%	0%	0%	0%	0%	
	Avg Size (mm)	2.57	2.82	3.11	2.69	2.98	2.99	2.83	2.79	3.21	2.25	2.74	3.11
<b>Quartile</b>	Max (mm)	29.21	39.88	46.74	24.64	39.88	32.00	29.21	32.51	34.29	25.40	33.02	46.74
	3rd Quartile (mm)	3.05	3.30	3.81	3.05	3.81	3.81	3.30	3.11	3.81	2.79	3.05	3.81
	Median (mm)	1.27	1.52	1.78	1.52	1.78	1.78	1.27	1.52	2.03	1.27	1.52	1.78
	1st Quartile (mm)	0.76	0.76	0.76	0.76	0.76	0.76	0.76	0.76	0.76	0.76	0.76	0.76
	Min (mm)	0.25	0.25	0.25	0.25	0.25	0.25	0.25	0.25	0.25	0.25	0.25	0.25
<b>Actual Event Frequency</b>	ALL EVENTS	16.6	20.5	22.2	5.0	5.7	6.5	5.4	7.0	7.4	6.2	7.8	8.3
	< 5 mm	14.2	17.1	17.7	4.3	4.5	5.0	4.7	6.0	6.0	5.6	6.7	6.6
	5-10 mm	1.9	2.7	3.5	0.5	0.8	0.9	0.4	0.8	1.1	0.6	0.8	1.3
	10-25 mm	0.5	0.6	0.9	0.2	0.3	0.5	0.3	0.2	0.3	< 0.1	0.2	0.4
	25-50 mm	< 0.1	< 0.1	< 0.1	0.0	< 0.1	< 0.1	< 0.1	0.0	< 0.1	0.0	< 0.1	0.0
	50-100 mm	0.0	0.0	0.0	0.0	0.0	0.0	0.0	0.0	0.0	0.0	0.0	0.0
	100-200 mm	0.0	0.0	0.0	0.0	0.0	0.0	0.0	0.0	0.0	0.0	0.0	0.0
>200 mm	0.0	0.0	0.0	0.0	0.0	0.0	0.0	0.0	0.0	0.0	0.0	0.0	

Table 4.14: As in Table 4.1 but for southern Alberta-Manitoba region (upper left) during November-December-January.

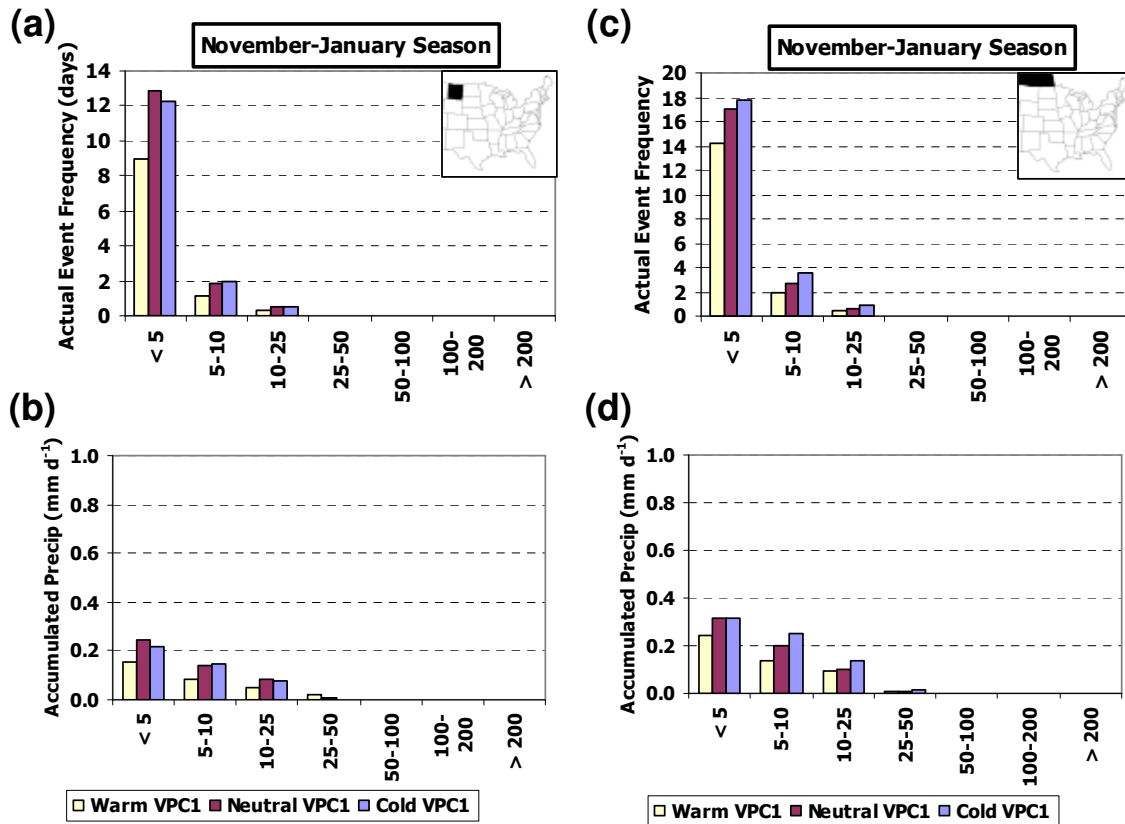


Fig. 4.12: As in Fig. 4.1 but for November-January precipitation in eastern Montana (a)-(b) and southern Alberta-Manitoba (c)-(d).

Daily precipitation totals of less than 10 mm contributed most to the overall seasonal and monthly composite totals in both regions during warm SSTA events, but during cold SSTA events the positive precipitation anomaly in southern Alberta-Manitoba arose from larger daily precipitation amounts. In eastern Montana, during warm TP SSTA events (compared to neutral SSTA events), although the seasonal precipitation received from all daily precipitation categories decreased (Fig. 4.13a), the majority of the seasonal composite precipitation difference came from daily amounts less than 10 mm, as the combined decreased of  $-0.14 \text{ mm d}^{-1}$  ( $-0.09 + -0.05 = -0.14$ ) comprised 82% of the total decrease of  $-0.18 \text{ mm d}^{-1}$  (Fig. 4.13a; Table 4.15). Further, most of this decrease in the seasonal anomaly arose from December and January (Table 4.15), although the monthly anomaly for November also decreased during warm SSTA events compared to neutral SSTA events. In southern Alberta-Manitoba, the

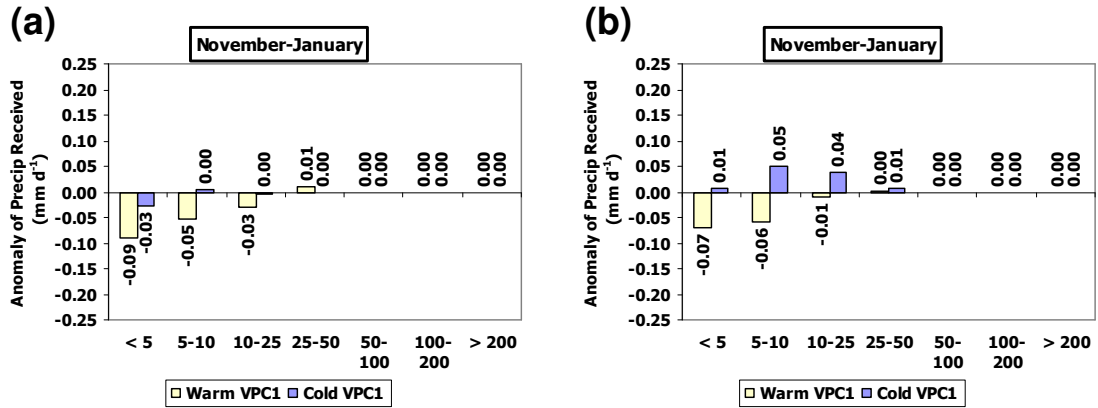


Fig. 4.13: As in Fig. 4.5, but for total November-January precipitation for (a) eastern Montana region in Fig. 4.12a and (b) southern Alberta-Manitoba region in Fig. 4.12c.

seasonal composite precipitation received during warm (cold) daily precipitation amounts of all sizes decreased (increased) compared to neutral TP SSTA events (Fig. 4.12d). In this region, while the precipitation received during warm (compared to neutral) SSTA events mainly decreased from daily amounts less than 10 mm (Fig. 4.13b; Table 4.16), that received during cold SSTA events increased mainly from daily amounts between 5-25 mm in December-January.

Precip Category	November-January Season			November			December			January		
	Warm	Neutral	Cold	Warm	Neutral	Cold	Warm	Neutral	Cold	Warm	Neutral	Cold
<5	0.156	0.247	0.222	0.151	0.210	0.211	0.130	0.244	0.205	0.177	0.270	0.236
5-10	0.086	0.139	0.147	0.100	0.148	0.147	0.073	0.132	0.131	0.081	0.135	0.153
10-25	0.042	0.081	0.077	0.067	0.088	0.067	0.031	0.071	0.067	0.025	0.078	0.092
25-50	0.009	0.006	0.000	0.018	0.010	0.000	0.005	0.003	0.000	0.005	0.004	0.000
50-100	0.000	0.000	0.000	0.000	0.000	0.000	0.000	0.000	0.000	0.000	0.000	0.000
100-200	0.000	0.000	0.000	0.000	0.000	0.000	0.000	0.000	0.000	0.000	0.000	0.000
>200	0.000	0.000	0.000	0.000	0.000	0.000	0.000	0.000	0.000	0.000	0.000	0.000
<b>TOTAL</b>	<b>0.293</b>	<b>0.475</b>	<b>0.446</b>	<b>0.336</b>	<b>0.455</b>	<b>0.425</b>	<b>0.239</b>	<b>0.450</b>	<b>0.402</b>	<b>0.287</b>	<b>0.488</b>	<b>0.481</b>

Precip Category	November-January Season			November			December			January		
	Warm	Neutral	Cold	Warm	Neutral	Cold	Warm	Neutral	Cold	Warm	Neutral	Cold
<5	53%	52%	50%	45%	46%	50%	55%	54%	51%	62%	55%	49%
5-10	29%	30%	33%	30%	32%	35%	30%	29%	33%	28%	28%	32%
10-25	14%	17%	17%	20%	19%	16%	13%	16%	17%	9%	16%	19%
25-50	3%	1%	0%	5%	2%	0%	2%	1%	0%	2%	1%	0%
50-100	0%	0%	0%	0%	0%	0%	0%	0%	0%	0%	0%	0%
100-200	0%	0%	0%	0%	0%	0%	0%	0%	0%	0%	0%	0%
>200	0%	0%	0%	0%	0%	0%	0%	0%	0%	0%	0%	0%

Table 4.15: As in Table 4.4 but for eastern Montana region (as delineated in upper left corner of Table 4.13) during November-December-January.

Precip Category	November-January Season			November			December			January		
	Warm	Neutral	Cold	Warm	Neutral	Cold	Warm	Neutral	Cold	Warm	Neutral	Cold
<5	0.245	0.314	0.323	0.222	0.263	0.292	0.218	0.321	0.301	0.277	0.337	0.355
5-10	0.141	0.202	0.253	0.126	0.192	0.200	0.145	0.193	0.277	0.141	0.208	0.262
10-25	0.072	0.098	0.141	0.093	0.105	0.119	0.091	0.080	0.141	0.028	0.103	0.154
25-50	0.004	0.006	0.013	0.000	0.008	0.014	0.009	0.004	0.013	0.002	0.007	0.012
50-100	0.000	0.000	0.000	0.000	0.000	0.000	0.000	0.000	0.000	0.000	0.000	0.000
100-200	0.000	0.000	0.000	0.000	0.000	0.000	0.000	0.000	0.000	0.000	0.000	0.000
>200	0.000	0.000	0.000	0.000	0.000	0.000	0.000	0.000	0.000	0.000	0.000	0.000
<b>TOTAL</b>	<b>0.461</b>	<b>0.621</b>	<b>0.730</b>	<b>0.441</b>	<b>0.568</b>	<b>0.625</b>	<b>0.463</b>	<b>0.597</b>	<b>0.732</b>	<b>0.448</b>	<b>0.654</b>	<b>0.784</b>

Precip Category	November-January Season			November			December			January		
	Warm	Neutral	Cold	Warm	Neutral	Cold	Warm	Neutral	Cold	Warm	Neutral	Cold
<5	53%	51%	44%	50%	46%	47%	47%	54%	41%	62%	51%	45%
5-10	31%	33%	35%	29%	34%	32%	31%	32%	38%	31%	32%	33%
10-25	16%	16%	19%	21%	19%	19%	20%	13%	19%	6%	16%	20%
25-50	1%	1%	2%	0%	1%	2%	2%	1%	2%	< 1%	1%	2%
50-100	0%	0%	0%	0%	0%	0%	0%	0%	0%	0%	0%	0%
100-200	0%	0%	0%	0%	0%	0%	0%	0%	0%	0%	0%	0%
>200	0%	0%	0%	0%	0%	0%	0%	0%	0%	0%	0%	0%

Table 4.16: As in Table 4.4 but for southern Alberta-Manitoba region (as delineated in upper left corner of Table 4.14) during November-December-January.

The composite constituent years that did not match the sign of the corresponding composite anomaly included 1976-77 and 1982-83 for eastern Montana in warm TP SSTA events and 1965-66 (1954-55) for southern Alberta-Manitoba in warm (cold) TP SSTA events. Fig. 4.14a indicates that eastern Montana observed below average November-January precipitation in every warm SSTA event except 1976-77 when well above normal January precipitation ( $+0.24 \text{ mm d}^{-1}$ ) brought the November-January season slightly above average ( $+0.01 \text{ mm d}^{-1}$ ). Additionally, especially strong December 1982 precipitation anomalies ( $+0.34 \text{ mm d}^{-1}$ ) brought that November-January seasonal anomaly near average. Table 2.2 indicates that both of these “exception” years were characterized by a negative phase of the Arctic Oscillation in November-January. In southern Alberta-Manitoba, of all the warm TP SSTA events, only in 1965-66 was the November-January seasonal precipitation anomaly positive (Fig. 4.14b), while during the cold TP SSTA events, only in 1954-55 was the seasonal precipitation anomaly below normal (Fig. 4.14c). For this region, the warm event exception year of 1965-66 was also characterized by a negative AO phase and the cold event exception year of 1954-55 by a positive phase of the NAO (Table 2.2). The effect of a negative AO phase on the warm SSTA event teleconnections will be investigated in Chapter 5.

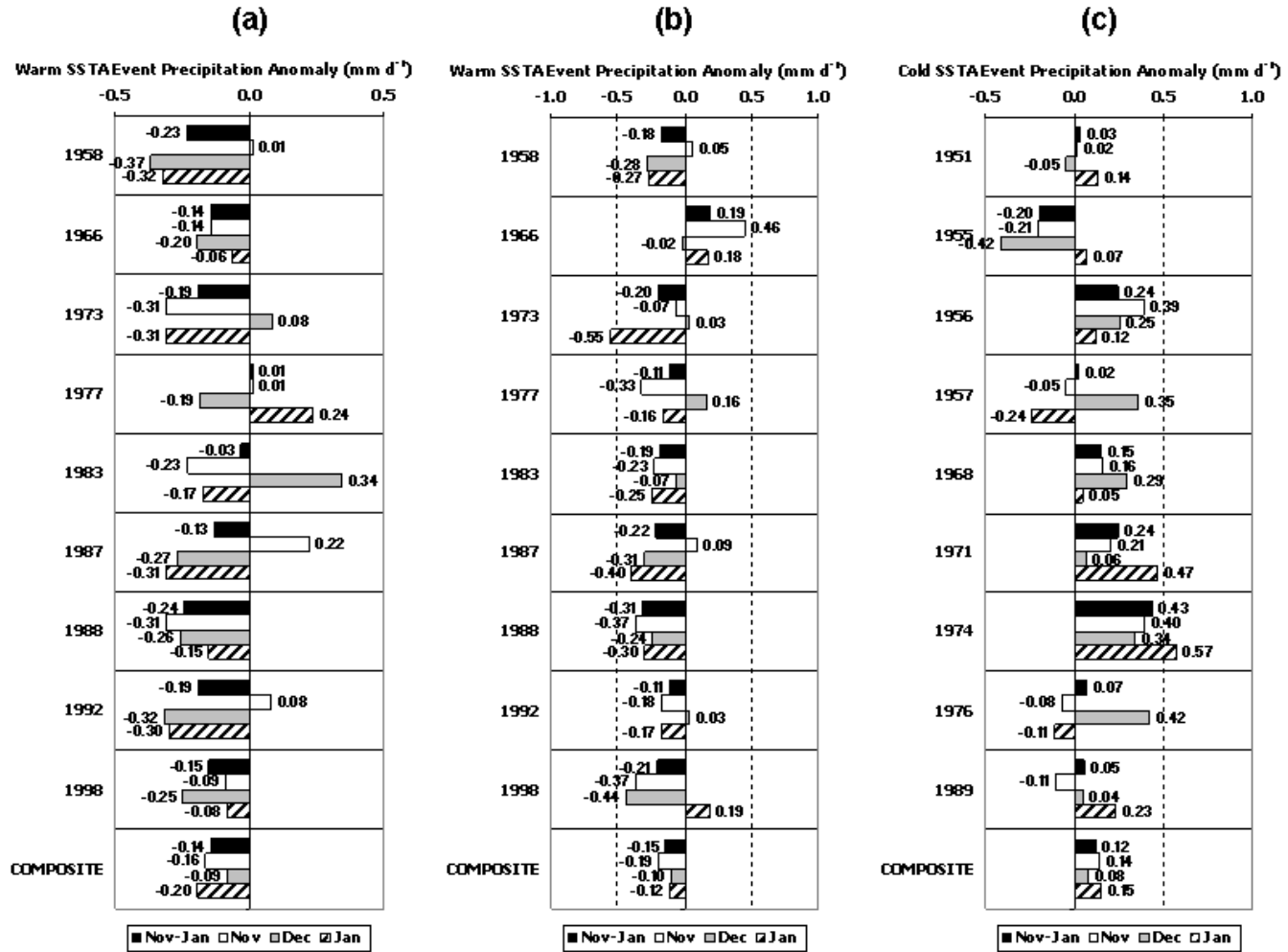


Fig. 4.14: (a) As in Fig. 2.1a but for November-January precipitation for eastern Montana region as delineated in Table 4.13. Indicated year corresponds to January of November-January season. (b) As in (a), but for November-January precipitation for southern Alberta-Manitoba region delineated in Table 4.14. (c) As in (b) but for cold SSTA events.

#### 4.3.1.5 NORTH TEXAS (JANUARY)

In addition to identifying the especially prominent associations along the Gulf coast during November-March, MRL98 demonstrated that north Texas January precipitation is nonlinearly related to TP SSTAs, with above average precipitation during warm eastern TP SSTA events but no consistent association during cold TP SSTA events. While the composite anomalies are small (around  $10 \text{ mm month}^{-1}$ , or  $0.3 \text{ mm d}^{-1}$ ), they are locally significant (Fig. 3.1e).

The present study further demonstrates the nonlinearity of north Texas precipitation and shows that it arises primarily from increases in the frequency of precipitation events of all size categories. Table 4.17 shows that the composite January precipitation anomaly for this region is  $+0.40 \text{ mm d}^{-1}$  during warm TP SSTA events, but that the negative composite anomaly during cold TP SSTA events is much smaller ( $-0.15 \text{ mm d}^{-1}$ ).

The above average January precipitation in north Texas was associated with an increase in both the frequency and precipitation accumulated from daily precipitation totals of all size categories, though daily amounts up to  $25 \text{ mm d}^{-1}$  contributed most to the monthly anomaly. Fig. 4.15a shows that the Actual Event Frequency of daily precipitation amounts of all sizes in the north Texas region (Table 4.17) increased during warm TP SSTA events compared to neutral TP SSTA events. This shift in the Actual Event Frequency was linked to an increase (relative to neutral SSTA events) in the precipitation accumulated from daily precipitation totals of all sizes (Table 4.18; Fig. 4.15b), although the increase for daily amounts between  $10\text{-}25 \text{ mm d}^{-1}$  of  $+0.204 \text{ mm d}^{-1}$  was more than double the increase in other categories. Consistent with the nonlinear aspect of this association mentioned above, the Actual Event Frequency during cold TP SSTA events is very similar to that during neutral SSTA events (Fig. 4.15a).

The indication from the warm TP SSTA composite anomaly is relatively consistent with the signs of the anomalies from the composite constituent years, while the anomalies during cold TP SSTAs suggest a weak relationship. The sign of the average anomaly is positive in 8 of the 9 warm TP SSTA composite constituent years, with 1988 being the only year not characterized by a positive precipitation anomaly (Fig. 4.16).

													
		<b>Jan</b>			<b>Mar</b>			<b>Mar</b>			<b>Dec</b>		
		<b>North Texas</b>			<b>Oklahoma-Kansas</b>			<b>Northern Great Plains</b>			<b>East Texas Louisiana</b>		
		<i>Warm</i>	<i>Neutral</i>	<i>Cold</i>	<i>Warm</i>	<i>Neutral</i>	<i>Cold</i>	<i>Warm</i>	<i>Neutral</i>	<i>Cold</i>	<i>Warm</i>	<i>Neutral</i>	<i>Cold</i>
<b>Aggregate Statistics</b>	Total (mm d <sup>-1</sup> )	1.16	0.70	0.61	2.53	1.82	1.06	1.83	1.17	0.61	4.76	3.50	3.26
	Anom (mm d <sup>-1</sup> )	0.40	-0.06	-0.15	0.75	0.04	-0.73	0.67	0.01	-0.55	1.08	-0.18	-0.43
<b>Relative Event Frequency</b>	Num Events	866	1974	739	2169	10588	1416	2252	11651	1832	2499	6310	2622
	< 5 mm	52%	59%	64%	42%	45%	45%	55%	60%	72%	50%	56%	52%
	5-10 mm	21%	18%	16%	21%	19%	22%	18%	17%	18%	12%	17%	14%
	10-25 mm	21%	19%	16%	26%	24%	19%	20%	18%	9%	20%	17%	20%
	25-50 mm	5%	4%	3%	9%	11%	12%	6%	5%	1%	12%	9%	11%
	50-100 mm	< 1%	< 1%	< 1%	2%	1%	2%	1%	< 1%	0%	5%	2%	3%
	100-200 mm	0%	< 1%	0%	< 1%	< 1%	< 1%	0%	0%	0%	1%	1%	1%
	>200 mm	0%	0%	0%	0%	0%	0%	0%	0%	0%	< 1%	0%	0%
	Avg Size (mm)	6.75	6.15	4.70	10.41	8.88	7.44	7.48	5.75	4.18	16.42	13.93	14.27
<b>Quartile</b>	Max (mm)	98.30	101.09	75.69	119.38	178.56	108.46	92.71	81.28	45.72	264.16	168.91	198.12
	3rd Quartile (mm)	9.40	8.13	6.60	13.97	12.70	10.67	9.72	7.11	5.08	21.97	18.48	18.03
	Median (mm)	3.81	3.05	2.54	5.84	5.08	4.06	3.81	2.79	2.03	8.38	7.11	7.11
	1st Quartile (mm)	1.27	1.02	0.76	1.78	1.78	1.52	1.27	1.02	0.76	2.54	2.29	2.03
	Min (mm)	0.25	0.25	0.25	0.25	0.25	0.25	0.25	0.25	0.25	0.25	0.25	0.25
<b>Actual Event Frequency</b>	ALL EVENTS	5.3	3.5	3.4	7.9	6.1	3.8	7.7	6.3	4.7	9.3	8.1	7.5
	< 5 mm	2.8	2.1	2.2	3.3	2.7	1.7	4.2	3.7	3.4	4.7	4.5	3.9
	5-10 mm	1.1	0.6	0.5	1.6	1.1	0.8	1.4	1.1	0.8	1.1	1.3	1.0
	10-25 mm	1.1	0.7	0.5	2.1	1.4	0.7	1.5	1.1	0.4	1.9	1.3	1.5
	25-50 mm	0.3	0.1	0.1	0.7	0.7	0.4	0.4	0.3	0.1	1.1	0.7	0.8
	50-100 mm	< 0.1	< 0.1	< 0.1	0.1	0.1	0.1	0.1	< 0.1	0.0	0.4	0.1	0.2
	100-200 mm	0.0	< 0.1	0.0	< 0.1	< 0.1	< 0.1	0.0	0.0	0.0	0.1	< 0.1	0.1
>200 mm	0.0	0.0	0.0	0.0	0.0	0.0	0.0	0.0	0.0	< 0.1	0.0	0.0	

Table 4.17: As in Table 4.1 but for individual regions in the Central and Southern U.S. Great Plains during January and March and eastern Texas-Louisiana in December.

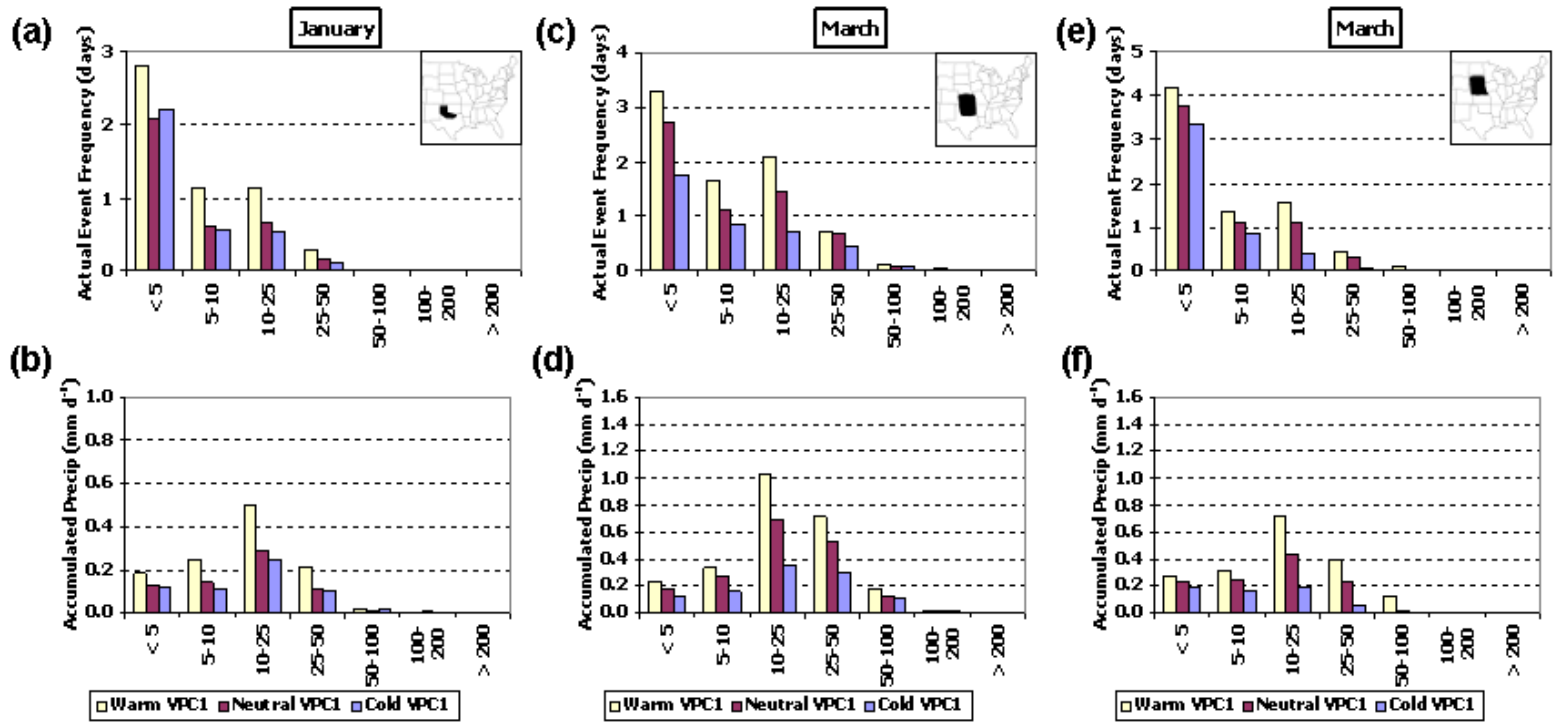


Fig. 4.15: (a) As in Fig. 4.1a but for January precipitation in north Texas region (upper right) delineated in Table 4.17. (b) As in Fig. 4.2b, but for January precipitation in north Texas region in (a). (c)-(d) As in (a)-(b) but for March precipitation in Oklahoma-Kansas region (upper right) in Table 4.17. (e)-(f) As in (c)-(d) but for northern Great Plains region (upper right).

Precip Category	Jan			Mar			Mar			Dec		
	North Texas			Oklahoma-Kansas			Northern Great Plains			East Texas Louisiana		
	Warm	Neutral	Cold	Warm	Neutral	Cold	Warm	Neutral	Cold	Warm	Neutral	Cold
<5	0.184	0.125	0.120	0.233	0.187	0.130	0.269	0.237	0.188	0.224	0.200	0.186
5-10	0.246	0.140	0.115	0.336	0.273	0.159	0.319	0.244	0.169	0.349	0.343	0.292
10-25	0.497	0.293	0.248	1.037	0.693	0.350	0.717	0.441	0.191	1.192	1.029	0.974
25-50	0.211	0.116	0.104	0.721	0.530	0.301	0.395	0.226	0.058	1.604	1.138	1.065
50-100	0.020	0.016	0.021	0.177	0.122	0.108	0.124	0.023	0.000	1.041	0.640	0.508
100-200	0.000	0.006	0.000	0.028	0.015	0.010	0.000	0.000	0.000	0.269	0.147	0.231
>200	0.000	0.000	0.000	0.000	0.000	0.000	0.000	0.000	0.000	0.086	0.000	0.000
<b>TOTAL</b>	<b>1.157</b>	<b>0.696</b>	<b>0.608</b>	<b>2.532</b>	<b>1.821</b>	<b>1.058</b>	<b>1.825</b>	<b>1.171</b>	<b>0.606</b>	<b>4.765</b>	<b>3.498</b>	<b>3.255</b>

Precip Category	Jan			Mar			Mar			Dec		
	North Texas			Oklahoma-Kansas			High Plains			East Texas Louisiana		
	Warm	Neutral	Cold	Warm	Neutral	Cold	Warm	Neutral	Cold	Warm	Neutral	Cold
<5	16%	18%	20%	9%	10%	12%	15%	20%	31%	5%	6%	6%
5-10	21%	20%	19%	13%	15%	15%	17%	21%	28%	7%	10%	9%
10-25	43%	42%	41%	41%	38%	33%	39%	38%	32%	25%	29%	30%
25-50	18%	17%	17%	28%	29%	28%	22%	19%	9%	34%	33%	33%
50-100	2%	2%	3%	7%	7%	10%	7%	2%	0%	22%	18%	16%
100-200	0%	1%	0%	1%	1%	1%	0%	0%	0%	6%	4%	7%
>200	0%	0%	0%	0%	0%	0%	0%	0%	0%	2%	0%	0%

Table 4.18: As in Table 4.4 but for individual regions (delineated in Table 4.17) in the Central and Southern Plains during January and March and in eastern Texas-Louisiana in December.

This year was characterized by a positive phase of the NAO and the PDO, and these climate system characteristics will be examined in Chapter 5 for their influence on the association between TP SSTAs and January precipitation in north Texas. In addition, while MRL98 did not specifically identify an association during cold TP SSTA events and the composite precipitation anomaly in Table 4.17 for north Texas during cold TP SSTA events is small, Fig. 4.16 suggests that a large positive anomaly in 1968 may have masked a stronger negative association during cold TP SSTA events, as 8 out of 12 cold SSTA events exhibited negative January precipitation anomalies.

#### 4.3.1.6 U.S. GREAT PLAINS (MARCH)

MRL98 demonstrated that March precipitation in the central U.S. Great Plains was linearly related to TP SSTAs. Positive precipitation anomalies spanned Oklahoma-South Dakota in the warm TP SSTA composite (Fig. 3.1i), while negative locally significant composite anomalies spanned the same region in the cold TP SSTA composite (Fig. 3.1j). Further, the composite anomalies were found to be around  $20 \text{ mm month}^{-1}$  (approximately  $0.6 \text{ mm d}^{-1}$ ), and in all of the warm (cold) TP SSTA events, the sign of

### North Texas January Precipitation Anomaly

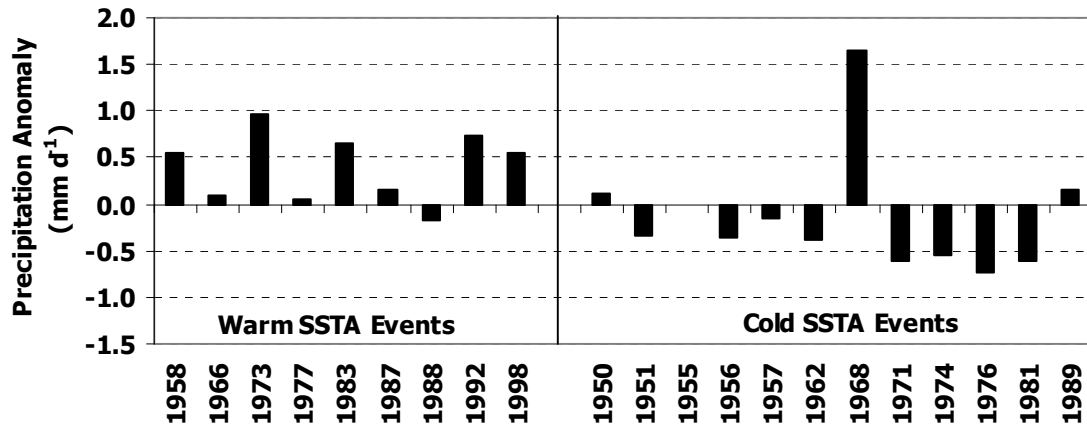


Fig. 4.16: Average January precipitation anomaly from 1950-92 mean in mm d<sup>-1</sup> for north Texas region delineated in Table 4.17.

the observed anomaly in the composite constituent years matched that of the composite anomaly (Table 3.1).

The general linearity of the March associations in MRL98 is largely supported in the frequency of daily precipitation amounts from Oklahoma to South Dakota. Fig. 4.15c,e shows that the Actual Event Frequency of daily precipitation amounts of all sizes (in Table 4.17) increased (decreased) during warm (cold) TP SSTA events, relative to neutral conditions, for both the Oklahoma-Kansas and Northern Great Plains regions. However, the largest changes in frequency occurred for daily precipitation amounts less than 25 mm during warm TP SSTA events, and for less than 50 mm during cold TP SSTA events. Consequently, changes in the relative frequency of the precipitation events were slightly different during warm TP SSTA events compared to cold SSTA events.

The amount of precipitation received by precipitation category in the Great Plains was mostly linearly related to TP SSTAs, with the anomalies arising principally from daily precipitation amounts greater than 10 mm. Fig. 4.15d,f indicates that the amount of precipitation received from each event category in the Oklahoma-Kansas and Northern Great Plains regions (located in Table 4.17) increases during warm SSTA events and decreases during cold TP SSTA events. However, the largest changes in amount of

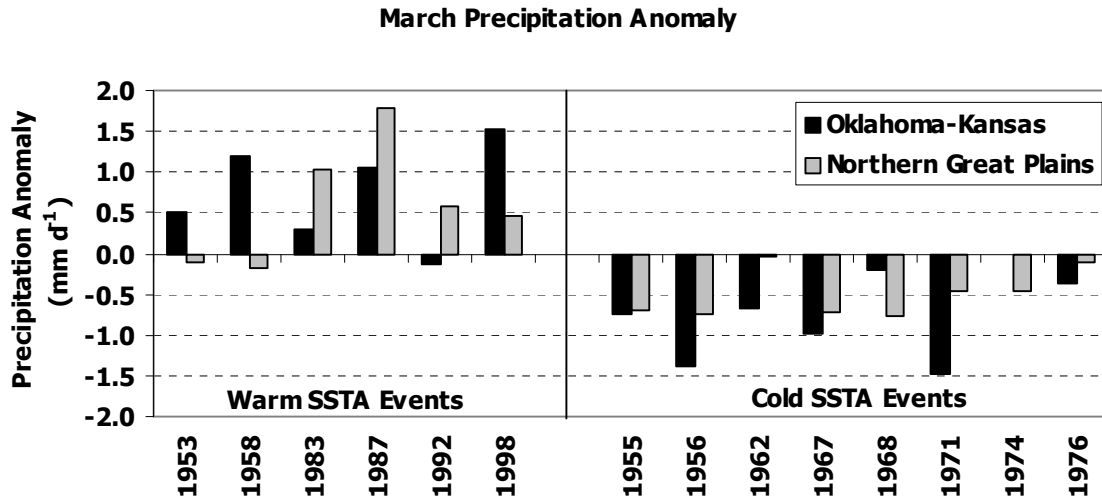


Fig. 4.17: Average March precipitation anomaly from 1950-92 mean in  $\text{mm d}^{-1}$  for Oklahoma-Kansas and Northern Great Plains regions delineated in Table 4.17.

precipitation received occurred for daily precipitation amounts greater than 10 mm during both warm and cold TP SSTA events.

Only a few years provide exceptions to the associations described above. For March precipitation events, the constituent years for the cold SSTA event composite all have negative precipitation anomalies except for 1974 in Oklahoma-Kansas, which is equal to climatology (Fig. 4.17). Additionally, the March precipitation anomalies for the constituent years for the warm SSTA event composites are all positive except for 1992 in Oklahoma-Kansas and 1953/1958 in the Great Plains. During both March 1953 and March 1958, the NAO was in a negative phase, but otherwise there were no significant distinguishing characteristics for these exception years.

#### 4.3.1.7 EAST TEXAS AND LOUISIANA (DECEMBER)

While MRL98 identified some associations between December monthly precipitation anomalies and eastern TP SSTA events, they did not find statistically significant associations for that month. Positive composite December precipitation anomalies occurred in a geographical region (Texas and lower Mississippi River valley)

that also exhibited positive anomalies in the January composite, which had high field significance (Fig. 3.1c,e). However, despite these December anomalies being rather large, nearly  $+50\text{mm month}^{-1}$  (about  $+1.6\text{ mm d}^{-1}$ ) in some parts of eastern Texas, they were not locally significant because of significant event-to-event variability in the sign of the precipitation anomaly (see Texas-to-Nebraska region in Table 3.1). The present more detailed investigation into the nature of these December anomalies, and documentation of the associated climate system characteristics that bring them about in some years, may help explain why other studies of monthly precipitation associations with TP SSTAs (e.g., M97, L97) also did not identify statistically significant December associations.

The positive December precipitation anomaly over eastern Texas and Louisiana during warm SSTA VPC1 events primarily arose from changes in the frequency of large precipitation events. Fig. 4.18a shows that the Actual Event Frequency for this region in Table 4.17 increased during warm SSTA VPC1 events compared to neutral TP SSTA events for daily precipitation amounts above 10 mm. Table 4.18 and Fig. 4.18b also indicate that the amount of precipitation received within precipitation categories less than 5  $\text{mm d}^{-1}$  and above 10  $\text{mm d}^{-1}$  was higher during warm TP SSTA events compared to neutral SSTA events, suggesting increasing importance of large magnitude precipitation events to the total composite precipitation anomaly. One of the largest increases occurred for precipitation events in the

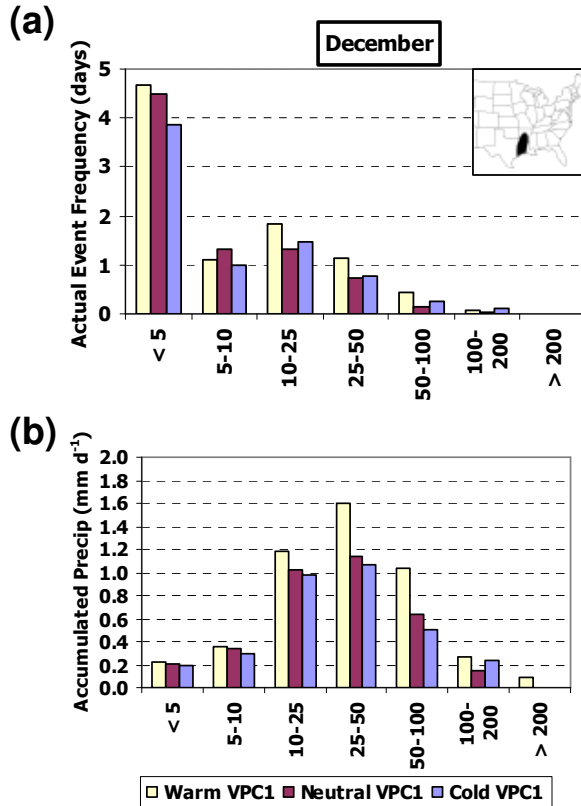


Fig. 4.18: (a) As in Fig. 4.1a but for December precipitation in the east Texas-Louisiana region (upper right). (b) As in Fig. 4.1b, but for December precipitation in east Texas-Louisiana region.

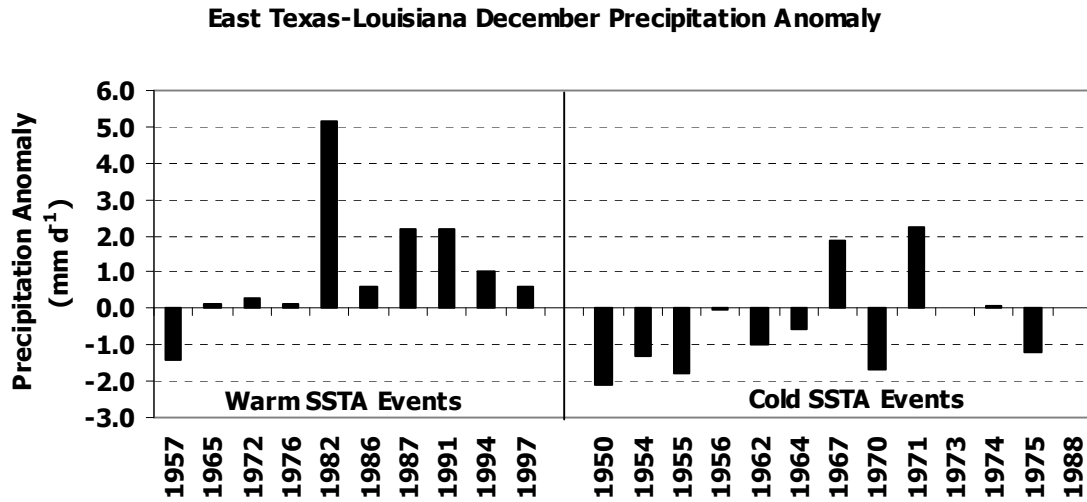


Fig. 4.19: Average December precipitation anomaly from 1950-92 mean in mm d<sup>-1</sup> for east Texas-Louisiana region delineated in Table 4.17.

25-50 mm d<sup>-1</sup> range, from which a monthly average of 1.604 mm d<sup>-1</sup> was received during warm TP SSTA events, compared to a monthly average of 1.138 mm d<sup>-1</sup> during neutral SSTA events (Table 4.18). During cold TP SSTA events, the Actual Event Frequency (Fig. 4.18a) and precipitation accumulated by daily category (Fig. 4.18b) are relatively similar to that during neutral SSTA events.

Analysis of the regional precipitation anomalies in individual composite constituent years suggests that this particular feature may exhibit decadal-scale trends, possibly helping to explain the lack of statistical significance of this feature in MRL98. Fig. 4.19 shows that for eastern TP SSTA events before and including 1976, positive precipitation anomalies were present in all but one case (1957), but they were very small. However, after 1976, 4 of 6 warm SSTA events exhibited precipitation anomalies exceeding 1 mm d<sup>-1</sup>, with the other 2 having anomalies around 0.6 mm d<sup>-1</sup>. With many previous authors documenting the presence of decadal-scale shifts in the climatology of atmospheric variables (e.g., Trenberth and Hurrell 1994, Graham 1994) and ecological data (e.g., Ebbesmeyer et al. 1991) after 1976, the delineation of weak and large magnitude events around the 1976/77 boundary merits further physical investigation. The relative difference in the magnitude of this association before and after the decadal-

scale shift that occurred in 1976-77 could help explain why the analysis of earlier authors did not show statistically significant associations between December precipitation and TP SSTAs, as the larger magnitude for the post-1976 events increases the standard deviation for the full analysis period (1950-2000), thereby raising the critical  $t$  value for 90% statistical significance.

#### 4.3.2 Associations with Central Tropical Pacific SSTA Events Only

While the previous section focused specifically on associations with eastern TP SSTAs (as measured by SSTA VPC1), this section now focuses on central TP SSTA events (as measured by SSTA UPC1). One of the more striking and robust nonlinear relationships that MRL98 identified involved a pronounced tendency toward below normal precipitation in the mid-Atlantic region during April of cold SSTA UPC1 (i.e., central TP) events. They demonstrated that locally significant composite April precipitation anomalies of about  $-25 \text{ mm month}^{-1}$  (about  $-0.8 \text{ mm d}^{-1}$ ) span much of the mid-Atlantic region in the cold SSTA UPC1 composites, while smaller and more varied positive precipitation anomalies that are not statistically significant are present in the warm SSTA UPC1 composite. No such relationship was present in the composites based on eastern TP SSTAs (VPC1), and so the following section deals with this association for April.

		April		
		Warm	Neutral	Cold
<b>Aggregate Stats</b>	Total (mm d <sup>-1</sup> )	3.64	3.01	2.11
	Anom (mm d <sup>-1</sup> )	0.71	0.08	-0.82
<b>Relative Event Frequency</b>	Num Events	1930	13780	2367
	< 5 mm	48%	52%	54%
	5-10 mm	16%	19%	19%
	10-25 mm	25%	20%	20%
	25-50 mm	7%	7%	6%
	50-100 mm	4%	1%	1%
	100-200 mm	< 1%	< 1%	0%
	>200 mm	0%	0%	0%
<b>Quartile</b>	Avg Size (mm)	9.77	8.59	7.80
	Max (mm)	115.6	126.75	77.98
	3rd Quartile (mm)	12.45	11.43	9.40
	Median (mm)	4.83	4.83	3.81
	1st Quartile (mm)	1.52	1.52	1.27
<b>Actual Event Frequency</b>	Min (mm)	0.25	0.25	0.25
	ALL EVENTS	11.7	10.7	9.0
	< 5 mm	5.6	5.6	4.8
	5-10 mm	1.9	2.0	1.7
	10-25 mm	2.9	2.2	1.8
	25-50 mm	0.8	0.7	0.5
	50-100 mm	0.5	0.1	0.1
	100-200 mm	< 0.1	< 0.1	0.0
>200 mm	0.0	0.0	0.0	

Table 4.19: As in Table 4.1 but for mid-Atlantic region (upper left) during April SSTA UPC1 events.

The present study shows that the negative precipitation anomalies associated with cold central TP (i.e., UPC1) SSTA events arise from decreases in the frequency of precipitation events of all sizes. The Relative Event Frequency changes little for the given precipitation categories, with the percentage of total precipitation events during cold UPC1 events remaining very close to that for neutral UPC1 SSTA events (Table 4.19). Further, Fig. 4.20a shows that the Actual Event Frequency in Table 4.19 of precipitation events in all categories decreases during cold SSTA UPC1 events compared to neutral SSTA events and only increases notably during warm SSTA UPC1 events for two categories. Fig. 4.20b demonstrates that the amount of precipitation received from daily precipitation amounts of all sizes decreases during cold SSTA UPC1 events compared to neutral TP SSTA events. However, the largest decrease in precipitation received occurs for daily precipitation amounts exceeding 10 mm d<sup>-1</sup> – for example, the amount of precipitation received from daily precipitation amounts between 10-25 mm d<sup>-1</sup> decreases to a monthly average of 0.450 mm d<sup>-1</sup> during cold SSTA UPC1 events from 0.744 mm d<sup>-1</sup> during neutral UPC1 events (Table 4.20). While the amount of precipitation received during warm TP SSTA UPC1 events is higher (compared to neutral SSTA events) for daily amounts above 10 mm d<sup>-1</sup>, MRL98 previously indicated that the associated composite anomaly (+0.71 mm d<sup>-1</sup>, Table 4.19) was not statistically significant using either local or regional significance tests.

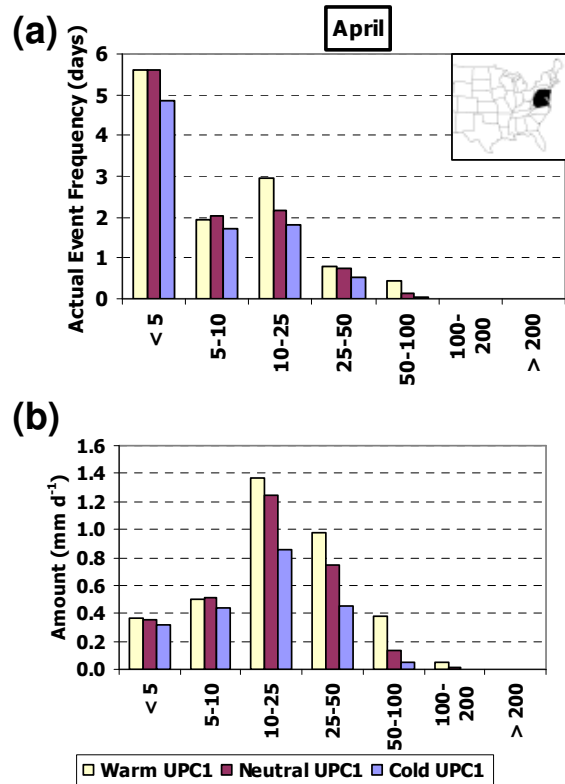


Fig. 4.20: (a) As in Fig. 4.1a but for April precipitation in mid-Atlantic region delineated in Table 4.17 during SSTA UPC1 events. (b) As in Fig. 4.1b, but for April precipitation in mid-Atlantic region during SSTA UPC1 events.

The negative composite April precipitation anomaly for cold UPC1 events is consistent across all individual constituent years. Fig. 4.21 shows that in each year with cold central TP SSTAs, negative precipitation anomalies prevailed in the mid-Atlantic region. The strongest precipitation anomalies occurred in 1950, 1971, and 1976, when observed precipitation anomalies exceeded  $-1.0 \text{ mm d}^{-1}$ .

Precip Category	April		
	Warm	Neutral	Cold
<5	0.367	0.356	0.322
5-10	0.504	0.509	0.436
10-25	1.370	1.248	0.854
25-50	0.978	0.744	0.450
50-100	0.378	0.138	0.051
100-200	0.045	0.012	0.000
>200	0.000	0.000	0.000
<b>TOTAL</b>	<b>3.642</b>	<b>3.006</b>	<b>2.113</b>

Precip Category	April		
	Warm	Neutral	Cold
<5	10%	12%	15%
5-10	14%	17%	21%
10-25	38%	42%	40%
25-50	27%	25%	21%
50-100	10%	5%	2%
100-200	1%	< 1%	0%
>200	0%	0%	0%

Table 4.20: As in Table 4.4 but for mid-Atlantic region delineated in Table 4.19 during April SSTA UPC1 events.

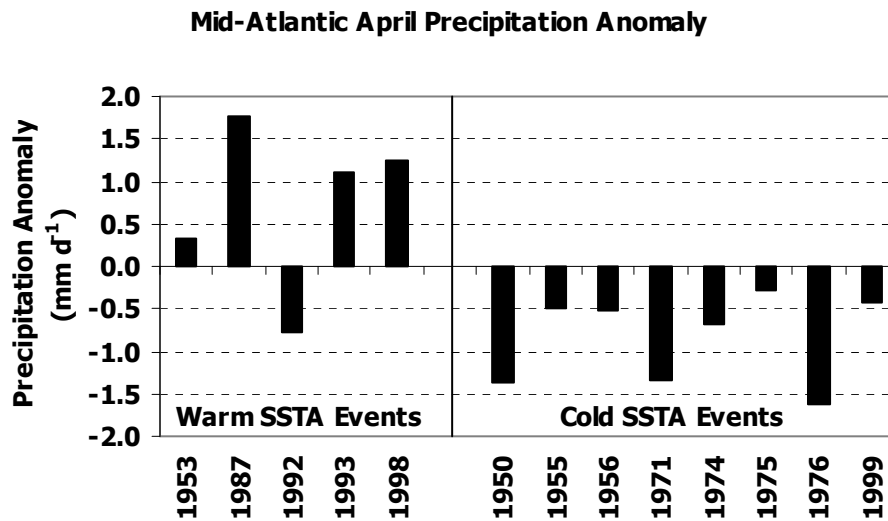


Fig. 4.21: Average April precipitation anomaly from 1950-92 mean in  $\text{mm d}^{-1}$  for mid-Atlantic region delineated in Table 4.19.

## 4.4 Temperature Results

The following section presents the details of the daily temperature results and parallels the precipitation results in Section 4.3. Again, the associations are separated according to the SSTA TP PC used to define the events, and results are provided for both warm and cold TP SSTA events for November-March. But, as in Section 4.3, if an association begins in March and extends into April or begins in October and extends in to November, then the October or April associations also are discussed.

### 4.4.1 Associations with Eastern Tropical Pacific SSTA Events

The following sections describe the daily event characteristics of maximum and minimum temperature anomalies in regions exhibiting a coherent association between monthly average daily maximum and/or minimum temperature anomalies and warm and cold TP SSTA VPC1 events as noted in Figs. 3.6-3.9. The regions examined in this section correspond to those described in Section 3.4.2 and listed in Table 3.3 and Table 3.4. In the discussion below, the nonlinear aspects of the associations are highlighted.

#### 4.4.1.1 U.S.-CANADIAN BORDER (DECEMBER-APRIL)

As indicated in Chapter 3, the monthly average of daily maximum/minimum temperatures along the U.S.-Canadian border and the southern tier of the U.S. are nonlinearly related to TP SSTAs. Fig. 3.6 demonstrated that during warm eastern TP SSTA events, positive composite anomalies for average December, January, February, and March daily maximum and minimum temperature all span much of the northern U.S. and southern Canada and also the eastern U.S. (December) and the central Plains (February-March). Additionally, negative composite January temperature anomalies are present in much of the southern U.S. in the composites of both daily maximum and minimum temperature. However, in the corresponding cold TP SSTA event composite (Fig. 3.7), locally significant anomalies of the opposite sign in similar regions are only present in the northern U.S. in February and the southern U.S. in January. The daily temperature extreme variability that produced this nonlinearity now is documented.

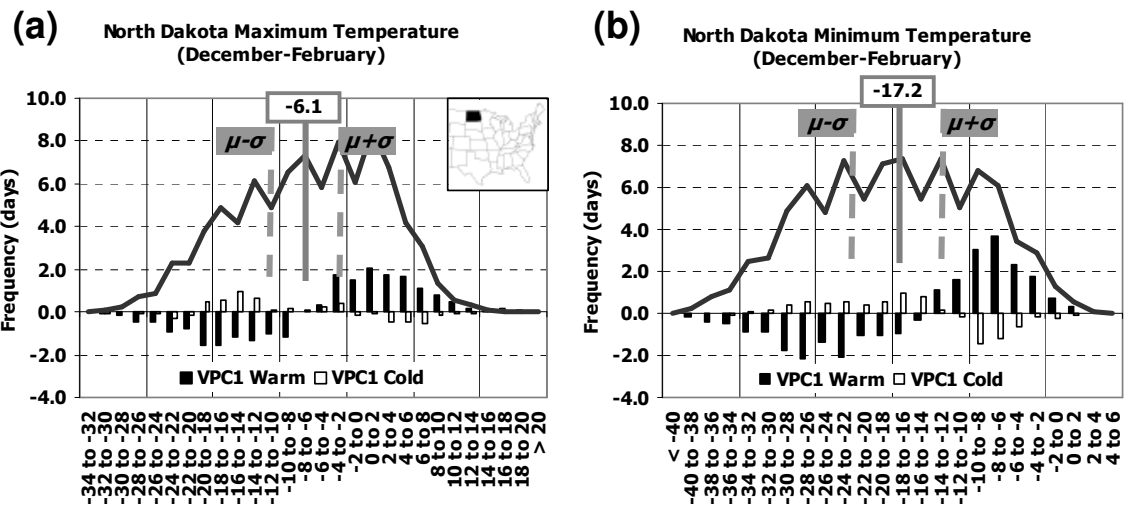


Fig. 4.22: (a) Frequency (indicated by solid line) of daily maximum temperatures ( $^{\circ}\text{C}$ ) during neutral SSTA VPC1 events in December-February for North Dakota region delineated in inset map, and associated anomaly (indicated by bars) during warm and cold SSTA VPC1 events. (b) As in (a) but for daily minimum temperatures. Category containing seasonal 1950-2000 mean daily temperature extreme ( $^{\circ}\text{C}$ ) is indicated by solid gray line. Dashed gray lines provide approximate indication of seasonal mean  $\pm$  one standard deviation.

In the northern U.S. Great Plains, the positive anomalies of daily maximum and minimum temperature in the individual monthly composites from December through February during warm eastern TP SSTA events (Section 3.4.2.1, Fig. 3.6) arose from a shift in the frequency of daily temperature extremes. Fig. 4.22 shows that, during warm VPC1 SSTA events in December-January-February, the distribution of daily maximum temperatures over North Dakota shifted to increase the frequency of days above  $-4^{\circ}\text{C}$  and decrease the frequency of days below  $-10^{\circ}\text{C}$ . In contrast, there were no such strong frequency shifts during cold SSTA VPC1 events, with only very slight changes in the opposite direction as warm SSTA events. Table 4.21 (top) further indicates that during warm TP SSTA events, there were on average 10 fewer days (relative to neutral SSTA events) during December-February with daily maximum temperatures below  $-9^{\circ}\text{C}$  (equal to the 1950-2000 seasonal mean minus one seasonal standard deviation, hereafter denoted  $\mu-\sigma$ ), and 10 more days with daily maximum temperature above the seasonal mean plus one standard deviation (hereafter denoted  $\mu+\sigma$ ). The minimum temperature distribution (Fig. 4.22b) indicates more frequent occurrences of higher than average minimum

	<b>&lt; Mean - 1<math>\sigma</math></b>	<b>&lt; Mean</b>	<b>&gt; Mean</b>	<b>&gt; Mean + 1<math>\sigma</math></b>
<b>Tmax</b>	< -9.0°C	< -6.1°C	> -6.1°C	> -3.2°C
Warm	-9.6	-10.8	+11.8	+9.7
Cold	+2.1	+2.2	-1.3	-1.9
<b>Tmin</b>	< -20.2°C	< -17.2°C	> -17.2°C	> -14.2°C
Warm	-10.2	-12.3	+14.3	+14.6
Cold	+2.0	+3.1	-3.0	-3.8

Table 4.21: For North Dakota region (delineated in upper right inset map in Fig. 4.22a), cumulative sum of frequency anomaly (compared to neutral SSTA events; displayed in Fig. 4.22) of daily maximum (Tmax, °C) and daily minimum (Tmin, °C) temperatures (in days) during December-February warm and cold SSTA VPC1 events. Sums are computed for daily extremes below seasonal 1950-2000 mean minus one standard deviation (“< Mean-1 $\sigma$ ”), below seasonal mean (“< Mean”), above seasonal mean (“> Mean”), and above the seasonal mean + one standard deviation (“> Mean+1 $\sigma$ ”). Seasonal mean and  $\pm 1\sigma$  range are indicated in Fig. 4.22.

temperatures than below average minimum temperatures, with 15 more days above  $\mu + \sigma$  and 10 fewer days below  $\mu - \sigma$  (Table 4.21, bottom). The frequency of neither daily maximum nor daily minimum temperatures exhibited a notable change during cold TP SSTA events compared to neutral SSTA events.

During December, positive anomalies in average daily maximum and minimum temperatures in the eastern U.S.-Canadian border region during warm SSTA VPC1 events (Section 3.4.2.1, Fig. 3.6) mostly were associated with a general shift in frequency of daily temperatures in the eastern U.S. to favor warmer daily extremes and also a notable reduction in the number of extreme negative daily temperature anomalies. Again, little consistent counterpart associations characterized cold SSTA VPC1 events. Fig. 4.23 shows that during warm SSTA events, extreme cold maximum temperature anomalies in western Pennsylvania were less frequent, with 5.1 fewer days (compared to neutral SSTA events) with maximum temperatures below the seasonal  $\mu - \sigma$  of +0.9°C (Table 4.22, top). These changes in event frequency were accompanied by relatively few days with maximum temperatures below -6°C, while the principal increases occurred for daily maximum temperatures between 4-10°C (Fig. 4.23a). Similarly, there were few daily minimum temperatures below -18°C during warm TP SSTA events, with the largest frequency increases for daily minimum temperatures being between -6°C and -4°C (Fig. 4.23b). In total, Table 4.22 (bottom) shows there were 3.7 fewer days with daily

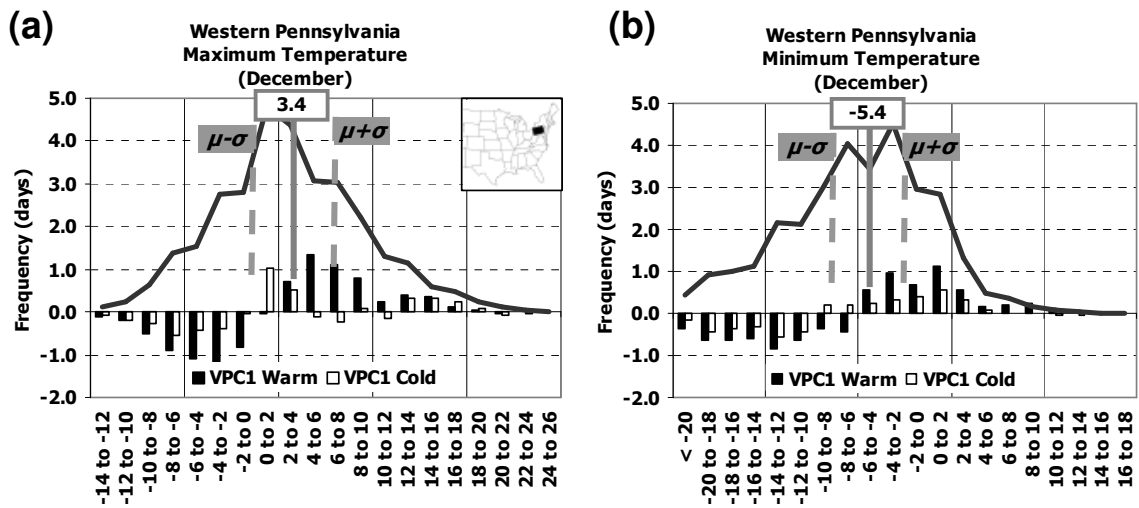


Fig. 4.23: As in Fig. 4.22 but for western Pennsylvania during December.

	< Mean - 1σ	< Mean	> Mean	> Mean + 1σ
<b>Tmax</b>	< 0.9°C	< 3.4°C	> 3.4°C	> 5.9°C
Warm	-5.1	-5.1	+4.4	+3.1
Cold	-1.9	-0.9	+0.4	+0.5
<b>Tmin</b>	< -8.0°C	< -5.4°C	> -5.4°C	> -2.8°C
Warm	-3.7	-4.5	+4.0	+3.0
Cold	-2.3	-1.9	+1.6	+1.3

Table 4.22: As in Table 4.21, but for western Pennsylvania region during December (Fig. 4.23).

minimum temperatures below  $-8.0^{\circ}\text{C}$  ( $\mu-\sigma$ ) and 3.0 more days above  $-2.8^{\circ}\text{C}$  ( $\mu+\sigma$ ). The counterpart totals for cold SSTA VPC1 events again were much smaller for both daily maximum and daily minimum temperatures (Table 4.22), consistent with the lack of significant composite anomalies noted in Section 3.4.2.1 (Fig. 3.7).

For warm (cold) SSTA VPC1 events, the warmer (colder) than average February-April temperatures in southeastern and south-central Canada (Section 3.4.2.1, Fig. 3.7) were linked to more frequent very warm (cold) daily temperature extremes. Fig. 4.24 shows that in southern Quebec, the frequency of daily maximum (minimum) temperatures above  $+8^{\circ}\text{C}$  ( $-6^{\circ}\text{C}$ ) during warm February-April SSTA events increased (compared to neutral SSTA events) and those for extremes under  $-6^{\circ}\text{C}$  ( $-14^{\circ}\text{C}$ ) increased during cold SSTA events. In total, Table 4.23 indicates that, compared to neutral SSTA events, there were on average 4.3 (4.5) more days during February-April warm SSTA

events with daily maximum (minimum) temperatures above the seasonal mean of  $+0.3^{\circ}\text{C}$  ( $-10.9^{\circ}\text{C}$ ) and 3.6 (4.1) more days during cold SSTA events with daily maximum (minimum) temperatures below the seasonal  $\mu-\sigma$  of  $-1.0^{\circ}\text{C}$  ( $-12.6^{\circ}\text{C}$ ). Southern Manitoba exhibited a similar relationship during March-April, as the occurrence of daily maximum (minimum) temperatures above  $+6^{\circ}\text{C}$  ( $-6^{\circ}\text{C}$ ) increased during warm SSTA VPC1 events compared to neutral SSTAs and those below  $-2^{\circ}\text{C}$  ( $-12^{\circ}\text{C}$ ) increased during cold SSTA events (Fig. 4.25). On average, there were 4.0 (5.9) more days with daily maximum (minimum) temperatures below  $+1.0^{\circ}\text{C}$  ( $-10.2^{\circ}\text{C}$ ) during cold SSTA events compared to neutral SSTAs and 3.4 (5.2) days above  $6.2^{\circ}\text{C}$  ( $-5.6^{\circ}\text{C}$ ) during warm SSTA events (Table 4.24).

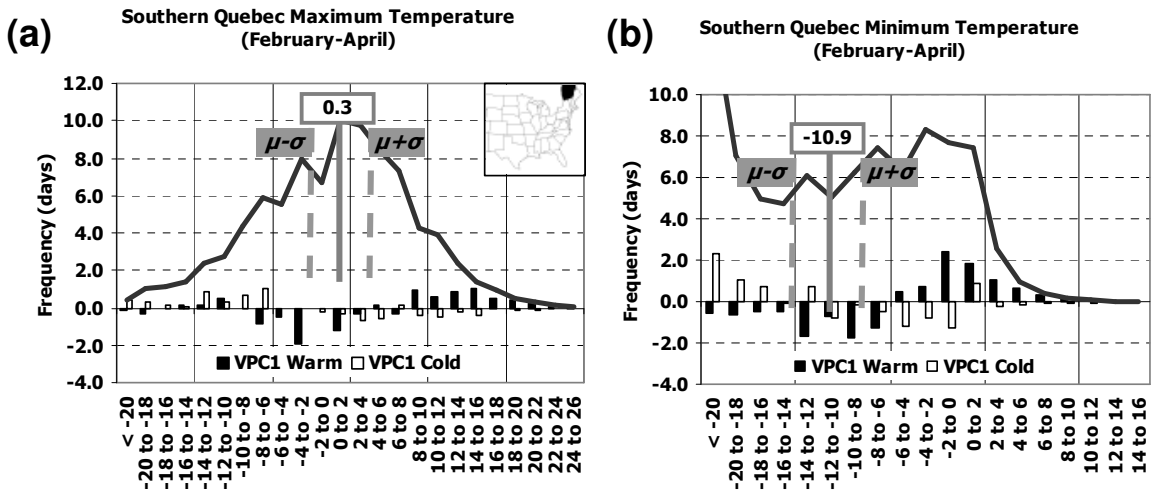


Fig. 4.24: As in Fig. 4.22 but for southern Quebec during February-April.

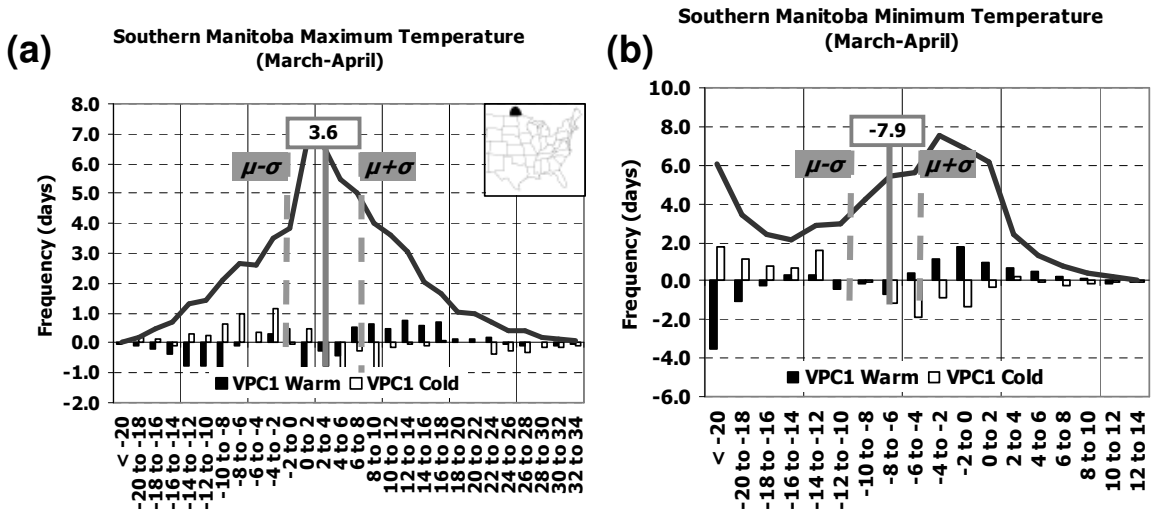


Fig. 4.25: As in Fig. 4.22 but for southern Manitoba during March-April.

	<i>&lt; Mean - 1σ</i>	<i>&lt; Mean</i>	<i>&gt; Mean</i>	<i>&gt; Mean + 1σ</i>
<b>Tmax</b>	<i>&lt; -1.0°C</i>	<i>&lt; 0.3°C</i>	<i>&gt; 0.3°C</i>	<i>&gt; 1.6°C</i>
Warm	-3.1	-3.2	+4.3	+4.3
Cold	+3.6	+3.5	-2.9	-2.9
<b>Tmin</b>	<i>&lt; -12.6°C</i>	<i>&lt; -10.9°C</i>	<i>&gt; -10.9°C</i>	<i>&gt; -9.1°C</i>
Warm	-2.2	-3.9	+4.5	+6.2
Cold	+4.1	+4.8	-3.8	-3.6

Table 4.23: As in Table 4.21, but for southern Quebec region during February-April (Fig. 4.24).

	<i>&lt; Mean - 1σ</i>	<i>&lt; Mean</i>	<i>&gt; Mean</i>	<i>&gt; Mean + 1σ</i>
<b>Tmax</b>	<i>&lt; 1.0°C</i>	<i>&lt; 3.6°C</i>	<i>&gt; 3.6°C</i>	<i>&gt; 6.2°C</i>
Warm	-2.3	-3.2	+3.5	+3.4
Cold	+4.0	+4.4	-3.7	-2.4
<b>Tmin</b>	<i>&lt; -10.2°C</i>	<i>&lt; -7.9°C</i>	<i>&gt; -7.9°C</i>	<i>&gt; -5.6°C</i>
Warm	-4.2	-4.9	+5.6	+5.2
Cold	+5.9	+5.9	-4.8	-2.9

Table 4.24: As in Table 4.21, but for southern Manitoba region during March-April (Fig. 4.25).

The consistency of the observed daily extreme temperature anomalies with respect to the overall warm and cold SSTA VPC1 event composites examined in Section 3.4.2.1 and this section now is discussed. First, for the December-February warm SSTA VPC1 relationships along the U.S.-Canadian border, the observed anomalies were generally inconsistent with the composite anomaly during only three of a total of eleven warm SSTA VPC1 events, and in southern U.S., the anomalies were inconsistent with the composites in four out of the eleven. Fig. 4.26a shows that in three December-February

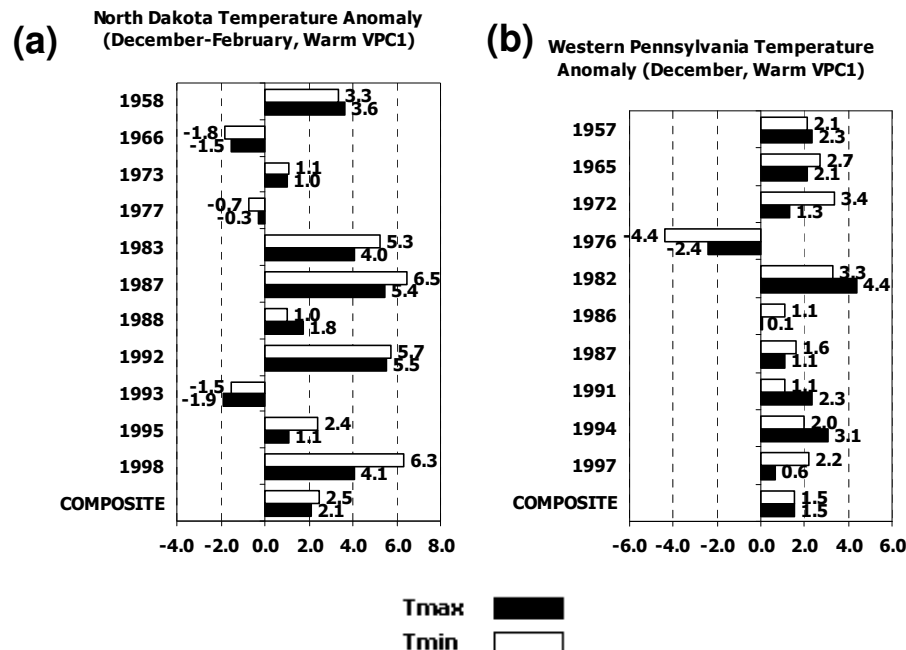
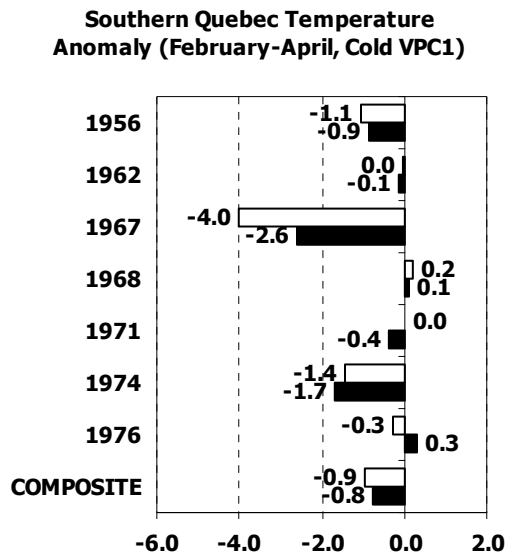


Fig. 4.26: Observed seasonal or monthly average daily maximum (solid bar) and minimum (open bar) temperature anomalies (in °C) in years classified as warm SSTA VPC1 events for (a) North Dakota region (Fig. 4.22) in December-February, and (b) western Pennsylvania region (Fig. 4.23) in December.

(a)



(b)

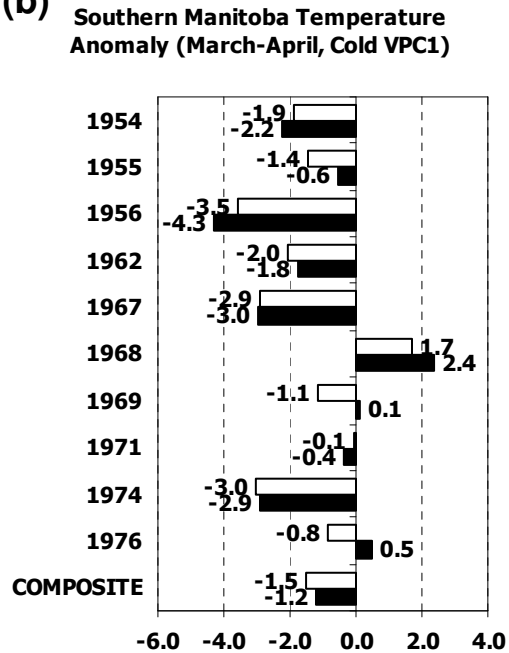


Fig. 4.27: As in Fig. 4.26 but for cold SSTA VPC1 events for (a) southern Quebec region (Fig. 4.24) during February-April, and (b) southern Manitoba region (Fig. 4.25) during March-April.

seasons (1965-66, 1976-77, and 1992-93), the average daily maximum and minimum temperature for the North Dakota region was below average instead of above average as indicated by the composite in Fig. 3.6a-f. The western Pennsylvania region also observed anomalies in December temperature extremes below average in one of these years (1976; Fig. 4.26b). In total, at least one region in the U.S.-Canadian border area observed anomalies inconsistent with the warm December-February SSTA composites in 1965-66, 1976-77, and 1992-93.

For the February-April cold SSTA VPC1 relationships discussed in this section, the observed anomalies in the U.S. Great Plains and southern Canada were inconsistent with the composite anomaly during only two out of ten cold SSTA events. Fig. 4.27a-b shows that in two February-April seasons (1968 and 1971), the average daily maximum and minimum temperatures for both the southern Manitoba and southern Quebec regions were above or very near average instead of below average as indicated by the composite in Fig. 3.7.

#### 4.4.1.2 CENTRAL U.S. GREAT PLAINS AND SOUTHERN TIER OF U.S. (DECEMBER-APRIL)

Focusing now on the southern U.S., additional nonlinear associations between daily temperature extremes and TP SSTAs during the same overall December-April time period are evident in positive December-February anomalies in the central and southern Plains. During cold SSTA VPC1 events (Section 3.4.2.1, Fig. 3.7a-f), this region observed a general increase in the frequency of warmer daily temperature extremes. Southeast Texas observed more daily maximum temperatures above  $+22^{\circ}\text{C}$  during cold SSTA VPC1 events than during neutral SSTA events during December-February (Fig. 4.28a). Similarly, the frequency of December daily maximum temperatures in western Kansas-Oklahoma decreased (compared to neutral SSTA events) for daily maximum temperatures below  $+6^{\circ}\text{C}$  and increased for those above  $+8^{\circ}\text{C}$  (Fig. 4.29a). Table 4.25 (Table 4.26) indicates that during cold VPC1 events, southeast Texas (western Kansas-Oklahoma) observed on average 7.7 (3.4) more days (compared to neutral SSTAs) with daily maximum temperatures above  $19.7^{\circ}\text{C}$  ( $11.9^{\circ}\text{C}$ ) during December-February (December) and 5.5 (4.0) less days below  $16.5^{\circ}\text{C}$  ( $6.8^{\circ}\text{C}$ ). The frequencies of daily minimum temperatures during cold December-February SSTA VPC1 events in southeast Texas exhibited similar characteristics as daily maximum temperatures (Fig. 4.28b), but those in western Kansas-Oklahoma showed no notable association with cold SSTA events (Fig. 4.29b). During warm December-February SSTA events, Fig. 4.28 shows that southeast Texas experienced a decrease in the frequency of daily maximum (minimum) temperatures above  $+20^{\circ}\text{C}$  ( $+12^{\circ}\text{C}$ ), while the frequency of December daily extremes in western Kansas-Oklahoma exhibited no notable characteristics. These associations during warm SSTA events are further examined in the next paragraph.

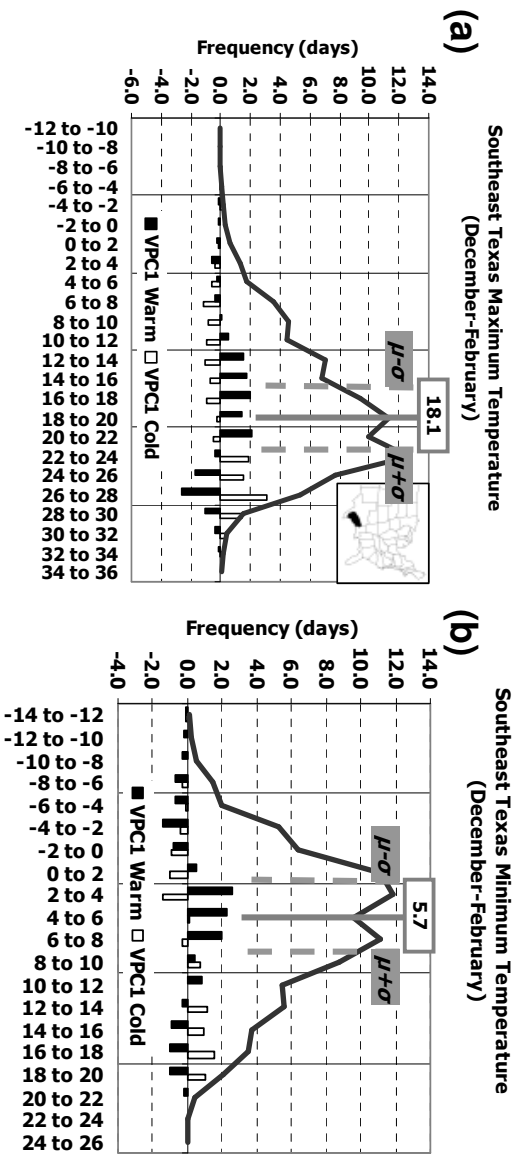


Fig. 4.28: As in Fig. 4.22 but for southeast Texas region during December-February.

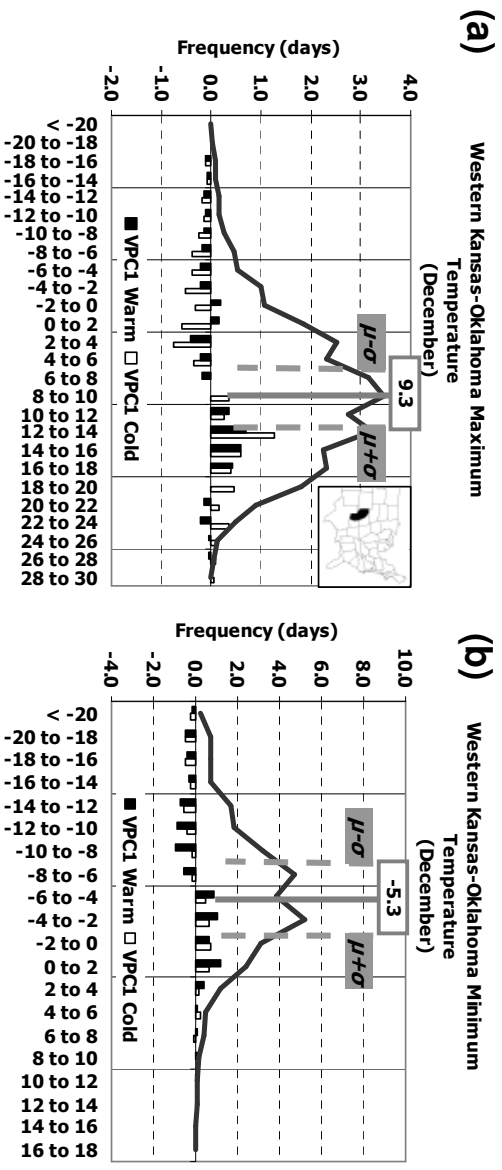


Fig. 4.29: As in Fig. 4.22 but for western Kansas-Oklahoma region during December.

	<b>&lt; Mean - 1<math>\sigma</math></b>	<b>&lt; Mean</b>	<b>&gt; Mean</b>	<b>&gt; Mean + 1<math>\sigma</math></b>
<b>Tmax</b>	< 16.5°C	< 18.1°C	> 18.1°C	> 19.7°C
Warm	+2.0	+4.0	-4.4	-4.4
Cold	-5.5	-6.4	+7.7	+7.7
<b>Tmin</b>	< 4.3°C	< 5.7°C	> 5.7°C	> 7.2°C
Warm	-1.2	-1.2	-0.1	-2.1
Cold	-4.2	-4.2	+5.1	+5.4

Table 4.25: As in Table 4.21, but for southeast Texas region during December-February (Fig. 4.28).

	<b>&lt; Mean - 1<math>\sigma</math></b>	<b>&lt; Mean</b>	<b>&gt; Mean</b>	<b>&gt; Mean + 1<math>\sigma</math></b>
<b>Tmax</b>	< 6.8°C	< 9.3°C	> 9.3°C	> 11.9°C
Warm	-1.5	-1.6	+1.7	+1.3
Cold	-4.0	-4.0	+3.7	+3.4
<b>Tmin</b>	< -6.9°C	< -5.0°C	> -5.0°C	> -3.1°C
Warm	-3.8	-4.4	+3.5	+2.5
Cold	-2.6	-2.7	+2.2	+1.6

Table 4.26: As in Table 4.21, but for western Kansas-Oklahoma region during December (Fig. 4.29).

Negative anomalies in January temperature extremes during the warm TP SSTA VPC1 event counterparts (Section 3.4.2.1, Fig. 3.6c-d) to the cold SSTA associations described on page 116 principally arose from a shift in the distributions of maximum temperatures, but the distribution of minimum temperatures also narrowed. Fig. 4.30 (Fig. 4.31) shows that for northern Georgia (southeast Texas), the frequency of daily maximum temperatures above +18°C (+22°C) decreased and those below +14°C (+20°C) increased. In northern Georgia, Table 4.28 indicates that there were on average 3.5 fewer (2.0 more) days with maximum temperatures above the monthly  $\mu+\sigma$  of +14.6°C (below the monthly  $\mu-\sigma$  of +9.3°C), while Table 4.27 shows that for southeast Texas, there were on average 4.0 fewer (1.8 more) days above the monthly  $\mu+\sigma$  of +19.6°C (below the monthly  $\mu-\sigma$  of +14.4°C). For daily minimum temperatures, the frequency of January temperature extremes near the monthly mean increases during warm SSTA events and the frequency of events in the tails generally decreases for both northern Georgia (Fig. 4.30b, Table 4.28) and southeast Texas (Fig. 4.31b, Table 4.27), with the largest decreases in the warm tail. For both regions, the associations during cold January SSTA VPC1 events are relatively minor, although the frequency of daily minimum temperatures below -2.8°C ( $\mu-\sigma$ ) in northern Georgia did decrease by on average 2.0 days (Table 4.28).

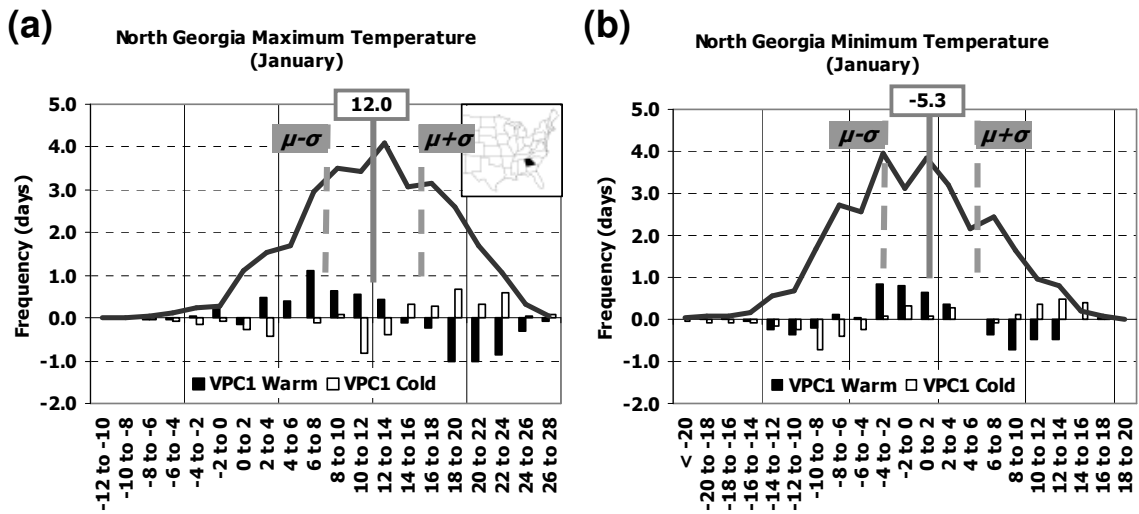


Fig. 4.30: As in Fig. 4.22 but for northern Georgia during January.

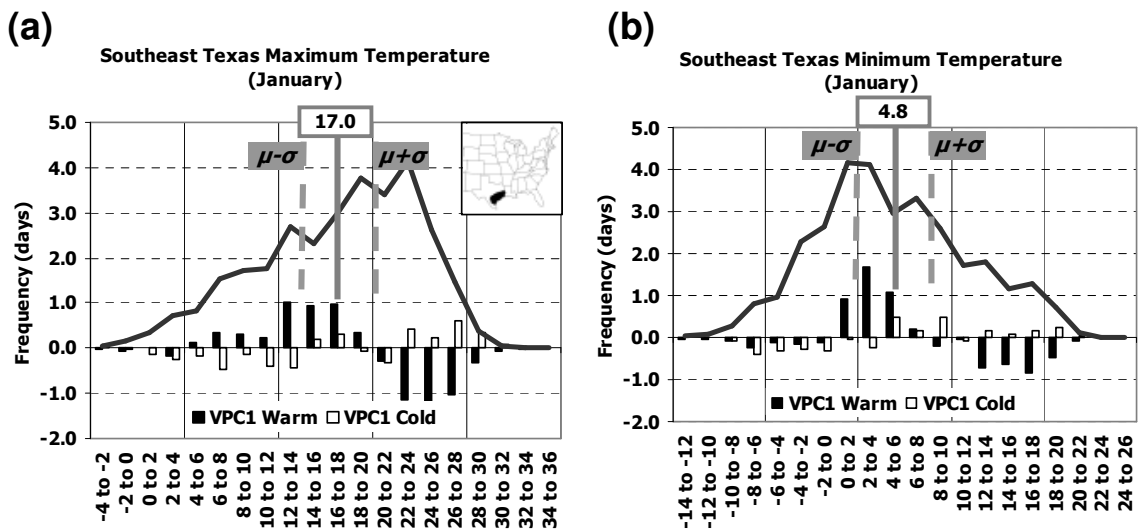


Fig. 4.31: As in Fig. 4.22 but for southeast Texas during January.

	<i>&lt; Mean - 1σ</i>	<i>&lt; Mean</i>	<i>&gt; Mean</i>	<i>&gt; Mean + 1σ</i>
<b>Tmax</b>	<i>&lt; 9.3°C</i>	<i>&lt; 12.0°C</i>	<i>&gt; 12.0°C</i>	<i>&gt; 14.6°C</i>
Warm	+2.0	+2.7	-3.2	-3.5
Cold	-1.2	-1.1	+2.0	+2.0
<b>Tmin</b>	<i>&lt; -2.8°C</i>	<i>&lt; 0.1°C</i>	<i>&gt; 0.1°C</i>	<i>&gt; 3.0°C</i>
Warm	-0.6	+1.0	-1.7	-2.0
Cold	-2.0	-1.6	+1.5	+1.3

Table 4.28: As in Table 4.21, but for northern Georgia region during January (Fig. 4.30).

	<i>&lt; Mean - 1σ</i>	<i>&lt; Mean</i>	<i>&gt; Mean</i>	<i>&gt; Mean + 1σ</i>
<b>Tmax</b>	<i>&lt; 14.4°C</i>	<i>&lt; 17.0°C</i>	<i>&gt; 17.0°C</i>	<i>&gt; 19.6°C</i>
Warm	+1.8	+2.7	-3.7	-4.0
Cold	-1.8	-1.6	+1.3	+1.4
<b>Tmin</b>	<i>&lt; 2.6°C</i>	<i>&lt; 4.8°C</i>	<i>&gt; 4.8°C</i>	<i>&gt; 7.0°C</i>
Warm	+0.1	+1.8	-2.8	-3.0
Cold	-1.5	-1.7	+1.2	+1.1

Table 4.27: As in Table 4.21, but for southeast Texas region during January (Fig. 4.31).

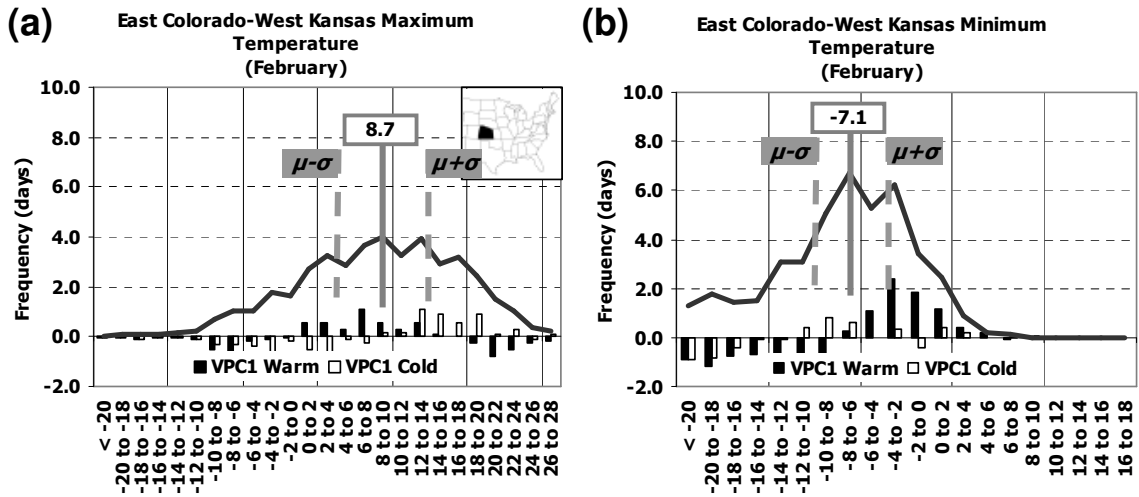


Fig. 4.32: As in Fig. 4.22 but for eastern Colorado-western Kansas during February.

	<i>&lt; Mean - 1σ</i>	<i>&lt; Mean</i>	<i>&gt; Mean</i>	<i>&gt; Mean + 1σ</i>
<b>Tmax</b>	<i>&lt; 5.2°C</i>	<i>&lt; 8.7°C</i>	<i>&gt; 8.7°C</i>	<i>&gt; 12.2°C</i>
Warm	-0.8	+0.6	-1.1	-2.0
Cold	-3.7	-4.1	+4.1	+2.8
<b>Tmin</b>	<i>&lt; -9.3°C</i>	<i>&lt; -7.1°C</i>	<i>&gt; -7.1°C</i>	<i>&gt; -4.9°C</i>
Warm	-5.9	-7.3	+7.0	+5.9
Cold	-1.9	-1.1	+0.6	+0.6

Table 4.29: As in Table 4.21, but for eastern Colorado-western Kansas region during February (Fig. 4.32).

In the central U.S. Plains, the positive anomalies in February daily minimum temperature anomalies during warm SSTA VPC1 events (Section 3.4.2.1, Fig. 3.6f) mainly arose from a decrease in the frequency of extreme cold events. Fig. 4.32b shows that the frequency of minimum temperatures in eastern Colorado-western Kansas below  $-14^{\circ}\text{C}$  in February decreased notably during warm SSTA VPC1 events, while the frequency of events above  $-8^{\circ}\text{C}$  is higher. Table 4.29 indicates that there were 5.9 fewer days with minimum temperature below  $-9.3^{\circ}\text{C}$  ( $\mu - \sigma$ ) compared to normal. Consistent with the lack of significant anomalies in the warm SSTA VPC1 composite (Fig. 3.6e) of February average daily maximum temperature in the eastern Colorado-western Kansas region, there are no notable changes in the frequency of February daily maximum temperatures in this region (Fig. 4.32a). During cold SSTA events, the frequency of daily maximum temperatures above  $+12^{\circ}\text{C}$  increases, while there are no significant changes in the frequency of daily minimum temperatures (Fig. 4.32).

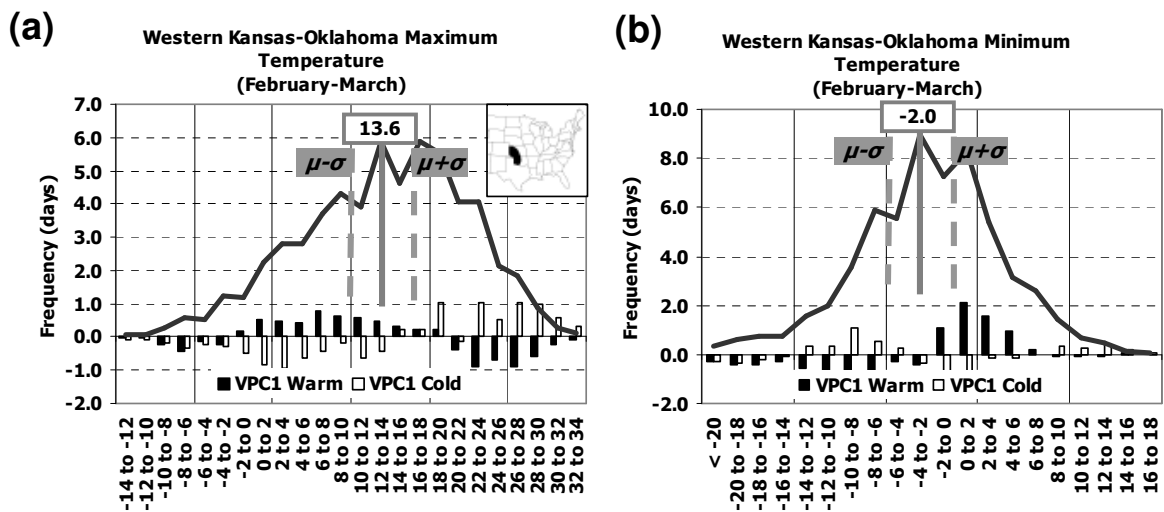


Fig. 4.33: As in Fig. 4.22 but for western Kansas-Oklahoma during February-March.

Also during February-March, positive anomalies in daily maximum temperatures in the central U.S. Great Plains during cold SSTA events (Section 3.4.2.1, Fig. 3.7e,g) were linked to more frequent warmer than average extremes. But for this season, there were no significant changes in daily minimum

temperatures. For example, in western Kansas-Oklahoma, the frequency of daily maximum temperatures during cold SSTA VPC1 events increased notably (compared to neutral SSTA events) for temperatures above +22°C, while frequencies of below normal daily maximum temperatures decreased over a wider range (Fig. 4.33a). Table 4.30 shows that there were on average 5.4 more days with maximum temperature above +16.0°C ( $\mu+\sigma$ ) in this area during February-March and 4.8 less days below 11.1°C ( $\mu-\sigma$ ). This is consistent with MRL98’s finding of drier than normal conditions in the central Plains during cold SSTA VPC1 events, as clear skies (which would likely accompany drier than normal conditions) can allow daytime temperatures to rise considerably. But

	<i>&lt; Mean - 1σ</i>	<i>&lt; Mean</i>	<i>&gt; Mean</i>	<i>&gt; Mean + 1σ</i>
<b>Tmax</b>	<i>&lt; 11.1°C</i>	<i>&lt; 13.6°C</i>	<i>&gt; 13.6°C</i>	<i>&gt; 16.0°C</i>
Warm	+1.9	+2.4	-2.9	-3.5
Cold	-4.8	-5.4	+5.9	+5.4
<b>Tmin</b>	<i>&lt; -3.5°C</i>	<i>&lt; -2.0°C</i>	<i>&gt; -2.0°C</i>	<i>&gt; -0.6°C</i>
Warm	-5.3	-5.3	+5.7	+4.6
Cold	+1.6	+1.6	-1.1	+0.1

Table 4.30: As in Table 4.21, but for western Kansas-Oklahoma region during February-March (Fig. 4.33).

the lack of an association with daily minimum temperatures suggests that this effect does not translate to nighttime radiative cooling.

The consistency of the observed daily extreme temperature anomalies with respect to the overall warm and cold SSTA VPC1 event composites examined in Section 3.4.2.1 and this section now is discussed. Fig. 4.34a-b indicates that SSTA VPC1 events after 1992 (1995) exhibited warmer than normal January temperatures in northern Georgia (southeast Texas), as opposed to the colder than normal temperatures indicated in the composite (Fig. 3.6). Also, February daily minimum temperatures were below average instead of above average in the eastern Colorado/western Kansas region during 1993 (Fig. 4.34c). In total, the southern U.S. observed December-February anomalies inconsistent with the warm SSTA composites in 1991-92, 1992-93, 1994-95, and 1997-98.

Lastly, for the December-February associations during cold SSTA VPC1 events in the U.S. Great Plains, the average daily maximum temperature anomalies were below normal instead of above normal during three out of twelve cold SSTA VPC1 events. Fig. 4.35a indicates that in two December-February seasons (1962-63 and 1967-68), the average daily maximum temperatures for the southeast Texas region was below normal instead of above normal as indicated by the composite in Fig. 3.7. Similarly, the western Kansas/Oklahoma region also observed December average daily maximum temperature anomalies below normal instead of above normal in 1967 and 1971 (Fig. 4.35b) while the observed February-March average daily maximum temperature anomalies for the same region were below normal instead of above normal in 1971 (Fig. 4.35c).

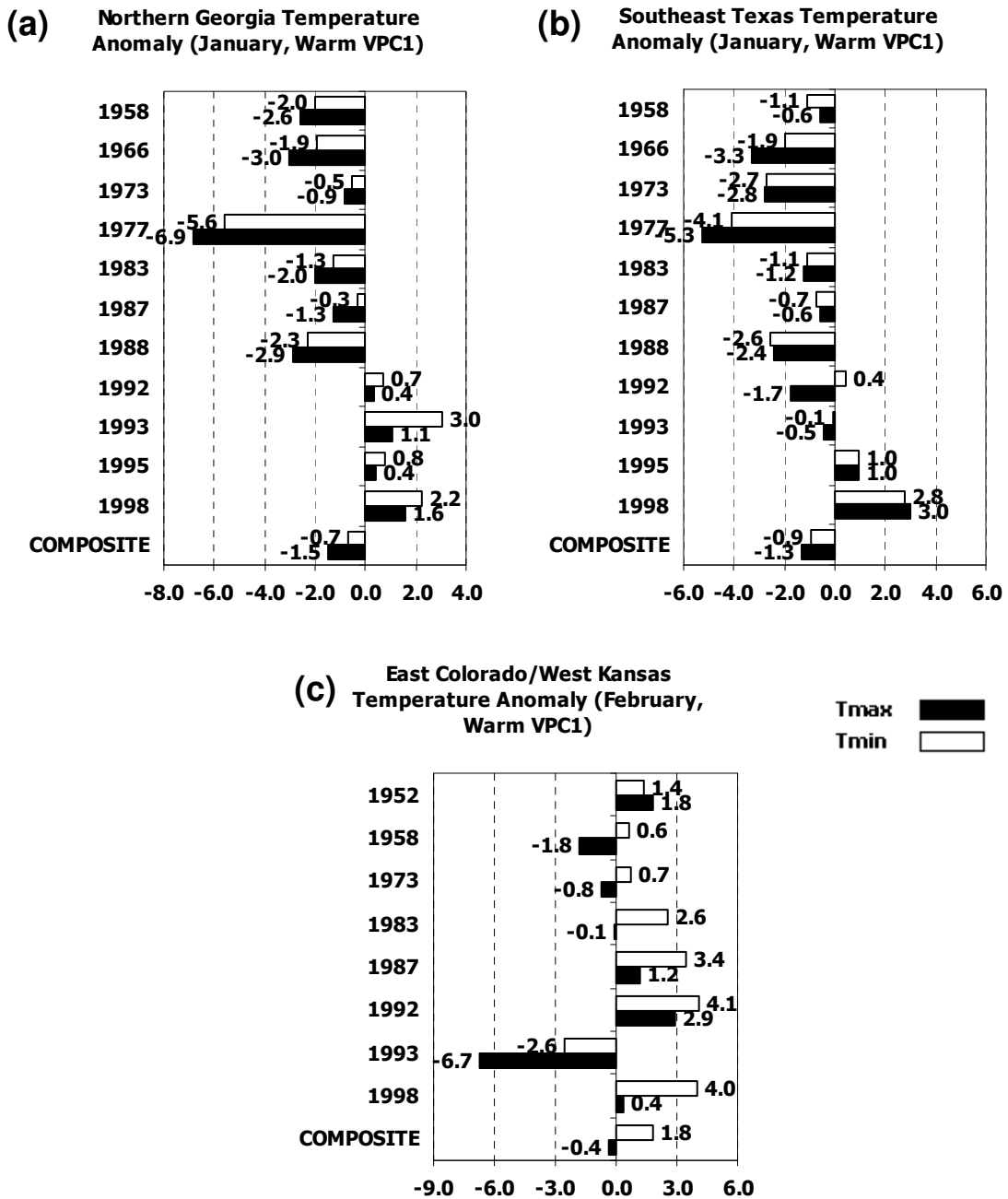


Fig. 4.34: As in Fig. 4.26 but for (a) northern Georgia region (Fig. 4.30) in January, (b) southeast Texas region (Fig. 4.31) in January, and (c) eastern Colorado/western Kansas region in February (Fig. 4.32)

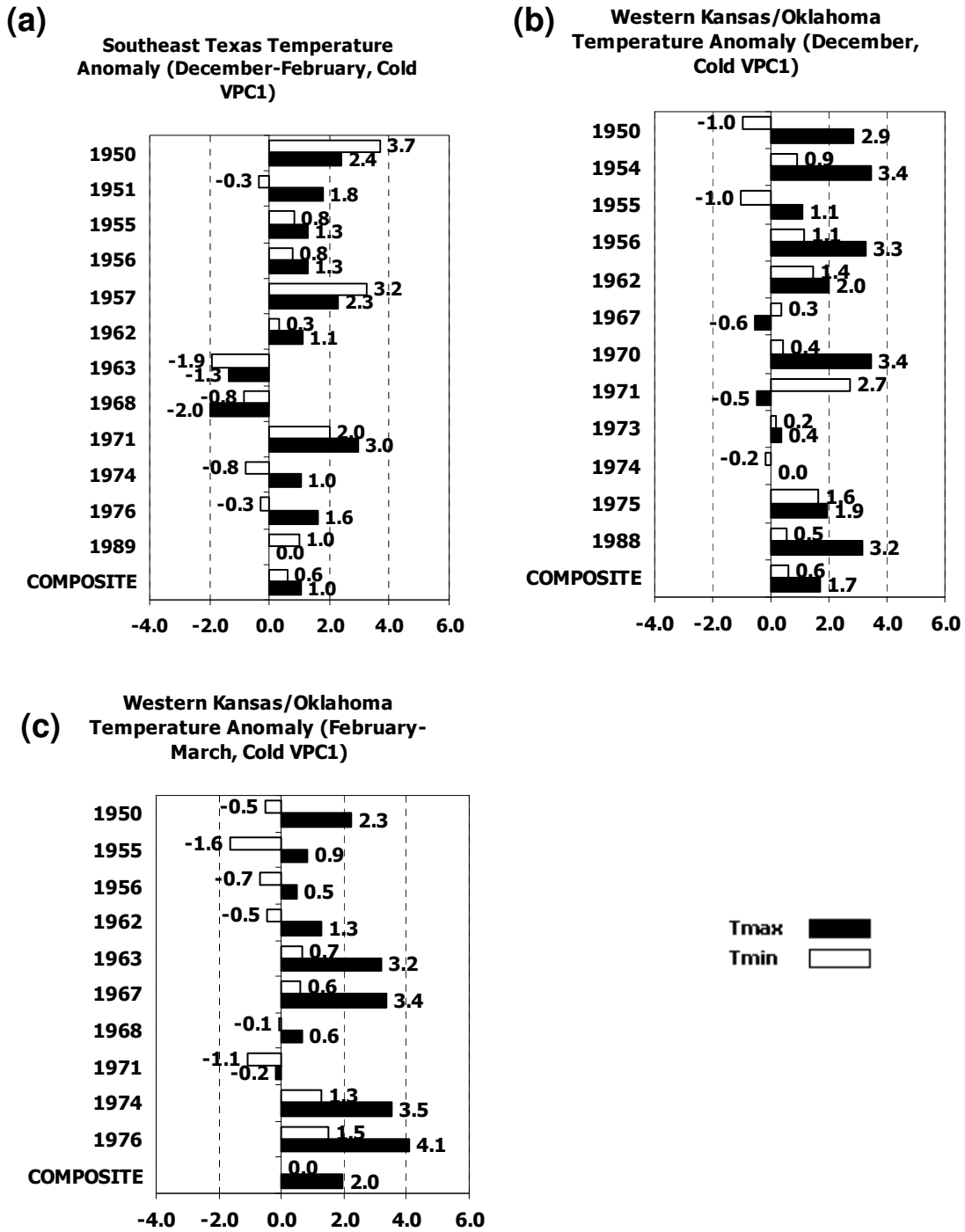


Fig. 4.35: As in Fig. 4.27 but for (a) southeast Texas region (Fig. 4.28) during December-February, (b) western Kansas/Oklahoma region (Fig. 4.29) during December, and (c) western Kansas/Oklahoma region (Fig. 4.33) during February-March.

#### 4.4.1.3 U.S. GREAT PLAINS (OCTOBER-NOVEMBER)

As indicated in Section 3.4.2.2, the monthly average of daily maximum temperatures for October-November in the U.S. Great Plains are broadly linearly related to TP SSTAs. Fig. 3.8 suggests that during warm TP SSTA events, negative composite anomalies of individual monthly averages of daily maximum temperatures during October-November span much of the U.S. east of the Rocky Mountains and are strongest throughout the Great Plains. Additionally, positive temperature anomalies span much of the eastern two thirds of the U.S. particularly in the October (but also November) composite of daily maximum temperature during cold TP SSTA events, although the concentration of statistically significant anomalies is different in the cold SSTA VPC1 composite (Fig. 3.9) compared to the warm composite. The area with the highest local statistical significance in both warm and cold SSTA VPC1 composites is the southern Plains. The daily temperature extreme variability associated with this relationship and its nonlinear characteristics now are documented.

The negative anomalies in monthly averages of daily maximum October-November temperature during warm SSTA VPC1 events in the northern and central U.S. Great Plains are associated with an increased frequency of much colder than average daily maximum temperatures, with no significant opposite association during cold TP SSTAs. Consistent with the warm October-November SSTA VPC1 composite monthly average daily minimum temperatures, the changes in frequency of daily minimum temperatures are weaker. Fig. 4.36a shows that in southern Minnesota, daily maximum temperatures less than +6°C are more frequent during warm SSTA VPC1 events compared to neutral SSTA events, while those more than +16°C are less frequent. In general, during warm October-November SSTA VPC1 events there are about 4.6 more days with daily maximum temperatures less than the seasonal  $\mu-\sigma$  of +8.2°C compared to neutral SSTA years, and 4.5 less days above the seasonal  $\mu+\sigma$  value of +12.1°C (Table 4.31). Similarly, eastern Nebraska (Fig. 4.37a) observed a decrease (increase) in all daily maximum temperature events below (above) +14°C during warm SSTA VPC1 events compared to neutral SSTA events, with 5.3 more days with daily maximum temperatures below the  $\mu-\sigma$  value of +12.6°C and 5.2 fewer days above the seasonal  $\mu+\sigma$  of +16.6°C (Table 4.32). During cold SSTA events, both southern Minnesota

(Fig. 4.36a) and eastern Nebraska (Fig. 4.37a) observed little change in frequency of daily maximum temperatures during cold TP SSTA events, consistent with the lack of statistically significant composite anomalies in the cold SSTA October-November composite (Fig. 3.9a,c). As for daily minimum temperatures, the changes in frequency during both warm and cold SSTA events relative to neutral TP SSTAs were very small (Fig. 4.36b, Fig. 4.37b).

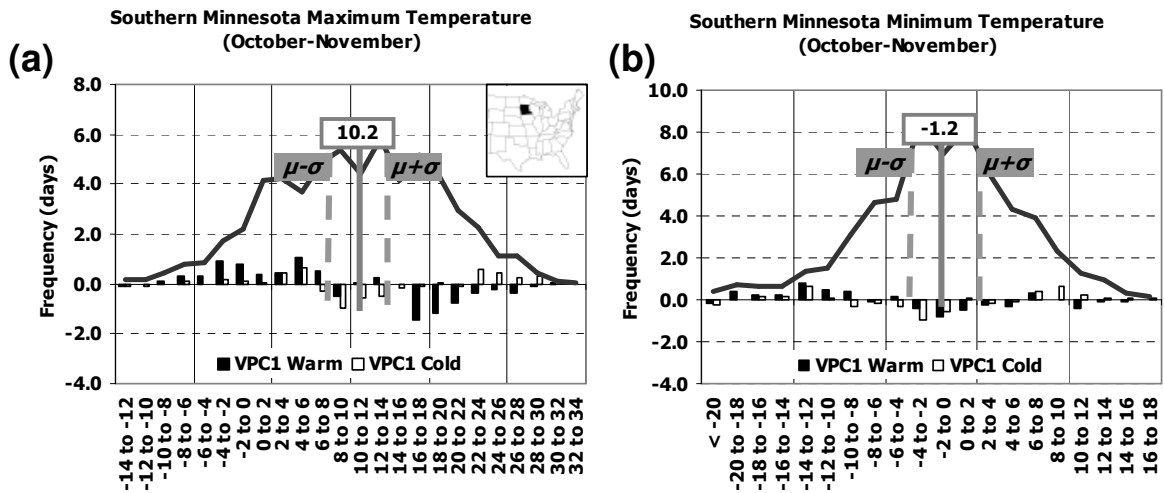


Fig. 4.36: As in Fig. 4.22 but for southern Minnesota region during October-November.

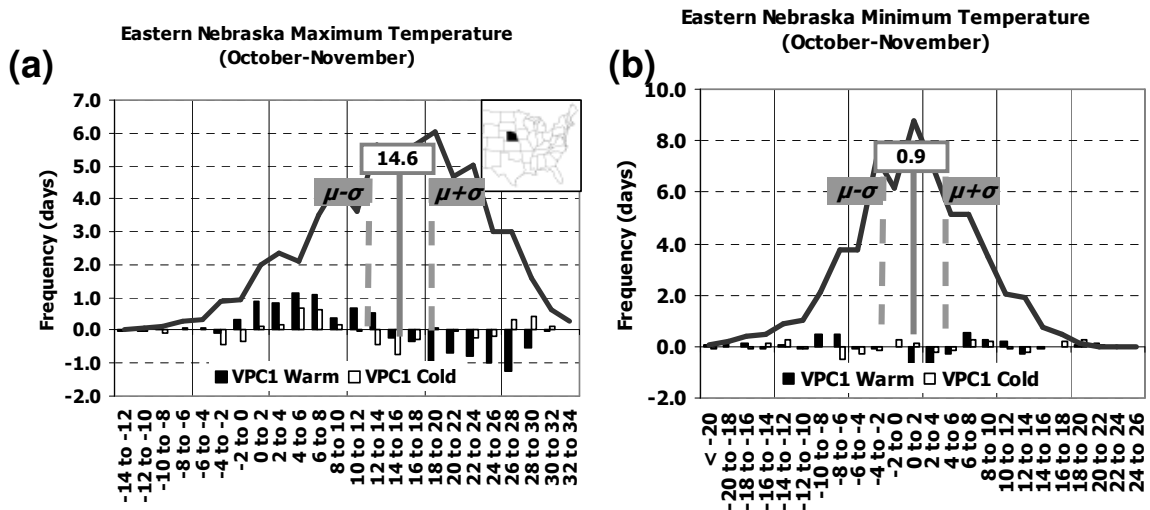


Fig. 4.37: As in Fig. 4.22 but for eastern Nebraska region during October-November.

	<b>&lt; Mean - 1<math>\sigma</math></b>	<b>&lt; Mean</b>	<b>&gt; Mean</b>	<b>&gt; Mean + 1<math>\sigma</math></b>
<b>Tmax</b>	< 8.2°C	< 10.2°C	> 10.2°C	> 12.1°C
Warm	+4.6	+4.2	-4.2	-4.5
Cold	+0.9	-0.1	+0.7	+1.2
<b>Tmin</b>	< -2.8°C	< -1.2°C	> -1.2°C	> 0.5°C
Warm	+2.5	+2.1	-1.3	-0.8
Cold	+0.0	-0.9	+1.5	+1.4

Table 4.31: As in Table 4.21, but for southern Minnesota region during October-November (Fig. 4.36).

	<b>&lt; Mean - 1<math>\sigma</math></b>	<b>&lt; Mean</b>	<b>&gt; Mean</b>	<b>&gt; Mean + 1<math>\sigma</math></b>
<b>Tmax</b>	< 12.6°C	< 14.6°C	> 14.6°C	> 16.6°C
Warm	+5.3	+5.8	-5.6	-5.2
Cold	+0.9	+0.5	+0.2	+0.5
<b>Tmin</b>	< -0.5°C	< 0.9°C	> 0.9°C	> 2.3°C
Warm	+1.1	+1.2	-0.3	+0.5
Cold	-0.7	-0.4	+0.3	+0.5

Table 4.32: As in Table 4.21, but for eastern Nebraska region during October-November (Fig. 4.37).

The changes in frequency of daily maximum temperatures in the southern Plains during warm TP SSTA events (Section 3.4.2.2, Fig. 3.8) compared to neutral SSTA events exhibited more linear characteristics, while those for daily minimum temperatures were not significant. In North Texas, the frequency of daily maximum temperatures below +20°C increased during warm TP SSTA events compared to neutral SSTA events, while those between +26°C and +32°C decreased (Fig. 4.38a). The region observed 4.8 more days with daily maximum temperatures below the seasonal  $\mu-\sigma$  value of +21.2°C and 4.2 fewer days above the seasonal  $\mu+\sigma$  value of +24.3°C (Table 4.33). Though the magnitude of the changes were small, Fig. 4.38a shows that during cold SSTA events, the region observed an increase (decrease) in the frequency of daily maximum temperatures between +26°C and +32°C (below +22°C). During cold SSTA events, the North Texas region observed 1.6 more days above the seasonal  $\mu+\sigma$  of 24.3°C and 1.6 fewer days below the seasonal  $\mu-\sigma$  of 21.2°C. As for daily minimum temperatures, the changes in frequency during both warm and cold SSTA events relative to neutral TP SSTAs were very small (Fig. 4.38b).

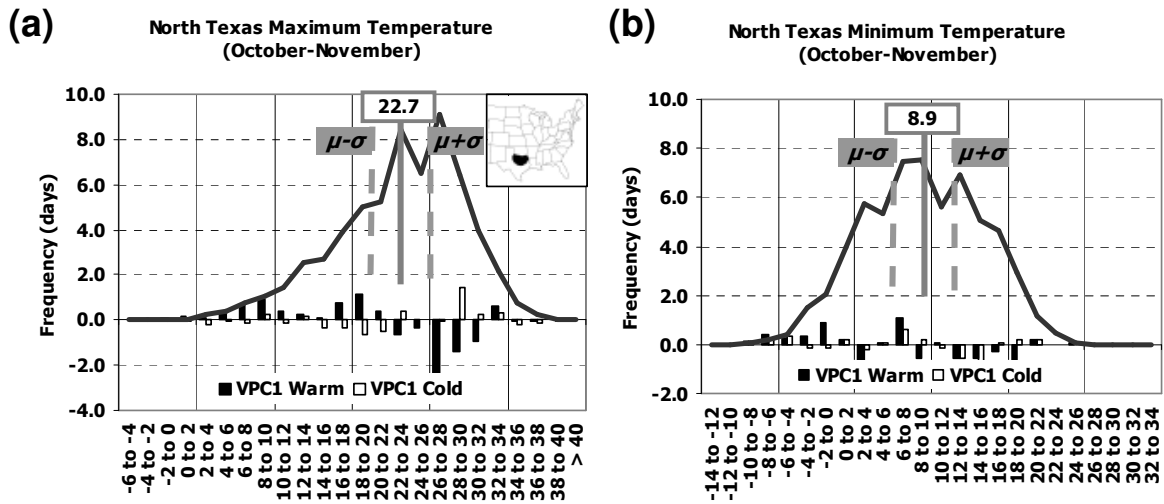


Fig. 4.38: As in Fig. 4.22 but for north Texas region during October-November.

	< Mean - 1σ	< Mean	> Mean	> Mean + 1σ
<b>Tmax</b>	< 21.2°C	< 22.7°C	> 22.7°C	> 24.3°C
Warm	+4.8	+5.2	-4.6	-4.2
Cold	-1.6	-2.0	+1.6	+1.6
<b>Tmin</b>	< 7.6°C	< 8.9°C	> 8.9°C	> 10.2°C
Warm	+1.5	+2.6	-2.0	-2.1
Cold	+0.5	+1.1	-1.3	-1.2

Table 4.33: As in Table 4.21, but for north Texas region during October-November (Fig. 4.38).

The observed average of the daily maximum temperature anomalies were above normal instead of below normal (as indicated by the warm SSTA VPC1 composite, Fig. 3.8) for all three regions discussed above during a total of four out of twelve October-November periods, including one during a negative AO phase and another in a positive AO phase. Fig. 4.39a-c indicates that during October-November 1965 (negative AO phase in November; Table 2.2), the average daily maximum temperatures were warmer than normal instead of colder than normal as indicated by the composite in Fig. 3.8. Additionally, during October-November 1994 (positive AO phase in November; Table 2.2) southern Minnesota and eastern Nebraska average daily maximum temperatures were warmer than normal (Fig. 4.39a-b). Other October-November periods

with warmer than normal (instead of colder than normal) average daily maximum temperatures included 1987 (southern Minnesota, Fig. 4.39a), 1951 (north Texas, Fig. 4.39c), and 1983 (north Texas, Fig. 4.39c). Consistent with the composite anomalies in Fig. 3.8, the observed anomalies of October-November average daily minimum temperatures in the same regions were near zero.

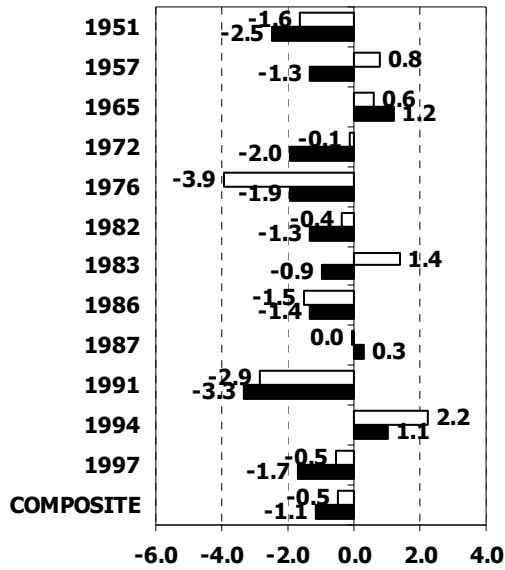
During cold October-November TP SSTA events, the observed average daily maximum temperature anomaly in the southern Plains was below normal instead of above normal in three out of eleven years. Fig. 4.39d shows that the average October-November daily maximum temperature anomaly in the North Texas region was below normal during 1961, 1967, and 1970. However, none of these October-November seasons were characterized by extreme phases of the AO or NAO (Table 2.2). Consistent with the composite anomalies in Fig. 3.9, the observed anomalies of October-November average daily minimum temperatures in the southern Plains were near zero.

#### **4.5 Summary of Daily Distribution Findings and Focus for Chapter 5**

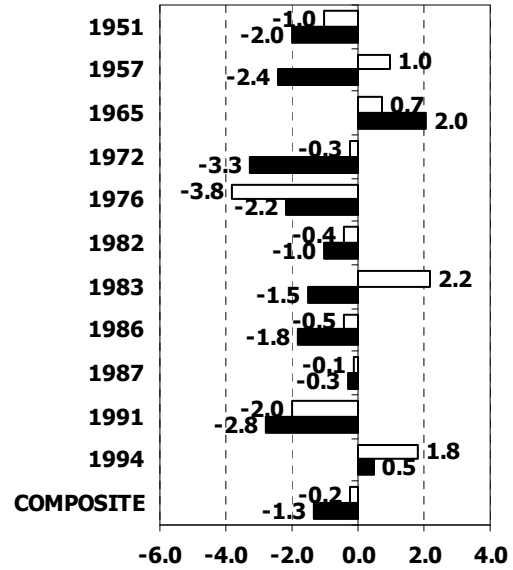
This Chapter has documented fully the properties of the daily precipitation and maximum/minimum temperature distributions for regions identified in Chapter 3 to exhibit statistically significant monthly total precipitation and mean temperature associations with TP SSTAs. The daily distribution characteristics described above for the coherencies in monthly total precipitation and monthly average daily maximum and minimum temperature are summarized in Table 4.34 and Table 4.35, respectively. This extensive documentation adds to the previous TP SSTA-based monthly teleconnection work of M97 and MRL98 by providing insight into the statistical distributions of daily data that underly the spatial patterns of the traditional monthly composite anomalies.

The analysis of the distribution of daily precipitation totals has identified multiple regions in which the change in the distribution is not uniform across all daily amounts. For example, during warm (cold) January-March SSTA VPC1 events, the frequency of daily precipitation totals in the southeastern U.S. increased (decreased) for moderate totals (10-100 mm d<sup>-1</sup>) but was unchanged for larger daily amounts (Table 4.34). The

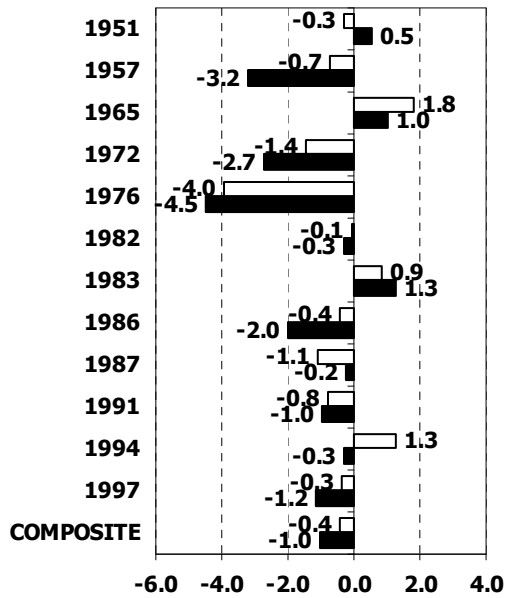
(a) Southern Minnesota Temperature Anomaly (October-November, Warm VPC1)



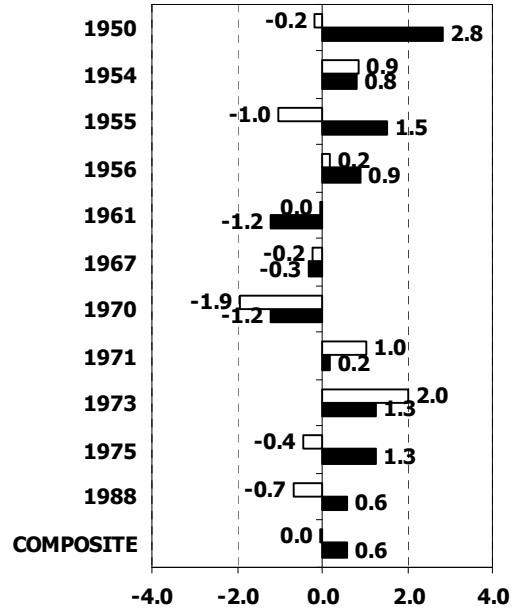
(b) Eastern Nebraska Temperature Anomaly (October-November, Warm VPC1)



(c) North Texas Temperature Anomaly (October-November, Warm VPC1)



(d) North Texas Temperature Anomaly (October-November, Cold VPC1)



Tmax   
 Tmin

Fig. 4.39: As in Fig. 4.26 but during warm October-November SSTA VPC1 events for (a) southern Minnesota region (Fig. 4.36), (b) eastern Nebraska region (Fig. 4.37), and (c) north Texas region (Fig. 4.38). (d) As in (c) but for cold SSTA events.

only exception was southern Florida during cold SSTA VPC1 events, which observed a decrease in the frequency of very large daily totals. During November, the change in frequency of daily totals was uniform across all sizes for the coastal regions during both warm and cold SSTA VPC1 events, but for a region from Oklahoma to Illinois, only larger daily amounts exhibited a decrease in frequency during cold SSTA events, with no associated change during warm SSTA events. But in the U.S. Great Plains, the change during warm SSTA VPC1 events was uniform across all sizes.

While the changes in the frequency of daily temperature extremes represents a shift in the distribution to favor events with daily anomalies having the sign of the composite anomaly for most regions, some regions exhibit changes that are not uniform. In the eastern U.S., very cold December daily maximum and minimum temperature anomalies were less frequent during warm TP SSTA events, while the southern U.S. in January experienced less frequent very warm daily maximum temperature anomalies (Table 4.35). October-November was characterized by less frequent very cool daily maximum temperature anomalies across the U.S. Great Plains during warm SSTA VPC1 events (Table 4.35). During cold SSTA VPC1 events, February-April generally was characterized by more frequent very cold daily maximum temperatures (Table 4.35).

In order to focus the examination of the teleconnection linkage chain from the TP to North America, the aforementioned precipitation and temperature results have been further summarized into key characteristics for five major regions for warm SSTA VPC1 events. These characteristics are presented in Table 4.36 and will be used to focus the analysis of the duration of consecutive days of anomalies with same sign and the documentation of the atmospheric conditions preceding the formation of these anomaly periods in Chapter 5.

Section	Period	Region	Sub-Region	Summary of Daily Precipitation Statistics
<i>VPCI Warm / Cold</i>				
4.3.1.1	JFM	Atlantic and Gulf of Mexico Coasts	South Florida	<b>Warm events:</b> Wet with more frequent daily precip events especially from 25-100 mm d <sup>-1</sup> <b>Cold events:</b> Dry with few daily large precip events <b>Exceptions:</b> 1958 (warm) 1967 1971 (cold)
			Far Southeast U.S. and Central Florida	<b>Warm events:</b> Wet with more frequent daily precip events 10-100 mm d <sup>-1</sup> <b>Cold events:</b> Dry with decrease in frequency of precip events 10-100 mm d <sup>-1</sup> <b>Exceptions:</b> 1958 (warm) 1967 1971 (cold)
			North-South Carolina	<b>Warm events:</b> Wet with more frequent daily precip events 10-100 mm d <sup>-1</sup> <b>Cold events:</b> Dry with decrease in frequency of precip events 10-100 mm d <sup>-1</sup> <b>Exceptions:</b> 1958 (warm) 1967 1971 (cold)
4.3.1.2	Nov	Southern and Midwest U.S.	Carolinas	<b>Warm events:</b> Wet with more frequent daily precip events of all sizes <b>Cold events:</b> Dry with few daily precip events >10 mm d <sup>-1</sup> <b>Exceptions:</b> 1965 1991 (warm)
			Florida	<b>Warm events:</b> Wet with more frequent daily precip events of all sizes <b>Cold events:</b> Dry with less frequent daily precip events of all sizes <b>Exceptions:</b> 1957 1965 1991 (warm) 1954 (cold)
			Gulf Coast	<b>Warm events:</b> Wet with more frequent daily precip events of all sizes <b>Cold events:</b> Dry with few daily precip events >10 mm d <sup>-1</sup> <b>Exceptions:</b> 1965 1991 1994 (warm) 1973 (cold)
			Texas	<b>Warm events:</b> None <b>Cold events:</b> Dry due to less frequent daily precip events >25 mm d <sup>-1</sup> <b>Exceptions:</b> None
			OK-IL Track	<b>Warm events:</b> None <b>Cold events:</b> Dry due to less frequent daily precip events >25 mm d <sup>-1</sup> <b>Exceptions:</b> 1973, 1975 (cold)
4.3.1.3	JF	Eastern Midwest and Western Appalachian Mountains	Eastern Midwest	<b>Warm events:</b> Dry with fewer daily precip events of all sizes <b>Cold events:</b> Wet during Feb. only due to increase in frequency of events 10-50 mm d <sup>-1</sup> <b>Exceptions:</b> 1998 (warm) 1968 (cold)
			Western Appalachians	<b>Warm events:</b> Dry due to lack of occurrence of large precip events (>25 mm d <sup>-1</sup> ) <b>Cold events:</b> Wet due to increase in frequency of all events <b>Exceptions:</b> 1973, 1998 (warm) 1968 1976 (cold; positive AO)
4.3.1.4	NDJ	Canadian Prairies	Eastern Montana	<b>Warm events:</b> Dry with fewer daily precip events in all categories, but especially for events < 10mm <b>Cold events:</b> None <b>Exceptions:</b> 1976-77 1982-83 (warm; low Arctic Oscillation)
			Southern Alberta-Manitoba	<b>Warm events:</b> Dry with fewer daily precip events in all categories, but especially for events < 10mm <b>Cold events:</b> Wet with more frequent precip events in all categories <b>Exceptions:</b> 1965-66 (warm; low Arctic Oscillation) 1954-55 (cold; positive NAO)

Table 4.34: Summary of daily precipitation event characteristics associated with TP SSTA events.

Section	Period	Region	Sub-Region	Summary of Daily Precipitation Statistics
<i>VPCI Warm / Cold</i>				
4.3.1.5	Jan	Southern Plains	North Texas	<b>Warm events:</b> Wet due to increase in frequency of all precipitation events <b>Cold events:</b> None <b>Exceptions:</b> 1988 (warm; positive NAO and PDO)
4.3.1.6	Mar	U.S. Great Plains	Oklahoma-Kansas	<b>Warm events:</b> Wet due to increase in frequency of all precipitation events <b>Cold events:</b> Wet due to decrease in frequency of all precip events <b>Exceptions:</b> 1992 (warm) 1974 (cold)
			High Plains	<b>Warm events:</b> Wet due to increase in frequency of all precipitation events <b>Cold events:</b> Wet primarily due to decrease in frequency of precip events exceeding 10 mm d <sup>-1</sup> <b>Exceptions:</b> 1953 1958 (warm; negative NAO)
4.3.1.7	Dec	Eastern Texas and Louisiana	---	<b>Warm events:</b> Wet due to increased relative frequency of precipitation events exceeding 25 mm d <sup>-1</sup> . However, magnitude was very large for events after the 1976/77 climate shift <b>Cold events:</b> None <b>Exception:</b> 1957
<i>UPCI Cold</i>				
4.3.2	Apr	Mid-Atlantic	---	Dry due to decrease in frequency of precipitation events of all sizes. <b>Exceptions:</b> None.

Table 4.34 (continued)

Section	Period	Region	Sub-Region	Summary of Daily Temperature Statistics	
				Maximum Temperature	Minimum Temperature
		<i>VPCl Warm</i>			
4.5.1.1	Dec-Feb	Northern Plains / Southern Canadian prairies	North Dakota	More frequent warm days (especially above -4°C) and less frequent cold days (below -10°C) <b>Exceptions:</b> 1966, 1977, 1993	More frequent extreme positive anomalies, less frequent negative anomalies, but comparatively larger occurrence of strong positive anomalies <b>Exceptions:</b> 1966, 1977, 1993
	Feb		East Colorado-Western Kansas	None	Less frequent extreme cold events <b>Exceptions:</b> 1966, 1973, 1977, 1988, 1993
	Mar		Minnesota-Wisconsin	None	Less frequent extreme cold events <b>Exceptions:</b> 1977, 1993
	Dec	Atlantic coast	Three Rivers	More frequent warm days, less frequent cold days (especially less frequent very cold days) <b>Exceptions:</b> 1976, 1986, 1997	More frequent warm days, less frequent cold days (especially less frequent very cold days) <b>Exceptions:</b> 1976
			Chesapeake Bay	More frequent warm days, less frequent cold days (especially less frequent very cold days) <b>Exceptions:</b> 1976	More frequent warm days, less frequent cold days (especially less frequent very cold days) <b>Exceptions:</b> 1976
			Western Pennsylvania	More frequent warm days, less frequent cold days (especially less frequent very cold days) <b>Exceptions:</b> 1976	More frequent warm days, less frequent cold days (especially less frequent very cold days) <b>Exceptions:</b> 1976
	4.5.1.2	Jan	Southeast U.S. / Texas	Carolinas	Less frequent very warm days (none above $\mu+c$ ) and more frequent cold days <b>Exceptions:</b> 1992, 1993, 1995, 1998
Southeast Texas				Less frequent very warm days (none above $\mu+c$ ) and more frequent cold days <b>Exceptions:</b> 1995, 1998	Less frequent very warm days and very cold days, more days near normal <b>Exceptions:</b> 1992, 1995, 1998
Northern Georgia				Less frequent very warm days (none above $\mu+c$ ) and more frequent cold days <b>Exceptions:</b> 1992, 1993, 1995, 1998	Less frequent very warm days and very cold days, more days near normal <b>Exceptions:</b> 1992, 1993, 1995, 1998
Western Texas				Less frequent very warm days (none above $\mu+c$ ) and more frequent cold days <b>Exceptions:</b> 1995, 1998	Less frequent very warm days and more frequent cooler than normal days <b>Exceptions:</b> 1958, 1992, 1993, 1995, 1998
4.5.1.3	Oct-Nov	Central U.S.	Southern Minnesota	More frequent very cool days, but no change in very warm days <b>Exceptions:</b> 1965, 1987, 1994	None
			Eastern Nebraska	More frequent very cool days, but no change in very warm days <b>Exceptions:</b> 1965, 1994	None
			Northern Texas	More frequent very cool days, but no change in very warm days <b>Exceptions:</b> 1951, 1965, 1983	None

Table 4.35: Summary of daily maximum and minimum event coherencies with TP SSTA events.

Section	Period	Region	Sub-Region	Summary of Daily Temperature Statistics	
				Maximum Temperature	Minimum Temperature
		<i>YPC1 Cold</i>			
4.5.1.2	Feb-Mar	Southern Plains	Western Kansas-Oklahoma	More frequent extreme cold days <b>Exceptions:</b> 1971	None
4.5.1.1	Feb-Apr	U.S.-Canada border	Southern Quebec	More frequent extreme cold days <b>Exceptions:</b> 1968, 1976	More frequent extreme cold days <b>Exceptions:</b> 1962, 1968, 1971
			Maire-New Brunswick	More frequent extreme cold days <b>Exceptions:</b> 1976	More frequent extreme cold days <b>Exceptions:</b> 1968, 1971
	Mar-Apr		Southern Manitoba	More frequent extreme cold days <b>Exceptions:</b> 1968, 1969, 1976	More frequent extreme cold days <b>Exceptions:</b> 1968

Table 4.35 (continued)

Table 4.36: Key regions and associated precipitation/temperature characteristics used to define target anomaly periods and focus examination of antecedent atmospheric conditions.

<b>Target Region</b>	<b>Period</b>	<b>Overall climate characteristics</b>
Northern Plains / Southern Canadian prairies	Dec-Feb	Warmer than normal temperatures due to more frequent warm days and less frequent cold days, but also drier than normal in the southern Canadian prairies due to less frequent precipitation events of all sizes
Southeast U.S.	Nov-Feb	Generally wet throughout the season due to more frequent precipitation events and cool in January due to less frequent warmer than normal days and more frequent cooler than normal days
Eastern Midwest	Jan-Mar	Generally warm and dry conditions, with fewer precipitation events of all sizes and more frequent warmer than normal days
Atlantic coast	Dec-Jan	Generally warmer than normal temperatures due to more frequent warm days and especially less frequent very cold days
Central Plains	Feb	Generally warm minimum temperatures due to lack of extreme cold minimum temperature events

## Chapter 5

### **Larger-Scale Atmospheric Phenomena Associated with Shifts in North American Daily Weather Event Distributions during Warm Tropical Pacific SSTA Events**

#### **5.1 Preamble**

In this Chapter, the larger-scale atmospheric relationships connecting TP SSTAs and North American climate are investigated. Chapter 3 delineated and characterized the regions for which monthly average North American precipitation and temperature were significantly linked to TP SSTAs. These associations were further refined in Chapter 4 by documenting, for the first time, the properties of daily weather event distributions underlying these monthly relationships. The final step, and goal of this Chapter 5, is to identify the associated larger-scale atmospheric conditions involved, thereby adding to the previous dynamical/physical understanding of the linkage between TP SSTAs and North American climate. The focus of this analysis is October through March during the key warm TP SSTA events identified in Section 2.4 and repeated here in Table 5.1. Those multiple-month warm events were selected to facilitate an examination of the atmospheric evolution under the regular forcing of warm TP SSTAs during October-March, the season with strongest statistical significance for both precipitation and temperature relationships, as indicated by MRL98 and Chapter 3. For this Chapter, the focus will be on warm TP SSTA events during the October-March season due to the comparatively higher attention given to documenting the physical aspects of and teleconnections associated with warm TP SSTA events in the literature (e.g., Rasmusson and Carpenter 1982, Ropelewski and Halpert 1986, Kunkel and Angel 1999, Compo et al. 2001) compared to cold TP SSTA events (e.g., Branstator and Trenberth 1988). Further, warm TP SSTA events have been more frequent in the last 25 years than cold TP SSTA events (Fig. 2.3a-b).

The research summarized in this Chapter had two components. The initial objective was to document the dynamical/physical teleconnection linkage chain between warm TP SSTAs and atmospheric circulation over the north Pacific Ocean and North America using the data and methods summarized in Sections 5.2 and 5.3. Through composite analysis of the NCEP/NCAR Reanalysis data, the general atmospheric conditions observed in the presence of the key warm SSTA events (Table 5.1) are described and compared to the findings of earlier authors (Section 5.4).

Significant deviations from the composite mean pattern for individual constituent years also are noted and related to the Arctic Oscillation (AO), which was often linked to exception years in Chapters 3 and 4. Next, the anomalous North American precipitation and temperature conditions linked to the monthly teleconnection relationships defined in Section 3.4 (and further refined in Sections 4.3 and 4.4) are described in terms of (a) the duration of the anomalies and (b) the antecedent atmospheric conditions through a targeted composite analysis of daily NCEP/NCAR Reanalysis data. Consistencies with the overall atmospheric patterns during warm TP SSTA events are described in Section 5.5, and a summary of key conclusions is provided in Section 5.6.

Table 5.1: As in Table 2.3, primary SSTA events for which physical/dynamical aspects of the teleconnection linkage chain from the tropical Pacific to North America will be documented.

<b>Period</b>	<b>Event Type</b>
1957-58	El Niño
1965-66	El Niño
1972-73	El Niño
1982-83	El Niño
1986-87	El Niño
1991-92	El Niño
1992-93	El Niño
1997-98	El Niño

## 5.2 Data

### 5.2.1 NCEP/NCAR Reanalysis Data

The principal data source used for identifying large-scale atmospheric patterns associated with warm TP SSTAs is the NCEP/NCAR Reanalysis data from 1950-2000. Motivated by the need to remove inhomogeneities from model-generated data sets due to the continuous upgrading of data assimilation systems, the NCEP/NCAR Reanalysis data

set was prepared using the spectral statistical interpolation system from the operational Medium Range Forecast model as of January 11, 1995 (Kalnay et al. 1996; Kistler et al. 2001). The assimilation system was used with a T62 spectral truncation and for 28 vertical levels. In the Reanalysis system, a full range of atmospheric variables are available on constant pressure surfaces. Two of the principal benefits of this data set are the regular  $2.5^\circ \times 2.5^\circ$  resolution latitude-longitude grid and the lack of missing data. In the present study, anomaly fields are calculated from the long-term climatological mean (from 1968-1996) provided with the NCEP/NCAR Reanalysis data set.

While problems have been noted with the moisture and energy budget aspects of the Reanalysis data, they do not have a material influence on the present investigation. Kistler et al. (2001) identified problems involving moisture parameters and snow cover near the poles. Further, Trenberth et al. (2002) noted problems when calculating energy budgets from the Reanalysis data. However, the present research examines 500mb geopotential height, 200mb zonal winds, and sea-level pressure (SLP), all of which have the highest reliability rating (“A”) in Kalnay et al. (1996), plus vertical motion in the tropics, which has a “B” reliability rating. While some effect of the above problems on the fields used in this study cannot be ruled out entirely, for the purposes of the present study (i.e., general atmospheric evolution in tropics and midlatitudes) the expected impact should be minimal.

### 5.2.2 *Cyclone Tracks*

To identify changes in storm tracks to complete the teleconnection linkage chain between warm TP SSTAs and North American precipitation and surface temperature, a cyclone track data base developed by NASA (2005) is used. This data base was produced by an objective method to identify low-pressure centers in SLP fields. Specifically, 12-hour observations are examined for local SLP minima that, in turn, are continuously tracked in successive 12-hour gridded fields. Cyclones must persist at least 36 hours before being so categorized (NASA 2005). Cyclone tracks were available for January 1961 through December 1998.

### **5.3 Methodology**

#### *5.3.1 Large-Scale Atmospheric Patterns Associated with warm TP SSTAs*

The first step in linking warm TP SSTAs to North American weather systems involved documenting the large-scale atmospheric flow associated with the warm TP SSTAs. The present research uses monthly composite analysis to identify the geopotential height, winds, sea-level pressure, and vertical motion patterns common to the warm TP SSTA events listed in Table 5.1. The spatial composite fields are supplemented with time-longitude and time-latitude composites to illustrate further the temporal evolution of the atmospheric anomalies. Where appropriate, differences between the characteristics of individual event years and the event mean composite are identified and associated with other atmospheric modes (particularly the AO).

#### *5.3.2 Intra-Month Characteristics of Anomalous North American Precipitation and Temperature*

Following the examination of the monthly mean atmospheric circulation fields associated with warm TP SSTAs, the intra-month characteristics of the associated North American precipitation and temperature patterns are documented using up to three types of analyses. First, to provide insight into the daily variability of the large scale fields, time-longitude cross-sections of daily average NCEP/NCAR reanalysis data are examined for cross-sections bisecting regions of key anomaly coherencies in seasonal mean atmospheric patterns. Second, a new data base was created that located local minima/maxima in 500mb geopotential height fields. Individual daily maps of NCEP/NCAR 500mb geopotential height anomalies were visually inspected to determine the locations of the local minima and maxima during October-March for the warm TP SSTA events listed in Table 5.1. The location (latitude/longitude) and magnitude of the central height anomalies were recorded to permit study of the evolution of the position and magnitude of anomaly centers.

Third, for the specific target regions that are selected from the monthly temperature/precipitation composites (Table 4.36), the daily event frequencies in Chapter 4 are extended by examining the temporal evolution of daily station anomalies. For the warm TP SSTA events listed in Table 5.1, the present research computes the

length of “runs” of consecutive days when the observed anomaly had the same sign as the corresponding composite anomaly for the target region. These periods will be called *targeted anomaly periods* (TAPs). Averaging the length of these anomalies during warm TP SSTA events provides information on the persistence of some of the anomaly features and offers some insight on how much (if at all) the atmosphere “locks” into a pattern to bring about the previously identified monthly average associations.

### 5.3.3 *Antecedent Atmospheric Conditions for Target Daily Periods*

Lastly, for each TAP, the antecedent atmospheric conditions over North America and the northern Pacific Ocean are documented for individual target regions for the warm TP SSTA events listed in Table 5.1. This involves compositing the daily 500mb height anomalies for 0 to 10 days before the TAP initiation, thereby identifying the general atmospheric evolution before the key period that brings about the anomaly in the monthly (and seasonal) composites. The full series of these composite fields – from Day (0) back through Day (-10) – is called a *time evolution composite* (TEC). The atmospheric pattern evolution in these TECs then is used to describe the final connection between TP SSTAs and the observed North American precipitation and temperature anomaly fields.

## 5.4 **Large-scale Atmospheric Features Linked to Warm TP SSTA Events**

### 5.4.1 *Seasonal and Monthly Composites*

During warm December-February TP SSTA events, strong SSTAs span much of the central and eastern TP, which displaces eastward the large-scale convection that otherwise resides over the western TP (e.g., Bjerknes 1966, 1969). As noted in Chapter 3 (e.g., Fig. 3.6), each calendar month from December to March is associated with extensive North American temperatures anomalies east of the Rockies during such warm TP SSTA events. The composite December-February warm SSTA field (Fig. 5.1) indicates positive SSTAs exceeding +1.0°C from the International Date Line to the South American coast, a region geographically coincident with MRL98’s UPC1 and VPC1 PC loading patterns. Further, the composite anomalies raise the actual SST field to above 28°C along the equator from 180° to 140°W and between the equator and 15°N from

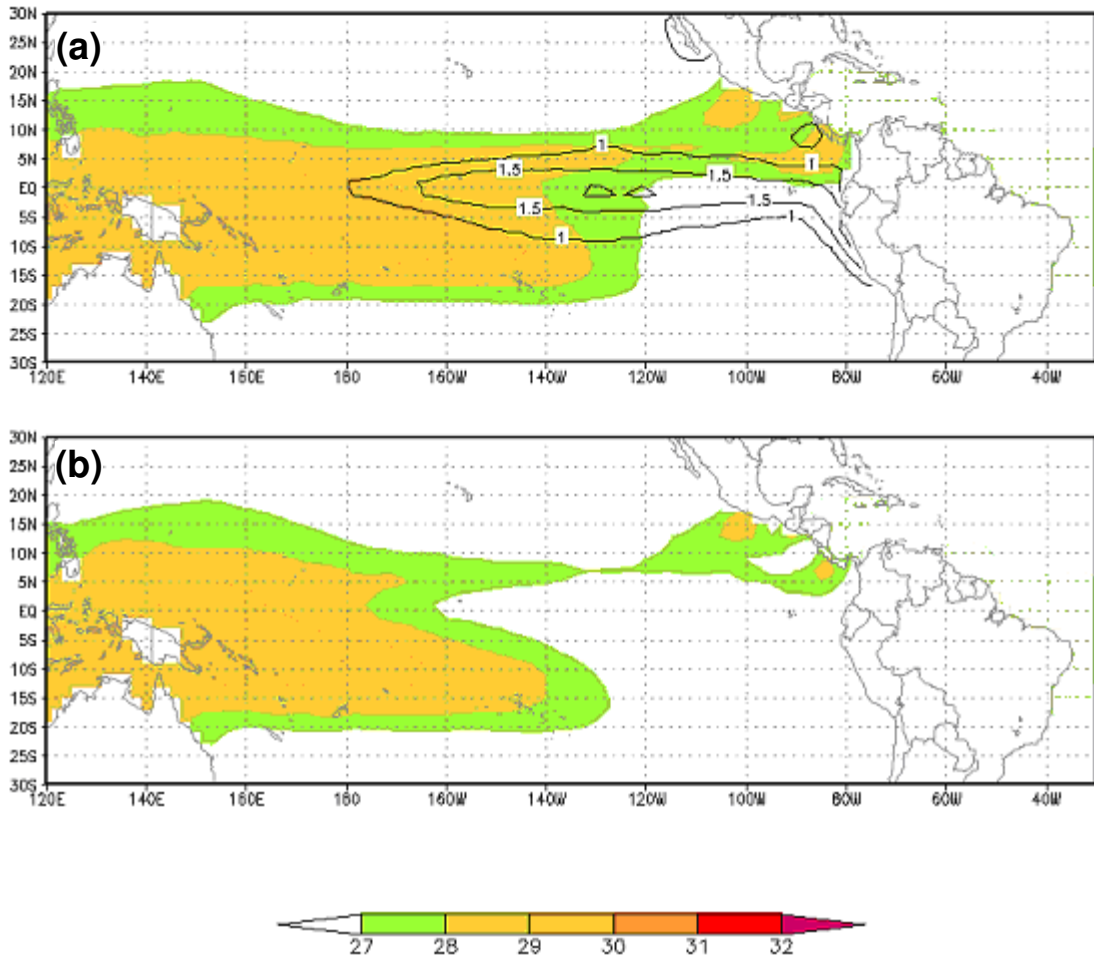


Fig. 5.1: (a) Composite SST anomalies (contoured, °C) and sea-surface temperatures (shaded, °C, bottom scale) during December-February for the warm SSTA VPC1 events listed in Table 2.3. (b) Climatological average sea-surface temperatures (shaded, °C, bottom scale) for December-February based on 1950-1999.

140°W to 80°W. Previous authors (e.g., Lau et al. 1997) have cited this 28°C threshold as indicative of significant overlying convection because of the inherent nonlinear relationship between water vapor and temperature. Using perpetual January forcing experiments, Gong (1998) demonstrated that in both the central and eastern TP, SSTs exceeding 28°C were associated with rising vertical motion and changes in the general atmospheric circulation, particularly the local Hadley circulation. (The association between rising motion and the local Hadley circulation has been described in detail by many other authors and is summarized in Peixoto and Oort (1992), pp. 157-160). The

finding that SSTs exceed the  $28^{\circ}\text{C}$  threshold in both the central and eastern TP supports the use of SSTA indices across the whole TP in examining TP-based teleconnections. Examples of such indices include the eastern TP-focused SSTA VPC1 and the central TP-focused SSTA UPC1 in the present study.

Associated with the SSTAs in Fig. 5.1 are upper-tropospheric circulation anomalies that enhance the subtropical jet stream. Fig. 5.2a shows that during December-February, negative zonal wind anomalies (i.e., less westerly) are located at 200mb directly over the equatorial Pacific SSTAs, with positive zonal wind anomalies (more westerly) across the subtropical Pacific around  $30^{\circ}\text{N}$  and around  $25^{\circ}\text{S}$ . These anomalies are consistent with a weakening of the Walker Circulation during El Niño events, as noted by other authors (e.g., Rasmusson and Carpenter 1982, Gong 1998). In addition, Fig. 5.2b exhibits positive (i.e., more northerly) meridional wind anomalies around  $160^{\circ}\text{W}$  and  $20^{\circ}\text{N}$ , just poleward of the region where positive SSTAs raise the ocean

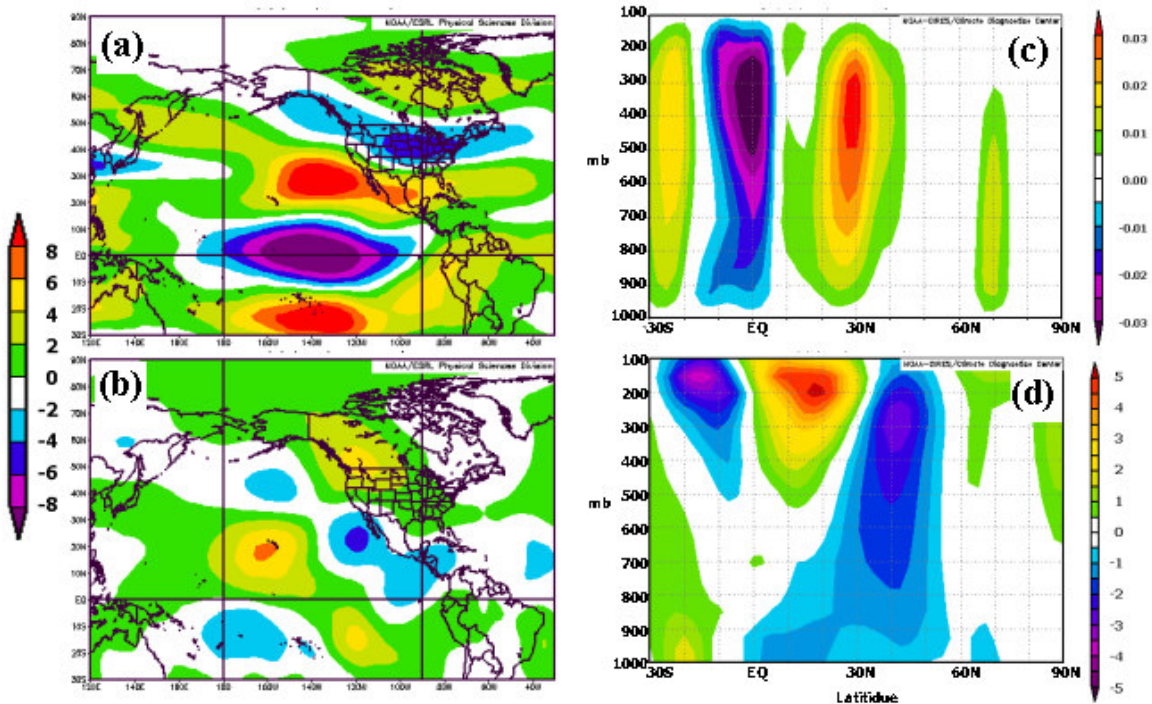


Fig. 5.2: Composite December-February wind anomalies ( $\text{m s}^{-1}$ ) for warm SSTA events (in Table 2.3) for (a) 200mb zonal wind and (b) 200mb meridional wind ( $\text{m s}^{-1}$ ). Composite December-February wind anomalies of (c) vertical motion ( $\text{mb s}^{-1}$ ) and (d) meridional wind ( $\text{m s}^{-1}$ ) for cross section from 1000mb to 100mb averaged over  $175^{\circ}\text{W}$  to  $155^{\circ}\text{W}$ .

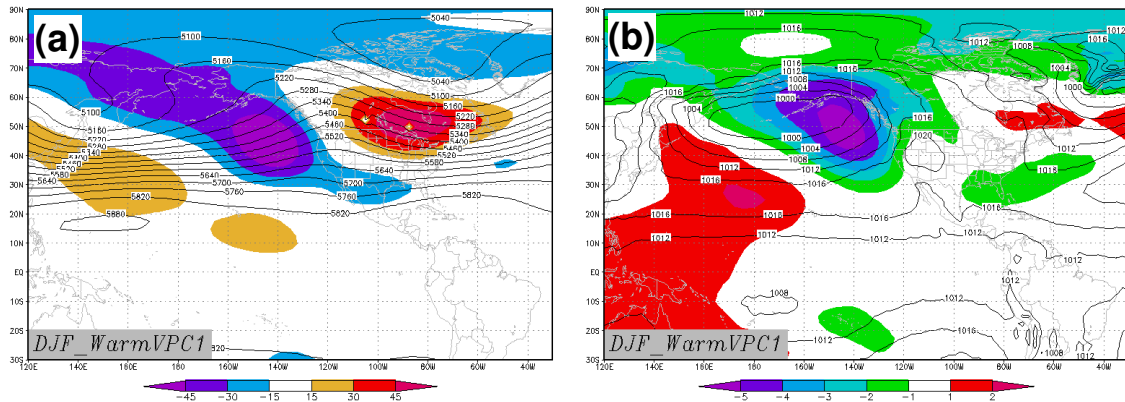


Fig. 5.3: Composite December-February (a) 500mb geopotential heights (contours, gpm) and anomalies (shaded, gpm, bottom scale) and (b) sea level pressure (contours, mb) and anomalies (shaded, mb, bottom scale) during warm SSTA VPC1 events.

temperatures above the  $28^{\circ}\text{C}$  convection threshold (Fig. 5.1), consistent with Gong (1998). This is the upper branch of a local anomalous vertical meridional circulation. Fig. 5.2d gives the composite meridional wind anomaly, which shows maximum anomalies near 200mb (southerly anomalies around  $25^{\circ}\text{N}$  and northerly anomalies around  $40^{\circ}\text{N}$ ) producing anomalous upper level convergence and descending motion around  $30^{\circ}\text{N}$ . This anomaly pattern is supported by the vertical motion anomalies in Fig. 5.2c, which also show enhanced rising motion around the equator. This constitutes a strengthening of the local Hadley circulation during warm TP SSTA events, consistent with the findings of other authors (e.g., Bjerknes 1966, 1969). In short, the SSTAs raise the actual ocean temperatures above the convective threshold, leading to enhanced rising motion near the equator overlain by upper tropospheric divergence, which increases convergence and descending motion around  $30^{\circ}\text{N}$  and strengthens the subtropical jet stream around  $30^{\circ}\text{N}$  as well.

The strengthening of the subtropical jet stream also is linked to decreases in geopotential height and seal-level pressure in the extratropical north Pacific. Fig. 5.3a indicates negative 500mb geopotential height anomalies centered at  $160^{\circ}\text{W}$  and  $45^{\circ}\text{N}$ , just poleward of the positive zonal wind anomalies associated with the enhanced subtropical jet stream (Fig. 5.2). In addition, this region is characterized by negative SLP anomalies (Fig. 5.3b) slightly east of the negative 500mb height anomalies (Fig. 5.3a). The position of the negative height anomalies is consistent with quasi-geostrophic (Q-G)

theory (Bluestein 1992, p. 339), as cyclonic vorticity advection ahead of the 500mb low would cause rising motion there, and surface convergence, thereby aiding the development of the anomalous surface low.

The principal features identified in the aforementioned seasonal mean composites also are present in the individual monthly composites for December-March and (to a lesser extent) November. Each of the monthly anomalies of 200mb zonal wind for December through March (Fig. 5.4b-e) exhibits a similar structure and magnitude as the December-February composite (Fig. 5.2a). The November 200mb zonal wind anomalies

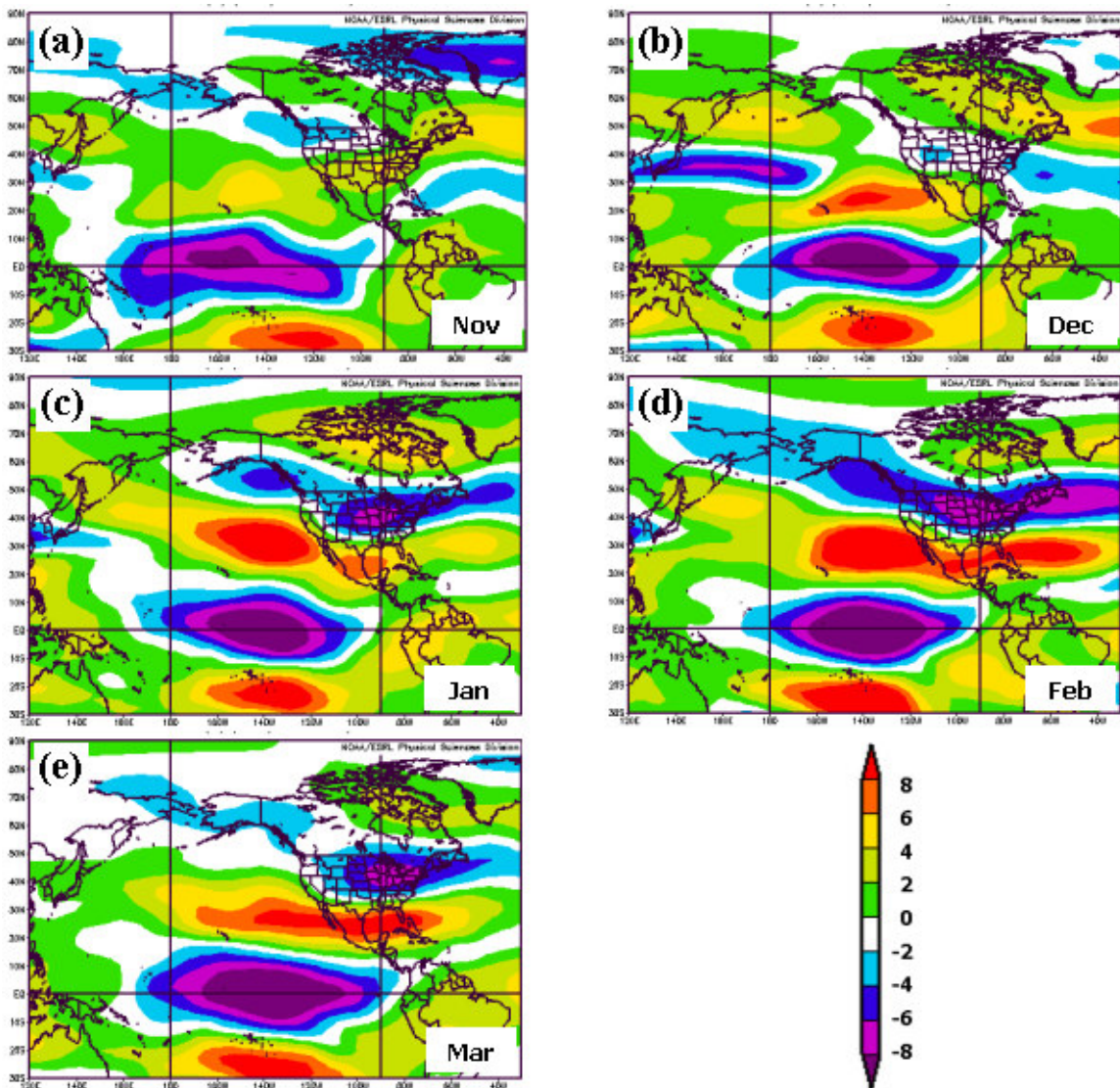


Fig. 5.4: As in Fig. 5.2a but for individual monthly composite 200mb zonal wind anomalies ( $\text{m s}^{-1}$ ) for November through March.

(Fig. 5.4a) are smaller in magnitude than for the composite (Fig. 5.2a). Similar common features are exhibited by 200mb meridional wind and 500mb height anomalies (not shown). This December-March coherence is consistent with the findings of MRL98, who demonstrated that the composite precipitation anomalies with the highest field significance occur in January-March when warm TP SSTAs are present in the central and eastern TP, and with the composites of monthly average daily maximum and minimum temperature anomalies in Chapter 3 (Fig. 3.6), which indicated that December-March are the months with composite values with the highest statistical significance.

The monthly and seasonal composites of SSTAs and large-scale atmospheric circulation presented in this section essentially reflect the findings of what now are classical studies. The composite SSTAs (Fig. 5.1) and sea level pressure anomalies (Fig. 5.3b) reflect Rasmusson and Carpenter's (1982) corresponding composites for the "Mature" phase of El Niño development, the December-February season following El Niño event initiation. The structure of the composite 500mb geopotential height anomalies (Fig. 5.3a) is similar to the composites of 700mb geopotential height anomalies in L97 and also to modes linked to the TP by Wallace et al.'s (1992) singular value decomposition and Wallace and Gutzler's (1981) correlation analysis. Further, both the 500mb height composite and the sea-level pressure anomalies reflect the findings of Bjerknes (1966) of an enhanced low in the Gulf of Alaska. Lastly, the 200mb wind anomalies (Fig. 5.2a-b, Fig. 5.4) and vertical circulation (Fig. 5.2c-d) are consistent with the weakening of the Walker Circulation and stronger local Hadley circulation in the vicinity of the stronger SSTAs (Bjerknes 1966; Kousky et al. 1984; Philander 1990, p. 20). In the following Sections, these background results will be built on through analyses, for the first time, of the associated intraseasonal atmospheric evolutions and differences among the warm SSTA events.

#### *5.4.2 Intra-month characteristics*

The position of daily negative 500mb height anomaly centers over the North Pacific and North America during warm TP SSTA events is consistent with the seasonal mean patterns presented in Section 5.4.1. Here, December-February 1957-1958 and 1982-1983 are examined as representative warm TP SSTA events, as the observed

500mb geopotential height anomalies in those seasons (Fig. 5.5) are particularly similar in structure to the pattern for the warm SSTA composite (Fig. 5.3). During these periods, the local maxima in the negative anomalies of 500mb geopotential height were frequently located in the region of negative seasonal mean anomalies in the northern Pacific Ocean (Fig. 5.5). Further, over North America, the positions of daily negative anomaly centers are located near the regions of positive 200mb zonal wind anomalies with very few centers in the regions of negative anomalies (Fig. 5.4), consistent with the strengthening and southward displacement of the southern storm track suggested by the structure of the 200mb zonal wind anomalies.

The negative daily anomaly centers in 500mb geopotential heights are also consistent with the precipitation anomalies in MRL98. Relatively few negative height anomaly centers were located in south central Canada (where MRL98 indicated below normal precipitation during warm central and eastern TP SSTA events). Conversely, clusters of anomaly centers are located along the southern tier of the U.S. in the region that MRL98 identified as having above normal precipitation during warm TP SSTA events. Additional documentation of the atmospheric conditions associated with these precipitation patterns is provided in Sections 5.5.1 and 5.5.2.

Fig. 5.6 suggests that the aforementioned daily negative 500mb height anomalies were maintained in the extratropical north Pacific Ocean for up to two weeks duration and did not progress eastward. December-February 1957-58 observed multiple periods (last half of December, first 3 weeks of January, last week of January, last 2 weeks of February) of negative height anomalies between 180° and 130°W of at least a week in duration, and in none of these cases did the anomalies move significantly eastward of 130°W (Fig. 5.6a). A similar characteristic was present in the December-February 1982-1983 500mb height anomalies (Fig. 5.6b), with two primary periods (last half of December and from mid January through February) of negative anomalies that did not move directly eastward. Similar characteristics of the 500mb height field were observed for all other warm TP SSTA events (not shown), except as noted in Section 5.4.3 below. Consequently, the seasonal mean relationships identified by earlier authors are associated

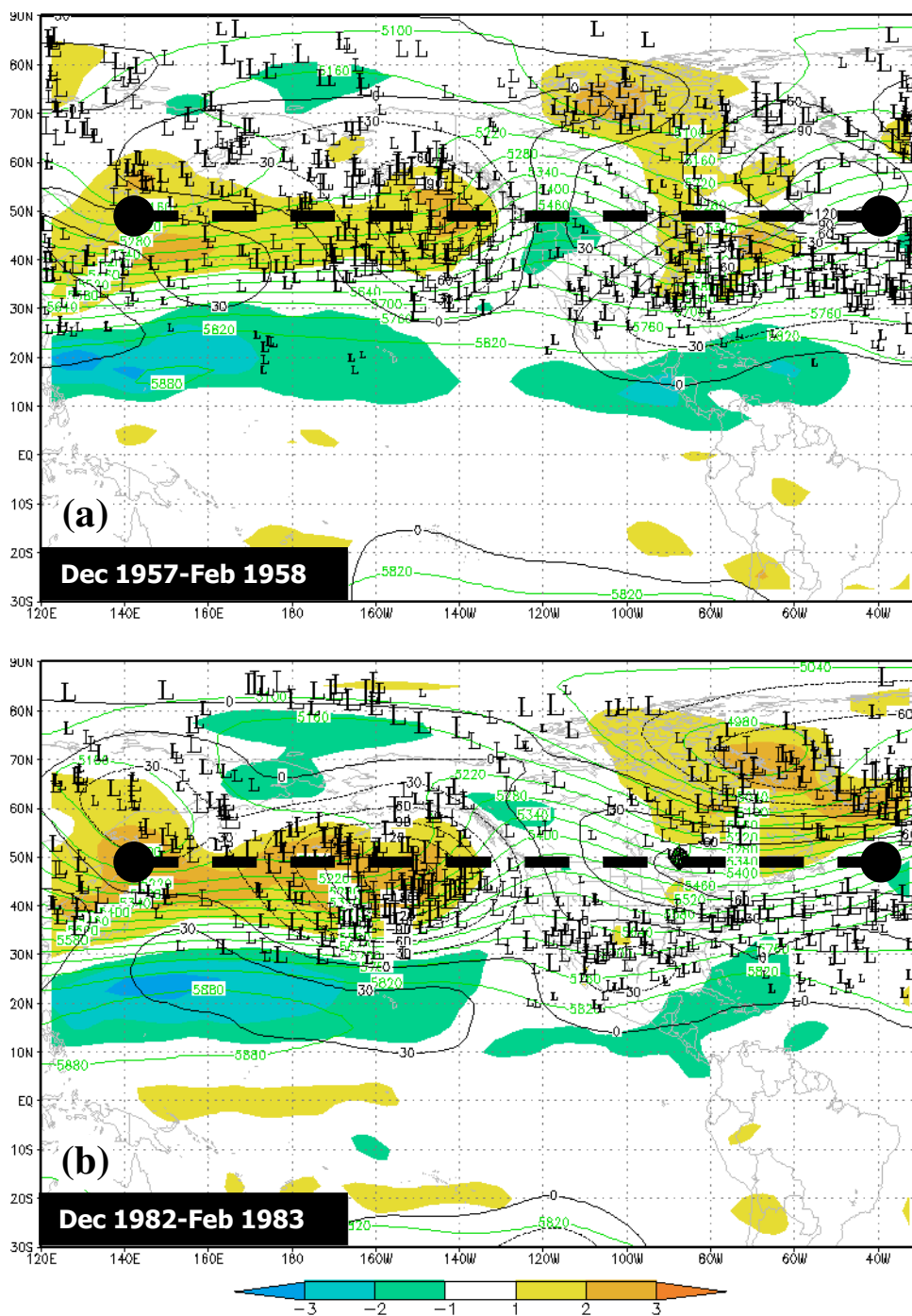


Fig. 5.5: Observed 500mb heights (light green lines, gpm), anomalies (black lines, gpm), average vorticity (shaded, in  $10^{-5} \text{ s}^{-1}$ ), and position of local maximum negative daily 500mb geopotential height anomalies (denoted by “L”) of at least 60m magnitude during (a) December-February 1957-58 and (b) December-February 1982-83. Size of letter “L” for plotted centers is proportional to size of 500mb height anomaly. Dashed barbell lines locate time-longitude cross-sections in Fig. 5.6.

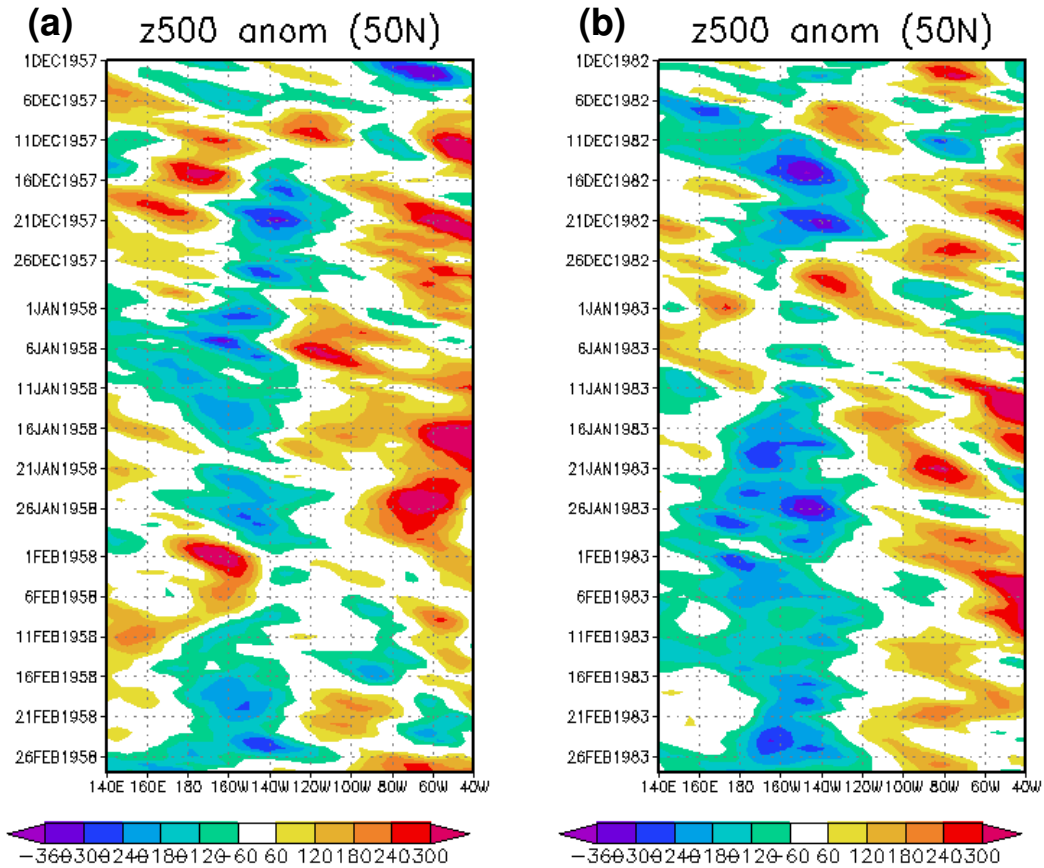


Fig. 5.6: Time-longitude pattern of daily mean 500mb height anomalies (gpm, averaged from 45°N to 55°N) from 140°E to 40°W during December-February (a) 1957-1958 and (b) 1982-83.

with persistent daily geopotential height anomalies that remained in the north Pacific for periods of two weeks or longer.

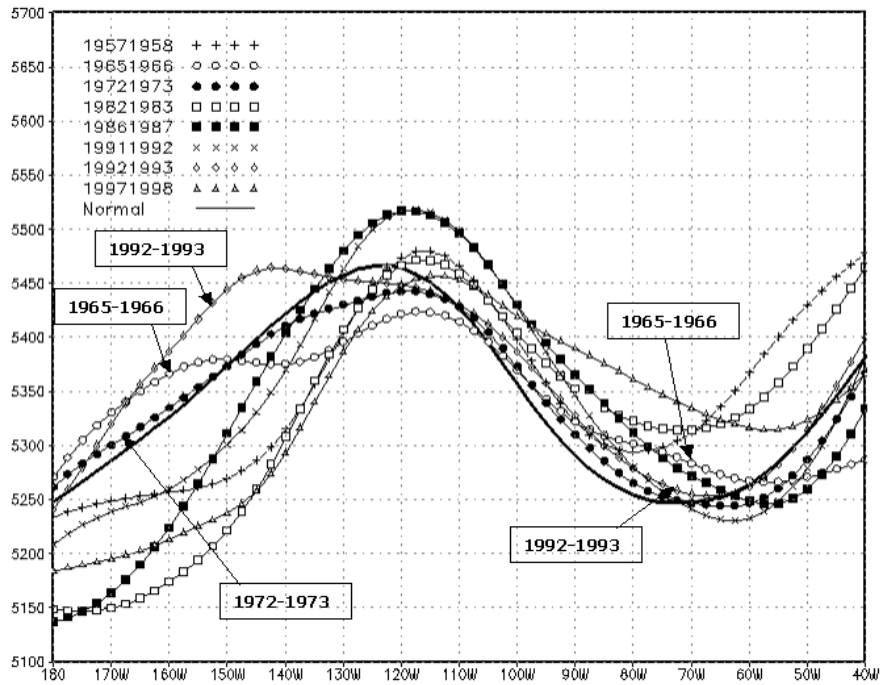
### 5.4.3 Individual event differences

An examination of the observed 500mb height anomalies in comparison to the warm SSTA composite (Fig. 5.3) identified three events with significant differences in large-scale atmospheric flow. Fig. 5.7a shows that the average December-February 500mb heights between 45-55°N exceeded the long-term mean during 1965-66, 1972-73, and 1992-93 between 180-150°W, while 500mb heights were well below normal in that sector during all other warm TP SSTA events. In these three cases, below normal heights were located farther east, from 150-110°W during 1965-66 and 1972-73 and 130-105°W for 1992-93 (Fig. 5.7a). Farther east, the observed geopotential height anomalies during

1965-66 and 1992-93 were above normal from 105-75°W (Fig. 5.7a) in the region of positive anomalies indicated by the composite 500mb height anomalies during warm TP SSTA events (Fig. 5.3a). Despite this match in the positive geopotential height anomalies over North America, both 1965-66 and 1992-93 were identified as exception years for daily maximum and minimum temperatures in the northern U.S. Great Plains, while 1972-73 was an exception year for daily minimum temperature in the central U.S. Great Plains and precipitation in the southwestern Appalachian Mountains region. In order to help explain these exception years, the large-scale atmospheric patterns during each of these events now are examined in turn.

The above lack of consistency between the observed 1965-66 500mb height anomalies and the composite based on warm TP SSTA events may be associated with the phase of the Arctic Oscillation (AO). Although December-February 1965-66 SSTs exceeded the 28°C convection threshold starting in June 1965 (Fig. 5.7b), an extreme negative AO phase occurred during January-February 1966. As described in Section 2.3.1, a negative AO phase before 1970 was characterized by a diminished polar vortex and negative 1000mb geopotential height anomalies over north central North America and increased geopotential height anomalies along 180° longitude in the far northern Pacific Ocean (Fig. 2.5a). This caused the positive 500mb height anomalies to form farther west than indicated in the warm SSTA event composite (Fig. 5.3a) during these months. Additionally, clusters of local minima in 500mb height anomalies were present in the far northwestern Pacific Ocean near 160°E to 180° as well as the far northeastern Pacific Ocean (Fig. 5.8). In the region where local minima are expected based on warm TP SSTA events more representative of the composite field (e.g., 1957-58 and 1982-83), local maxima were present (Fig. 5.9). Consequently, the lack of negative 500mb geopotential height anomalies in the North Pacific and warm temperature anomalies in the northern U.S. Great Plains can be attributed to the strong negative AO phase.

(a) December-February 500 mb Height – Average from 45-55°N



(b) Equatorial SST Averaged From 165-140°W

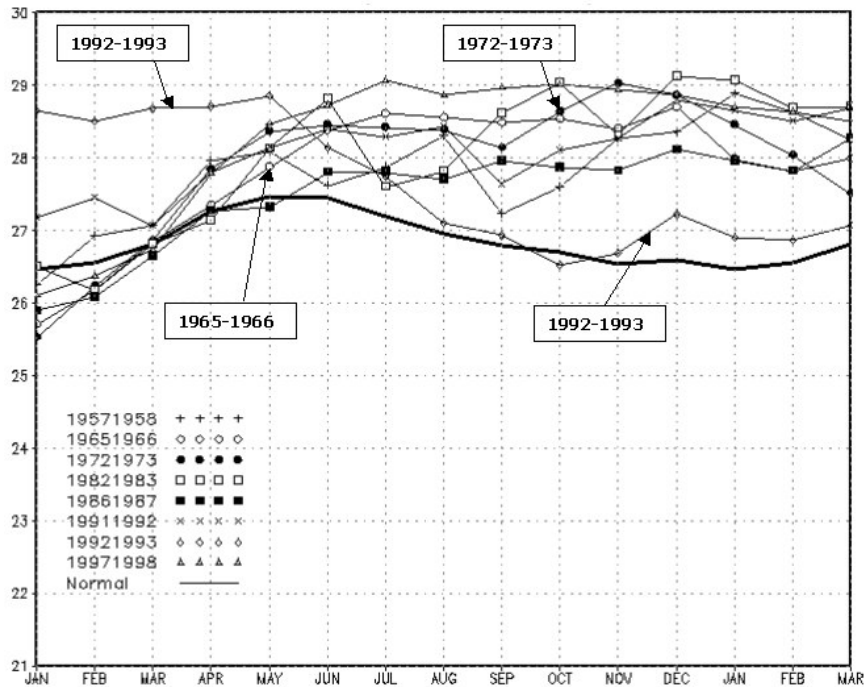


Fig. 5.7: (a) Observed December-February 500mb heights (gpm) averaged from 45-55°N for warm TP SSTA events in Table 2.3 compared to average for 1968-96 (thick solid line). (b) Average SSTs (°C) compared to average for 1979-95 (thick solid line) along the equator from 165-140°W for warm SSTA events in Table 2.3.

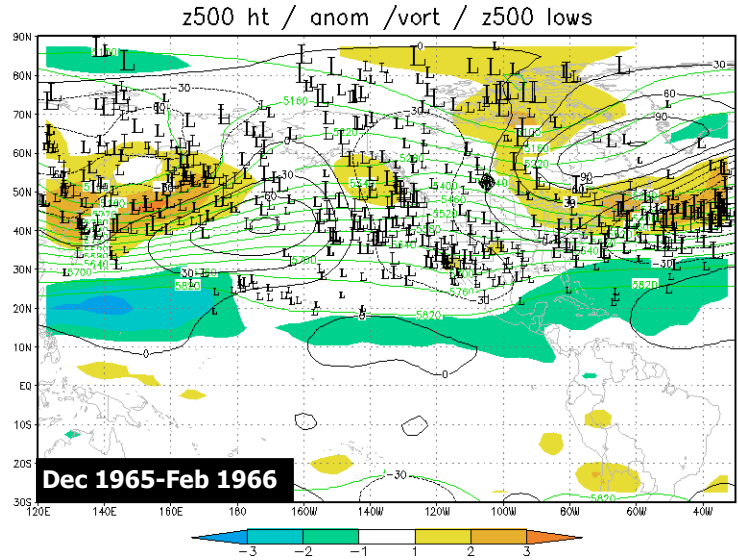


Fig. 5.8: As in Fig. 5.5 but for warm TP SSTA event in 1965-66.

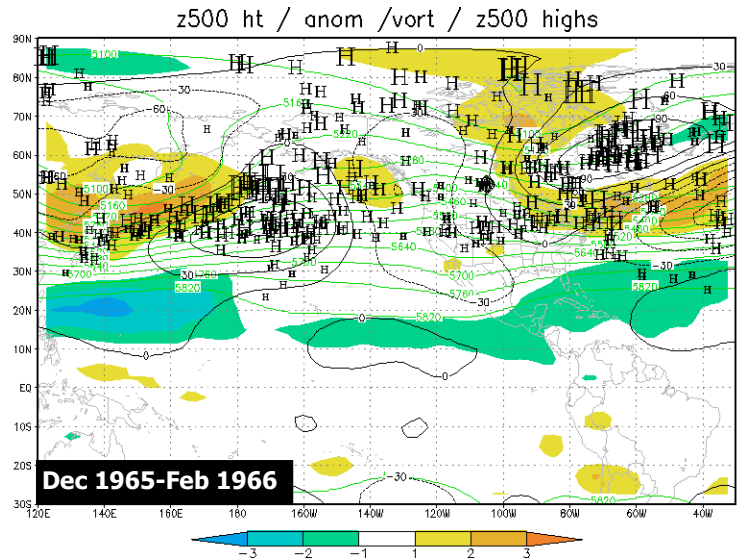


Fig. 5.9: As in Fig. 5.8 but for positive 500mb height anomaly centers plotted with an “H”.

The abnormally high 500mb geopotential heights in the north Pacific during 1972-73 were linked to a strong positive AO phase during early December 1972. The strong positive AO phase is associated with high pressure (and high geopotential heights) in the northern Pacific Ocean around 180° longitude and, for much of early December 1972, very strong geopotential height anomalies spanned the north Pacific in the center of

influence of the AO (Fig. 5.10). However, even with this AO-induced forcing, the local Hadley circulation was enhanced (not shown), as the near equatorial SSTs from 165°W-140°W were well above 28°C in December 1972 (Fig. 5.7b). Just north of the associated zonal wind anomalies, cut-off lows formed on December 1 and December 11, 1972 (Fig. 5.10). Consequently, both the tropical SST-based (negative height anomalies from 30-40°N) and AO-based (positive height anomalies north of 40°N) atmospheric responses were occurring in early December, with the AO displacing the tropical SST-based response farther south than it otherwise would have been. However, once the AO-based north Pacific ridge dissipated in mid-December 1972, a geopotential height pattern that formed was more similar to that for the warm TP SSTA event composite (Fig. 5.11). This atmospheric pattern continued until February 1973, when the negative geopotential height anomaly center shifted farther east (Fig. 5.12) as equatorial SSTs rapidly dropped, with the monthly average for February 1973 being very near the 28°C threshold (Fig. 5.7b). The AO also returned to a positive phase (Feb 1973 AO index ~ +0.8), further contributing to the deviation of the overall atmospheric pattern in the north Pacific from that of the warm SSTA event composite. As a result, the deviation of the large-scale atmospheric flow during December-February 1972-73 from that in the warm TP SSTA composites can be explained by the existence of a positive phase of the AO.

Although the AO or NAO were not in an extreme phase during the 1992-1993 warm SSTA event, the weak 500mb geopotential height response can be explained by the overall magnitude of the TP SSTs. Fig. 5.7b shows that the SSTs during 1992-93 were the lowest of all the eight key SSTA events examined in this Chapter (Table 5.1). Although the SSTs were warmer than normal west of 160°W, climatologically they usually are above 28°C in this region anyway (Fig. 5.1b). Consequently, the convective forcing in the TP did not expand to the east as in the other warm TP SSTA events. The average December-February 1992-93 500mb geopotential height field exhibited a strong positive anomaly in the northern Pacific Ocean (Fig. 5.13).

In this Section 5.4.3, the observed differences in large-scale atmospheric flow between warm TP SSTA events have been examined and associated with other atmospheric modes where possible. These large-scale flow differences can be used to

explain the observed deviations of North American precipitation and temperature patterns from the composite precipitation patterns described by MRL98 and the temperature extreme patterns discussed in Chapter 3. In the next section, the characteristics of North American temperature and precipitation corresponding to each of the key themes in Table 4.36 will be examined and, where possible, linked to the differences in the large-scale atmospheric patterns.

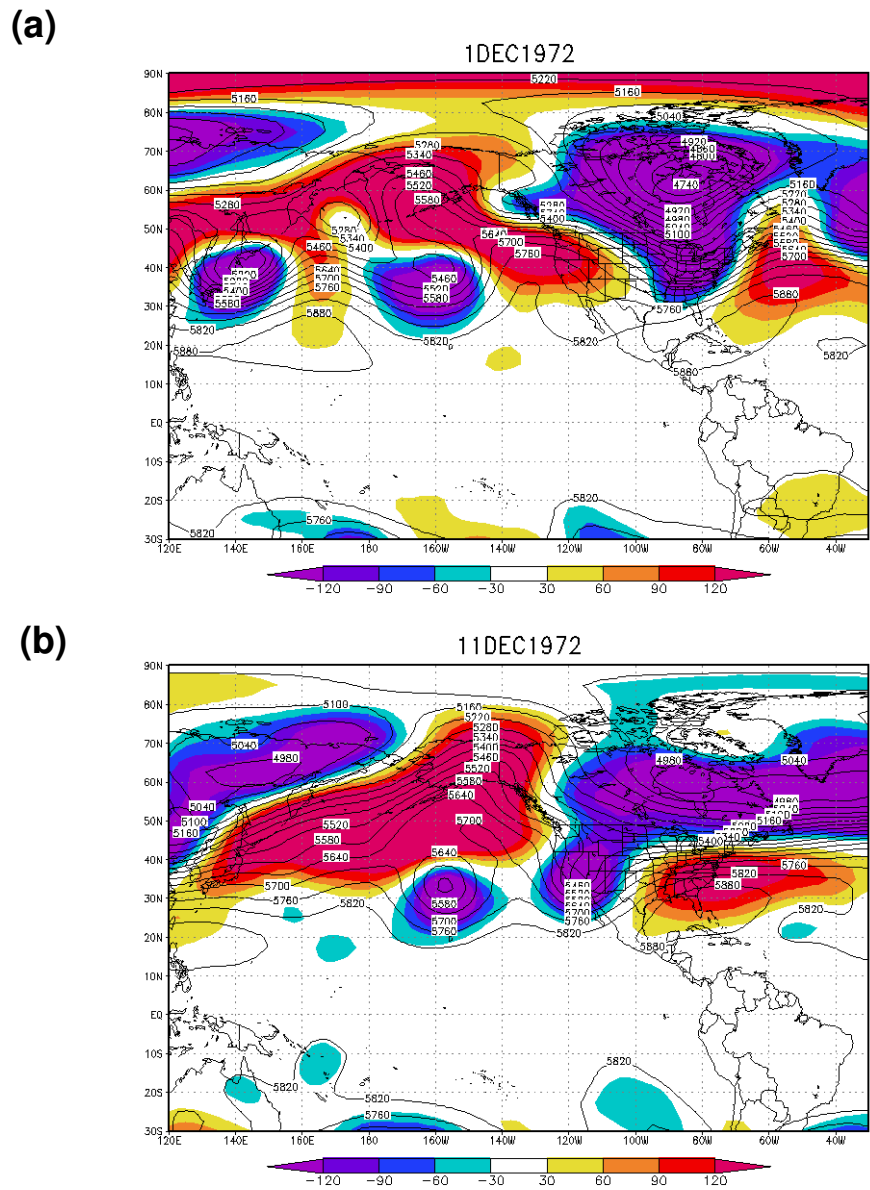


Fig. 5.10: Observed 500mb geopotential height (solid lines) and anomalies (shading) in geopotential meters for (a) 1 December 1972 and (b) 11 December 1972. Shading is given by indicated legend.

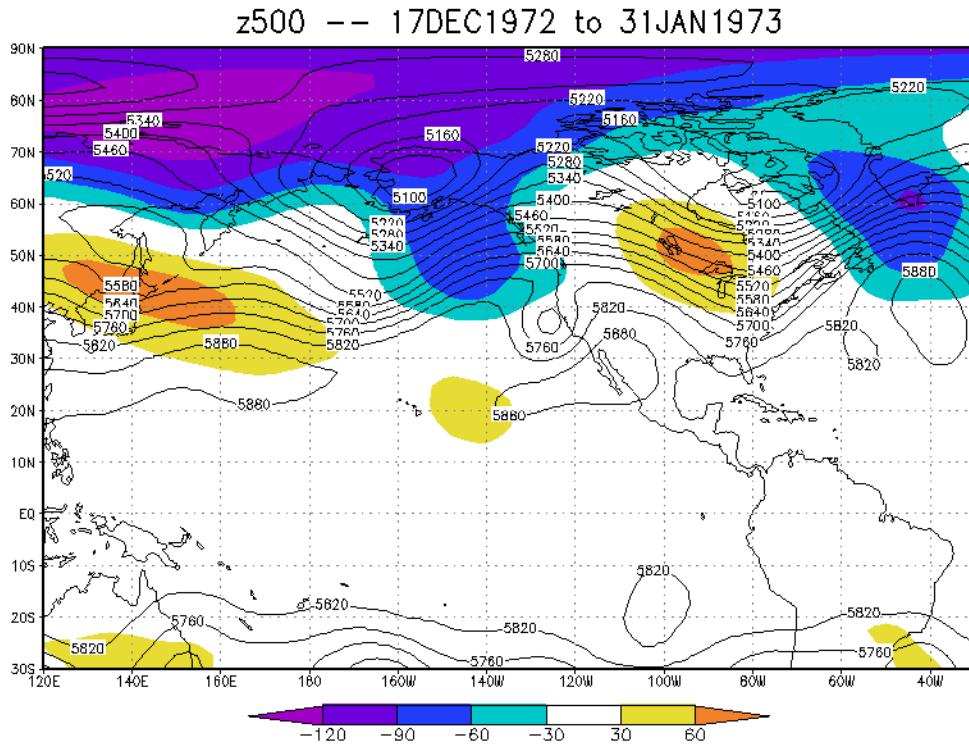


Fig. 5.11: As in Fig. 5.10 but for average from 17 December 1972 to 31 January 1973.

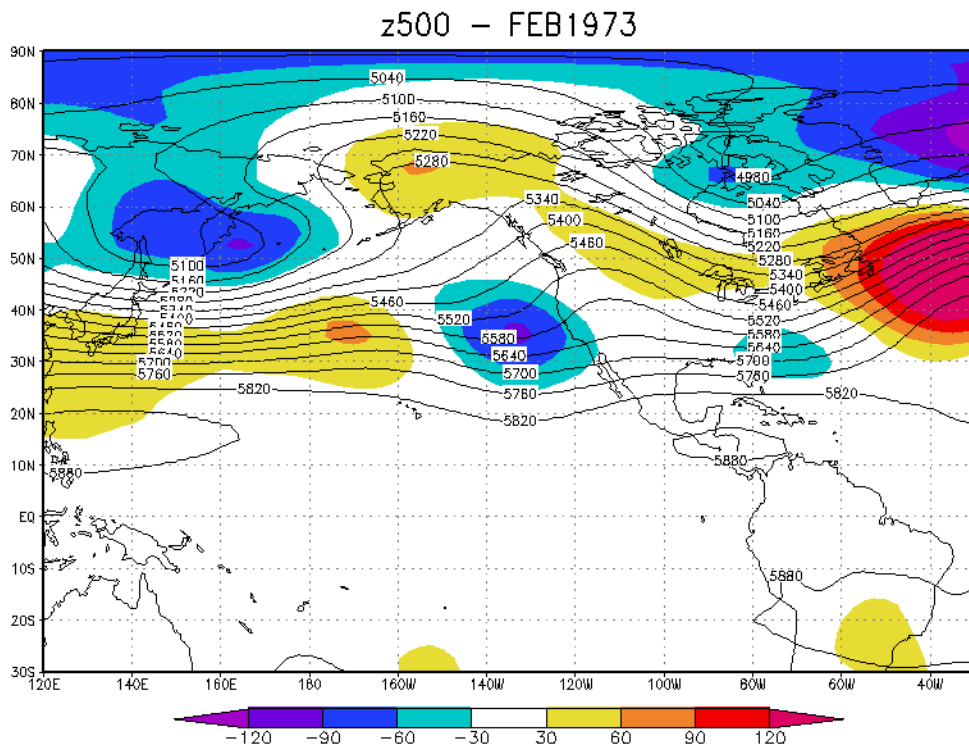


Fig. 5.12: As in Fig. 5.10 but for average from 1-28 February 1973.

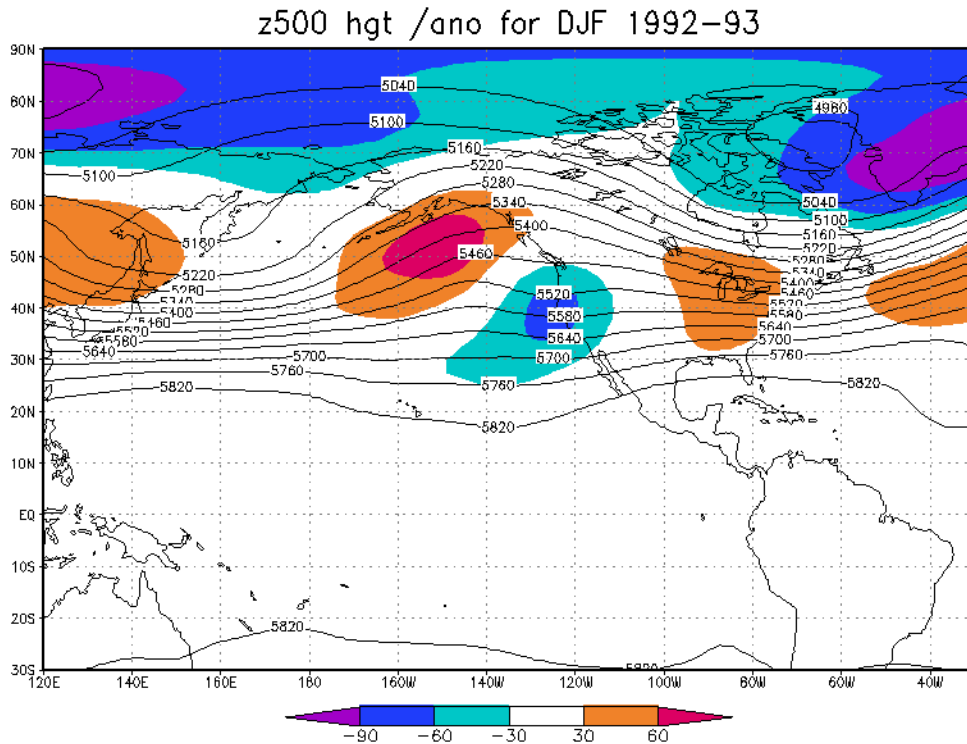


Fig. 5.13: As in Fig. 5.10 but for average from 1 December 1992 to 28 February 1993.

### 5.5 Characteristics of Anomalous North America Weather Associated with Warm Tropical Pacific SSTA Events

In this section, the temporal precipitation and temperature characteristics of key North American target regions are described and related to the observed larger-scale atmospheric patterns described in Section 5.4. The target regions in this analysis were obtained by summarizing the characteristics of the monthly anomaly fields outlined in Chapter 3, and are given in Table 4.36. For each of these fields, the frequency of “runs” of precipitation and temperature anomalies are examined, along with their antecedent atmospheric conditions. When possible, connections will also be made with the daily event distribution characteristics of the region as outlined in Chapter 4.

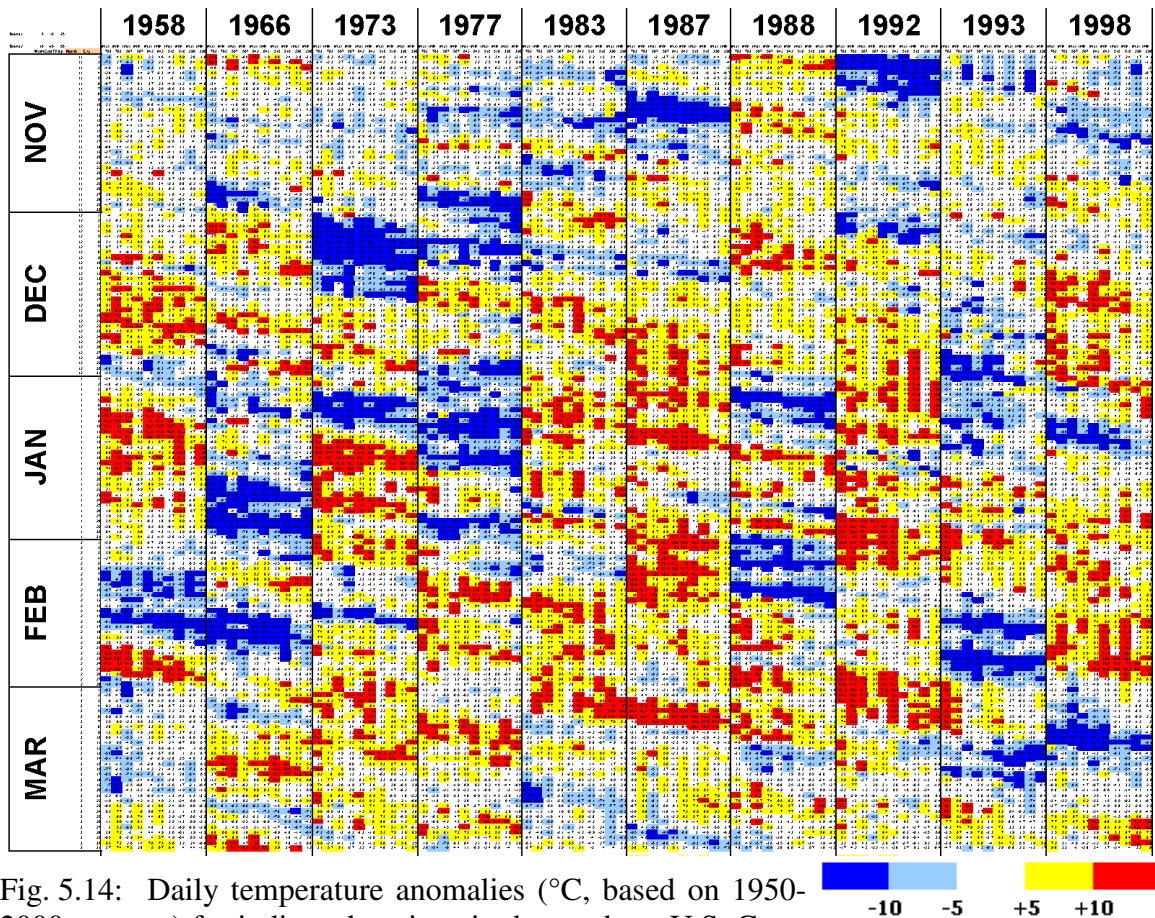
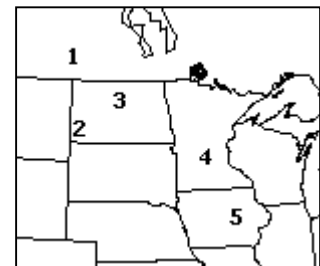


Fig. 5.14: Daily temperature anomalies ( $^{\circ}\text{C}$ , based on 1950-2000 average) for indicated stations in the northern U.S. Great Plains. Each row in the table corresponds to one day from November through March. Order of stations in column is Station 1 Tmax, Station 1 Tmin, Station 2 Tmax, Station 2 Tmin, etc., with station numbers according to number in inset map. Data are presented for November-March periods for warm SSTA events in Table 5.1 plus two other events (1976-77 and 1987-88) for comparison. Year indicated in column headings corresponds to January-March. Temperature ( $^{\circ}\text{C}$ ) shading is according to given legend.



### 5.5.1 Northern U.S. Great Plains and Southern Canadian Prairies – Warm and Dry (November-February)

The generally warm and dry conditions observed from November through February during warm TP SSTA events in the northern U.S. Great Plains and southern Canadian Prairies were linked to persistent warm temperature anomalies and the lack of notable cold outbreaks. Fig. 5.14 shows that during many of the warm SSTA VPC1

events, stations in the northern U.S. Great Plains (embedded within the positive composite anomaly coherency in Fig. 3.6a,c,e) observed extended periods (lasting nearly a month at times) of strong positive temperature anomalies with relatively few extensive cold periods. This was especially true during 1957-58, 1982-83, 1986-87, 1991-92, and 1997-98. During the 1965-66, 1976-77, and 1992-93 events (all of which were listed in Section 3.4.4.2 as being exceptions to the generally warm conditions), extensive cold periods were present in the region from December through February. No such cold periods occurred during the aforementioned warm northern U.S. Plains winters. These associations also are consistent with the findings in Section 4.4.1.1 that the warm surface temperature association was linked to an increase in the frequency (relative to those with neutral SSTAs) of days with very warm temperatures and decrease in frequency of days with colder than normal temperatures.

The positive daily maximum temperature TAPs that contributed to the positive composite temperature anomalies for the northern U.S. Great Plains during warm TP SSTA events had a particularly long duration. Fig. 5.15 makes two key points in that regard. First, in the northern U.S. Great Plains, positive TAPs of at least 8 days duration were generally more frequent during warm TP SSTA events than in all other years. By integrating the area under the TAP length curve, it was found that there were on average more than 32 December-February days during warm TP SSTA events that were part of at least an 8-day long TAP, compared to 12 such days during all other years. Further, the frequency of TAPs of at least 8 days in duration was higher than the frequency of warm SSTA events. (If warm TP SSTAs were not indicative of TAP duration, this frequency would equal the frequency of warm SSTA events.) Second, Fig. 5.15 shows that TAPs with duration of 19 days or longer *almost exclusively* occurred during warm SSTA events. During eight warm TP SSTA events, there were 6 TAPs of at least 19 days in duration. During the other 44 years, there was only one (24 days in duration, 1/6/1990 through 1/29/1990). Consequently, in the presence of warm SSTAs, long stretches of warmer than normal conditions in the northern Plains were frequently observed.

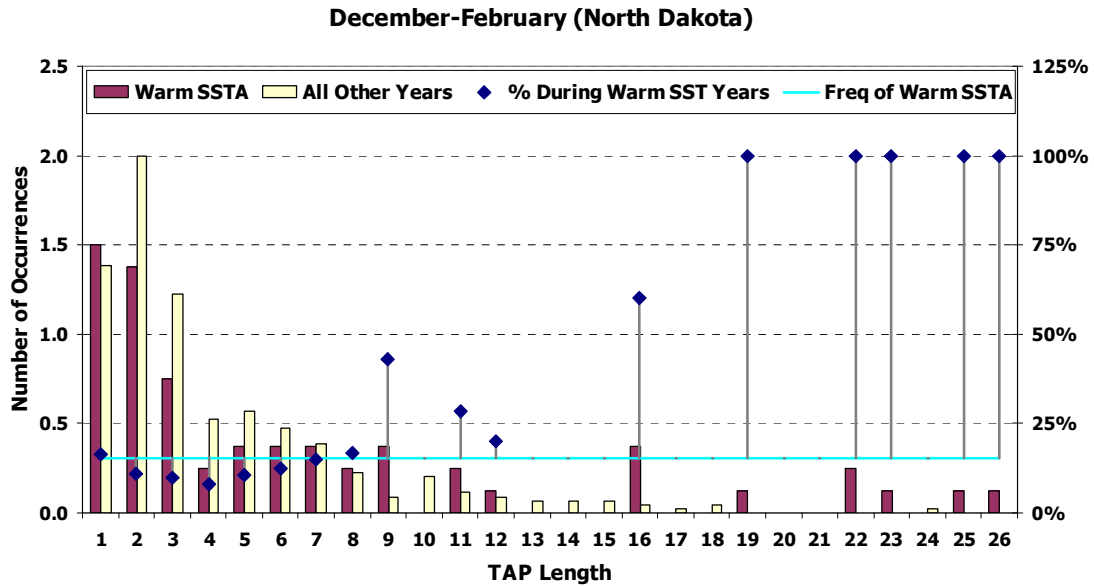


Fig. 5.15: Analysis of length of positive TAPs for average daily maximum temperatures in the North Dakota region (as delineated in Table 4.21) during December-February. A positive TAP is a period with consecutive daily maximum temperature anomalies (based on 1950-2000 average) of at least 3°C. Histogram bars: Average frequency (left axis) of positive TAPs with the duration indicated on abscissa during the warm SSTA events in Table 5.1 (dark bars) and all other years (lighter bars). Plotted diamonds: Percentage of time (right axis) that a TAP of that duration occurred during warm SSTA events. (For example, 100% = All TAPs with that length occurred during a warm TP SSTA event.) Solid thin line: Percentage (right axis) of years that are warm TP SSTA events (8 events divided by 52 periods = 18%).

Combining the large-scale atmospheric patterns described in Section 5.4 with the time evolution composites (TECs) for the TAPs described above suggests that the occurrence of persistent warm periods were associated with the deflection of the northern storm track even farther north. The positive anomalies in the 500mb geopotential height composite over central North America (Fig. 5.3a) indicate a weaker than normal trough there, geographically coincident with the positive composite anomalies of monthly average daily maximum/minimum temperature in Fig. 3.6. Further, Day(0) of the TEC (Fig. 5.16a) indicates strong negative geopotential height anomalies in the north Pacific at the beginning of long stretches of anomalously warm periods in North Dakota. Ahead of these negative anomalies on Day (0), positive 500mb geopotential height anomalies were located in northwestern North America (Fig. 5.16a). These findings suggest that positive

height anomalies occurred downstream of the intensified low in the north Pacific induced by the cyclonic shear from the advection of earth vorticity into the mid-latitudes by the enhanced local Hadley circulation. This is consistent with both the indication of positive 500mb geopotential height anomalies around 45-55°N east of 130°W during two of these warm SSTA events (1957-58 and 1982-83; Fig. 5.6a-b) and the positive composite anomalies of monthly average daily maximum and minimum temperatures in the northern U.S. Great Plains (Fig. 3.6). This unusually strong ridging deflected storm systems traversing western North America farther north than normal. Lower than normal precipitation in south-central Canada and the northern U.S. Great Plains also was observed due to a reduced frequency of active storm systems, consistent with the composite precipitation anomalies indicated by MRL98.

Fig. 5.16 further indicates an east Asian origin of the negative geopotential height anomalies in the north Pacific and the warmer than normal temperatures in the northern U.S. Great Plains during warm TP SSTA events. The negative anomaly center in the north Pacific is linked to negative 500mb geopotential height anomalies propagating from Asia on Day (-8) of the positive TAP for the North Dakota region (Fig. 5.16e). These negative geopotential height anomaly coherencies then increased in magnitude on Day (-6) and Day (-4) as they moved into the region north of the advection of earth's vorticity into mid-latitudes (Fig. 5.16c-d). The intensification of this trough then led to the positive geopotential height anomalies in northwestern North America, which began forming on Day (-4) and continued to strengthen until Day (0) (Fig. 5.16a-c). This atmospheric flow would allow vorticity impulses to be deflected to the north over the ridge, in a manner consistent with Hoskins and Karoly (1981) who showed that wavetrains from a source near 30°N (the latitude reached by the wave moving off Asia by Day -6 to Day -4, as shown in Fig. 5.16c-d) propagate along Great Circle routes. Consequently, the TEC for North Dakota suggests that the origins of the ridge associated with warmer than normal temperatures in the northern U.S. Great Plains were located in eastern Asia eight days before the warm temperatures began.

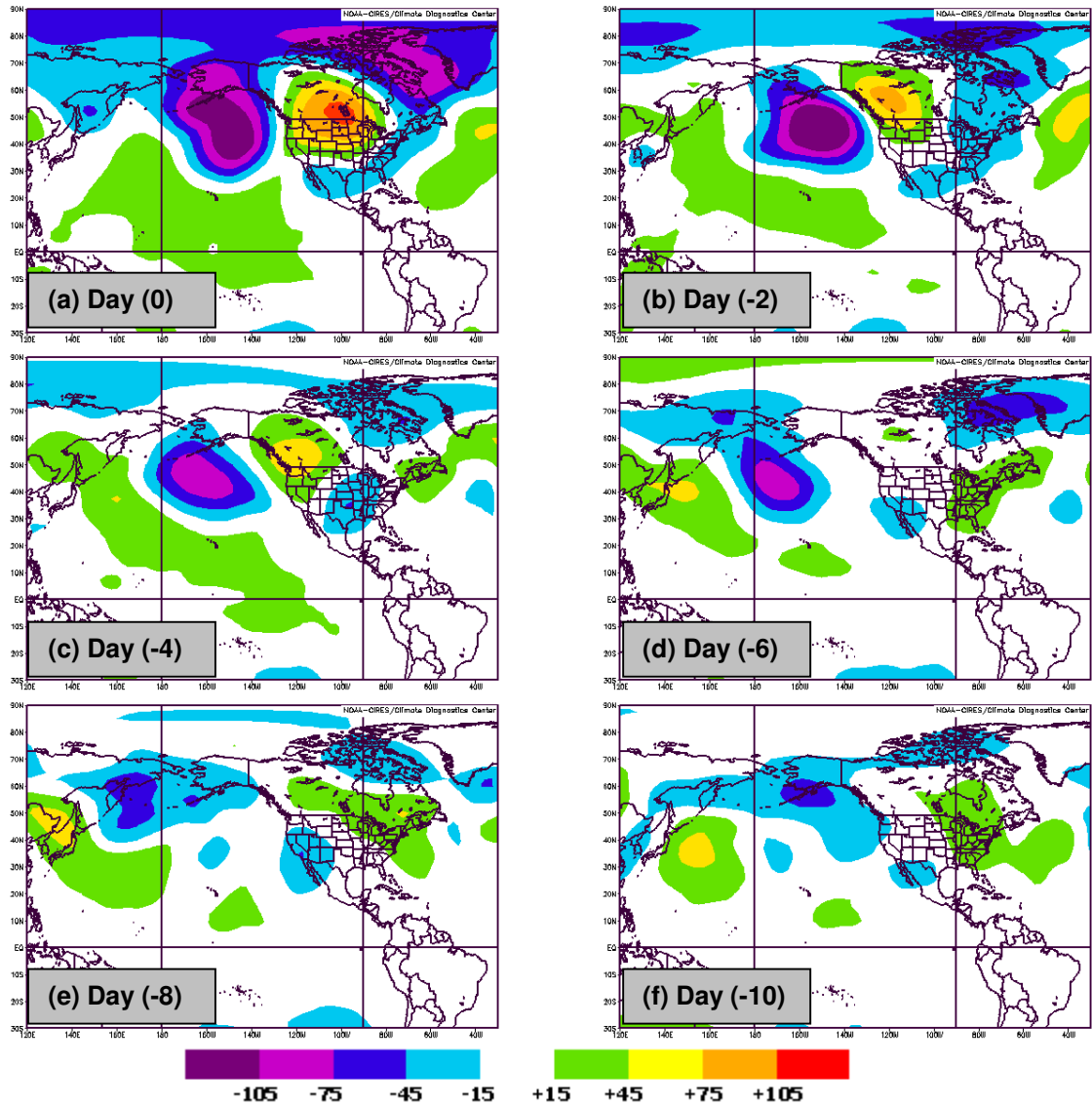


Fig. 5.16: Time evolution composites (TECs) (as defined in Section 5.3.3) of 500mb geopotential height anomalies (gpm) for days preceding onset of warm temperatures in North Dakota (as delineated in Table 4.21) during December-February of warm TP SSTA composite. TECs correspond to (a) Day (0), the day that the target anomaly period (TAP) began, (b) Day (-2), two days before TAP beginning, (c) Day (-4), (d) Day (-6), (e) Day (-8), and (f) Day (-10).

The end of the positive TAP in North Dakota was linked to troughs moving into the northwestern Pacific Ocean on Day (-6) from the end of the TAP, dissipating the anomalously strong Aleutian Low and enabling the ridge over northwestern North America to progress eastward. Fig. 5.17d shows a weak anomalous trough moving off

the Asian continent on Day (-6), intensifying by Day (-4) (Fig. 5.17c), and then leading to a breakup of the strong Aleutian low on Day (-2) (Fig. 5.17b), resulting in a much weakened Aleutian low by Day (0) and the end of the warmer than normal temperatures, with the ridge then moving farther to the east (Fig. 5.17a).

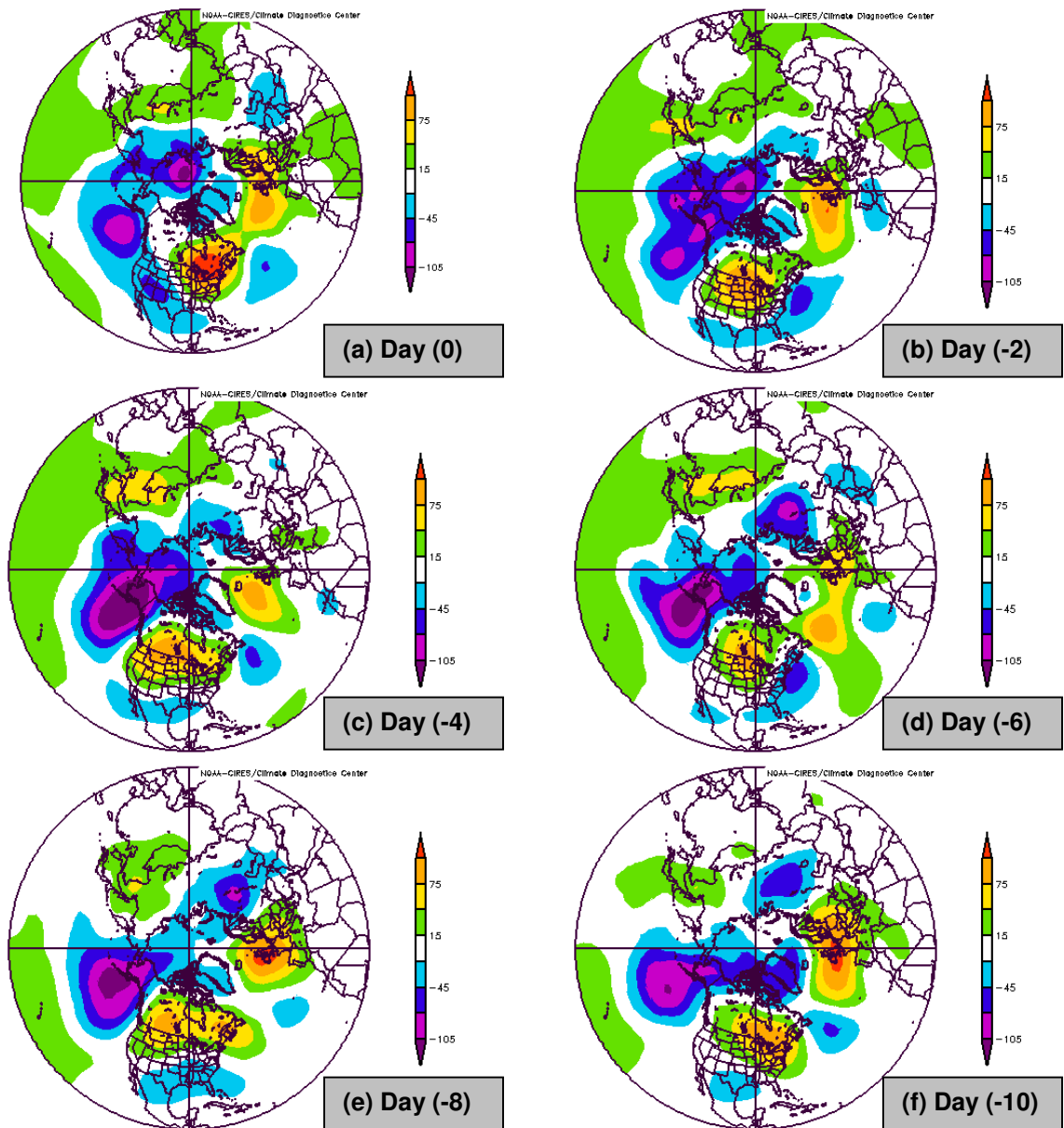


Fig. 5.17: As in Fig. 5.16 but where Day (0) corresponds to the end of the Target Anomaly Period (TAP).

The warm TP SSTA events in Table 5.1 that previously were categorized as exceptions to the warm temperature association in the southern Canadian Prairies/northern U.S. Great Plains (1965-66, 1992-93; Table 4.35) were characterized by more frequent periods of persistent cold temperatures and increased extratropical cyclone activity in the western U.S. Fig. 5.14 shows that the northern U.S. Great Plains observed periods of colder than normal temperatures in December-February 1965-66 and December-February 1992-93, with periods of generally warmer than normal temperatures in the other years in Table 5.1. During the warm TP SSTA events with warmer than normal temperatures in the northern U.S. Great Plains, there was relatively little cyclone activity in the western U.S. (Fig. 5.18). However, in the exception years cited above (1965-66 and 1992-93), there was more cyclone activity in the western U.S., especially in 1992-93 (Fig. 5.19). This increased cyclone activity in the western U.S. is consistent with the large-scale process described in Section 5.4.3 during these two exception years. In 1965-66, the low geopotential height anomalies did not enable a strong ridge to develop over western North America and prevent extratropical cyclones from moving into the western U.S. In 1992-93, the lack of SSTs above 28°C in the equatorial region from 165-140°W did not support negative geopotential height anomalies in the north-central Pacific and positive anomalies in western North America, which enabled extratropical cyclones to track across the western U.S.

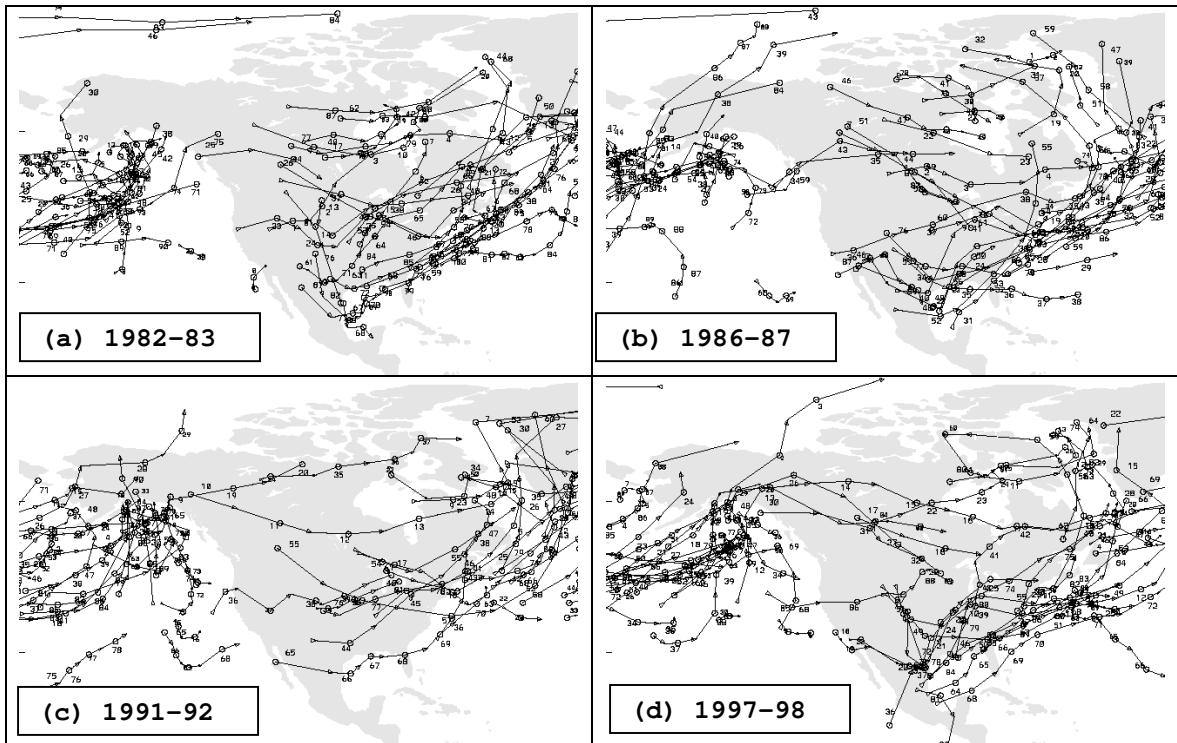


Fig. 5.18: Tracks of extratropical cyclones (in SLP) during December-February for selected warm eastern TP SSTA events as recorded in the NASA Atlas of Extratropical Storm Tracks (NASA 2005). Tracks given for December-February of (a) 1982-83, (b) 1986-87, (c) 1991-92, and (d) 1997-98. Small numbers represent the day of the season that particular cyclone was observed.

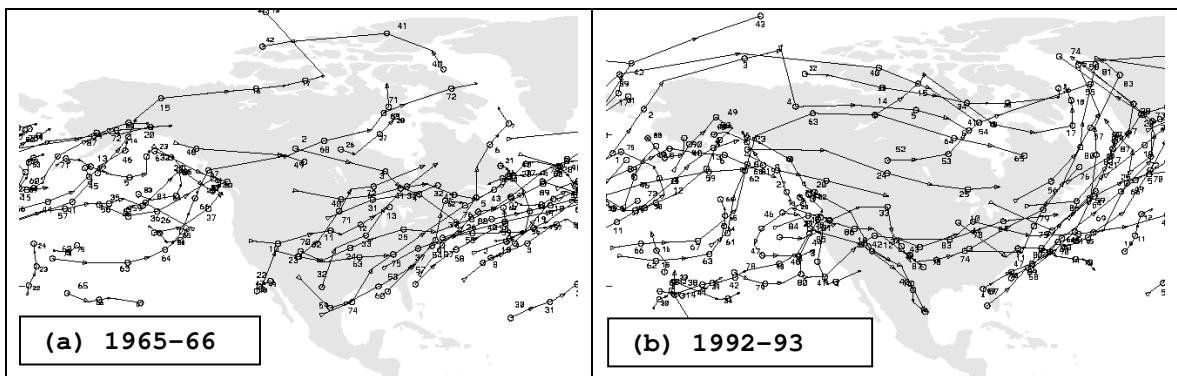


Fig. 5.19: As in Fig. 5.18 but for (a) 1965-66 and (b) 1992-93.

### 5.5.2 Dry Eastern Midwest and Wet-Cool South (January-March)

For the observation of dry conditions in the eastern Midwest (Section 4.3.1.3) and wet/cold conditions in the southern U.S. (Sections 4.3.1.1 and 4.4.1.1), the temporal structure of the surface climate anomalies suggests that the precipitation relations tended to arise from persistent anomaly periods, but the temperature association did not exhibit a similar structure. Fig. 5.20 (Fig. 5.21) shows that for the wet (dry) association over Georgia (eastern Midwest), the frequency of the associated TAPs lasting at least 3 days was higher than the frequency of warm SSTA event occurrence. This included one extensive period of 13 days where no station in the target Midwest region received any rainfall, and a period of this duration only occurred in the presence of warm SSTAs. But for the temperature association in Georgia-Alabama, the typical length of the TAPs was not consistently outside the range of what would be expected due to the frequency of warm SSTA events (Fig. 5.22).

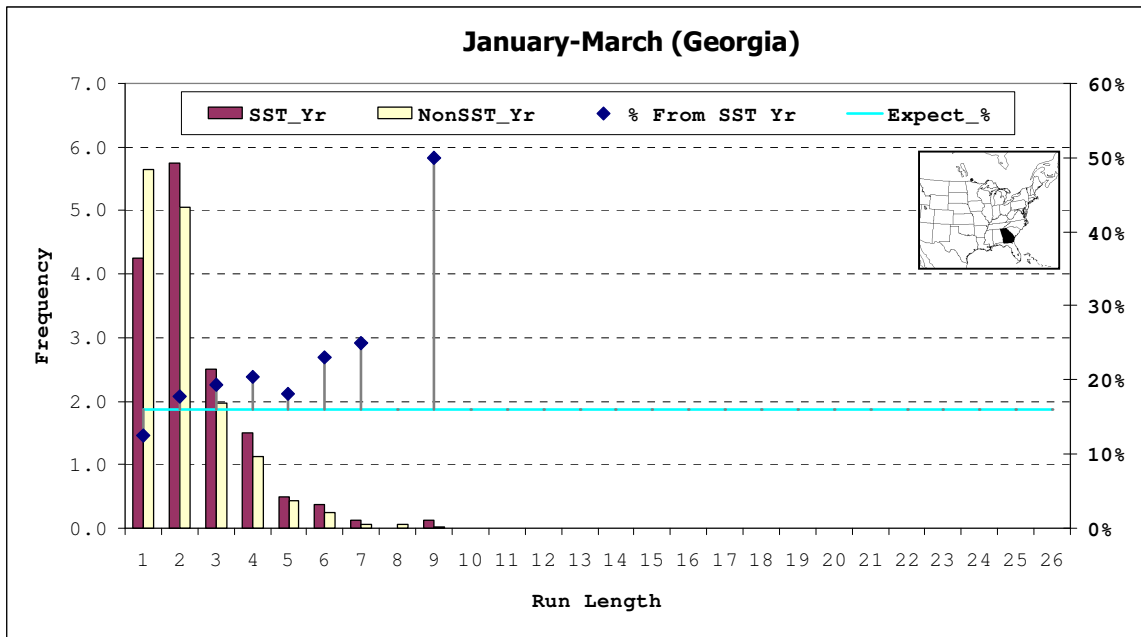


Fig. 5.20: As in Fig. 5.15, but for length of wet events over all stations in Georgia (delineated in inset map, upper right) during January-March. A wet event was defined as at least one day with at least 1 mm of precipitation.

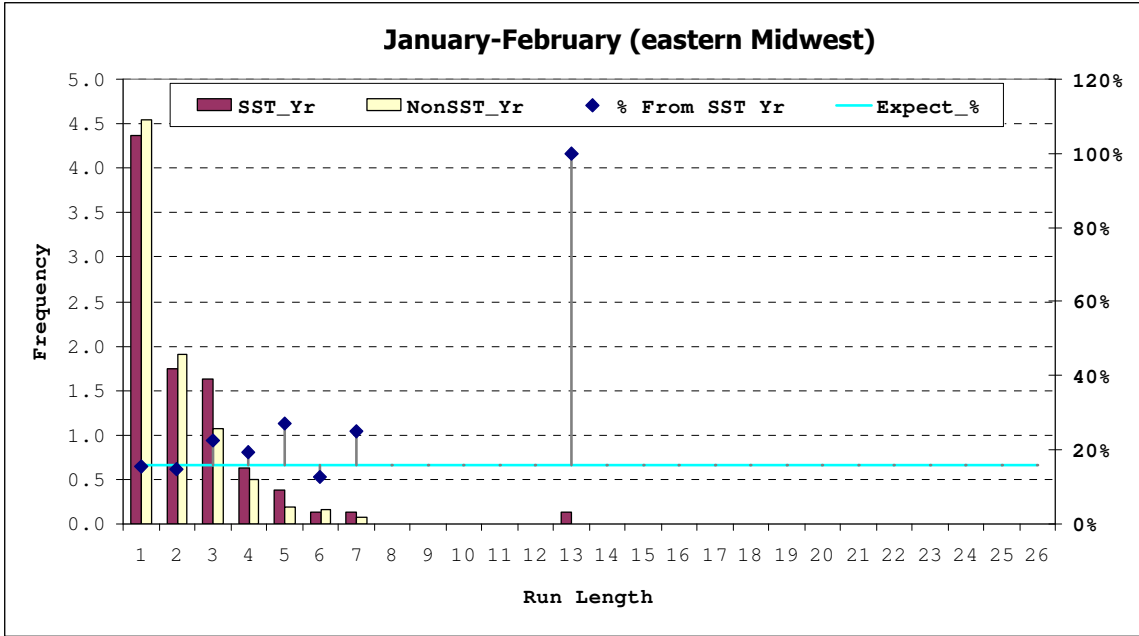


Fig. 5.21: As in Fig. 5.20, but for periods of zero precipitation for stations in the eastern Midwest (as delineated in Table 4.10) during January-February.

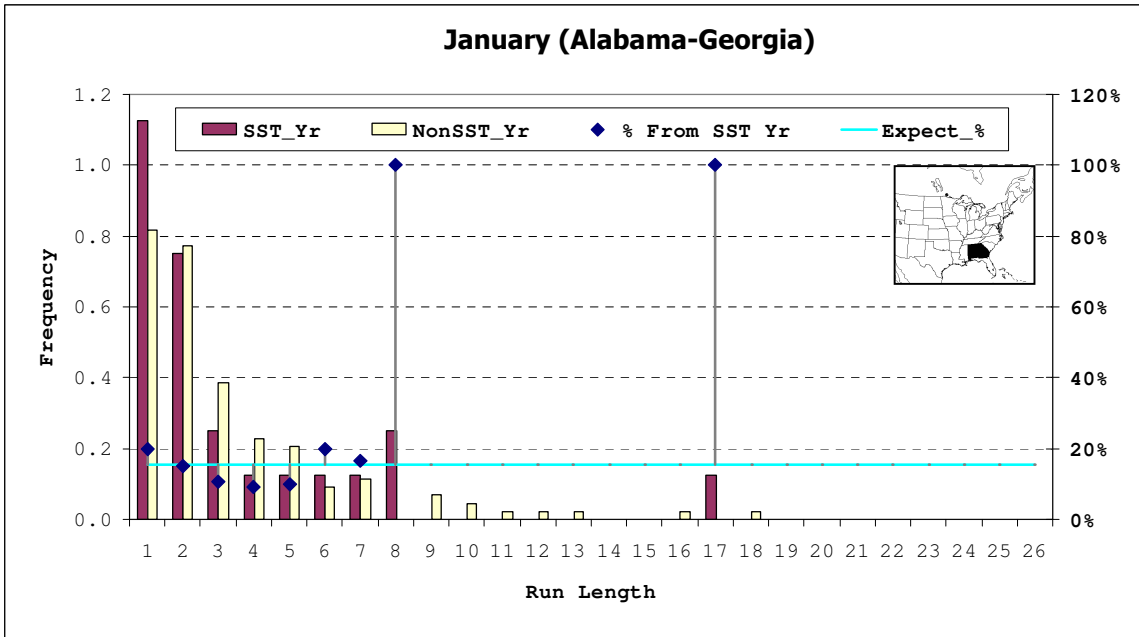


Fig. 5.22: As in Fig. 5.15, but for maximum temperature averaged over all stations in Alabama-Georgia (delineated in inset map, upper right) during January.

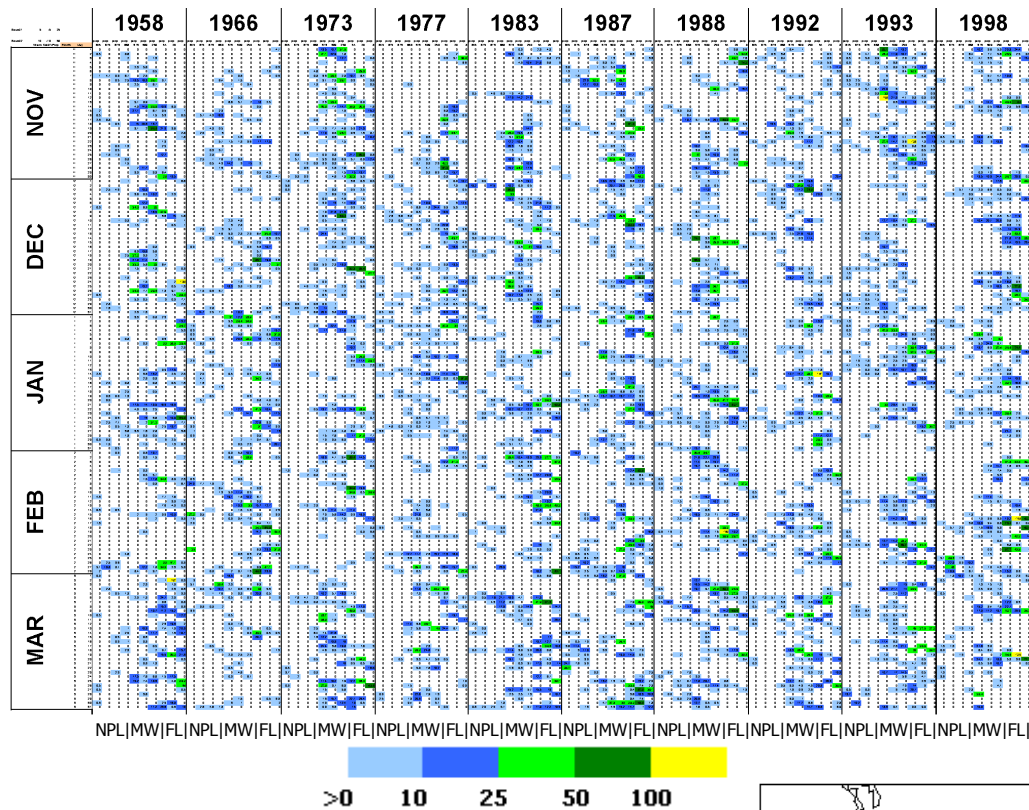


Fig. 5.23: As in Fig. 5.14, but for daily precipitation totals (mm) from November through March observed at stations from the northern U.S. Plains to Florida. Inset map gives order of stations within each SSTA event column. Small letters at foot of column further indexes stations as Northern Plains (“NPL”, Columns 1-4), Midwest (“M”, Columns 5-7), and Florida (“FL”, Columns 8-10). Year indicated in column headings corresponds to January-March. Precipitation shading (mm) is according to given legend.

The dry eastern Midwest and wet/cold southern U.S. associations are associated with a more active southern storm track in the U.S. during warm SSTA events. Fig. 5.23 shows that especially during January-March, there were several periods where the eastern Midwest observed only light precipitation while the southeast U.S. experienced frequent precipitation events, with a notable amount of heavy events. This is consistent with an active southern storm track and was observed in nearly all warm SSTA events, as shown in Section 4.3.1.1. Further, Fig. 5.24 (Fig. 5.25) shows that in the days preceding precipitation in Georgia (southeast Texas), an anomalous low established over southern

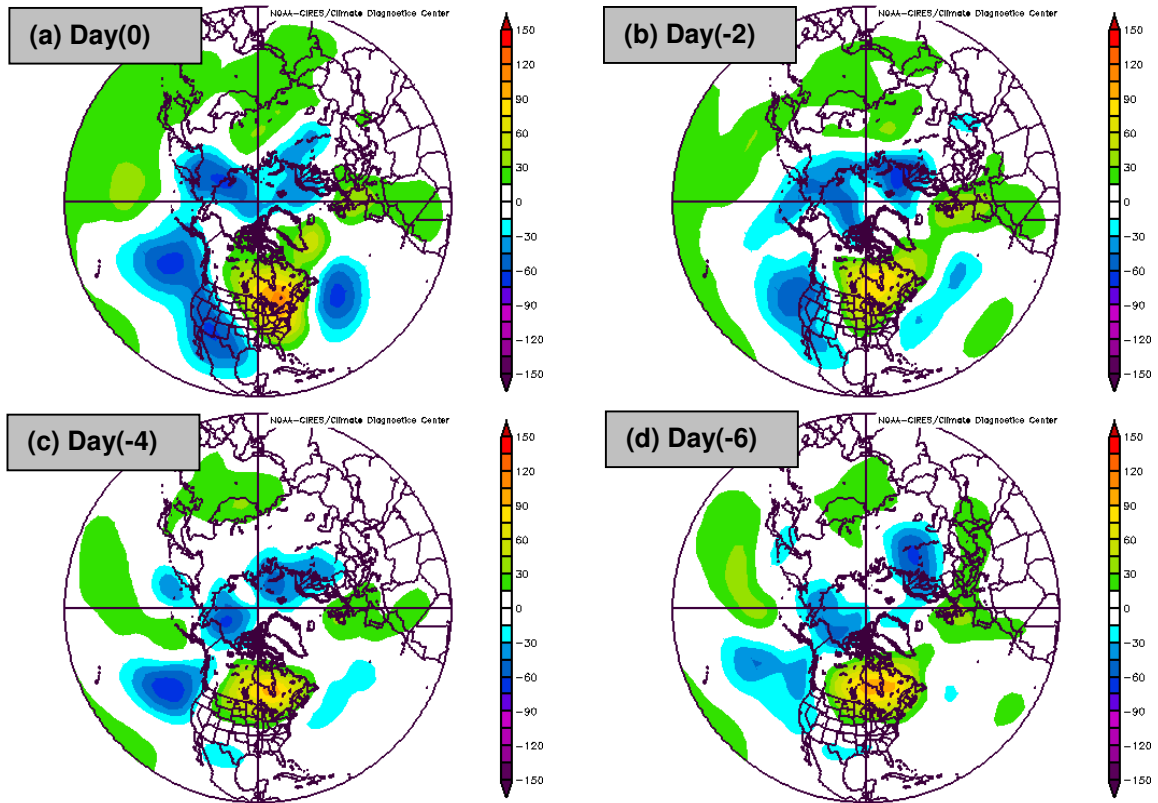


Fig. 5.24: As in Fig. 5.16 but for precipitation in Georgia (inset map in Fig. 5.20) for January-February-March.

California-Arizona and northern Mexico, providing a vorticity source for the formation of low-pressure systems to track across the southern U.S. as anomalous high pressure over the Great Lakes moves east. The establishment of an anomalous low over the southwestern U.S. is consistent with the broad indications of Hoskins and Karoly (1981), who show that a wavetrain emanating from an upper level vorticity source at 30°N (which in the present case formed just north of the anomalous upper-tropospheric wind anomalies in the central Pacific as shown in Fig. 5.2) can become trapped and propagate into the southwestern U.S.

The wet relationship in the south also is consistent with the cold temperature association. Increased precipitation often is associated with more cloudiness, keeping daytime maximum temperatures low. The higher amounts of moisture results in more net surface radiation being used to evaporate water instead of warming the atmosphere through sensible heat transfer. However, the increased moisture counterbalanced this

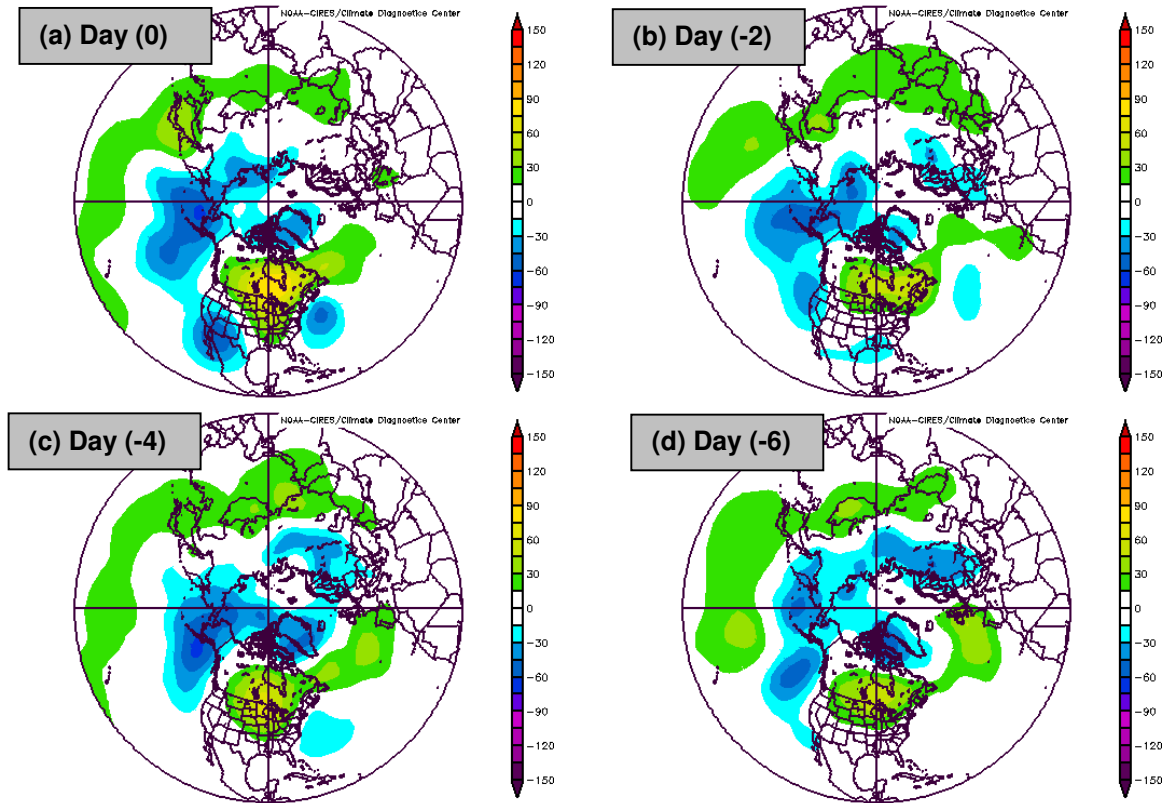


Fig. 5.25: As in Fig. 5.16 but for precipitation in southeast Texas (see inset map #6 in Fig. 3.6) for November- February.

effect in minimum temperatures, as dewpoints would have been higher. Collectively, these relationships can also help explain why the surface temperature composites of Fig. 3.6(c-d) for January show more significant maximum temperature anomalies than minimum temperature anomalies.

### 5.5.3 Warm Eastern U.S. (December)

The positive December temperature anomalies in the eastern U.S. (Section 3.4.2.1) were associated with periods of warmer than normal temperatures with a shorter duration than for the northern U.S. Great Plains. For example, Fig. 5.26 shows that during the warm TP SSTA events in Table 5.1, Pennsylvania observed continuous periods of warmer than normal temperatures, the positive anomaly in monthly average daily maximum and minimum temperatures lasting anywhere from two days to around a week. The duration of these periods is shorter than the durations of up to two weeks

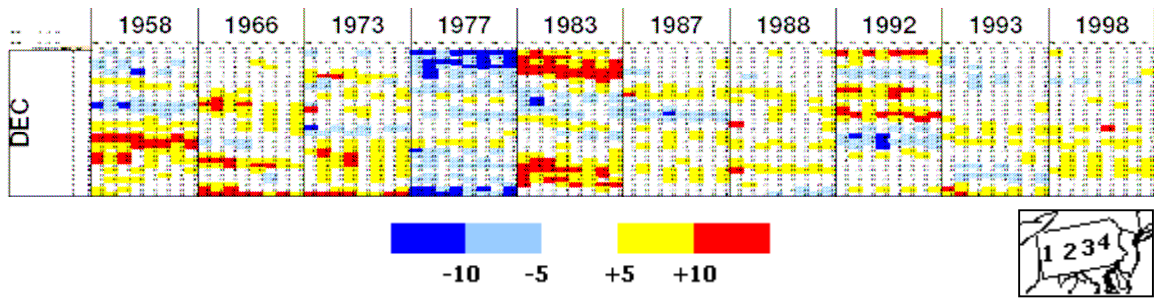


Fig. 5.26: As in Fig. 5.14 but for December daily maximum and minimum temperatures ( $^{\circ}\text{C}$ ) for stations in Pennsylvania indicated in inset map. Order of stations in column is Station 1 Tmax, Station 1 Tmin, Station 2 Tmax, Station 2 Tmin, etc. Column heading corresponds to year of following January (in order to facilitate comparison to Fig. 5.14).

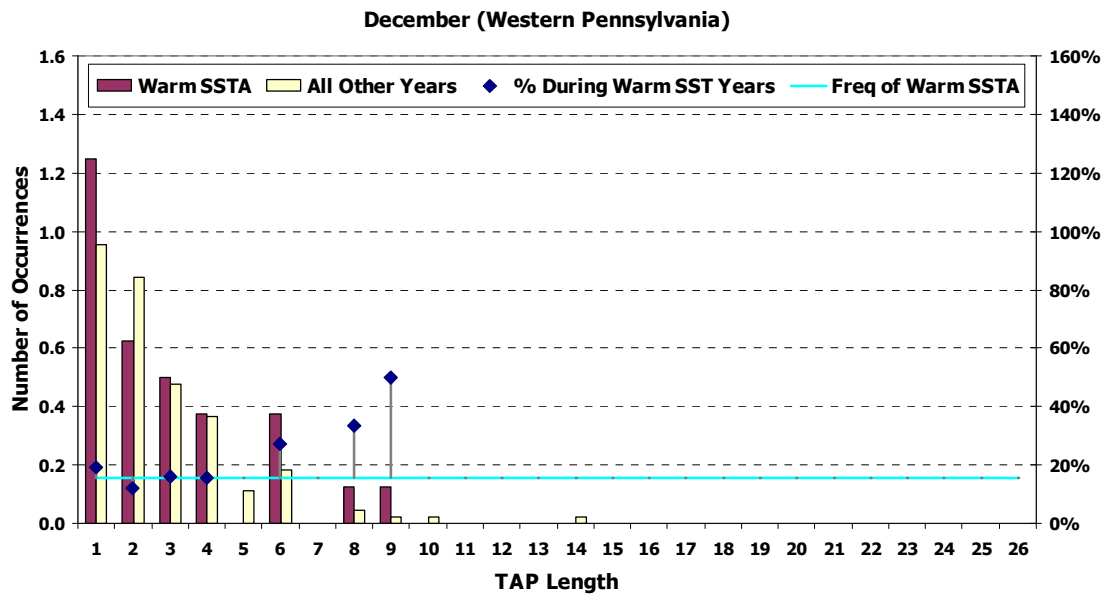


Fig. 5.27: As in Fig. 5.15 but for positive TAPs in western Pennsylvania region as delineated in Table 4.22.

observed in the northern U.S. Great Plains (Fig. 5.14). Warm TP SSTA years with particularly strong periods of warmer than normal December temperatures in Pennsylvania included 1957 and 1982.

Analysis of the TAPs associated with the warmer than normal temperatures during warm TP SSTA events in the eastern U.S. further supports the indication that warmer than normal temperatures have a maximum duration of around one week. For example, Fig. 5.27 shows that western Pennsylvania TAPs of almost all durations were

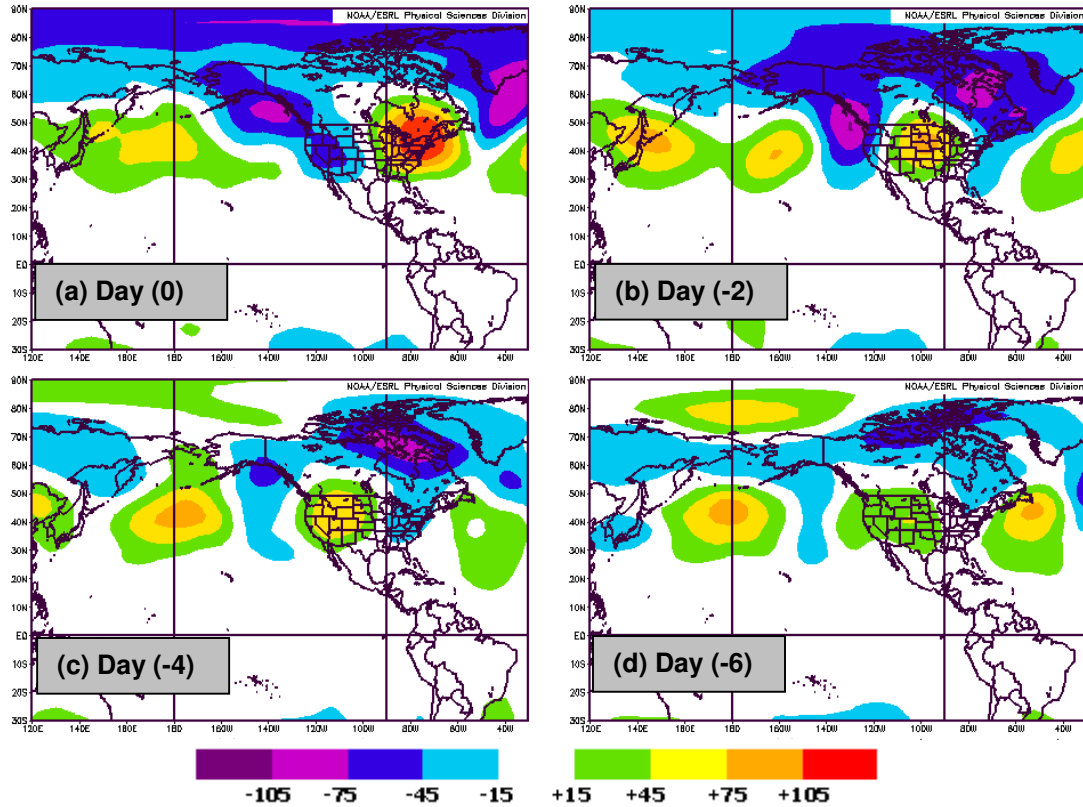


Fig. 5.28: As in Fig. 5.16 but for positive TAPs in western Pennsylvania.

more frequent during warm TP SSTA events than during all other years, but the longest TAP duration was around 9 days, much shorter than the maximum duration of TAPs associated with the northern U.S. Great Plains (Fig. 5.15).

The warmer than normal temperatures in the eastern U.S. have large-scale atmospheric flow origins in western North America. The TECs associated with the positive western Pennsylvania TAPs indicate that on Day (0) of the beginning of warmer than normal temperatures there, strong positive 500mb geopotential height anomalies are located over the northeastern U.S. (Fig. 5.28a). On Day (-2), these anomalies were located in the northern U.S. Great Plains (Fig. 5.28b), while on Day (-4) and Day (-6) they were in the western U.S. (Fig. 5.28c-d). This progression of the anomalies suggests that the same atmospheric pattern that created the warming in the northern U.S. Great Plains (larger ridge in central North America deflecting storm tracks farther to the north) accounts for the warmer than normal eastern U.S. as well.

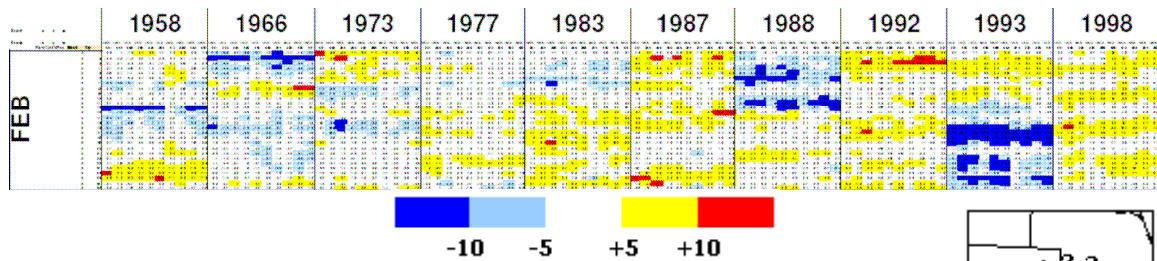


Fig. 5.29: As in Fig. 5.14 but for February daily minimum temperatures ( $^{\circ}\text{C}$ ) for stations in eastern Colorado/western Kansas indicated in inset map. Order of stations in column is Station 1 Tmin, Station 2 Tmin, Station 3 Tmin, etc.

#### 5.5.4 Warm Daily Minimum Temperatures in Central U.S. Plains (February) and Northern/Central Plains to Ohio Valley (March)

The warmer than normal December daily minimum temperature anomalies in the central U.S. Great Plains (Section 3.4.2.1) were associated both with the lack of significant periods of colder than normal temperatures and with periods of warmer than normal daily minimum temperatures of less than about one week in duration. Fig. 5.29 shows that during the warm TP SSTA events in Table 5.1, eastern Colorado/western Kansas observed relatively few periods of notably colder than normal daily minimum temperatures (consistent with Section 4.4.1.1), except for the years previously noted (in Table 4.35) as exception years (1966, 1973, 1993). During these exception years (and in 1977 and 1988, two warm SSTA years not included in Table 5.1 because they didn't match the 3 of 6 month requirement, but are included in Fig. 5.29 to illustrate the duration of periods of colder than normal daily minimum temperatures in this region), periods of colder than normal daily minimum temperatures were observed with durations of about 3-7 days. But during the warm TP SSTA years, these cold periods were not observed, and instead there occurred periods of warmer than normal daily minimum temperatures with durations less than about 7 days. The duration of these warmer periods is shorter than the durations of up to two weeks observed in the northern U.S. Great Plains (Fig. 5.14).

Analysis of the TAPs associated with the colder than normal daily minimum temperatures during warm TP SSTA events in the central U.S. Great Plains further

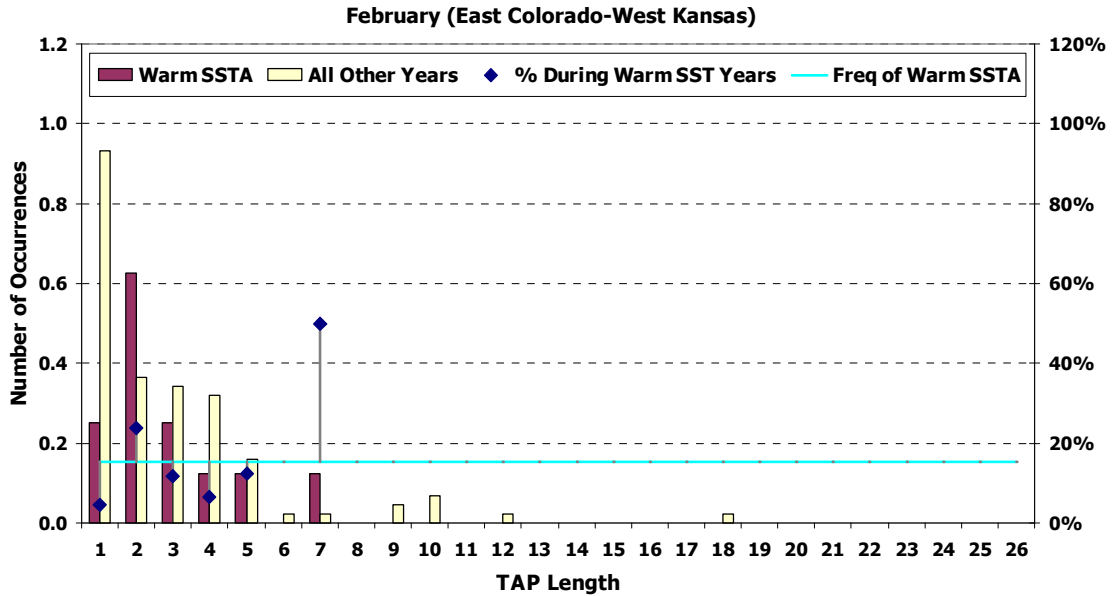


Fig. 5.30: As in Fig. 5.15 but for negative TAPs in eastern Colorado/western Kansas region as delineated in Table 4.29.

supports the indication of fewer periods of colder than normal daily minimum temperatures of all durations. For example, Fig. 5.30 shows that for the eastern Colorado/western Kansas region, TAPs of almost all durations (but especially one day) were less frequent during warm TP SSTA events than during all other years. The frequency of TAPs with duration of 7 days was higher than the frequency of warm TP SSTA years (Fig. 5.30), but this TAP (and the TAP of 5 days in length) was observed during the 1993 exception year (not shown).

The origins of periods of colder than normal daily minimum temperatures in the central U.S. Great Plains during all non-warm TP SSTA event years are linked to positive geopotential height anomalies in the North Pacific Ocean, whereas warm SSTA events are associated with an anomalous trough. This helps explain the lack of extreme cold daily minimum temperatures in the central U.S. Great Plains in February during warm TP SSTA events. The TECs associated with colder than normal February daily minimum temperatures in the central U.S. Great Plains during all years except warm TP SSTA events coincide with negative 500mb height anomalies in the western U.S. and positive 500mb height anomalies in the northern Pacific Ocean on Day (0) (Fig. 5.31a). This

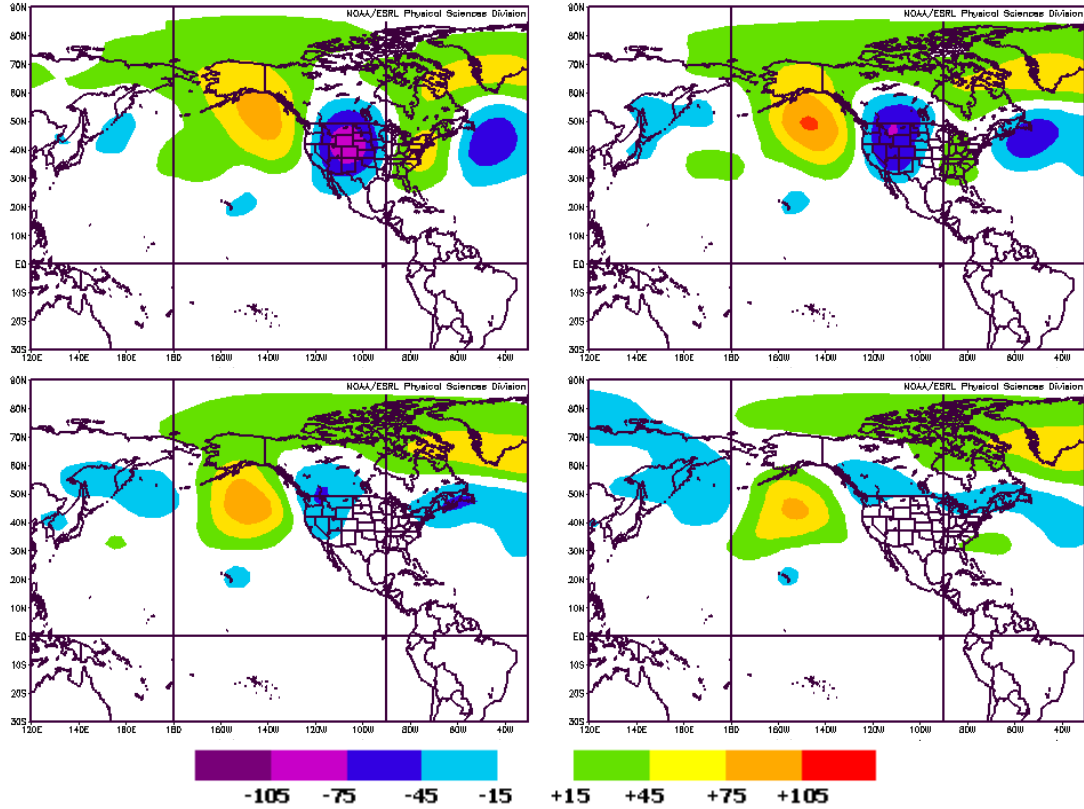


Fig. 5.31: As in Fig. 5.16 but for negative TAPs in eastern Colorado/western Kansas region during all years except warm SSTA events.

pattern is inverted from the typical 500mb geopotential height pattern in this sector (Fig. 5.3a). For Day (-1) through Day (-3), the positive geopotential height anomalies continue to be present in the northern Pacific Ocean (Fig. 5.31b-d). Consequently, during warm TP SSTA events, the negative height anomalies in the northern Pacific Ocean is not conducive to the favorable pattern (i.e., strong ridge in northern Pacific with a downstream trough in western North America) that would support cold daily minimum temperatures in the central U.S. Great Plains.

## 5.6 Summary

This Chapter has presented a full teleconnection linkage chain associating warm TP SSTAs with observed patterns of winter daily temperature extremes and daily precipitation totals in North America. The regional precipitation and temperature

coherencies identified in Chapter 3 and their associated daily distribution properties described in Chapter 4 have been used to (a) identify the duration of consecutive days of daily precipitation and temperature anomalies underlying the composite values and (b) focus the analysis of antecedent large-scale atmospheric patterns.

Most of the precipitation and temperature coherencies associated with TP SSTAs are specifically related to the presence of a large-scale trough in the northern Pacific Ocean and a downstream ridge over western North America. These features, also, are modified during the positive and negative phase of the AO. During the positive AO phase, the positive 500mb height anomalies over North America shift farther west to the northern Pacific Ocean, displacing the negative geopotential height anomalies from the TP SST forcing farther south (Fig. 5.32). During the negative AO phase, the positive

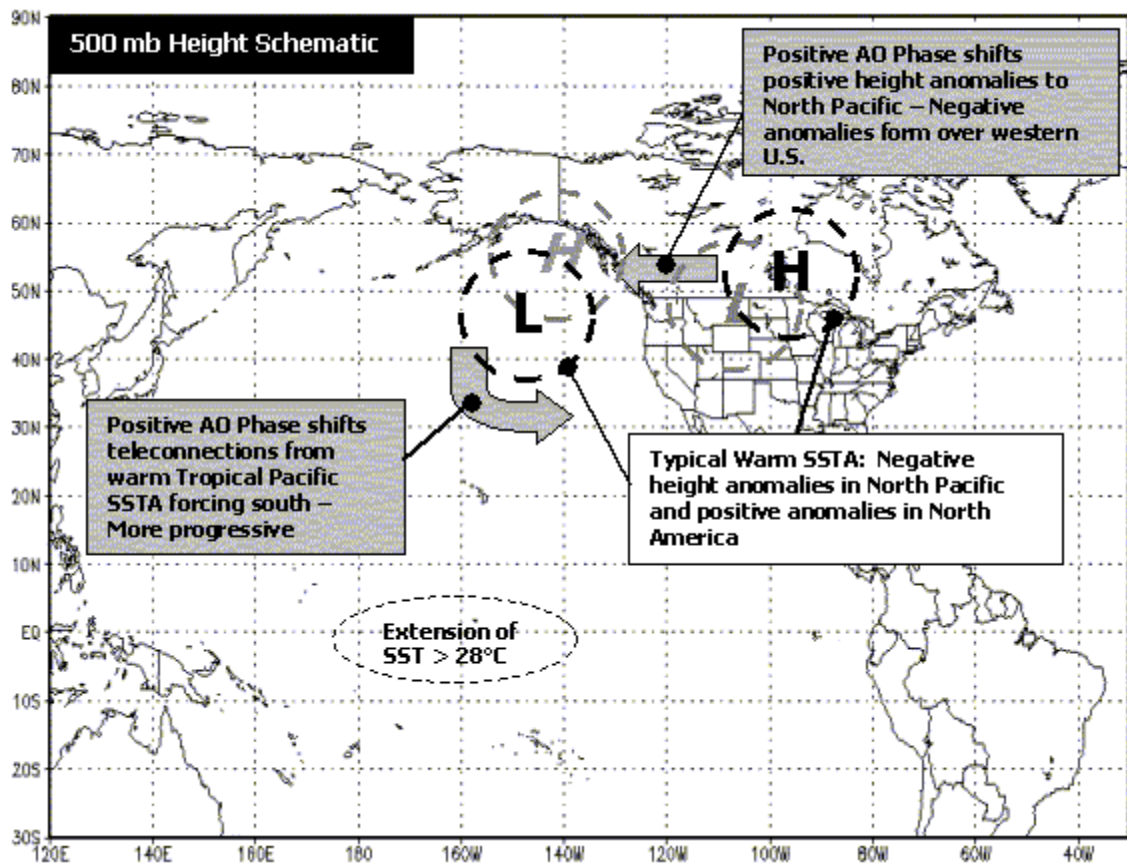


Fig. 5.32: Illustration of the role of the positive phase of the Arctic Oscillation on the 500mb geopotential height patterns during warm TP SSTA events. Black lines provide position of negative and positive anomaly centers during warm TP SSTA events and gray lines provide displaced positions during positive Arctic Oscillation phases.

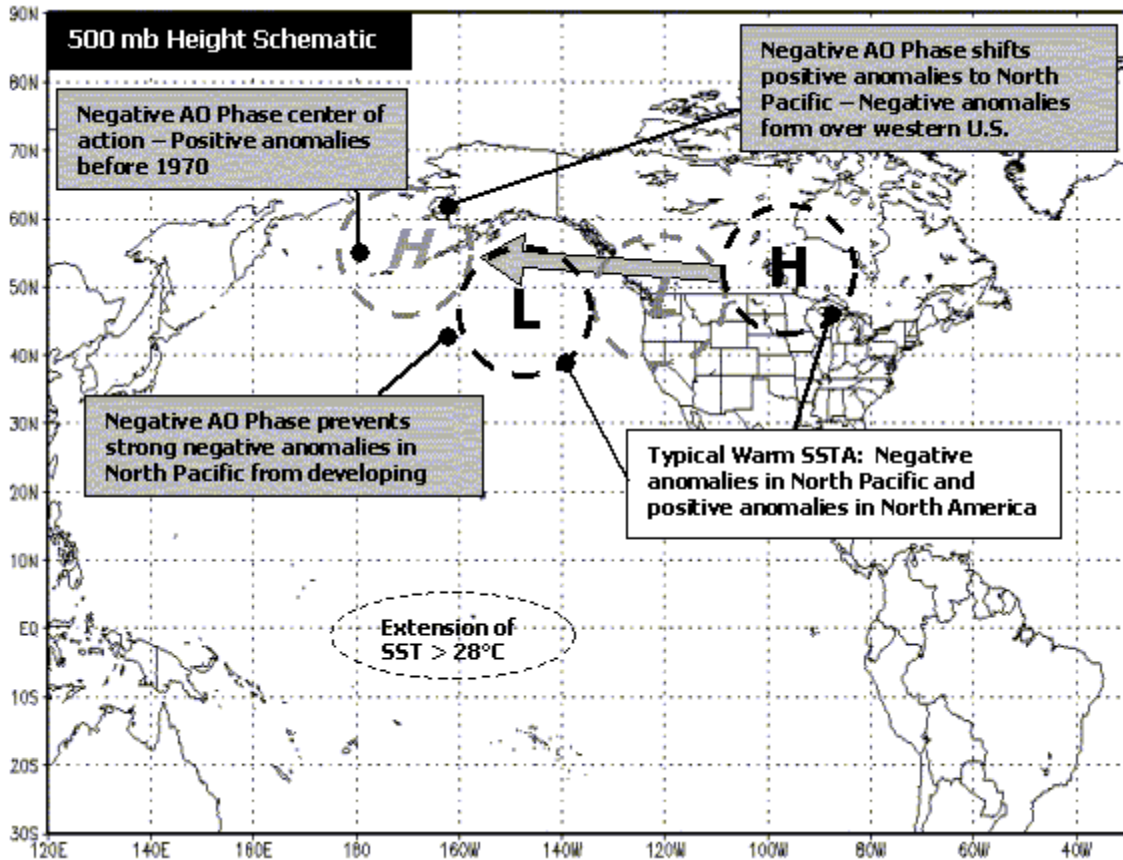


Fig. 5.33: Illustration of the role of the negative phase of the Arctic Oscillation on the 500mb geopotential height patterns during warm TP SSTA events. Black lines provide position of negative and positive anomaly centers during warm TP SSTA events and gray lines provide displaced positions during negative Arctic Oscillation phases.

anomalies also shift much farther west into the northern Pacific Ocean as positive geopotential height anomalies along 180° longitude favor the formation of the anomalous ridge in that area and the negative 500mb height anomalies (linked to anomalous TP SST forcing) farther east over the western coast of North America.

This Chapter has built on previous research in three different manners. First, it has fully documented the temporal characteristics of the North American climate anomalies during warm TP SSTA events. Second, the antecedent larger-scale atmospheric conditions for those anomalies have been identified and related to large-scale atmospheric patterns linked to warm TP SSTAs. Lastly, this research has discussed possible reasons that other atmospheric modes (namely the AO) could disrupt the teleconnections of the typical North American precipitation and temperature patterns. All

of these findings have helped form a full teleconnection linkage chain connecting TP SSTAs to North American climate.

## Chapter 6

### Summary and Conclusions

#### 6.1 Preamble

The principal objective of this research was to address the need for a comprehensive physical explanation on the daily level of the seasonal and monthly mean relationships between tropical Pacific (TP) sea-surface temperature anomalies (SSTAs) and North American precipitation and temperature. To address this need, this research jointly analyzed both the spatial and temporal properties of the North American precipitation and temperature associations with TP SSTA events and the atmospheric conditions preceding the development and occurrence of these anomalies. The present research has used unique analyses of daily precipitation and temperature data for central and eastern North America (east of the Rocky Mountains) and daily atmospheric conditions across the TP, North Pacific Ocean, and North America during 1950-2000. These analyses, focusing on properties of the daily precipitation and temperature data and their antecedent larger-scale atmospheric conditions, have extended the knowledge of the associations between TP SSTAs and North American climate. Some of the key conclusions now are summarized and discussed, and key comments are provided on future research that could be based on these findings.

#### 6.2 Associations Between Tropical Pacific SSTAs and Monthly Averages of Daily Maximum and Minimum Temperatures

One of the key contributions was the full documentation of the teleconnections between TP SSTAs and monthly averages of daily maximum and daily minimum temperatures in central and eastern North America. Previous investigations (e.g., Livezey et al. 1997, hereafter L97) seeking the associations with TP SSTAs focused only on monthly or seasonal average temperatures. The present research was the first to separately analyze the monthly average of the daily maximum and minimum

temperatures. This enabled the identification of some associations in maximum temperature or minimum temperature only, as summarized below. Using the precipitation-based work of Montroy et al. (1998, hereafter MRL98) as a foundation, the present research fully identified the monthly average daily maximum and minimum temperatures linked to both warm and cold TP SSTA events.

Chapter 3 identified the regions characterized by monthly averaged daily maximum and daily minimum temperature that are significantly related to TP SSTA events. For some of the regions (e.g., northern U.S. Great Plains, southern U.S.), this research provided additional quantitative detail to associations identified by earlier authors (e.g., Ropelewski and Halpert 1986, hereafter RH86; L97). The new results delineated regions for which daily minimum temperatures (only) are linked to warm TP SSTA events (e.g., central U.S. Great Plains in February) and some regions where the association involves daily maximum temperatures (only) and warm TP SSTA events (U.S. Great Plains in October-November) or cold TP SSTA events (e.g., southern U.S. Great Plains in February-March).

Additionally, Chapter 3 highlighted the nonlinear characteristics of some of the daily temperature associations with TP SSTAs. Such nonlinearity characterized nearly all regions exhibiting an association with TP SSTA events. For example, southern Manitoba March-April daily maximum and minimum temperatures were below average during cold TP SSTA events but exhibited no significant anomaly during warm TP SSTA events. Only L97 previously had identified some of these characteristics, but their study was limited by the coarse resolution of the climate division data they used. The use of fine-resolution temperature data in the present study (for an ~110 km x 110 km station distribution) enabled the identification of smaller scale regional features such as the lack of cold February outbreaks in the eastern Colorado-western Kansas region during warm TP SSTA events, even though cold TP SSTA events produce warm February temperatures in that area.

Finally, as in MRL98, the examination of monthly data enabled further refinement of earlier associations mentioned by other authors. Chapter 3 indicates that the cool association identified by RH86 during negative Southern Oscillation (i.e., warm

TP SSTA) events is strongest for January temperatures, when the most robust relationships occur for daily maximum temperature. Also, the warm association RH86 noted for the northern U.S. Great Plains is demonstrated here to be strongest in December-February for monthly average of daily maximum temperatures, whereas this link extends into March for monthly average daily minimum temperatures.

### **6.3 Daily Distribution Properties of Monthly Precipitation and Temperature Teleconnection Relationships**

Chapter 4 made additional key contributions through the full documentation of changes in daily precipitation and temperature extreme distributions associated with both warm and cold TP SSTA events. Previous investigations involved either regional studies or larger-scale analyses with a coarse grid, with no full fine-resolution examination on a continental scale of the daily weather patterns that typically occur during warm and cold TP SSTA events and produce regional temperature and precipitation anomaly patterns. The current study has provided a full list of the changes in daily precipitation and temperature patterns associated with the monthly scale temperature relationships identified in Chapter 3 and counterpart precipitation relationships first identified in MRL98 for 1950-92 and in Chapter 3 through 2000.

While in many cases the frequency changes in daily precipitation distributions during warm TP SSTA events were uniform across daily precipitation totals of all sizes, some regions were characterized by distribution changes that differed based on daily precipitation total. For example, in the southeastern U.S., the increased monthly precipitation during January-March warm TP SSTA events generally resulted from more frequent daily totals above  $10 \text{ mm d}^{-1}$ , whereas the increased November precipitation there for the same events stemmed from increased daily totals of all sizes. Further, the below average January precipitation in the southwestern Appalachian Mountain region during warm TP SSTA events was associated with the lack of occurrence of very large ( $>25 \text{ mm d}^{-1}$ ) daily precipitation totals. During cold TP SSTA events, that area's below average November precipitation principally was associated with a reduced frequency of larger ( $>10 \text{ mm d}^{-1}$ ) events.

The analysis of the daily distribution of monthly average daily temperature extremes in Chapter 4 further quantified the monthly mean associations described in Chapter 3. For many regions (e.g., the northern U.S. Great Plains, the southern U.S., and the U.S. Atlantic coast), changes in daily temperature distributions reflected a shift to favor temperature anomalies with the same sign as the anomaly generally observed during those SSTA events. (For example, positive temperature anomalies during warm SSTA events reflected more frequent warmer than average daily temperature observations and less frequent cooler than average daily temperature observations.) However, some regions were associated with the lack of occurrence of daily temperature extremes far from the mean only. The positive February anomalies in monthly average daily minimum temperature in the central U.S. Great Plains during warm TP SSTA events mainly arose from the lack of occurrence of observations well below the monthly mean. Also, the cooler than average January daily maximum temperatures in the southern U.S. during warm TP SSTA events were associated principally with relatively few observations well above the monthly mean.

For all of the temperature and precipitation distribution changes noted in Chapters 3 and 4, the years that were exceptions to the relationship generally observed during warm TP SSTA events were also fully documented and found to coincide principally with strong phases of the Arctic Oscillation (AO). Both the negative and positive phase of the AO were linked to years when the sign of the observed precipitation and/or temperature anomaly in some of the target regions in Chapter 3 (e.g., warmer than average temperatures in the Northern U.S. Great Plains, above average precipitation along the Atlantic and Gulf coasts, and below average precipitation in the Midwest and Ohio valley) did not match that of the composite value. The negative AO phase was primarily linked to observations of precipitation and temperature in the northern U.S. Great Plains/south central Canada (e.g., 1965-66), while the positive AO phase was linked to precipitation in the midwestern and southeastern U.S. (e.g., 1972-73). The nature of the modulation by each of these AO phases is summarized in Section 6.5 below.

The key result of Chapter 4 is a full documentation of the changes in the frequency of daily precipitation and temperature observations linked to the more

traditional monthly associations in Chapter 3. This establishes the focus for the last step in the analysis in Chapter 5, where the duration of these anomaly periods are documented and the atmospheric conditions preceding their formation are documented.

#### **6.4 Duration of Daily Precipitation and Temperature Anomaly Periods and Antecedent Atmospheric Conditions**

The present research employed a unique analysis methodology to identify the persistence of the key daily precipitation and temperature anomalies in North America during warm and cold TP SSTA events, and the atmospheric conditions over North America and the north Pacific Ocean preceding them. The specific focus of this analysis was October-March during warm TP SSTA events persisting over multiple months. Earlier authors had not investigated these associations using daily atmospheric flow and daily precipitation and other surface data and instead focused only on monthly and/or seasonal means (in this larger-scale forcing context).

The North American climate anomalies with the longest duration during warm TP SSTA events are the temperature anomalies in the northern U.S. Great Plains and south-central Canada. These regions experienced noticeably warmer than average temperatures that last for as many as 14 consecutive days during December-March (Fig. 6.1). The maximum duration of the warmer than average December temperatures in the eastern U.S. during warm TP SSTA events was about one week, while the cooler than normal February temperatures in the central U.S. Great Plains typically lasted about 5 days (Fig. 6.1). The above average precipitation in the southeastern U.S. during warm January-March SSTA events was associated with increased frequency of wet periods 3-9 days in length, while the contemporaneous below average precipitation association in the eastern Midwest was linked with increased frequency of dry periods 3-7 days in duration (Fig. 6.1).

The antecedent larger-scale atmospheric conditions for the principal North American regional climate anomalies during warm TP SSTA events involved positive 500mb height anomalies over North America and negative 500mb height anomalies over

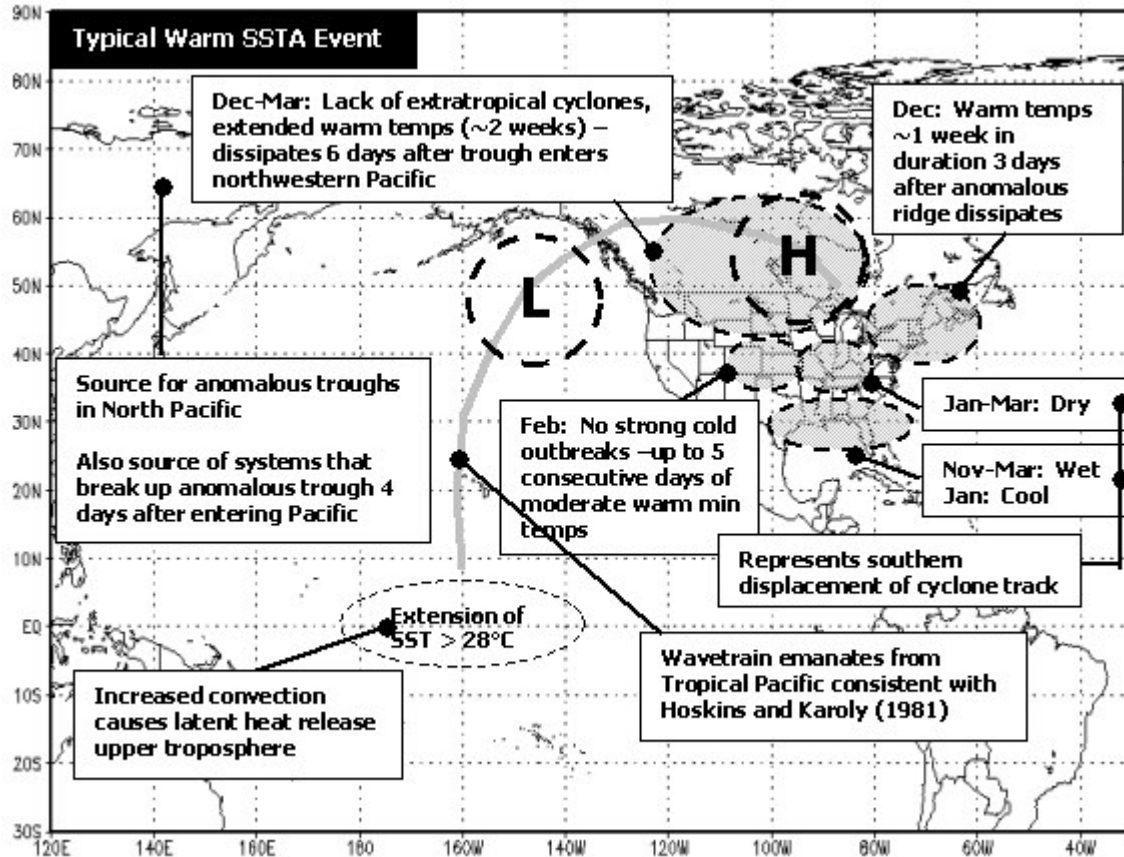


Fig. 6.1: Illustration of key atmospheric processes and North American precipitation and temperature associations during a typical warm TP SSTA event.

the northern Pacific Ocean. The evolution of these conditions in the northern U.S. Great Plains exhibited the negative 500mb height anomalies in the northern Pacific Ocean six days earlier [Day(-6)] and the positive 500mb height anomalies beginning to form over western North America on Day (-4) (Fig. 6.1). Similarly, the above average temperatures in the eastern U.S. began after positive 500mb height anomalies in central North America moved eastward starting on Day (-3) (Fig. 6.1). This is consistent with the positive geopotential height anomalies associated with the warmer than normal temperatures in the northern U.S. Great Plains moving eastward. The increased precipitation in the southeastern U.S. and in southern Texas also are linked to positive 500mb height anomalies in central North America as well as negative such anomalies in the northern Pacific Ocean up to six days before the onset of precipitation events involved.

The end of the periods of anomalously low geopotential heights over the north Pacific Ocean originates from troughs moving into the northwestern Pacific from northeast Asia. Before the end of warmer than average temperatures in the northern U.S. Great Plains, negative geopotential height anomalies move off northeast Asia on Day (-6). On Day (-2), the negative height anomalies over the north Pacific Ocean dissipate while the positive anomalies over central North America remain until they move farther east, ending the warmer than average temperatures in the northern U.S. Great Plains on Day (0). In summary, the movement of an anomalous trough into the northwestern Pacific Ocean was associated with the dissipation of the trough in the northern Pacific Ocean 4 days later and the end of the warmer than average temperatures in the northern U.S. Great Plains 6 days later (Fig. 6.1).

## **6.5 Influence of Other Atmospheric Modes on Teleconnections from Tropical Pacific to North America**

The present research has focused not only on identifying the atmospheric flow patterns common to most warm TP SSTA events, but also on the influence of other atmospheric modes on warm TP-North American teleconnections. Previous investigations have involved the influence of other atmospheric modes on North American climate (by simply stratifying some warm SSTA years by phase of another atmospheric mode) but not in the context of developing a physical teleconnection linkage chain from the TP to North America. This study found that the atmospheric mode with the largest modulation influence on teleconnections between the TP and North America is the AO. Both positive and negative AO phases can modulate the influence of warm TP SSTA events on North American atmospheric circulation patterns and regional precipitation/temperature anomalies. The positive AO phase especially influenced the temperature patterns in December 1972 and precipitation patterns in the Midwestern and southeastern U.S. in January-March 1973. In a strong positive AO phase, the Northern Hemisphere circumpolar vortex strengthens and geopotential heights increase near 180° longitude north of 55°N. This geopotential height increase occurs where negative geopotential height anomalies are expected over the north Pacific Ocean during warm TP

SSTA events due to the presence of enhanced convection in the central TP. This north Pacific geopotential height increase displaces the influence in the geopotential height field of the TP SSTA-based forcing farther south and further lowers geopotential heights in central and western North America where positive geopotential height anomalies are normally located during warm TP SSTA events.

The negative AO phase also can influence the association between TP SSTA events and North American precipitation and temperature, such as during December-February 1965-66. During a negative AO phase, the Northern Hemisphere circumpolar vortex weakens and positive geopotential height anomalies occur in the polar regions and along 180° longitude south to ~40°N. This development combines with the above TP-based convective forcing to displace the positive geopotential height anomalies farther west than is typically the case during warm TP SSTA events. These positive anomalies then support negative anomalies downstream in western North America. The negative anomalies in western North America are consistent with the occurrence of more cold air outbreaks in the northern U.S. Great Plains and south-central Canada.

Although the Pacific Decadal Oscillation (PDO) was not found to be associated with the central and eastern North American precipitation and temperature patterns, in the present study this doesn't mean that the PDO should not be considered further in the warm TP SSTA context. The present study focused on central and eastern North America, and the PDO influence on surface climate could be principally on the western U.S. But, more importantly, it is likely that multidecadal atmospheric-oceanic trends in the north Pacific Ocean need to be addressed when investigating the role of the PDO for teleconnections between the TP and North America. Proper interpretation of the AO modes required an accounting of the decadal-scale trends in the north Pacific (Sections 2.3.1 and 5.4.3).

## **6.6 Synopsis of Association between Tropical Pacific SSTAs and North American Precipitation and Temperature**

After identifying the North American regions with precipitation and temperature observations exhibiting monthly mean coherencies with warm TP SSTA events in Chapter 3, documenting the changes in the underlying daily precipitation and temperature distributions in Chapter 4, further identifying the duration of these anomalies in the first portion of Chapter 5, and associating their antecedent atmospheric conditions with the larger-scale atmospheric patterns accompanying warm TP SSTA events, the physical teleconnection linkage chain from the TP to North America was more complete than previously documented. What follows is a synopsis of how TP SSTAs modify the environment within which weather systems evolve in North America, demonstrating how the building blocks of daily weather systems come together to form the observed monthly and seasonal mean associations.

During warm TP SSTA events, the warmer than normal SSTs induce enhanced convection there, which is displaced farther to the east from its usual location in the western TP, leading to an enhanced local Hadley circulation across the north-central tropical Pacific between  $180^\circ$  and  $150^\circ\text{W}$ . This creates positive advection of Earth's vorticity toward the northern subtropical region, enhancing the subtropical jet stream. Further, the latent heat release in the upper troposphere establishes a wavetrain as outlined in Hoskins and Karoly (1981) that favors negative geopotential height anomalies in the northern Pacific Ocean around  $35\text{-}55^\circ\text{N}$  latitude and  $160\text{-}140^\circ\text{W}$  longitude (Fig. 6.1). These negative anomalies also are supported by the enhanced subtropical jet stream. They are initiated by a cyclonic system moving off northeast Asia into the northern Pacific region that is favorable for development, and once this wave begins to intensify, it remains locked there for periods ranging from 5 to 16 days. Downstream from the negative geopotential height anomalies in the north Pacific, a region of positive geopotential height anomalies forms over north-central North America, also consistent with Hoskins and Karoly (1981). The negative anomalies remain until a cyclonic system moving off northeast Asia gets strong enough to help "kick" the anomalous trough in the north Pacific eastward into the U.S.

The positive geopotential height anomalies in north-central North America are associated with the patterns of observed daily anomalies outlined in Chapter 4. During December-March, the strengthening of the climatological ridge in this region prevents cyclonic systems from moving into western Canada and down into the northern U.S. Great Plains, decreasing the frequency of precipitation days in southern Canada and the northern U.S. Plains (during December-January), along with enhanced (reduced) frequencies of warmer (colder) than normal maximum and minimum temperatures (during December-March). Simultaneously, the storm track across the southern U.S. is enhanced, resulting in the increased frequency of precipitation events to a small extent in Texas during November-March (with the exception of December) but mainly in the far southeastern U.S. for daily totals at least  $10 \text{ mm d}^{-1}$  during January-March. During this time, at least one month of especially heavy precipitation typically is observed in south Florida. With the positive height anomalies over western and central North America preventing cyclonic systems from tracking into the U.S. from Canada, both south-central Canada and the Midwestern U.S. observe a decrease in daily precipitation totals of all sizes. Also, a small region just west of the Appalachian Mountains in January does not receive large precipitation totals exceeding  $25 \text{ mm d}^{-1}$ . Lastly, the positive height anomalies in the north-central U.S. also prevent cyclonic systems from moving either down the Plains out of Canada or over the Rockies and into the Central U.S. Great Plains. This feature prevents the advection of very cold Canadian air from northerly winds behind the system that would allow for at least a couple very clear evenings and very cold minimum temperatures in the central U.S. Great Plains.

## **6.7 Comments on Context Provided by Key Atmospheric Flow Studies**

As mentioned in the previous paragraph, the present results are consistent with the Rossby wavetrain propagation pattern proposed in Hoskins and Karoly (1981). Their idealized response to low-level TP SST forcing generally supported two “rays” of wave propagation, one that traveled nearly a great-circle route, forming a wavetrain stretching into northern Canada, and one that was “trapped” more toward the equator (Fig. 6.1). These tracks are evident in the observations associated with the eight significant SSTA

events examined in this study, as the 500mb height anomalies reflect a great circle track from the TP (positive geopotential height anomalies) to the northern Pacific Ocean (negative) to western North America (positive) and further to the southeastern U.S. (positive) where the subtropical storm track is more active.

The present study also supports the findings of Namias, who associated the North Pacific SSTs with atmospheric variability over North America. Namias demonstrated an association between cooler than average north Pacific SSTs and an overlying negative geopotential height pattern, with downstream positive geopotential heights over north-central North America. In the present investigation, it was shown that positive TP SSTAs are linked to negative geopotential height (and therefore atmospheric circulation) anomalies in the north Pacific both at upper levels and at the surface (Section 5.4.1). The cyclonic circulation anomalies at the surface can help induce negative SSTAs in the north Pacific that Namias associated with variations in atmospheric flow downstream over North America. Moreover, Fig. 6.2 indicates that the composite SSTAs for all warm SSTA events in Table 5.1 after 1980 exhibited negative north Pacific SSTAs from 30-45°N latitude and 170-140°W longitude, a region examined by Namias (e.g., 1959, 1969).

While confirming the Namias “approach” to some extent the present investigation also gives some support to the Wallace “approach” that includes the AO as an independent entity. It was demonstrated here that extreme AO phases (both positive and negative) can help modulate the association between TP SSTAs and atmospheric flow over North America linked to observed precipitation and temperature anomalies there.

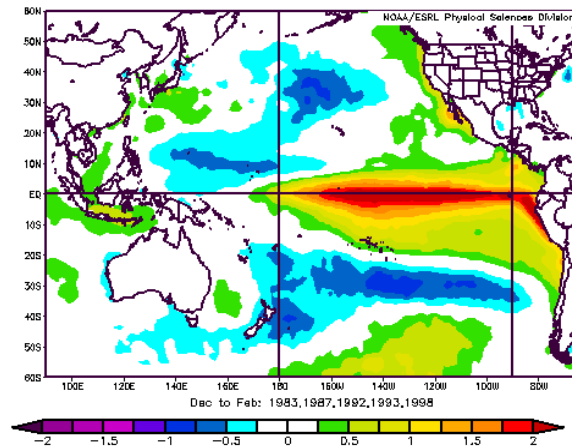


Fig. 6.2: Composite December-February SSTAs (°C) during 1982-83, 1986-87, 1991-92, 1992-93, and 1997-98 using optimal interpolation SST data of Reynolds et al. (2002).

Further, the present identification of persistent AO phases with the above effect supports the functioning of the AO as an independent phenomenon. This also encourages its consideration in how it modulates the key North American climatic variations associated with TP SSTA teleconnections during October-March.

In addition to the above support for the AO as an independent phenomenon modulating teleconnections between the TP and North American winter climate, new work focusing on the northern Pacific Ocean would further the understanding of the exact role of the AO. Fig. 2.4 suggests that the region exhibiting the strongest correlation magnitudes with the AO index is the Arctic region, with the correlations in the northern Pacific Ocean approximately one-half of those near the pole. Further, Trenberth and Hurrell (1994) have identified a North Pacific mode of atmospheric variability that focuses specifically on this region. Because the present research showed that the AO modulates the TP-North America teleconnection through the “center of action” in the north Pacific Ocean, it is possible that use of an index more representative of variability in the north Pacific Ocean could provide greater understanding of the “exception years” (i.e., the years when the observed atmospheric flow and surface climate anomalies do not match those of most warm TP SSTA events) than the AO (Section 5.4.3). Trenberth and Hurrell (1994) define a North Pacific Index (Fig. 6.3) that focuses on sea-level pressure variability in the northern Pacific Ocean in the exact region where the negative geopotential height and sea-level pressure anomalies form in the northern Pacific Ocean during warm TP SSTA events (Section 5.4.3). This index is only weakly correlated (+0.31 in December-February) with the AO index in Fig. 2.4, suggesting that it could be a more representative measure of the atmospheric flow that brings about the above exception years noted in Sections 3.4.4 and 4.5. Consequently, additional research into these “exception” years using this index would be a useful extension of the analysis presented in Section 5.4.3 and summarized in Section 6.5.

## **6.8 Framework for Future Modeling Investigations**

The present observation-based research has provided a comprehensive framework within which several numerical modeling investigations now can be conducted. For the

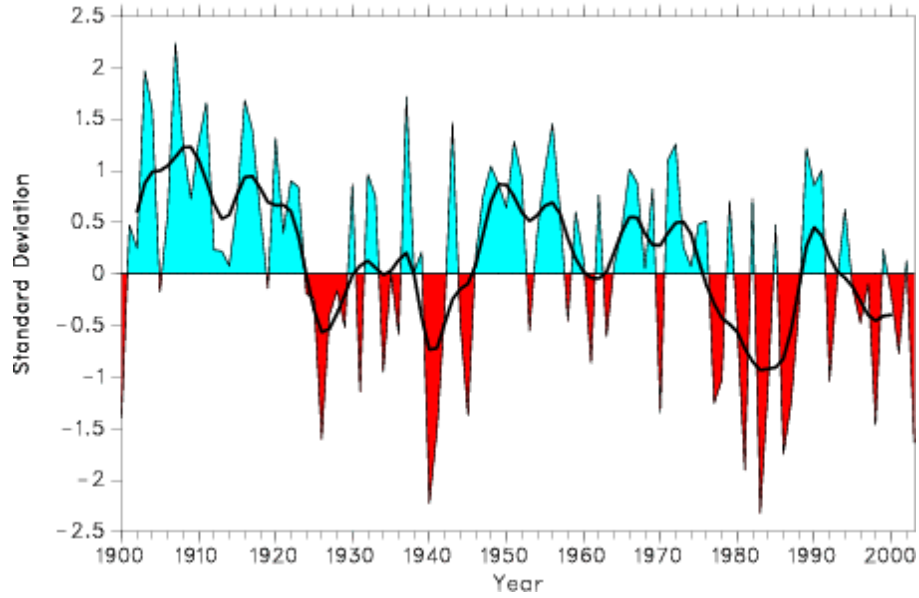


Fig. 6.3: Yearly North Pacific Index provided by the Climate Analysis Section, NCAR, Boulder, USA. Index represents the area-weighted sea level pressure from 30-65°N latitude and 160°E-140°W. Method of calculation is as in Trenberth and Hurrell (1994). Figure reproduced from Hurrell (2006). Smooth trend line is obtained using 11-year running mean.

observational period of record (since 1950), the present research has highlighted North American regions that experience pronounced seasonal and monthly climate anomalies associated with warm TP SSTA events. Consequently, the present research has provided target anomalies to replicate in numerical modeling experiments. Such a replication would provide a further confirmation of the observation-based associations described here and would offer an additional diagnostic tool by which to add more detail to the physical teleconnection linkage chain between the TP and North America.

The temporal and spatial characteristics of the observed anomalies to be investigated in these modeling studies would determine the type of model to be used. The present research utilized a high-resolution set of daily precipitation totals and daily maximum/minimum temperature observations, facilitating the identification of some characteristic warm TP SSTA associated anomalies in focused regions with limited spatial extent (e.g., negative February minimum temperature anomalies in the central U.S. Great Plains and decreased January precipitation in the southwestern Appalachian

Mountain region during warm TP SSTA events). These associations now could be investigated using nested regional models that capture influences of local topography and vegetation cover in order to determine the relative role of orographic forcing and changes in local energy balance on these highly regionalized anomalies. Additionally, a model that captures the impact of cloud cover on the local energy balance would be essential to examining the differences in daily maximum and minimum temperatures, as cloud cover can limit both incoming radiation but also outgoing radiation from the surface. This would be particularly essential in examining the west and cool southeastern U.S. that this research has outlined as a key characteristic of warm TP SSTA events

Modeling investigations into anomaly patterns with a longer duration would require a model capturing synoptic-scale variability. For example, the northern U.S. Great Plains was found to experience warm anomalies lasting for 2 weeks or longer (Section 5.5.1). A modeling investigation into these types of anomalies would require use of a fine-resolution model such as the operational MRF model run by the National Centers for Environmental Prediction (NCEP), similar to the studies of Barsugli et al. (1999) and Compo et al. (2001). However, anomaly periods of this duration extend beyond the synoptic scale (2-7 days) and into the intraseasonal time scale (8-45 days). In order to properly model these longer anomaly periods, a model that effectively represents intraseasonal processes would be required, such as the RegCM model (e.g., Giorgi and Mearns 1999).

Lastly, the finding that the AO modulates the atmospheric response to TP forcing could be tested using a nested modeling experiment, involving using a larger scale climate model to drive the boundary conditions of a regional climate model that can properly represent important polar climate factors. One of the key benefits of such a modeling study would be increasing the sample size, as the observational record is limited to roughly 50 years of data observing the behavior of both the AO and TP-forced climate variations. However, a model that could properly represent the AO would be required. Some large-scale models, including the operational MRF model used to develop the NCEP/NCAR Reanalysis data, do not represent snow cover well. AO variability is influenced significantly by the variations in snow cover in the Arctic

regions. But snow cover is assigned a reliability rating of “C” in Kalnay et al. (1996), suggesting that a model such as the NCEP MRF model would be needed to produce an effective AO representation. One possibility is to utilize a one-way nested modeling experiment using a regional model properly capturing polar processes uniquely associated with the AO (e.g., snow cover development, sea ice formation). Such a study has not yet been published.

## REFERENCES

- Barlow, M., S. Nigam, E. H. Berbery, 2001: ENSO, Pacific decadal variability, and U.S. summertime precipitation, drought, and stream flow. *J. Climate*, **14**, 2105-2128.
- Barnett, T. P., and R. C. J. Somerville, 1983: Advances in short-term climate prediction. *Rev. Geophys.*, **21**, 1096-1102.
- Barnett, T. P., and Coauthors, 1994: Forecasting global ENSO-related climate anomalies. *Tellus*, **46A**, 381-397.
- Barnett, T. P., K. Arpe, L. Bengtsson, M. Ji, and A. Kumar, 1997: Potential predictability and AMIP implications of midlatitude climate variability in two general circulation models. *J. Climate*, **10**, 2321-2329.
- Barnston, A. G., and R. E. Livezey, 1987: Classification, seasonality and persistence of low-frequency atmospheric circulation patterns. *Mon. Wea. Rev.*, **115**, 1083-1126.
- Barnston, A. G., and R. E. Livezey, 1989: A closer look at the effect of the 11-year solar cycle and the quasi-biennial oscillation on Northern Hemisphere 700 mb height and extratropical North American surface temperature. *J. Climate*, **2**, 1295-1313.
- Barnston, A. G., R. E. Livezey, and M. S. Halpert, 1991: Modulation of Southern Oscillation-Northern Hemisphere mid-winter climate relationships by the QBO. *J. Climate*, **4**, 203-217.
- Barsugli, J. J., J. S. Whitaker, A. F. Loughe, P. D. Sardeshmukh, and Z. Toth, 1999: The effect of the 1997/98 El Niño on individual large-scale weather events. *Bull. Amer. Meteor. Soc.*, **80**, 1399-1411.
- Berlage, H. P., 1966: The Southern Oscillation and world weather. *K. Ned. Meteor. Inst., Meded. Verh.*, **88**, 1-152.
- Bjerknes, J., 1966: A possible response of the atmospheric Hadley circulation to equatorial anomalies of ocean temperature. *Tellus*, **18**, 820-829.
- Bjerknes, J., 1969: Atmospheric teleconnections from the equatorial Pacific. *Mon. Wea. Rev.*, **97**, 163-172.
- Blanford, H. F., 1884: On the connection of Himalayan snowfall and seasons of drought in India. *Proc. R. Soc. London*, **37**, 3-22.
- Blanford, H. F., 1886: *Rainfall of India*. Memoirs, India Meteorological Department, 3, 658 pp.
- Bluestein, H. B., 1992: Synoptic-Dynamic Meteorology in Mid-Latitudes. Volume I: Principles of Kinematics and Dynamics. Oxford Press, 431 pp.
- Bowman, K. P., 1989: Global patterns of the quasi-biennial oscillation in total ozone. *J. Atmos. Sci.*, **46**, 3328-3343.
- Cane, M. A., and S. E. Zebiak, 1985: A theory of El Niño and the Southern Oscillation. *Science*, **228**, 1084-1087.
- Cattell, R. B., 1966: The scree test for the number of factors. *Multivar. Behav. Res.*, **1**, 245.
- Cayan, D. R., K. T. Redmond, and L. G. Riddle, 1999: ENSO and hydrologic extremes in the western United States. *J. Climate*, **12**, 2881-2893.

- Compo, G. P., P. D. Sardeshmukh, and C. Penland, 2001: Changes of sub-seasonal variability associated with El Niño. *J. Climate*, **14**, 3356-3374.
- CPC, cited 2006: Extended Range Outlooks. [Available online at [http://www.cpc.ncep.noaa.gov/products/forecasts/extended\\_range\\_outlooks.shtml](http://www.cpc.ncep.noaa.gov/products/forecasts/extended_range_outlooks.shtml).]
- Ebbesmeyer, C. C., D. R. Cayan, D. R. McLain, F. H. Nichols, D. H. Peterson, and K. T. Redmond, 1991: 1976 step in the Pacific climate: Forty environmental changes between 1968-1975 and 1977-1985. In J. L. Betancourt and V. L. Tharp, [ed.], *Proc. Seventh Annual Pacific Climate Workshop, April 1990, Asilomar, CA*. Calif. Dept. of Water Res., Interagency Ecological Studies Program Tech. Rep. 26.
- Gershunov, A. and T. P. Barnett, 1998: Inter-decadal modulation of ENSO teleconnections. *Bull. Amer. Met. Soc.*, **79**, 2715-2725.
- Giorgi, F. and Mearns, L. O., 1999: Introduction to special section: Regional climate modeling revisited, *J. Geophys. Res.*, **104**, 6335-6352.
- Gong, X., 1998: Recent interdecadal variations in the tropical atmosphere: Evidence and idealized GCM simulations. Ph.D. Dissertation, University of Oklahoma, 221 pp.
- Graham, N. E., 1994: Decadal-scale climate variability in the tropical and North Pacific during the 1970s and 1980s: observations and model results. *Climate Dynamics*, **10**, 135-162.
- Gray, W. M., C. W. Landsea, P. W. Mielke, Jr., and K. J. Berry, 1992: Predicting Atlantic seasonal hurricane activity 6-11 months in advance. *Wea. Forecasting*, **7**, 440-455.
- Halpert, M. S., and C. F. Ropelewski, 1992: Surface temperature patterns associated with the Southern Oscillation. *J. Climate*, **5**, 577-593.
- Hastenrath, S., 1994: *Climate Dynamics of the Tropics*. Kluwer Academic Publishers, Dordrecht, The Netherlands. 488 pp.
- Higgins, R. W., J. E. Janowiak, and Y.-P. Yao, 1996: A gridded hourly precipitation data base for the United States (1963-1993). NCEP/Climate Prediction Center Atlas No. 1, U. S. Dept. of Commerce, National Oceanic and Atmospheric Administration. [Available online at: [http://nic.fb4.noaa.gov/research\\_papers/ncep\\_cpc\\_atlas/1/](http://nic.fb4.noaa.gov/research_papers/ncep_cpc_atlas/1/)]
- Higgins, R. W., J.-K. E. Schemm, W. Shi, and A. Leetmaa, 2000: Extreme precipitation events in the western United States related to tropical forcing. *J. Climate*, **13**, 793-820.
- Higgins, R. W., A. Leetmaa, and V. E. Kousky, 2002: Relationships between climate variability and winter temperature extremes in the United States. *J. Climate*, **15**, 1555-1572.
- Hildebrandsson, H. H., 1897: Quelques recherches sur les entres d'action de l'atmosphere. *K. Sven. Vetenskaps akad. Handl.*, **29**, 1-33.
- Hodges, G., 2000: The new cold war. Stalking arctic climate change by submarine. *National Geographic*, **113**, 30-41.
- Hoskins, B. J., and D. J. Karoly, 1981: The steady linear response of a spherical atmosphere to thermal and orographic forcing. *J. Atmos. Sci.*, **38**, 1179-1196.
- Horel, J. D., 1981: A rotated principal component analysis of the interannual variability of the northern hemisphere 500mb height field. *Mon. Wea. Rev.*, **109**, 2080-2092.
- Hurrell, J. W., 1995: Decadal trends in the North Atlantic Oscillation region temperatures and precipitation. *Science.*, **269**, 676-679.

- Hurrell, J. W., cited 2006: Climate Indices: The North Pacific Index. [Available on-line at <http://www.cgd.ucar.edu/cas/jhurrell/npindex.html>.]
- Janowiak, J. E., and G. D. Bell, 1998: Changes in the seasonal distribution of daily U.S. temperature, precipitation, and snowfall associated with the ENSO cycle. *Proc., 23rd Climate Diagnostics and Prediction Workshop*, Miami, FL, Climate Prediction Center/NCEP, 319-322.
- Kahya, E., and J. A. Dracup, 1994: The influence of type 1 El Niño and La Niña events on streamflows in the Pacific Southwest of the United States. *J. Climate*, **7**, 965-976.
- Kaiser, H. F., 1958: The Varimax criterion for analytic rotation in factor analysis. *Psychometrika*, **23**, 187.
- Kalnay, E. and Coauthors, 1996: The NCEP/NCAR Reanalysis 40-year Project. *Bull. Amer. Meteor. Soc.*, **77**, 437-471.
- Kiladis, G. N., and H. F. Diaz, 1989: Global climatic anomalies associated with extremes in the Southern Oscillation. *J. Climate*, **2**, 1069-1090.
- Kistler, R., and Coauthors, 2001: The NCEP-NCAR 50-year Reanalysis: Monthly means CD-ROM and documentation. *Bull. Am. Meteor. Soc.*, **82**, 247-268.
- Kousky, V. E., M. T. Kagano, and I. F. Cavalcant, 1984: A review of the Southern Oscillation: Oceanic-atmospheric circulation changes and related rainfall anomalies. *Tellus*, **36A**, 490-504.
- Kumar, K. K., M. K. Soman, and K. R. Kumar, cited 1998: Seasonal Forecasting of Indian Summer Monsoon Rainfall: A Review. [Available on-line from <http://www.met.rdg.ac.uk/~daves/Monsoon/LrfReview.html>]
- Kunkel, K. E., and J. R. Angel, 1999: Relationship of ENSO to snowfall and related cyclone activity in the contiguous United States. *J. Geophys. Res.*, **104**, 19425-19434.
- Kushnir, Y., W. A. Robinson, I. Bladé, N. M. J. Hall, S. Peng, and R. Sutton, 2002: Atmospheric GCM response to extratropical SST anomalies: Synthesis and evaluation. *J. Climate*, **15**, 2233-2256.
- Lamb, P. J., and R. A. Pepler, 1987: North Atlantic Oscillation: Concept and an application. *Bull. Amer. Meteor. Soc.*, **68**, 1218-1225.
- Latif, M., T. P. Barnett, M. A. Cane, M. Flugel, N. E. Graham, H. von Storch, J.-S. Xu, and S. E. Zebiak, 1994: A review of ENSO prediction studies. *Climate Dyn.*, **9**, 167-179.
- Lau, K.-M., H.-T. Wu, and S. Bony, 1997: The role of large-scale atmospheric circulation in the relationship between tropical convection and sea surface temperature. *J. Climate*, **10**, 381-392.
- Livezey, R. E., A. Leetmaa, M. Masutani, H. Rui, M. Ji, and A. Kumar, 1997: Teleconnective response of the Pacific/North American region atmosphere to large central equatorial Pacific SST anomalies. *J. Climate*, **10**, 1787-1820.
- Lockyer, N., and W. J. S. Lockyer, 1902: On some phenomena which suggest a short period of solar and meteorological changes. *Proc. R. Soc. London*, **70**, 500.
- Lockyer, N., and W. J. S. Lockyer, 1904: The behavior of the short-period atmospheric pressure variation over the earth's surface. *Proc. R. Soc. London*, **73**, 457-470.
- Mantua, N. J., S. R. Hare, Y. Zhang, J. M. Wallace, and R. C. Francis, 1997: A Pacific decadal climate oscillation with impacts on salmon. *Bull. Amer. Meteor. Soc.*, **78**, 1069-1079.

- Mantua, N. J., cited 2005: Pacific Decadal Oscillation (PDO). [Available on-line at <http://tao.atmos.washington.edu/pdo/>.]
- McCreary, F. E., 1959: Stratospheric winds over the tropical Pacific Ocean. *Bull. Amer. Meteor. Soc.*, **40**, 370.
- Mo, K. C., and R. W. Higgins, 1998: Tropical convection and precipitation regimes in the western United States. *J. Climate*, **11**, 2404-2423.
- Montroy, D. L., 1997: Linear relation of North American precipitation to equatorial Pacific sea surface temperature anomalies. *J. Climate*, **10**, 541-558.
- Montroy, D. L., M. B. Richman, and P. J. Lamb, 1998: Observed nonlinearities of monthly teleconnections between tropical Pacific sea surface temperature anomalies and central and eastern North American precipitation. *J. Climate*, **11**, 1812-1835.
- Murphy, R. C., 1923: The oceanography of the Peruvian littoral with reference to the abundance and distribution of marine life. *Geogr. Rev.*, **13**, 64-85.
- NASA, cited 2005: Atlas of Extratropical Storm Tracks. [Available online at <http://www.giss.nasa.gov/data/stormtracks/>.]
- Namias, J., 1959: Recent seasonal interaction between North Pacific waters and the overlying atmospheric circulation. *J. Geophys. Res.*, **64**, 631-646.
- Namias, J., 1969: Seasonal interactions between the North Pacific Ocean and the atmosphere during the 1960s. *Mon. Wea. Rev.*, **97**, 173-192.
- Namias, J., and D. R. Cayan, 1981: Large-scale air-sea interactions and short period climate fluctuations. *Science*, **214**, 869-876.
- NCDC, cited 2005: Climate division data. [Available online at <http://www.ncdc.noaa.gov/oa/climate/onlineprod/drought/ftppage.html>.]
- Nicholls, N., 1989: Sea surface temperatures and Australian winter rainfall. *J. Climate*, **2**, 965-973.
- Nicholls, N., and A. Kariko, 1993: East Australian rainfall events: Interannual variations, trends, and relationships with the Southern Oscillation. *J. Climate*, **6**, 1141-1152.
- North, G. R., T. L. Bell, R. F. Calahan, and F. J. Moeng, 1982: Sampling errors in the estimation of empirical orthogonal functions. *Mon. Wea. Rev.*, **110**, 699-706.
- Peixoto, J. P., and A. H. Oort, 1992: *Physics of Climate*, American Institute of Physics, 520pp.
- Philander, S. G. H., 1990: *El Niño, La Niña, and the Southern Oscillation*. Academic Press, 289 pp.
- Power, S., T. Casey, C. Folland, A. Colman, and V. Mehta, 1999: Inter-decadal modulation of the impact of ENSO on Australia. *Climate Dyn.*, **15**, 319-324.
- Power S., F. Tseitkin, V. Mehta, B. Lavery, S. Torok, and N. Holbrook, 1999: Decadal climate variability in Australia during the twentieth century. *Int. J. Climatol.*, **19**, 169-184.
- Rasmusson, E. M., and T. H. Carpenter, 1982: Variations in tropical sea surface temperature and surface wind fields associated with the Southern Oscillation/El Niño. *Mon. Wea. Rev.*, **110**, 354-384.
- Reynolds, R.W., N.A. Rayner, T.M. Smith, D.C. Stokes, and W. Wang, 2002: An improved in situ and satellite SST analysis for climate. *J. Climate*, **15**, 1609-1625.

- Richman, M. B., 1986: Rotation of principal components. *J. Climatol.*, **6**, 293-333.
- Richman, M. B., and P. J. Lamb, 1985: Climatic pattern analysis of three- and seven-day summer rainfall in the central United States: Some methodological considerations and a regionalization. *J. Climate Appl. Meteor.*, **24**, 1325-1343.
- Richman, M. B., and P. J. Lamb, 1987: Pattern analysis of growing season precipitation in southern Canada. *Atmosphere-Ocean*, **25**, 137-158.
- Rogers, J. C., 1984: The association between the North Atlantic Oscillation and the Southern Oscillation in the northern hemisphere. *Mon. Wea. Rev.*, **112**, 1999-2015.
- Ropelewski, C. F., and M. S. Halpert, 1986: North American precipitation and temperature patterns associated with the El Niño Southern-Oscillation. *Mon. Wea. Rev.*, **114**, 2352-2362.
- Ropelewski, C. F., and M. S. Halpert, 1987: Global and regional scale precipitation patterns associated with the El Niño/Southern Oscillation. *Mon. Wea. Rev.*, **115**, 1606-1626.
- Ropelewski, C. F., and M. S. Halpert, 1989: Precipitation patterns associated with the high index phase of the Southern Oscillation. *J. Climate*, **2**, 268-284.
- Ropelewski, C. F., and M. S. Halpert, 1996: Quantifying Southern Oscillation-precipitation relationships. *J. Climate*, **9**, 1043-1050.
- Skinner, B. D., D. Changnon, M. B. Richman, and P. J. Lamb, 1999: Damaging weather conditions in the United States: A selection of data quality and monitoring issues. *Climatic Change*, **42**, 69-87.
- Smith, S. R., J. J. O'Brien, and J. M. Patten, 2001: Regional snowfall distribution associated with ENSO. *Preprints, Symp. on Climate Variability, the Oceans, and Societal Impacts*, Amer. Meteor. Soc., Albuquerque, New Mexico, 19-26.
- Stone, R., and A. Auliciems, 1992: SOI phase relationships with rainfall in eastern Australia. *Int. J. Climatol.*, **12**, 625-636.
- Stone, R. C. G. L. Hammer, and T. Marcussen, 1996a: Prediction of global rainfall probabilities using phases of the Southern Oscillation Index. *Nature*, **384**, 252-255.
- Stone, R. C., N. Nicholls, and G. Hammer, 1996b: Frost in northeast Australia: trends and influences of phases of the Southern Oscillation. *J. Climate*, **9**, 1896-1909.
- Thompson, D. W. J., cited 2005: Indices of the Annular Modes. [Available online at [http://www.atmos.colostate.edu/ao/Data/ao\\_index.html](http://www.atmos.colostate.edu/ao/Data/ao_index.html).]
- Thompson, D. W. J., and J. M. Wallace, 1998: The Arctic Oscillation signature in the wintertime geopotential height and temperature fields. *Geophys. Res. Lett.*, **25**, 1297-1300.
- Thompson, D. W. J., and J. M. Wallace, 2000: Annular modes in the extratropical circulation. Part I: Month-to-month variability. *J. Climate*, **13**, 1000-1016.
- Thompson, D. W. J., and D. J. Lorenz, 2004: The signature of the annular modes in the tropical troposphere. *J. Climate*, **17**, 4330-4342.
- Trenberth, K. E., and D. A. Paolino Jr., 1980: The Northern Hemisphere sea-level pressure data set: Trends, errors and discontinuities. *Mon. Wea. Rev.*, **108**, 855-872.
- Trenberth, K. E., and J. W. Hurrell, 1994: Decadal atmosphere-ocean variations in the Pacific. *Clim. Dyn.*, **9**, 303-319.

- Trenberth, K. E., D. P. Stepaniak, and J. M. Caron, 2002: Accuracy of atmospheric energy budgets. *J. Climate*, **15**, 3343-3360.
- van Loon, H., and J. C. Rogers, 1978: Seesaw in winter temperatures between Greenland and northern Europe. Part I: General description. *Mon. Wea. Rev.*, **106**, 296-310.
- Walker, G. T., 1923: Correlation in seasonal variations of weather. VII. A preliminary study of world weather. *Mem. Indian Meteorol. Dept.*, **24**, 75-131.
- Walker, G. T., 1924: Correlation in seasonal variations of weather. IX. A further study of world weather. *Mem. Indian Meteorol. Dept.*, **24**, 275-332.
- Walker, G. T., and E. W. Bliss, 1932: World Weather V. *Mem. Roy. Meteor. Soc.*, **4**, 53-83.
- Wallace, J. M., 2000: North Atlantic Oscillation/Northern Hemisphere annular mode: Two paradigms—One phenomenon. *Quart. J. Roy. Meteor. Soc.*, **126**, 791-806.
- Wallace, J. M., and D. S. Gutzler, 1981: Teleconnections in the geopotential height field during the Northern Hemisphere winter. *Mon. Wea. Rev.*, **109**, 784-812.
- Wallace, J. M., and D. W. Thompson, 1981: Teleconnections in the geopotential height field during the Northern Hemisphere winter. *Mon. Wea. Rev.*, **109**, 784-812.
- Ward, M. N., and C. K. Folland, 1991: Prediction of seasonal rainfall in the north Nordeste of Brazil using eigenvectors of sea-surface temperature. *Int. J. Climatol.*, **11**, 711-743.
- Wilks, D. S., 1995: *Statistical Methods in Atmospheric Sciences*, Academic Press, 467pp.
- Wolter, K., and M. S. Timlin, 1998: Measuring the strength of ENSO – how does 1997/98 rank? *Weather*, **53**, 315-324.
- Wolter, K., R. M. Dole, and C. A. Smith, 1999: Short-term climate extremes over the continental U.S. and ENSO. Part I: Seasonal Temperatures. *J. Climate*, **12**, 3255-3272.
- Wyrtki, K., 1975: El Niño – The dynamic response of the equatorial Pacific Ocean to atmospheric forcing. *J. Phys. Oceanogr.*, **5**, 572-584.
- Zebiak, S. E., and M. A. Cane, 1987: A model El Niño/Southern Oscillation. *Mon. Wea. Rev.*, **115**, 2262-2278.
- Zhang, Y., J. M. Wallace, and D. S. Battisti, 1997: ENSO-like interdecadal variability: 1900-1993. *J. Climate*, **10**, 1004-1020.